HYDROMETEOROLOGICAL REPORT NO. 49

Probable Maximum Precipitation Estimates, Colorado River and Great Basin Drainages

REPRINTED 1984

U.S. DEPARTMENT OF COMMERCE
NATIONAL OCEANIC AND ATMOSPHERIC ADMINISTRATION
U.S. DEPARTMENT OF ARMY
CORPS OF ENGINEERS

Silver Spring, Md.

U.S. DEPARTMENT OF COMMERCE
NATIONAL OCEANIC AND ATMOSPHERIC ADMINISTRATION

U.S. DEPARTMENT OF THE ARMY
CORPS OF ENGINEERS

HYDROMETEOROLOGICAL REPORT NO. 49

Probable Maximum Precipitation Estimates, Colorado River and Great Basin Drainages

REPRINTED 1984

Prepared by
E. Marshall Hansen,
Francis K. Schwarz, and John T. Riedel
Hydrometeorological Branch
Office of Hydrology
National Weather Service

Silver Spring, Md.

For sale by the Superintendent of Documents, U.S. Government Printing Office
Washington, D.C. 20402

Stock No. 003-017-00408-2

ERRATA

Page

45, line 6: Change "summary" to "summer."

68, line 22: Add a closing parenthesis after "spreading out."

115, figure 4.5: Some latitude markings (ticks) on the 110th, 115th, and 120th meridians are incorrectly positioned; such markings should agree with those on the 105th and 125th meridians.

118, line 4: Change the period (.) to a colon (:) at the end of the line.

119, table 4.3, number 3: Change "1945" to "1943."

147, line 16: Change to read "figures 3.11a to d (Revised)."

148, step A.2,
149, step B.4,
152, title,
154, title: In computing the reduction for elevation for local-storm PMP, use mean basin elevation (mean elevation of area enclosed by basin boundary and limiting isohyet of storm pattern if areal distribution is used) instead of lowest (minimum) elevation in drainage. [In the example given on pages 154 and 155, if the mean elevation of 6500 ft had been used instead of the lowest (minimum) elevation, a somewhat reduced local storm PMP would have been computed.]

150, step B.1: Change to read "figures 3.11a to d (Revised)."

150, step B.5: Change to read "(table 3.9)."

151, line 2: Change to read "Area 878 mi^2."

151, line B.5: Change to read "(table 3.9)."

CONTENTS

TABLES

FIGURES

PROBABLE MAXIMUM PRECIPITATION ESTIMATES, COLORADO RIVER AND GREAT BASIN DRAINAGES

E. Marshall Hansen, Francis K. Schwarz, and John T. Riedel
Hydrometeorological Branch
Office of Hydrology
NOAA, National Weather Service, Silver Spring, Md.

ABSTRACT. This study gives general-storm probable maximum precipitation (PMP) estimates for durations between 6 and 72 hours and for area sizes between 10 and 5,000 mi^2 (26 and 12,950 km^2), for any location in the Colorado River and Great Basin drainages. Total PMP is determined as the sum of convergence and orographic PMP components. Estimates are given for each month.

The study also provides estimates for local-storm PMP. In addition to the above drainages these estimates are provided for all of California. The estimates cover durations between 15 minutes and 6 hours and drainage areas between 1 and 500 mi^2 (2.6 and 1,295 km^2). Local-storm PMP is applicable to the warm season between May and October.

Comparisons are given between PMP estimates and the greatest observed rainfalls of record, 100-yr frequency rainfall and statistically derived PMP. A step-by-step outline of the procedure for computing PMP estimates is presented with examples for both the general and local storm.

1. INTRODUCTION

1.1 Purpose of Report

The purpose of this report is to present the material necessary to compute estimates of probable maximum precipitation for any watershed up to 5,000 mi^2 (12,950 km^2) for durations up to 72 hours in the Colorado River or Great Basin drainages. The material for preparing an estimate makes up only a small portion of this text; the bulk of the report consists of data and studies required to develop the criteria. The local-storm criteria presented in this report also cover the Pacific Ocean drainage of California.

1.2 Authorization

Authorization for the study was given in a memorandum from the Office of Chief of Engineers, Corps of Engineers, dated July 8, 1971. In conferences between representatives of the Corps of Engineers and the National Weather Service it was agreed the study should cover the Colorado River drainage and interior drainages of Nevada, Utah, and California. As thunderstorm PMP had not been previously considered for the Pacific Ocean drainages in California, it was subsequently agreed to expand this portion of the study.

1.3 Scope

Estimates of general-storm probable maximum precipitation (PMP) in this report cover the region between the crest of the Sierra Nevadas on the west and the Continental Divide on the east. To the north, the region extends to the southern limits of the Columbia River drainage and to the south to the U. S. border. This study region is shown in figure 1.1.

The shaded portion of the study region in figure 1.1 is a zone (to the west of the Continental Divide) where the PMP values are considered least certain. Detailed generalized PMP estimates including seasonal variation are not available for the slopes immediately east of the Continental Divide. PMP gradients in this region can influence PMP estimates west of the Divide. A future PMP study covering the area east of the Divide is needed before there will be comparable confidence in PMP over the contiguous portion of the Southwestern States.

General-storm PMP estimates may be obtained for basin sizes from 10 to 5,000 mi^2 (26 to 12,950 km^2) for durations from 6 to 72 hours. Values can be computed for each month.

Intense local summer thunderstorms can produce rain for short durations over small basins that exceed the rain potential from general storms. Chapter 4 gives these criteria for durations from 15 minutes to 6 hours covering basin sizes up to 500 mi^2 (1,295 km^2). The thunderstorm PMP estimates cover not only the primary study region defined above but also the remainder of California except a small section of the northern coastal region.

The meteorological background and discussions have been kept to a minimum. A companion report (Schwarz and Hansen 1978) contains detailed descriptions of the meteorology of storms and other major meteorological analyses.

1.4 Definition of Probable Maximum Precipitation

Probable maximum precipitation (PMP) is defined (American Meteorological Society 1959) as "...the theoretically greatest depth of precipitation for a given duration that is physically possible over a particular drainage basin at a particular time of year." We recognize there are yet unknowns in the complicated atmospheric processes responsible for extreme rainfalls. Thus, methods used for deriving PMP include making judgments based on record storms and meteorological processes related to them. Results of studies are considered estimates because changes are likely as our understanding increases.

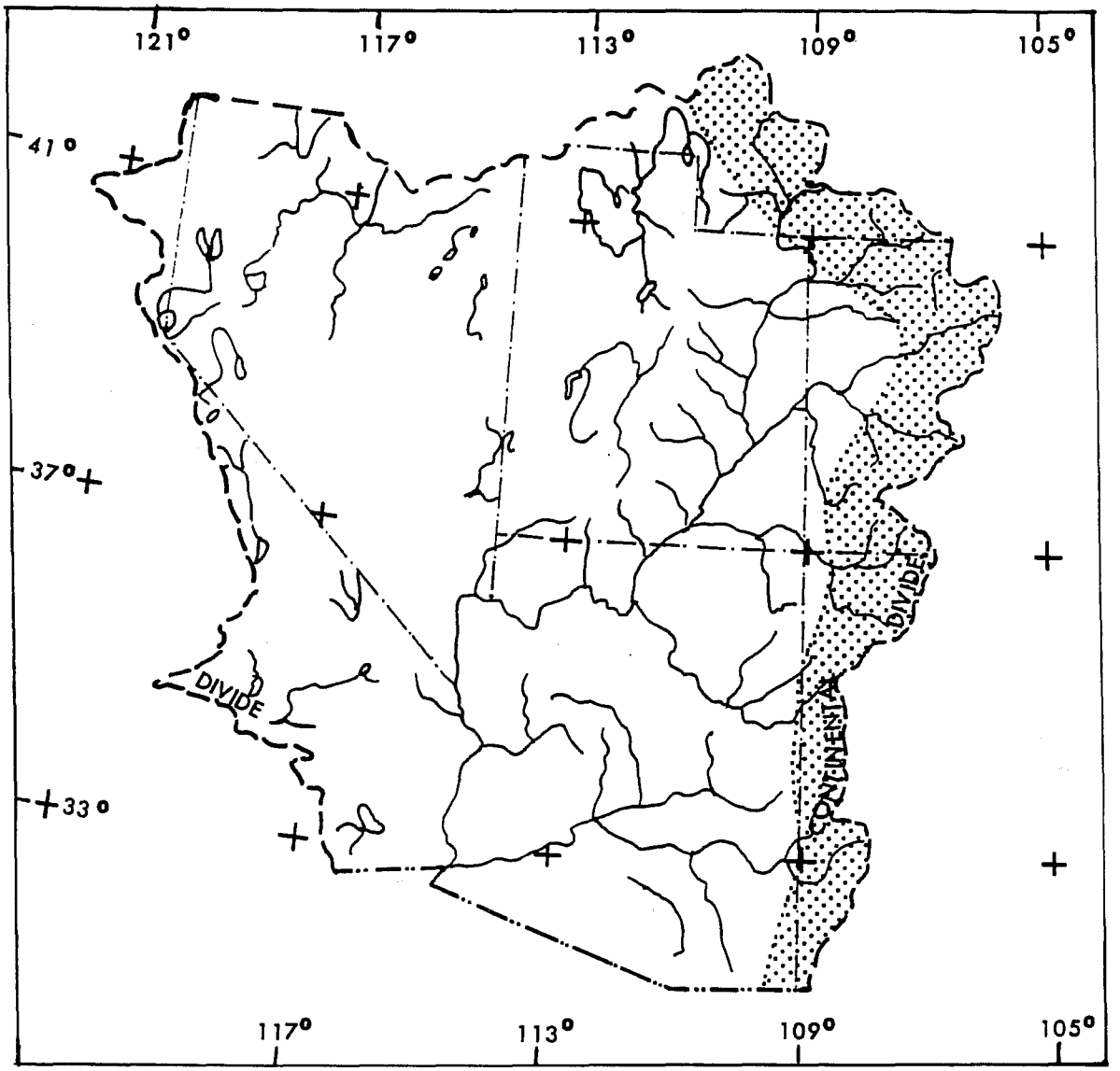

Figure 1.1.--Primary study area, Colorado River and Great Basin drainages. Criteria for shaded portion are considered of lesser reliability.

In this derivation of PMP we assume that the record storms during the past 80 or so years are representative of the climate of extreme precipitation. PMP estimates therefore do not allow for changes in climate.

Experience gained from PMP studies in other regions gives additional guidance to procedures and methods used. This then points to an operational definition of PMP; i.e., estimates by hydrometeorologists of upper limits of rainfall, supplied to engineers for use in hydrologic design. Quoting from Operational Hydrology Report No. 1 (World Meteorological Organization 1973), "Whatever the philosophical objection to the concept, the operational definition leads to answers that have been examined thoroughly by competent meteorologists and engineers and judged as meeting the requirements of a design criterion."

1.5 Methods of This Report

Estimation of general storm PMP of this report uses basically the same procedure used in two studies for adjoining regions; to the west (U. S. Weather Bureau 1961) and to the north (U. S. Weather Bureau 1966a). First, essentially nonorographic PMP, also termed convergence PMP (precipitation due to atmospheric processes), is estimated. Then orographic PMP (precipitation from moist air forced upward by mountain slopes and the triggering of rainfall near first upslopes) is estimated. The two components of PMP are then added together. The convergence PMP is based on moisture-maximized rains of record, reduced for mountain barriers and elevations. Consideration was given to convergence PMP from the adjoining studies. Orographic PMP, for the most part, was not based on the orographic precipitation computation model used in adjoining regions (U. S. Weather Bureau 1961 and 1966a). Reasons for this departure are spelled out in chapter 3. The model is not suited for the meteorological conditions accompanying the main PMP storm prototype for much of the Southwest, partly because the topography is too complicated. Alternate methods for estimating orographic PMP are discussed in chapter 3.

The method used for local or thunderstorm PMP was to adjust the most intense storm values for maximum moisture and develop a 1-hr PMP map for 1 mi^2 (2.6 km^2). The regional pattern of this map took into account maximum 1-hr rainfalls from recorder stations and broad-scale terrain features. Depth-duration and depth-areal variations to extend the estimates to other durations and larger areas were based on record storms.

1.6 Organization of Report

General-storm convergence PMP estimates are developed in chapter 2 and general storm orographic PMP in chapter 3. PMP for small areas from intense thunderstorms is covered in chapter 4. Checks on the general level of PMP are discussed in chapter 5; while chapter 6 gives procedures for and examples of use of the developed criteria.

We at times refer to the study region as the Southwest or the Southwestern States. Frequent reference will be made to studies for two adjoining regions. These are the Columbia River drainage, Hydrometeorological Report No. 43 (U. S. Weather Bureau 1966a) and the Pacific Ocean drainages of

California, Hydrometeorological Report No. 36 (U.S. Weather Bureau 1961). Hereafter they will be referred to as HMR No. 43 and HMR No. 36, respectively.

2. CONVERGENCE COMPONENT OF PMP

2.1 Introduction

2.1.1 Method of Determining General-Storm PMP

We noted in chapter 1 that the method for determining general-storm PMP in this study was to make separate estimates of orographic and nonorographic PMP; to judge the regional, seasonal, depth-area, and depth-duration variations of each component; and then to add the components for an estimate of total PMP. This method is comparable to that used for general-storm PMP estimates to the west and north (HMR No. 36 and No. 43). Development of nonorographic PMP, or convergence PMP, is the subject of this chapter.

2.1.2 Definition of Convergence PMP

Nonorographic precipitation can be defined as precipitation resulting from atmospheric processes not affected by terrain. Lifting and therefore cooling of moist air are necessary for major precipitation. Lifting or vertical motion can be produced by horizontal convergence of air at lower levels; hence, the term "convergence" for nonorographic precipitation. Under this definition all precipitation in regions with no abrupt changes in elevation is classified as convergence. Convergence and orographic precipitation can occur simultaneously.

2.1.3 General Storm Relation to Local Storm

In the United States east of approximately the 105th meridian, many extreme small area rainfalls have occurred within longer storm periods in which general rains cover larger areas. In contrast, experience has shown that the greatest short-duration rainfalls over small areas in the intermountain region come from intense local storms (thunderstorms) as opposed to general-storm situations. For the Southwestern States, therefore, separate estimates of local-storm PMP are given in chapter 4. While most extreme point rainfalls of record in the Southwest States have been isolated with regard to space and time, this does not negate the occurrence of lesser thunderstorm rains imbedded in the general PMP storm prototype. The point to be emphasized is that the local thunderstorm, the greatest potential rainfall threat for small areas and short durations, is an isolated event in time and space in the Southwestern States, while less intense thunderstorm occurring within general-storm rains are the key for general-storm convergence PMP.

2.1.4 Convergence PMP for Adjoining Regions

The Southwest States Region is bounded on the west by the Pacific Ocean drainage of California. Convergence PMP estimates for that drainage (HMR No. 36) were based on multiplying greatest observed ratios of P/M_s by M_x (observed precipitation, P, divided by storm moisture, M_s, multiplied by maximum moisture, M_x). The P/M_s ratios were associated with rains at least-orographic locations such as on the floor of the Central Valley of California. Enveloping values of P/M_s and a regional pattern of M_x were used to determine a basic convergence PMP index map for 10 mi^2 (26 km^2) for 6 hours duration.

For the Columbia River drainage to the north (HMR No. 43), similar procedures for estimating convergence PMP were used. The major difference from HMR No. 36 was that regional patterns of convergence PMP were determined for each month, October through June. These monthly maps incorporated the seasonal variations of maximum observed 1-day precipitation at groups of least-orographic stations as well as the seasonal variation of maximum moisture.

In developing convergence PMP for the present study, reasonable consistency was maintained with values for the two adjoining regions.

Also of some interest are PMP estimates for the United States east of the 105th meridian (Schreiner and Riedel 1978, and Riedel et al. 1956). For these studies, the effects of steepening slopes near the 105th meridian in Colorado and New Mexico were not taken into account. Thus, the PMP estimates to the east of the steep slopes of the Rocky Mountains should be considered nonorographic. The steep slopes east of the Continental Divide separate by distances up to 300 miles (483 km), the region of those studies from that of the present study. Sharp gradients in precipitation potential are expected in this intervening region that do not allow detailed comparisons of PMP between the two studies. Some overall general consistency checks can be made, such as the effect of moisture sources on PMP patterns, etc. Checks of this nature have been considered in this study.

2.1.5 Summary of Procedure

The approach for convergence PMP in this study follows after but is not identical with that for HMR Nos. 36 and 43. Instead of developing P/M_s ratio envelopes, the greatest moisture-maximized observed rainfalls for least-orographic locations were enveloped. This is equivalent to the previous studies [(P/M_s) envelope x $M_x = (P \times M_x/M_s)$ envelope]. Monthly patterns of highest moisture and seasonal trends in maximum observed precipitation were used as guides in interpolating between locations of highest moisture-maximized rainfalls. The resulting patterns are consistent with patterns of convergence PMP in HMR No. 43 and No. 36. The 1000-mb (100-kPa) convergence PMP estimates were then reduced for effective elevation and barrier. Depth-duration (from 6 to 72 hours) and depth-area (from 10 to 5,000 mi^2, 26 to 12,950 km^2) relations were based on maximum observed precipitation in least-orographic areas of the Southwestern States and those from eastern states data respectively. These procedures are in general agreement with those used in HMR No. 36 and HMR No. 43.

2.2 Mid-Month 1000-mb (100-kPa) Convergence PMP Maps, 24 hrs, 10 mi^2 (26 km^2)

2.2.1 Envelopment of Maximum Observed Rainfalls

Record storm rainfall is the underpinning to any PMP study. We need two restrictions to our data sample. First, extreme isolated thunderstorm values are not appropriate for development of general-storm convergence PMP. Such values rather are the basis for the local-storm PMP estimates of chapter 4. Secondly, in this section we are concerned with only the convergence component of record storm amounts. No consistent method has been found for separating total observed storm precipitation into convergence and orographic components; however, we can restrict the data to observed maxima in least-orographic regions of the Southwest.

Least-orographic regions are subjectively determined zones (shown in fig. 2.1) outlined on a 1:2,000,000 scale topographic map. The boundary of each subregion depicted on the figure is not significant other than to enclose a group of at least five stations whose precipitation we believe to be least influenced by orography. An appreciation for the complex terrain and an aid in determining general limits for these subregions was gained by two of the authors (Riedel and Hansen) during a 2-day series of overflights in 1972. We recognize that some substantial orographic features remain within the least-orographic boundaries shown in figure 2.1 but stations selected within these subregions were judged not to be significantly influenced by orography. An attempt was made to obtain an equal number of stations in each subregion, but this was difficult to maintain. Station storm totals exceeding 5 inches (127 mm) in 24 hours or less in the subregions were extracted from the historical records. The five storms meeting this criterion are listed in table 2.1. One other storm for Porter, N.M., east of the region of interest, is listed for comparison. Meteorological descriptions of each of the events is given in the companion report (Schwarz and Hansen 1978). Each storm total is the result of thunderstorms sustained over a period of 6 hours or more within a more general precipitation storm. This distinguishes them from the isolated thunderstorm events used for local-storm PMP.

The locations of storms listed in table 2.1 are shown in figure 2.2. San Luis, Mexico lies just south of the study region. Since the exact duration of the San Luis 1-day storm amount (Secretaria de Recursos Hydrolicos 1970) could not be determined, a duration of 24 hours was used.

Two of the 5 values in table 2.1, at Bug Pt., Utah and Dove Ck. 10 SW, Colo., occurred in the September 4-6, 1970 storm. These stations near the edge of an outlined least-orographic region (see fig. 2.1) reported rainfalls of 6.50 inches (165 mm) and 6.00 inches (152 mm), respectively. They are on a high plateau at elevations of 6600 and 6900 feet (2012 and 2103 m) respectively. Analysis of orographic PMP in the following chapter shows that some minimum-orographic effect is necessary over this subregion. Analyses of other notable general storms for the region (i.e. the September 4-7 and 11-13, 1939 and August 28-30, 1951 Arizona storms), disclosed that maximum precipitation for these storms occurred primarily in orographic regions. Total storm amounts were all less than 3 inches (76 mm) at least-orographic stations.

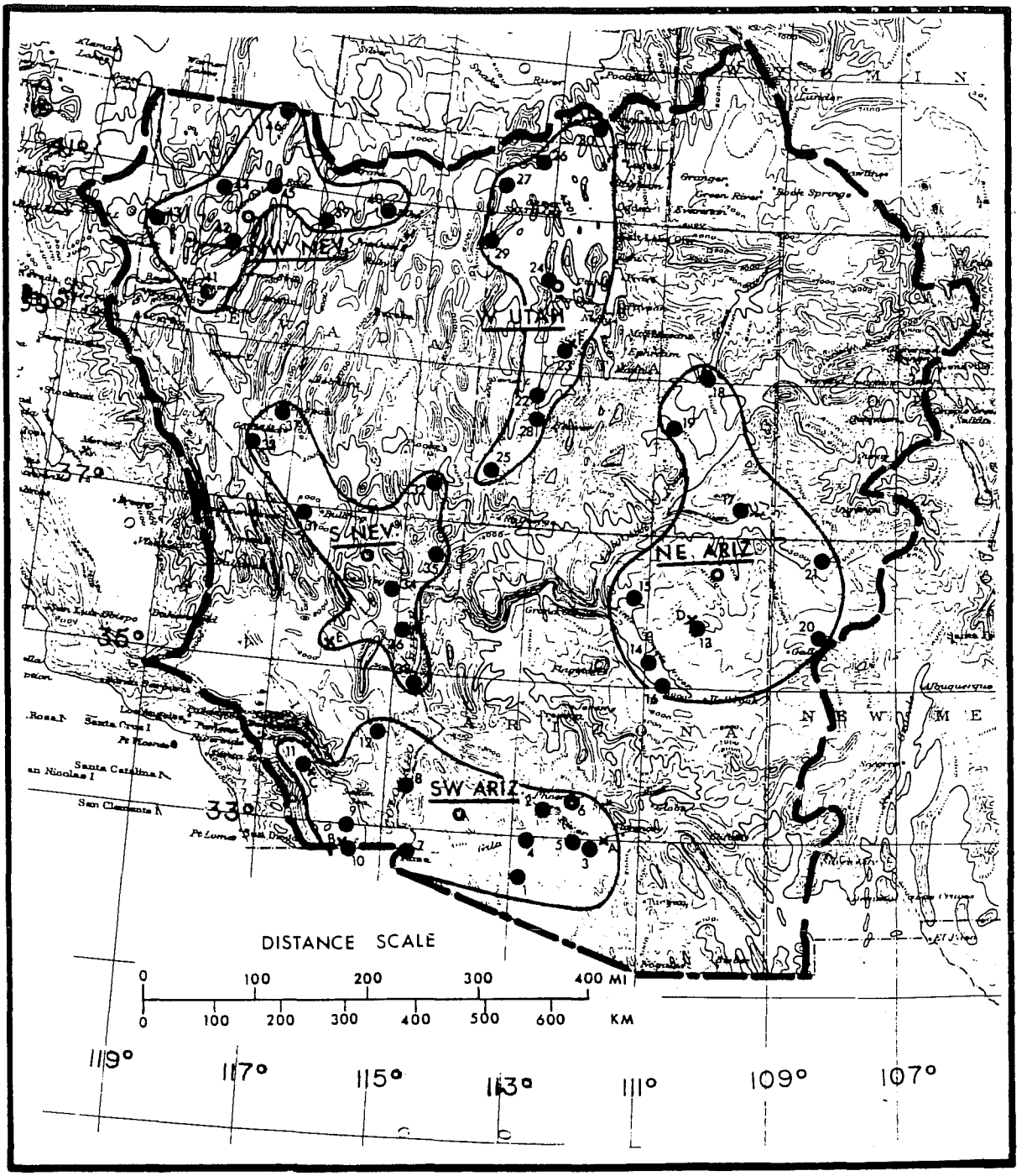

Figure 2.1.--Location of stations used in studies of 1- and 3-day rainfall. Numbered stations listed in table 2.2. Letters by X-stations refer to additional stations listed in table 2.4. Least-orographic regions considered for grouping stations into subregions enclosed by solid lines. Double circles indicate approximate midpoints for each subregion discussed in section 2.2.1.

Table 2.1.--Most extreme general-storm convergence rainfalls

Storm location	Date	Amount in.	Amount (mm)	Duration hr	Elevation ft	Elevation (m)	Elev. Adj.	Dura. Adj.	Moist Adj.	Adj. Storm Amt. in.	Adj. Storm Amt. (mm)
Indio, Calif. (33°43, 116°14)	9-24-39	6.45	(164)	6	20	(6)	100	141	134	12.2	(310)
Casa Grande Ruins, Ariz. (33°00, 111°33)	8-1-06	5.4	(137)	6.5	1400	(427)	113	128	116	9.1	(231)
San Luis, Sonora, Mex. (32°30, 114°48)	11-26-67	7.64	(194)	24*	0	(0)	100	100	120	9.2	(234)
Dove Ck.10SW,Colo. (37°45, 108°55)	9-5-70	6.00$^{\Delta}$	(152)	12	6900	(2103)	208	115	111	15.9	(404)
Bug Pt., Utah (37°38, 109°05)	9-5-70	6.50$^{\Delta}$	(165)	12	6600	(2012)	200	115	111	16.6	(422)
Porter, N. M. (35°13, 103°17)	10-10-30	9.91	(252)	24	4100	(1250)	152	100	148	22.3	(566)

*Duration has not been verified.

$^{\Delta}$Has some orographic contamination.

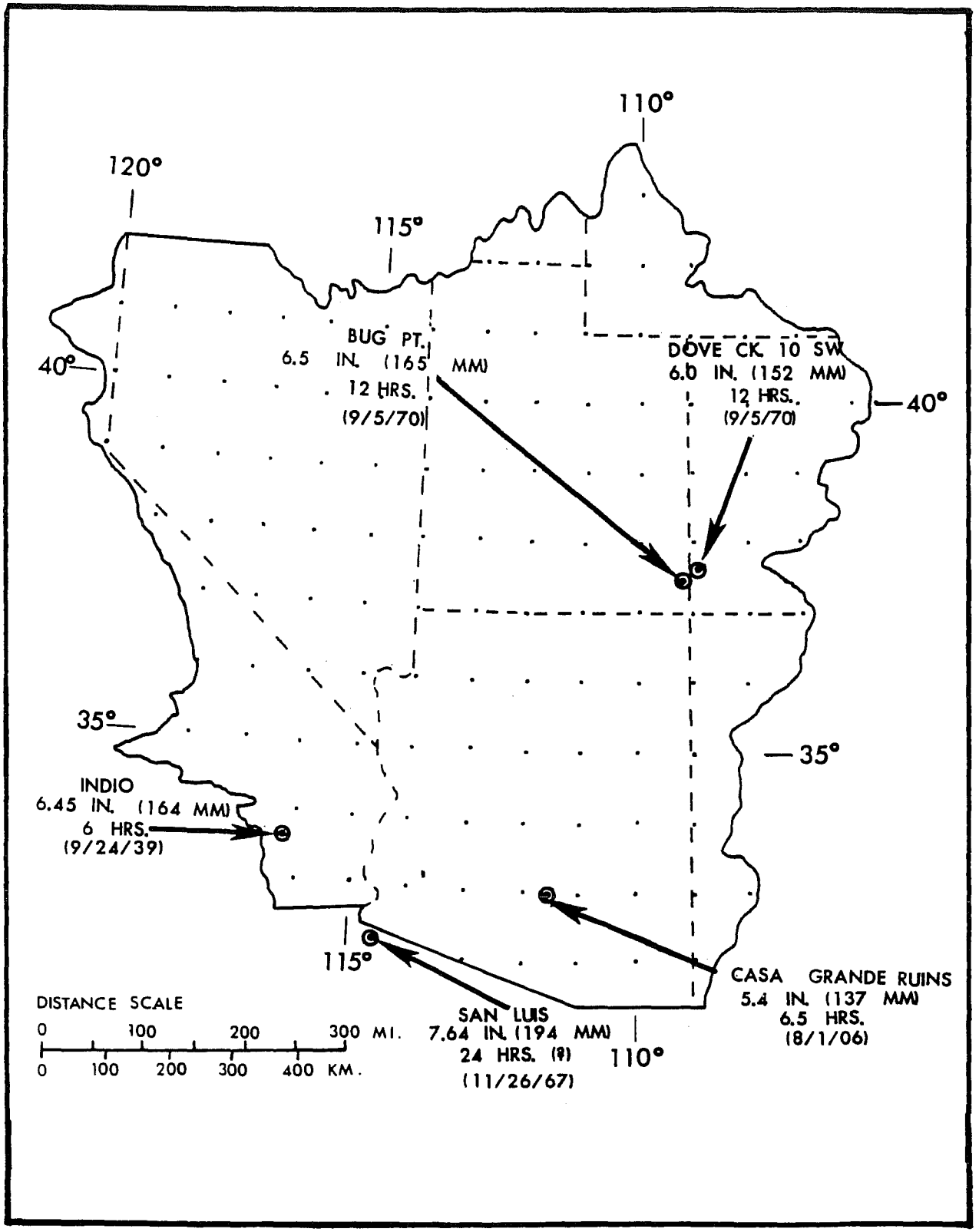

Figure 2.2.--Location of most extreme general-storm convergence rainfalls in the Southwest.

The major nonsummer general storms such as February 3-8, 1937, November 25-28, 1905 and December 14-17, 1908, also indicated less than 3 inch (76 mm) total storm amounts for least-orographic stations. Taken collectively, and excluding the Porter storm, the amounts listed in table 2.1 are the greatest known general-storm convergence point rainfalls for the Southwest.

The storm values were adjusted to a common elevation and duration, and to optimum moisture conditions. The adjustments are as follows:

a. Adjustment for elevation. The events of table 2.1 were adjusted to sea level (assumed 1000 mb, 100 kPa). This adjustment is the ratio of the available precipitable water above 1000 mb (100 kPa) to that available above the surface. Where adjustments were necessary, the precipitable water was determined using the storm 12-hr persisting 1000-mb (100-kPa) dew point and assuming a pseudo-adiabatic saturated atmosphere (U. S. Weather Bureau 1951a).

b. Adjustment for duration. A generalized durational variation determined for convergence PMP was applied to obtain a common duration of 24 hours for all the storms. Reference is made to figures and tables discussed in section 2.4 for the generalized relation. A monthly 6/24-hr ratio was interpolated from the appropriate map (figs. 2.25 to 2.27) at the location of storm rainfall. Entering table 2.7 or figure 2.20 with the 6/24-hr ratio and the duration of the rain amount gives the factor by which the rain amount needs to be adjusted to provide an estimated amount for the 24-hr duration.

c. Adjustment for maximum moisture. One of the steps in estimating PMP is to adjust observed storms to the maximum moisture potential for the storm location and date. Maximum 12-hr persisting 1000-mb (100-kPa) general-storm dew points (Schwarz and Hansen 1978) were used in this adjustment. The adjustment assumes a pseudo-adiabatic lapse rate with a saturated atmosphere and is the ratio of precipitable water for the maximum 1000-mb (100-kPa) dew point to that for the storm dew point at a location representative of the inflow moisture. A further maximization was made by allowing the maximum 12-hr persisting 1000-mb (100-kPa) dew point to be read 15 days toward the seasonal maximum.

2.2.2 Enveloping 12-hr Persisting Dew Points

Enveloping 12-hr persisting dew points have been developed and presented in HMR Nos. 36 and 43 and on a national basis in the Climatic Atlas (Environmental Science Services Administration 1968). The companion volume to the present study (Schwarz and Hansen 1978) updates the data for the Southwest and develops both general- and local-storm 12-hr maximum persisting 1000-mb (100-kPa) dew points.

2.2.3 Regional Patterns

The adjusted storm amounts in the last column of table 2.1 were plotted at their respective locations on a map (not shown). The few data points provided the lowest level of convergence PMP to be considered at these locations but were insufficient to define a regional pattern.

One approach to regional patterns was based on maximum 1-day precipitation for each month in the least-orographic regions in the Southwest. All long-record (>20 years) stations considered least-orographic within each subregion are listed in table 2.2 and are located by numbered dots in figure 2.1. Maximum monthly 1-day rains were obtained from Technical Paper No. 16 (Jennings 1952) and supplemented by recent records through 1970. Averaged maximum values, by month within each subregion, were helpful but not sufficient to define regional patterns, due primarily to the small number of data points. A further step of adjusting the data to a common elevation and for upwind barriers did not help materially.

Additional guidance for regional patterns of 1000-mb (100-kPa) convergence PMP came from analysis of moisture potential. The Climatic Atlas (Environmental Science Services Administration 1968) presents charts of maximum persisting 12-hr 1000-mb (100-kPa) dew points covering the 48 conterminuous states. These charts were used because they portray the broadscale moisture patterns influencing the Southwest. The use of revised moisture charts for the Southwest would not affect the conclusions on moisture patterns based on that Atlas. Figure 2.3 shows examples of schematic charts adapted from the January and August dew point charts from the Atlas. These schematics suggest the source of atmospheric moisture for the region. The solid lines are used to imply moisture from the Gulf of Mexico, while the dashed lines suggest moisture from Pacific Ocean sources. The change in orientation of the dashed lines between January and August reflects a change from mid-latitude storms in winter and spring to moisture surges from tropical latitudes in late summer. The dotted lines represent smoothing in the transition zone between the two moisture sources.

The moisture patterns for each of the months give guidance to the pattern of regional variation but not to magnitude of precipitation. They show that the tropical Pacific moisture source has its greatest influence over the southwest region from May through October.

The Gulf of Mexico is recognized by many researchers as a source for much of the day-to-day precipitation over the Southwest. However, such rainfall occurrences are not representative of conditions for extreme precipitation (Hansen 1975a, 1975b). Precipitation climatology studies of the Southwest by Schwarz and Hansen (1978) supports this interpretation.

2.2.4 Seasonal Variation

Clues to regional patterns of 1000-mb (100-kPa) convergence PMP for each month can also be obtained from analyses of seasonal trends in precipitation data at various locations. Therefore, the seasonal variations of the maximum 1-day precipitation for the stations in least-orographic subregions shown in figure 2.1 and listed in table 2.2 were analyzed. Seasonal charts, figures 2.4a to 2.4e, show monthly averages within each subregion by open circles, along with an eye-smoothed curve (short dashes).

In figure 2.4a to 2.4e the regionally averaged 1-day maximum precipitation curves have a summertime maximum in all five regions except northwest Nevada, which shows a summer minimum and bimodal winter and late spring maximum.

Table 2.2.--Stations within least-orographic regions for which daily precipitation was available for 20 years or more before 1970.

Station	Years of rec. thru 1970	Latitude	Longitude	Elevation ft.	(m)
Southwest Arizona					
*1. Ajo, Ariz.	66	32°22	112°52	1763	(537)
2. Buckeye, Ariz.	70	33°22	112°35	888	(271)
3. Casa Grande, Ariz.	63	32°53	111°45	1390	(424)
4. Gila Bend, Ariz.	70	32°57	112°43	737	(225)
5. Maricopa, Ariz.	59	32°57	112°00	1242	(379)
6. Phoenix, Ariz	72	33°28	112°04	1083	(330)
7. Yuma, Ariz	100	32°44	114°36	138	(42)
8. Blythe, Calif.	58	33°37	114°36	268	(82)
9. Brawley, Calif.	58	32°59	115°32	-119	(- 36)
10. Calexico, Calif.	47	32°40	115°30	3	(1)
11. Indio, Calif.	71	33°43	116°14	20	(6)
12. Iron Mt., Calif.#	22	34°08	115°08	922	(281)
Northeast Arizona					
13. Jeddito, Ariz.	35	35°46	110°08	6700	(2042)
14. Leupp, Ariz.	22	35°17	110°58	4700	(1433)
15. Tuba City, Ariz.	46	36°08	111°15	4936	(1504)
16. Winslow, Ariz.	55	35°01	110°44	4880	(1487)
17. Bluff, Utah	59	37°17	109°33	4320	(1317)
18. Green River, Utah	64	39°00	110°09	4087	(1246)
19. Hanksville, Utah	45	38°25	110°41	4456	(1358)
20. Crownpoint, N.Mex	63	35°40	108°13	6978	(2127)
21. Farmington, N. Mex.	64	36°43	108°12	5300	(1615)
Western Utah					
22. Black Rock, Utah	48	38°45	113°02	4860	(1481)
23. Deseret, Utah	77	39°18	112°38	4541	(1384)
24. Dugway, Utah#	20	40°10	113°00	4359	(1329)
25. Enterprise B.Jct., Utah#	30	37°43	113°39	5220	(1591)
26. Kelton, Utah	52	41°45	113°08	4225	(1288)
27. Lucin, Utah	45	41°22	113°50	4413	(1345)
28. Milford, Utah	49	38°25	113°01	5029	(1533)
29. Wendover, Utah	66	40°44	114°02	4239	(1292)
30. Malad, Idaho	57	42°11	112°16	4420	(1347)
Southern Nevada					
31. Beatty, Nev.	34	36°54	116°45	3314	(1010)
32. Caliente, Nev.	29	37°37	114°31	4402	(1342)
33. Goldfield, Nev.	45	37°43	117°13	5700	(1737)
34. Las Vegas, Nev.	47	36°10	115°09	2006	(611)
35. Logandale, Nev.	30	36°35	114°25	1400	(427)
36. Searchlight, Nev.	35	35°28	114°55	3540	(1079)
37. Tonopah, Nev.	44	38°04	117°14	6101	(1860)
38. Needles, Calif.	22	34°46	114°38	913	(278)
Northwest Nevada					
39. Battle Mt., Nev.	81	40°37	116°52	4528	(1380)
40. Elko, Nev.	109	40°50	115°47	5075	(1547)
41. Fallon Exp. Sta., Nev.	73	39°27	118°47	3965	(1209)
42. Lovelock, Nev.	73	40°12	118°28	3977	(1212)
43. Sand Pass, Nev.	49	40°19	119°48	3900	(1189)
44. Sulphur, Nev.	34	40°54	118°40	4044	(1233)
45. Winnemucca, Nev.	82	40°54	117°48	4314	(1316)
46. McDermitt, Nev.#	20	42°00	117°43	4427	(1349)

*Location identification number in figure 2.1.

[Station information from Technical Paper No. 16 (Jennings 1952) except when noted by # from hourly precipitation records.]

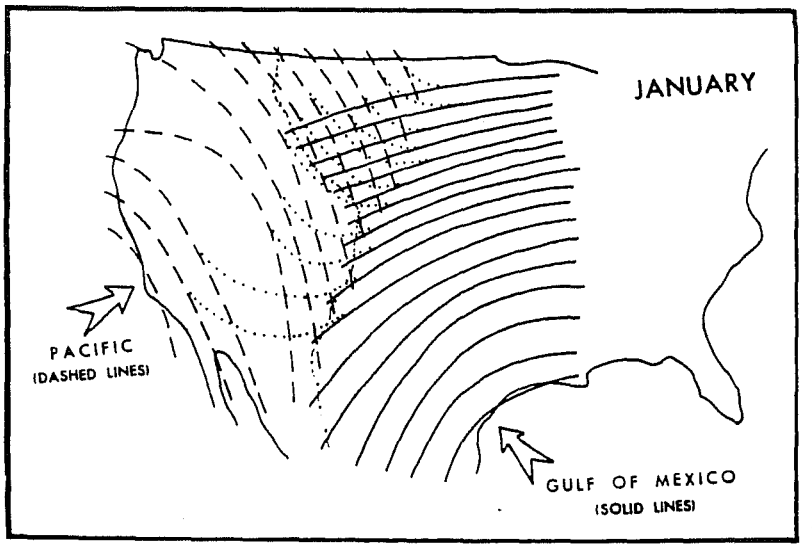

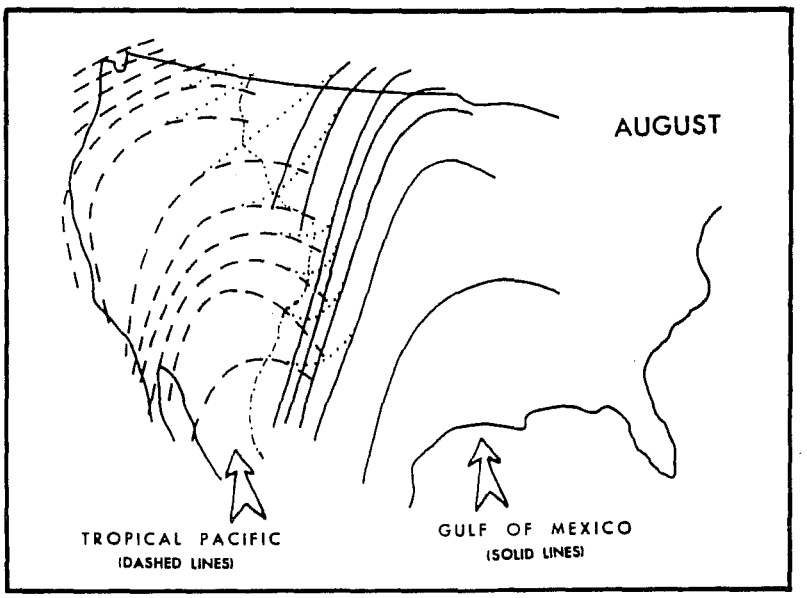

LEGEND

·—·—·—· **CONTINENTAL DIVIDE**

····· **TRANSITION LINES**

Figure 2.3.--Examples of schematic diagrams depicting moisture sources (arrows) implied by gradients of 12-hr persisting 1000-mb (100-kPa) dew points, January and August.

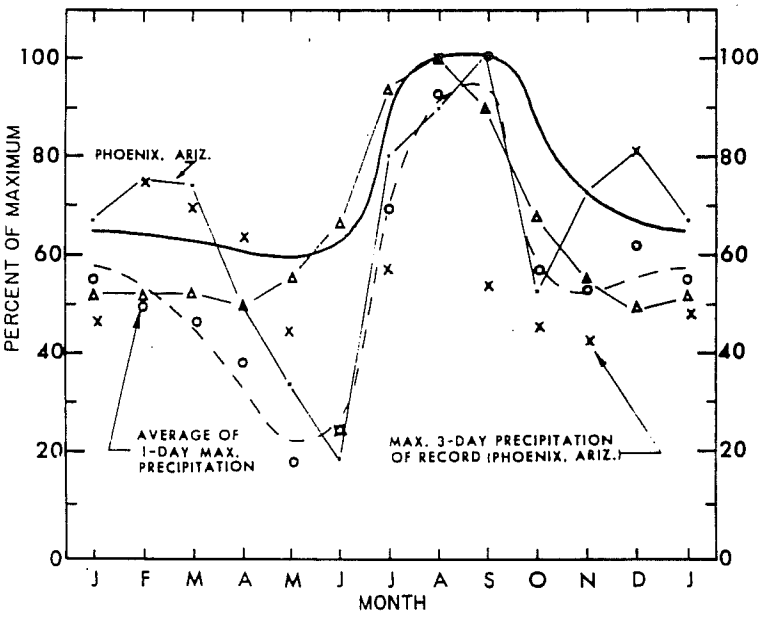

a. Southwest Arizona

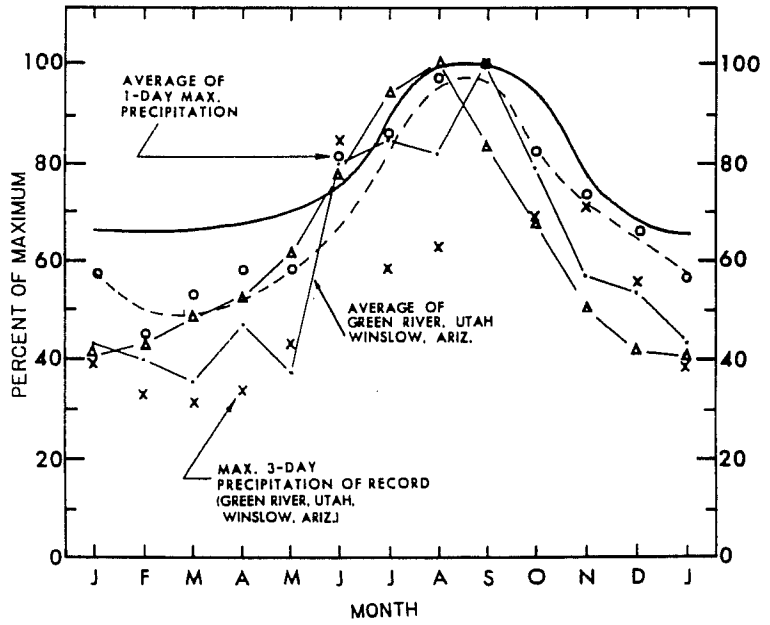

b. Northeast Arizona

△——△—— Maximum precipitable water at subregion midpoint
– – – – – "Eye" smoothed 1-day station average (stations listed in table 2.2)
·——·—— 0.02 probability level of 3-day maximum rains
———— 1000-mb (100-kPa) convergence PMP at subregion midpoint taken from analyses in figures 2.5 to 2.16

Figure 2.4.--Seasonal variation of convergence PMP and supporting data for least-orographic subregions. All values given in percent of the maximum monthly value for that parameter.

c. Western Utah

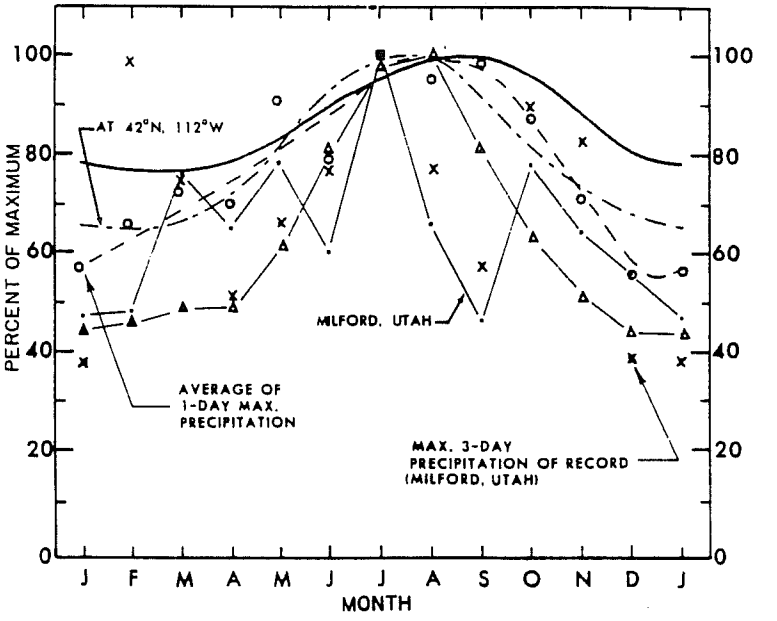

d. Southern Nevada

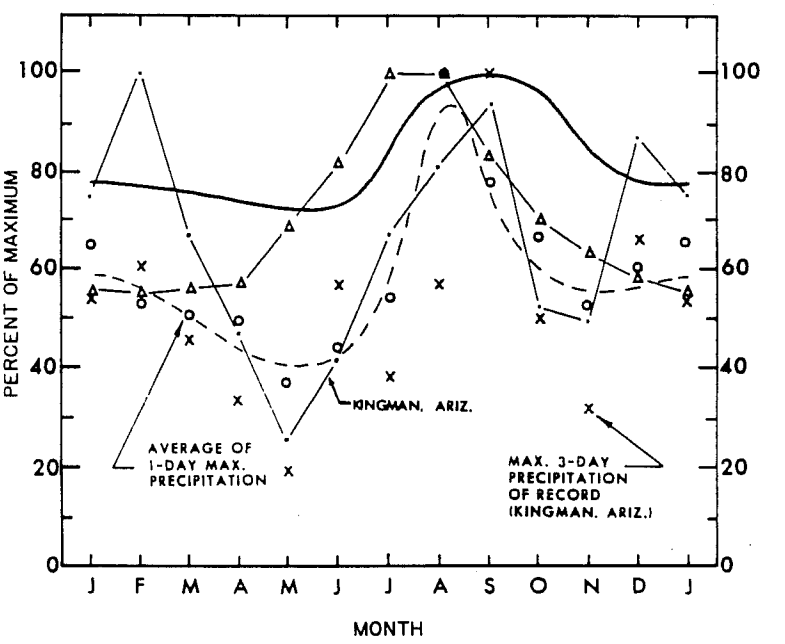

— — — — Convergence PMP (HMR No. 43)
—▲— Maximum precipitable water at subregion midpoint
- - - - - "Eye" smoothed 1-day station average (stations listed in table 2.2)
•—•— 0.02 probability level of 3-day maximum rains
——— 1000-mb (100-kPa) convergence PMP at subregion midpoint taken from analyses in figures 2.5 to 2.16

Figure 2.4.--Seasonal variation of convergence PMP and supporting data for least-orographic subregions. All values given in percent of the maximum monthly value for that parameter.

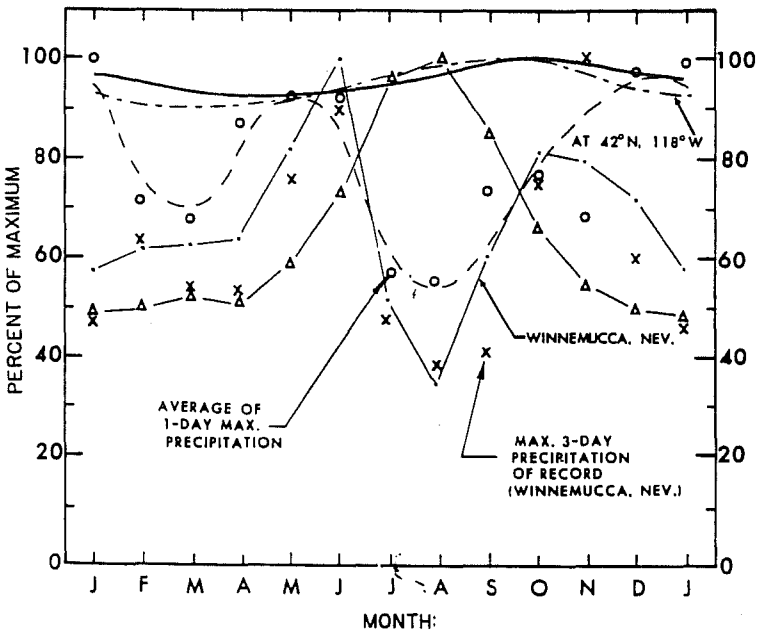

e. Northwest Nevada

– – – – Convergence PMP (HMR No. 43)
Δ—Δ— Maximum precipitable water at subregion midpoint
– – – – – "Eye" smoothed 1-day station average (stations listed in table 2.2)
·—·— 0.02 probability level of 3-day maximum rains
———— 1000-mb (100-kPa) convergence PMP at subregion midpoint taken from analyses in figures 2.5 to 2.16

Figure 2.4.--Seasonal variation of convergence PMP and supporting data for least-orographic subregions. All values given in percent of the maximum monthly value for that parameter.

Southwest Arizona and southern Nevada show spring minimums while northeast Arizona has a late winter minimum and western Utah has a winter minimum. The 1-day maximum values from June to November very likely are influenced by local-storm rainfalls.

Another rainfall statistic considered was maximum 3 consecutive observation day precipitation. These data reduce some of the bias due to thunderstorm rainfall, particularly in summer when short-duration thunderstorms predominate. In addition to the maximum for each month, the 0.02 probability level of maximum 3 consecutive observation-day precipitation was computed for stations in each subregion. This is shown on figures 2.4a to 2.4e by dot-dashed lines. The 0.02 probability level was computed using the Fisher-Tippett type I distribution fitted by the method of Gumbel from the series of maximum monthly values for each year from approximately 50 years of record (1912-61) for one station within each subregion. Kingman, Ariz., while somewhat beyond the regional limits, was used for the southern Nevada subregion.

In figures 2.4a to e, the seasonal trends in the 1- and 3-day data are comparable with some exceptions, most notably between October and February in northwest Nevada (fig. 2.4e) in which the trends appear opposed. Some rather large differences occur for specific months as in September in figures 2.4a, c, d, and e, and February in figures 2.4a and c. All five figures show the seasonal tendency of the 0.02 probability values to generally follow the trends in the 1- and 3-day data. A large exception for one month appears in the 0.02 probability peak in February in figure 2.4d.

In additon to the maximum rainfall data, an index to moisture potential was considered for additional input to the seasonal variation problem. Potential moisture in the form of precipitable water associated with the maximum 12-hr persisting dew points was determined. The dew points were read from the analyses developed for the Southwest general storms (Schwarz and Hansen 1978) at mid-points of each subregion. These data have been entered on figures 2.4a to 2.4e in percent of maximum precipitable water amount (dash triangle curve). All five subregions show late summer maxima (July or August) with broad minimums through the winter months, extending into spring.

Figures 2.4c and 2.4e, also show seasonal curves of 24-hr 1000-mb (100-kPa) convergence PMP (alternate long-short dashes) taken from HMR No. 43 at the southern edge of the region of that report. Although HMR No. 43 covers only the months of October to June, the data were extended through the remaining months by simple extension of smoothed curves. Table 2.3 gives the smoothed values considered at these two locations.

Table 2.3.--Seasonal variations of 1000-mb (100-kPa) convergence PMP for 24 hrs, from HMR No. 43 (U. S. Weather Bureau 1966a).

Location		Jan	Feb	Mar	Apr	May	Jun	July	Aug	Sept	Oct	Nov	Dec
42°N 118°W	in.	8.60	8.45	8.37	8.46	8.50	8.70	(8.93)	(9.18)	(9.30)	9.20	9.00	8.75
(Northwest Nevada)	mm	218	215	213	215	216	221	(227)	(233)	(236)	234	229	222
42°N 112°W	in.	8.30	8.15	8.40	9.25	10.30	11.80	(12.72)	(12.80)	(11.70)	10.50	9.28	8.55
(Northern Utah)	mm	211	207	213	235	262	300	(323)	(325)	(297)	267	236	217

Values in parentheses estimated from interpolation, based on smooth seasonal distribution.

2.2.5 PMP Storm Prototypes

Another consideration before we can develop mid-month convergence PMP maps is to determine what type(s) of storm(s) is (are) likely to produce general-storm PMP in the Southwest, and the seasonal and regional variations of the general storm.

An extensive review of the meteorology of Southwestern storms is presented, with examples, in the companion volume (Schwarz and Hansen 1978). Nevertheless, brief comments are included here to establish the trend in storms that are considered representative of producing rainfall of PMP magnitude.

Through most of the Southwest, the decadent tropical cyclone is considered the PMP prototype for the period from the end of June to mid-October. Examples of record are the storms of September 1939, August 1951, and September 1970. In the southern portion of the region during the cool season, fronts and storm centers from the Pacific Ocean produce major rains. Slow-moving to stagnant frontal situations, as in December 1955 and January 1916, are examples.

The summer tropical cyclone is not likely to penetrate into the northwest or extreme northeast corners of the study area. For all-season PMP in the northwest portion, storms with more westerly moisture flows can enter the region around the north end of the Sierra Nevada range. This has led to the conclusion that northwest Nevada would have a seasonal influence more closely allied to northern California, where the October 1962 storm produced extreme rains.

The northeast corner, particularly north of the Uinta Mountains and east of the Wasatch Mountains, can be influenced by moisture flows from the east that have spilled around the northern end of the Rocky Mountains in Colorado. Although no prototype storm for this northeast corner has yet been observed, the June 1964 storm that struck the Montana Rockies is an example of the type of storm that could affect this portion of the Southwest. Thus, seasonally, the northeast corner is similar to the eastern boundary region in HMR No. 43.

Exact boundaries for the zone of influence of each type of storm have not been delineated. Rather, their influence has been incorporated in part by adjustments in the barrier elevation chart (see section 2.3) to account for the expected flows, and in part by the seasonal variations built into the convergence PMP analyses through tie-ins to peripheral studies. To understand the result and effectiveness of these methods, see the discussion in chapter 5 on checks on PMP level.

2.2.6 Development of 10-mi^2 (26-km^2) 24-hr Convergence PMP

In the development of seasonal maps of convergence PMP a number of considerations were used as guidance. Not necessarily in the order of importance, These were to:

a. Envelop all maximized values of observed rainfall in least-orographic areas without explicit transposition.

b. Recognize trends in seasonal variations established by data from least-orographic stations.

c. Recognize the potential summertime maximum precipitation represented by the seasonal variation of maximum precipitable water.

d. Fit a pattern that is in accord with tracks of extreme rain-producing storms.

e. Observe regional variations caused by influences of different prototype storms.

This formed the nucleus of the scheme for developing Southwest convergence PMP. Since the Northwest PMP report presented monthly maps of convergence PMP (except July to September), these were selected as the point of beginning. The California PMP report does not provide a seasonally variable pattern of convergence PMP although values are given for October through April. Therefore, some discontinuity existed between the Northwest and the California results. Most important was the fact that the patterns of gradients between the two studies were compatible.

The procedure began by simply extending the gradient patterns of 1000-mb (100-kPa) convergence PMP from the Northwest into the Southwest. The maximized value at Indio (table 2.1) gives the limiting magnitude for the month of September at that location. The eye-smoothed 1-day data curve of figure 2.4a was used to get an initial seasonal variation of magnitude at Indio taking the September value as 100%. It was obvious that the deep minimum in spring of this seasonal curve was not in agreement with a consistent pattern of extended gradients from HMR No. 43. The Indio seasonal curve was modified by increasing the spring values to be more in line with the broad winter-spring minimum shown by the moisture curve in figure 2.4a.

From this beginning the next consideration was how to treat the west slopes of the Rocky Mountains. East of the 105th meridian HMR No. 51 (Schreiner and Riedel 1978) shows a tight gradient of PMP having a NE-SW orientation of isohyets of PMP. Because the general level of convergence PMP for the Southwest is much less than that shown by HMR No. 51, it is necessary to create a tight gradient somewhere between these two regions. PMP for the mountainous region between the Continental Divide and 105th meridian has yet to be studied in detail. We assume that much of the decrease in magnitude of PMP from HMR No. 51 will be concentrated near the Divide. Therefore, a tighter gradient was maintained along the west slopes of the Rockies than over most of the remainder of the Southwestern Region.

Considerations c, d, and e were particularly involved with interpretation of the pattern of PMP gradients during the period of summer maximum precipitation, expected to come from a decadent tropical cyclone. The influence of this PMP prototype storm through much of the region is especially important in the southern portion of the region, closest to the source of moisture, and extends from July to September. This causes the isohyets to become aligned more east-west at lower latitudes. An assumption of equal likelihood of the summer prototype general storm between July and early October is supported by monthly distributions of eastern Pacific tropical cyclones (Rosendal 1962, Serra 1971, Baum 1974). Thus a rather broad seasonal maximum in convergence PMP results through the southern portion of the Southwest.

With these considerations in mind, a preliminary set of monthly PMP maps was constructed tying magnitudes and gradients along the north to HMR No. 43, along the west to HMR No. 36, and using the Indio maximized value as a control on the magnitude in the southwest section. Pattern and magnitude in the eastern sections were controlled to a lesser extent by HMR No. 51.

Seasonal values of convergence PMP were read for mid-points of the five least-orographic subregions from these preliminary maps and compared to the 1-day, 3-day, and moisture curves shown in figures 2.4a to 2.4e. Smoothing and adjusting of the set of preliminary maps resulted in a consistent series of seasonal curves and maps.

The finalized set of 1000-mb (100-kPa) 10-mi^2 (26-km^2) 24-hr convergence PMP maps is presented in figures 2.5 to 2.16. Whereas, the initial maps began as extensions of the isohyets in HMR No. 43, the final maps after smoothing no longer maintain the direct association. For some individual months differences in magnitude of up to 1 inch exist at some border locations. The greatest differences in pattern between these two studies occur in April and November, both considered transition months in terms of synoptic storm influences.

Final mid-month convergence PMP values were read from figures 2.5 to 2.16 for the least-orographic regions and seasonal curves for these points plotted in terms of percent of the greatest of the 12 values in figures 2.4a to 2.4e (heavy solid lines) for comparison with the data. In figure 2.4a, convergence PMP preserves the summer maximum and broadens the peak, as intended, to include the summer prototype storm over the longer period. A similar remark can be made about the convergence PMP curve in figure 2.4b.

In western Utah, figure 2.4c, the convergence PMP curve peaks in September. This is a month later than the eye-smoothed 1-day rainfall curve and the curve from HMR No. 43. The PMP maximum in September results from extension beyond the data to consider the influence of late summer tropical cyclones.

The peak in convergence PMP in figure 2.4d (Southern Nevada) is noticeably later than the moisture curve and somewhat later than the 1-day data, being broadly centered about the 3-day maximum in September.

In figure 2.4e (northwest Nevada), the convergence PMP curve has a small amplitude with a broad maximum centered on October. The October maximum is in agreement with the fall prototype storm with westerly inflow in northern California.

The resulting 1000-mb (100-kPa) convergence PMP maps of figures 2.5 to 2.16 describe a set that is generally consistent with considerations listed at the beginning of this section. With the exception of western Utah and northwest Nevada the patterns show prominent summer maxima similar to maximum moisture, but tend to show much less variation from summer to winter than do the moisture curves in all five regions. The seasonal variation of the convergence PMP should be less than the variation of moisture alone since the greater efficiency of storms in the cooler season compensates to some extent for less available moisture.

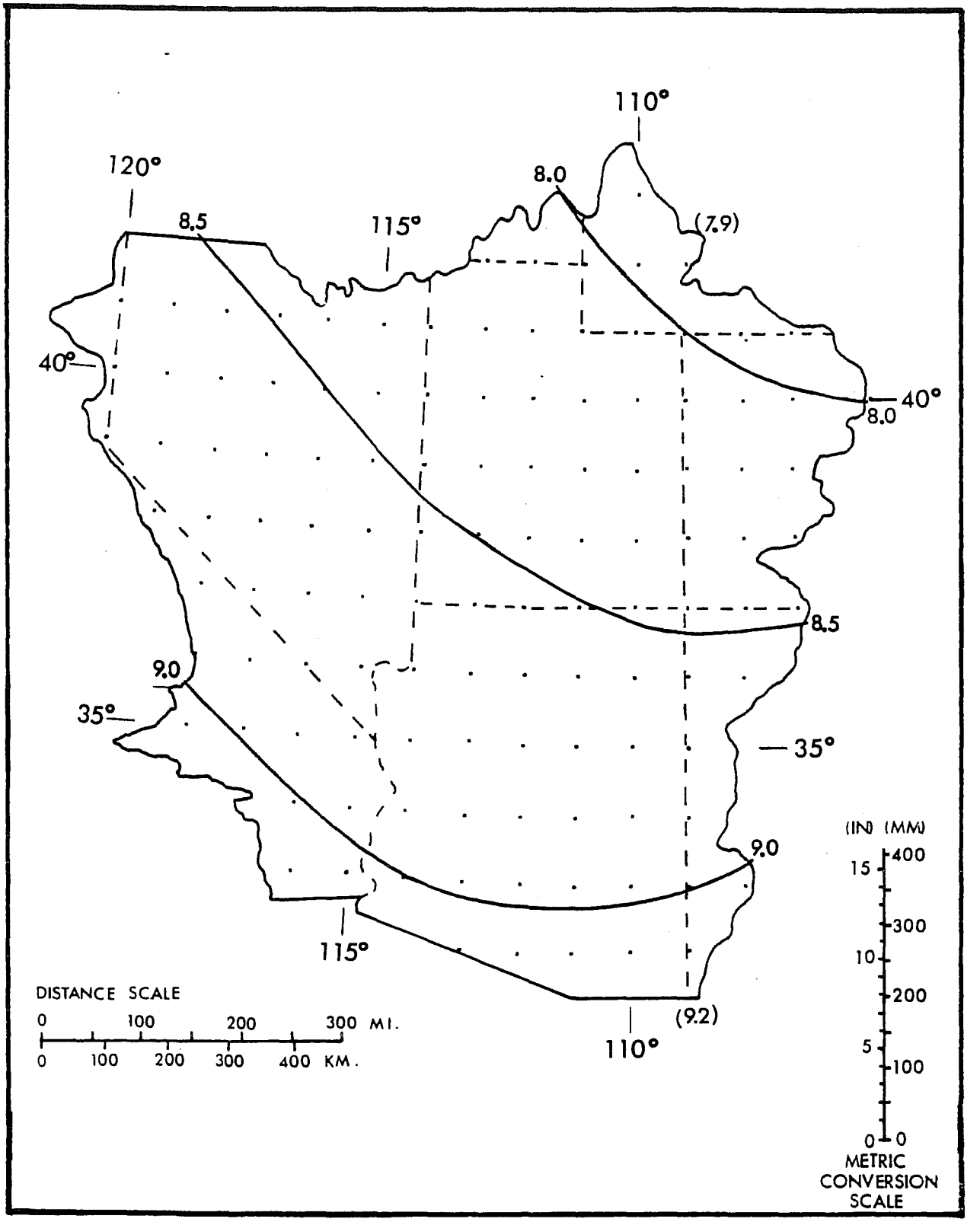

Figure 2.5.--1000-mb (100-kPa) 24-hr convergence PMP (inches) for 10 mi^2 (26 km^2) for January. Values in parentheses are limiting values and are to facilitate extrapolation beyond the indicated gradient.

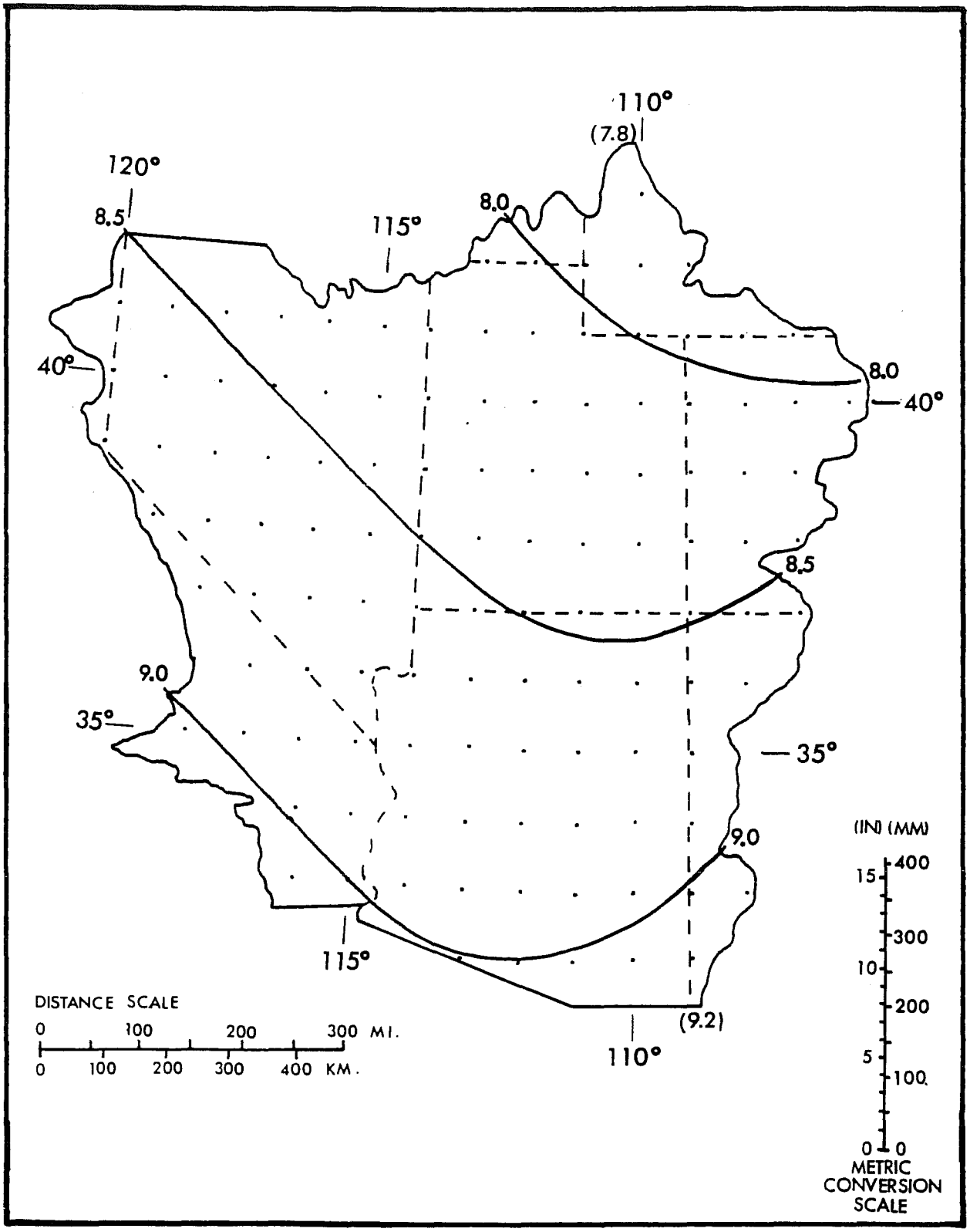

Figure 2.6.--1000-mb (100-kPa) 24-hr convergence PMP (inches) for 10 mi^2 (26 km^2) for February. Values in parentheses are limiting values and are to facilitate extrapolation beyond the indicated gradient.

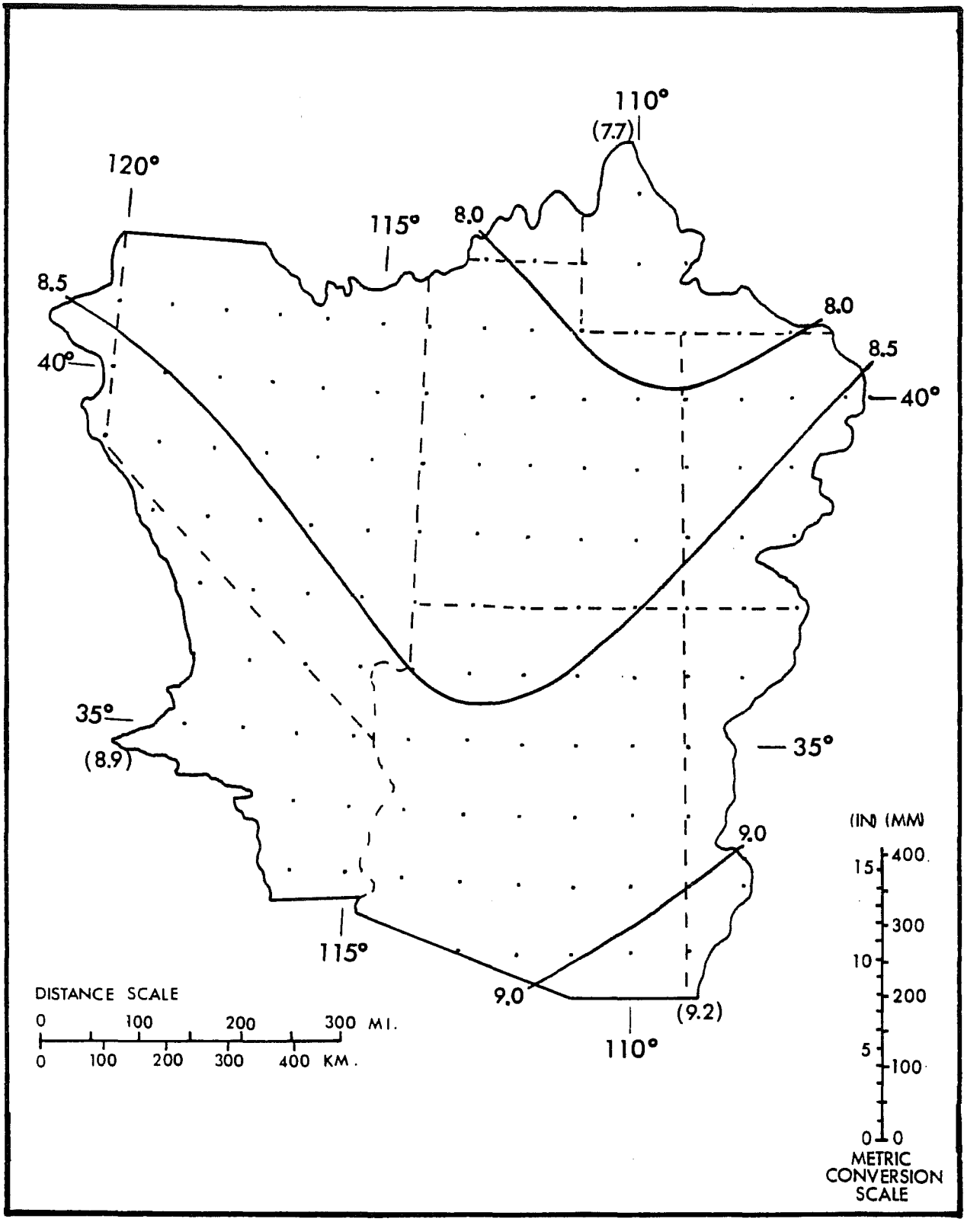

Figure 2.7.--1000-mb (100-kPa) 24-hr convergence PMP (inches) for 10 mi^2 (26 km^2) for March. Values in parentheses are limiting values and are to facilitate extrapolation beyond the indicated gradient.

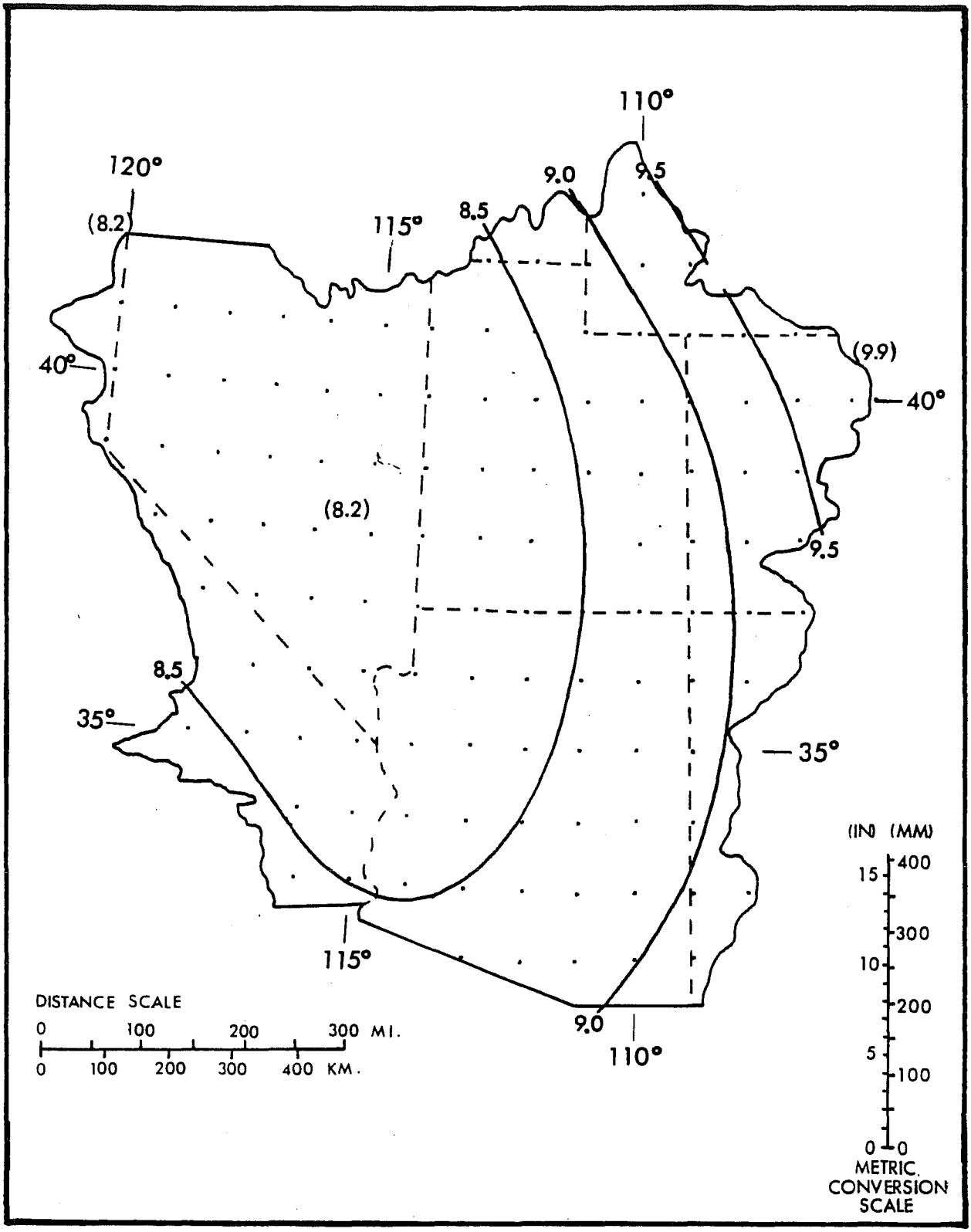

Figure 2.8.--1000-mb (100-kPa) 24-hr convergence PMP (inches) for 10 mi^2 (26 km^2) for April. Values in parentheses are limiting values and are to facilitate extrapolation beyond the indicated gradient.

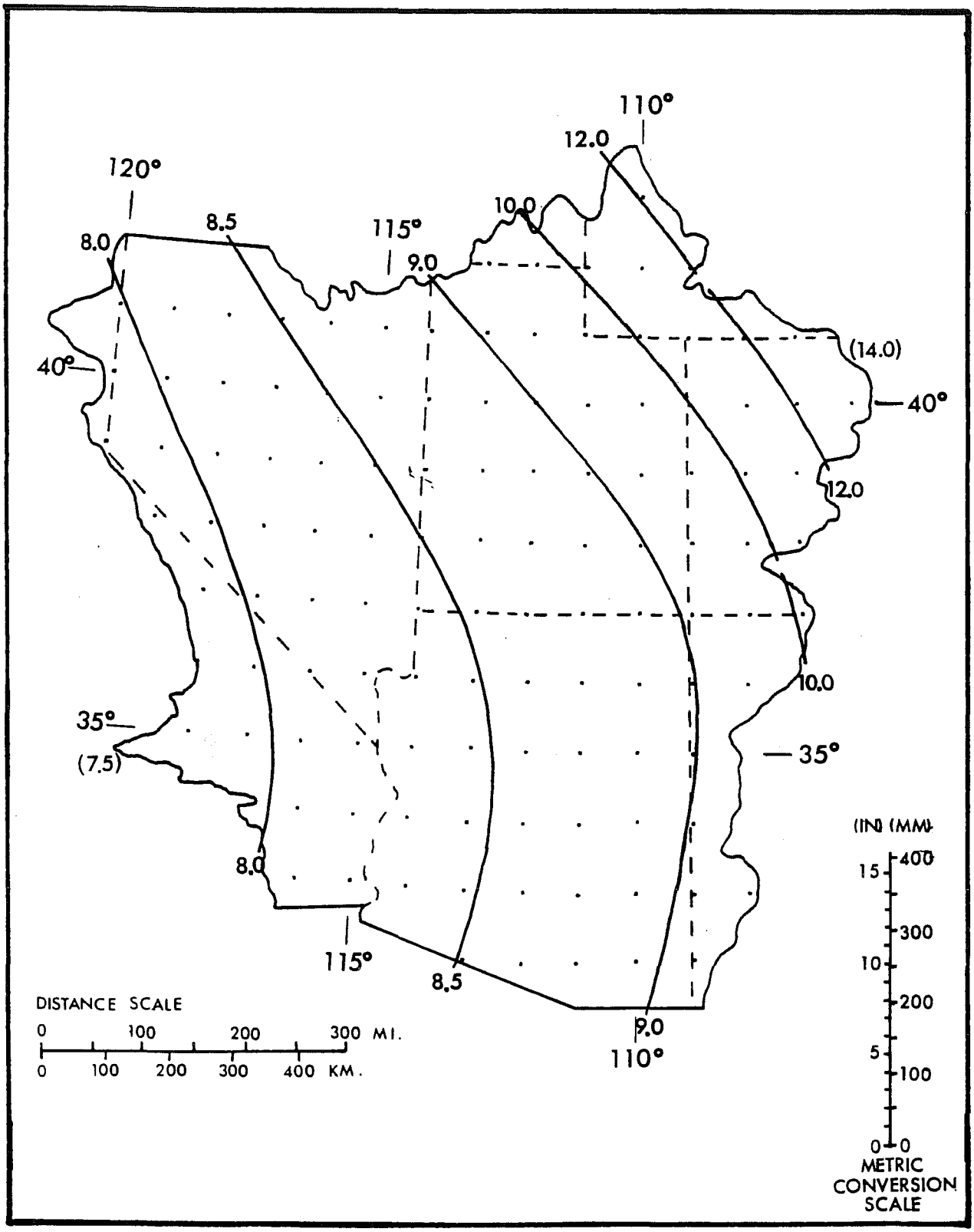

Figure 2.9.--1000-mb (100-kPa) 24-hr convergence PMP (inches) for 10 mi^2 (26 km^2) for May. Values in parentheses are limiting values and are to facilitate extrapolation beyond the indicated gradient.

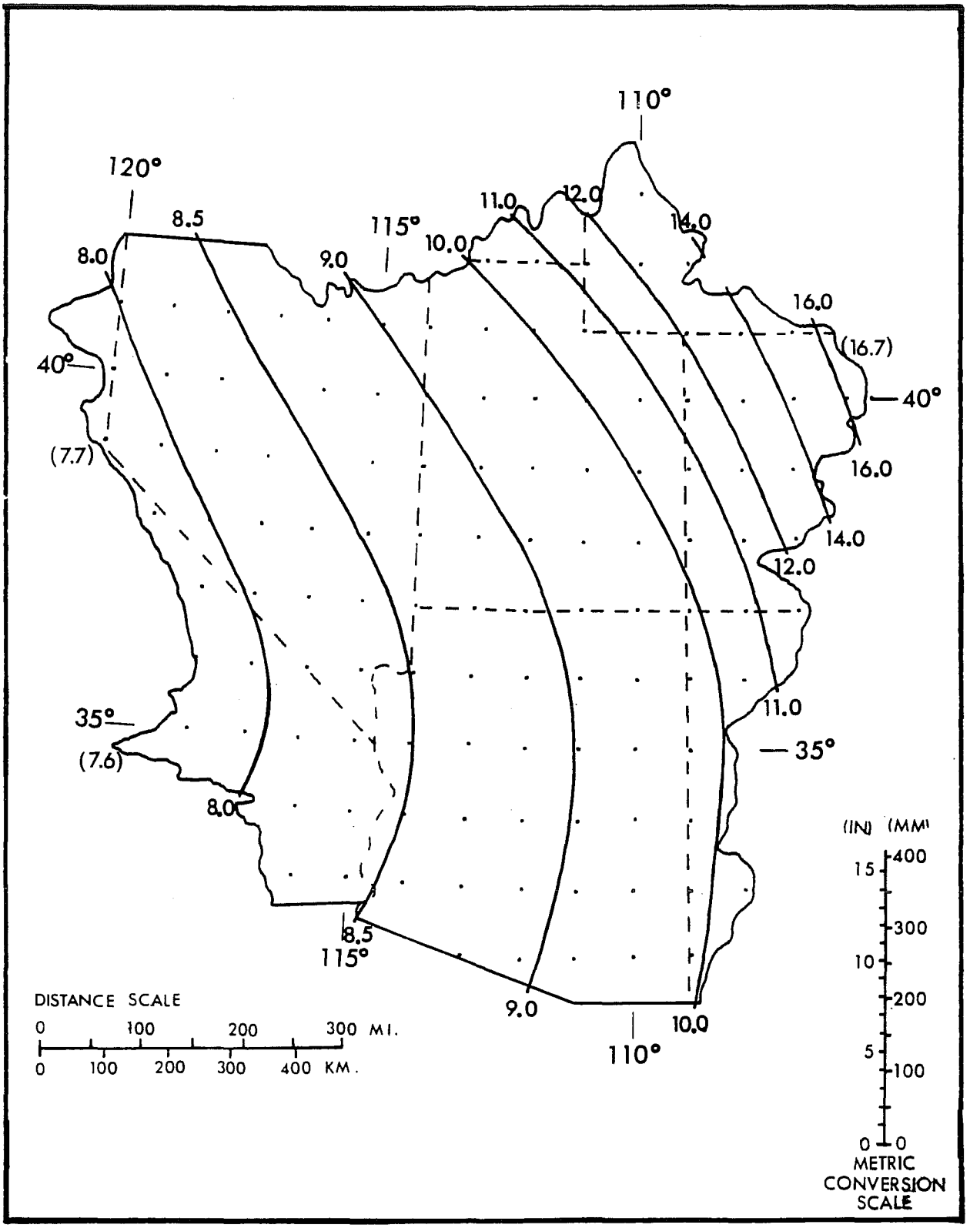

Figure 2.10.--1000-mb (100-kPa) 24-hr convergence PMP (inches) for 10 mi^2 (26 km^2) for June. Values in parentheses are limiting values and are to facilitate extrapolation beyond the indicated gradient.

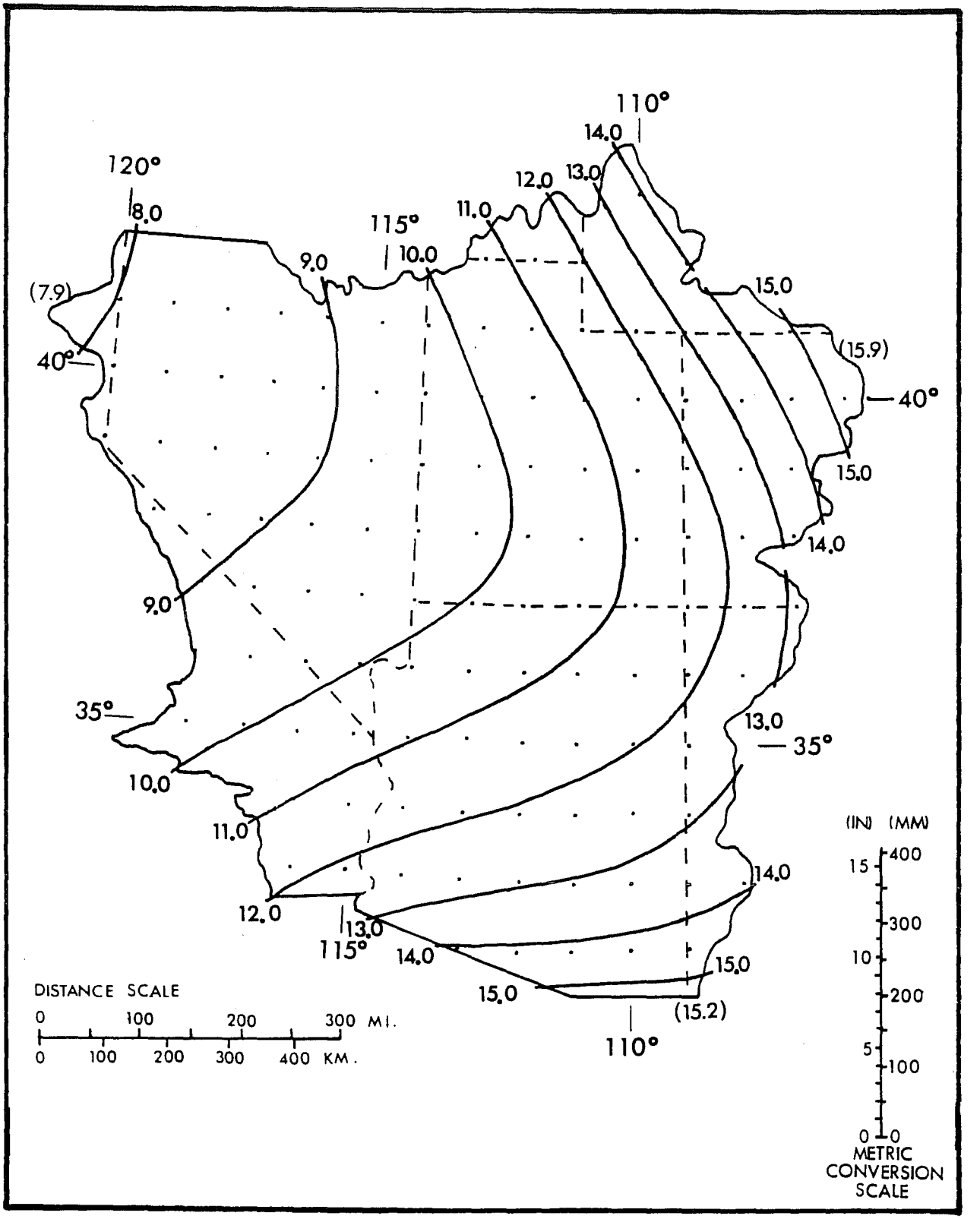

Figure 2.11.--1000-mb (100-kPa) 24-hr convergence PMP (inches) for 10 mi² (26 km²) for July. Values in parentheses are limiting values and are to facilitate extrapolation beyond the indicated gradient.

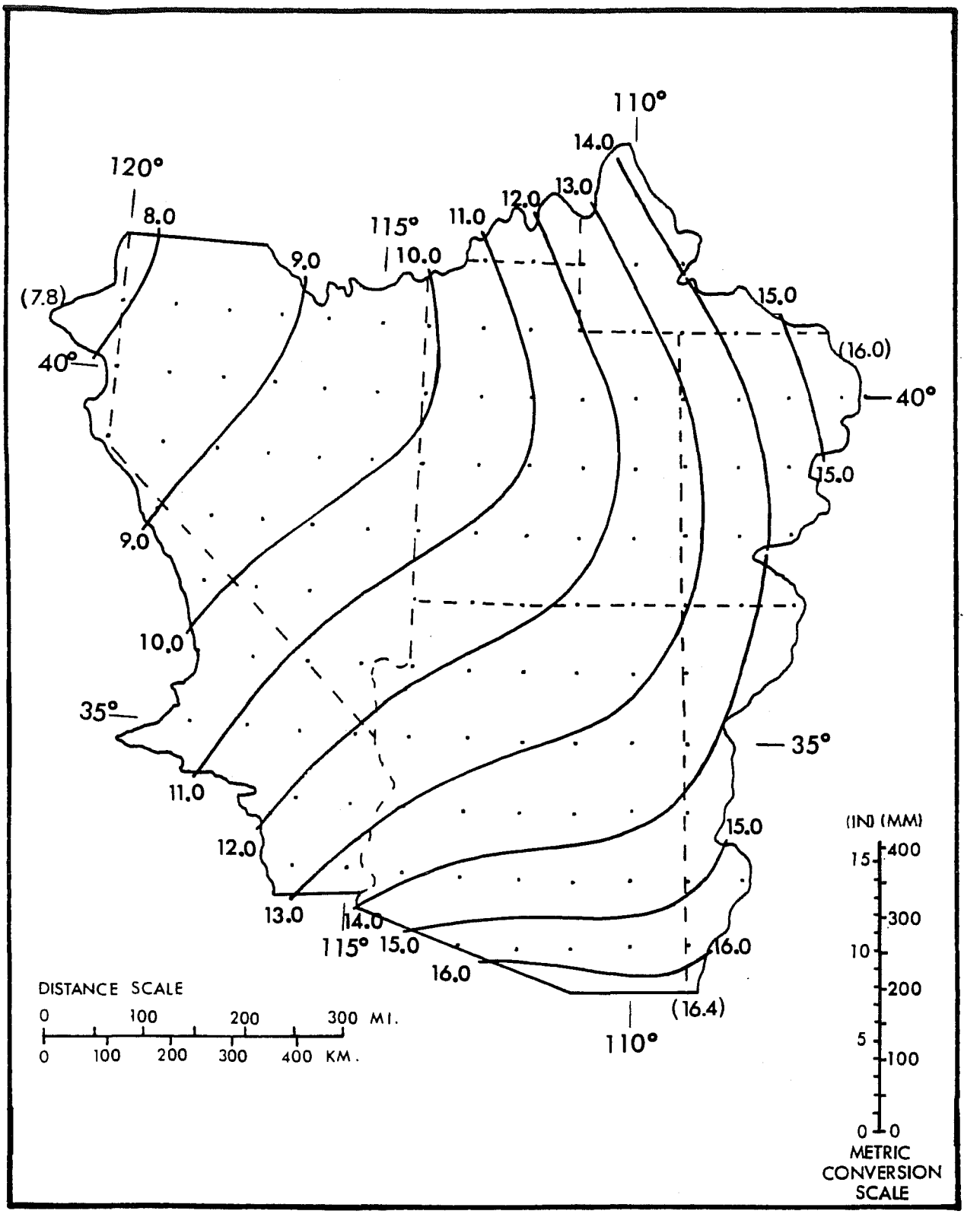

Figure 2.12.--1000-mb (100-kPa) 24-hr convergence PMP (inches) for 10 mi^2 (26 km^2) for August. Values in parentheses are limiting values and are to facilitate extrapolation beyond the indicated gradient.

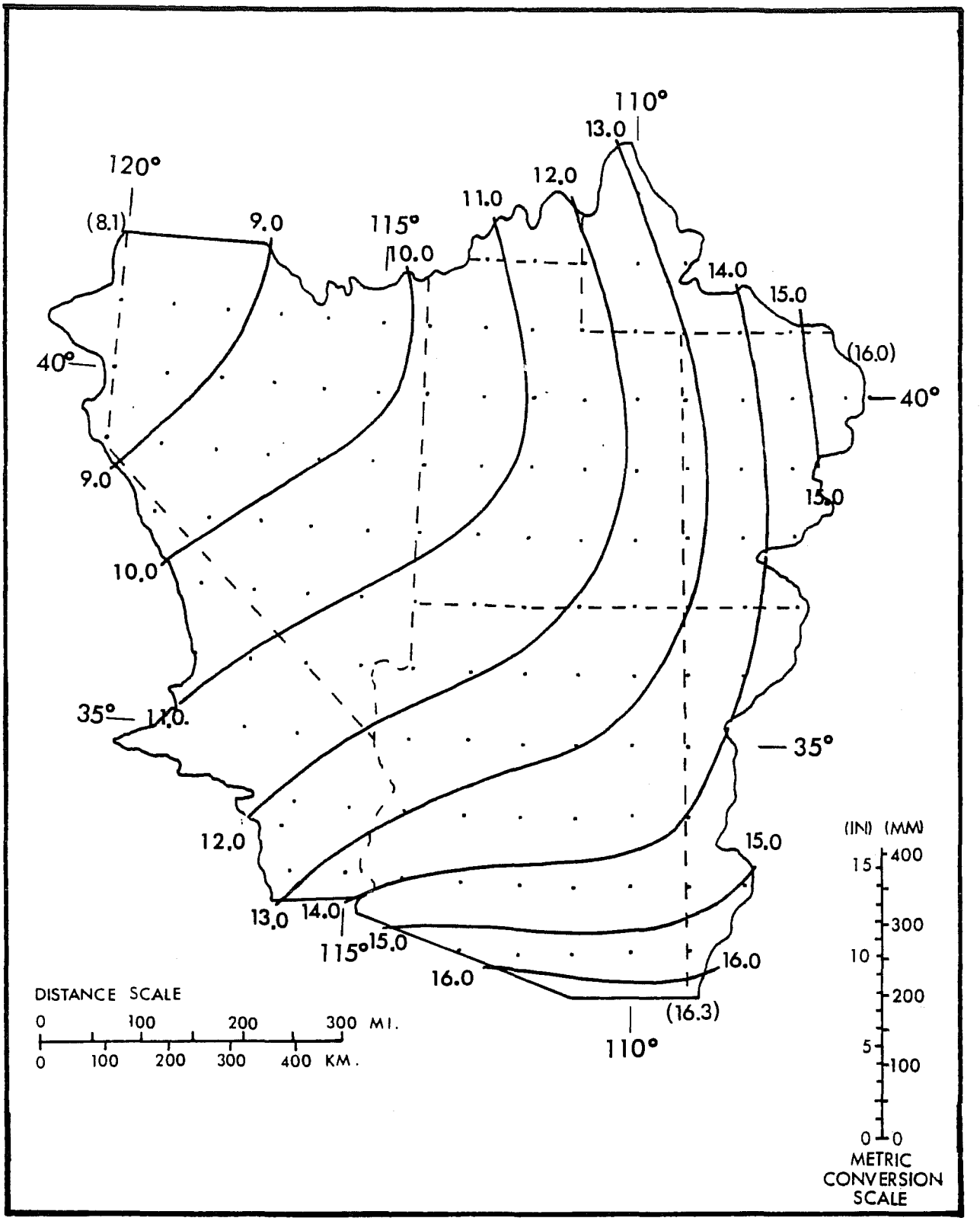

Figure 2.13.--1000-mb (100-kPa) 24-hr convergence PMP (inches) for 10 mi^2 (26 km^2) for September. Values in parentheses are limiting values and are to facilitate extrapolation beyond the indicated gradient.

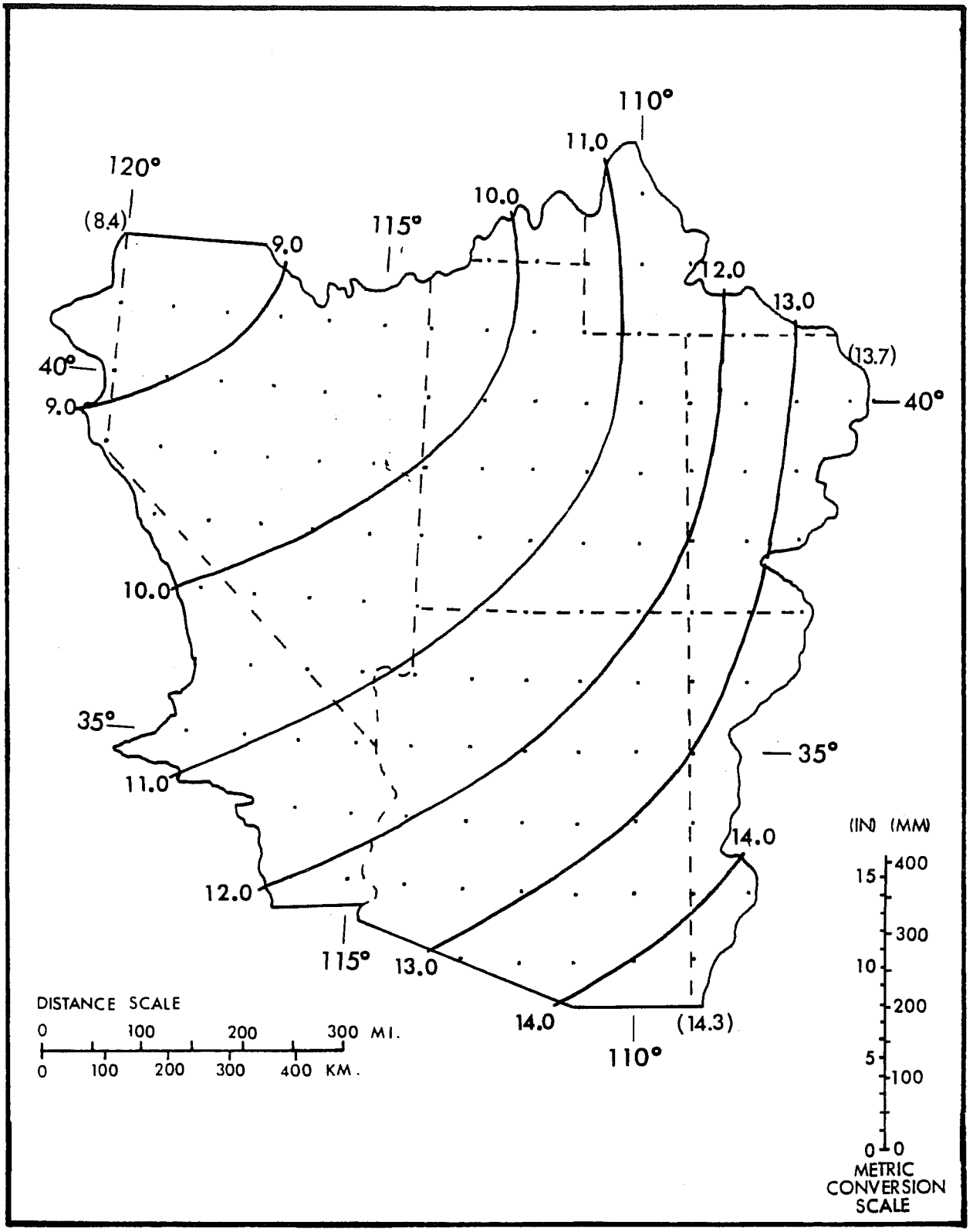

Figure 2.14.--1000-mb (100-kPa) 24-hr convergence PMP (inches) for 10 mi^2 (26 km^2) for October. Values in parentheses are limiting values and are to facilitate extrapolation beyond the indicated gradient.

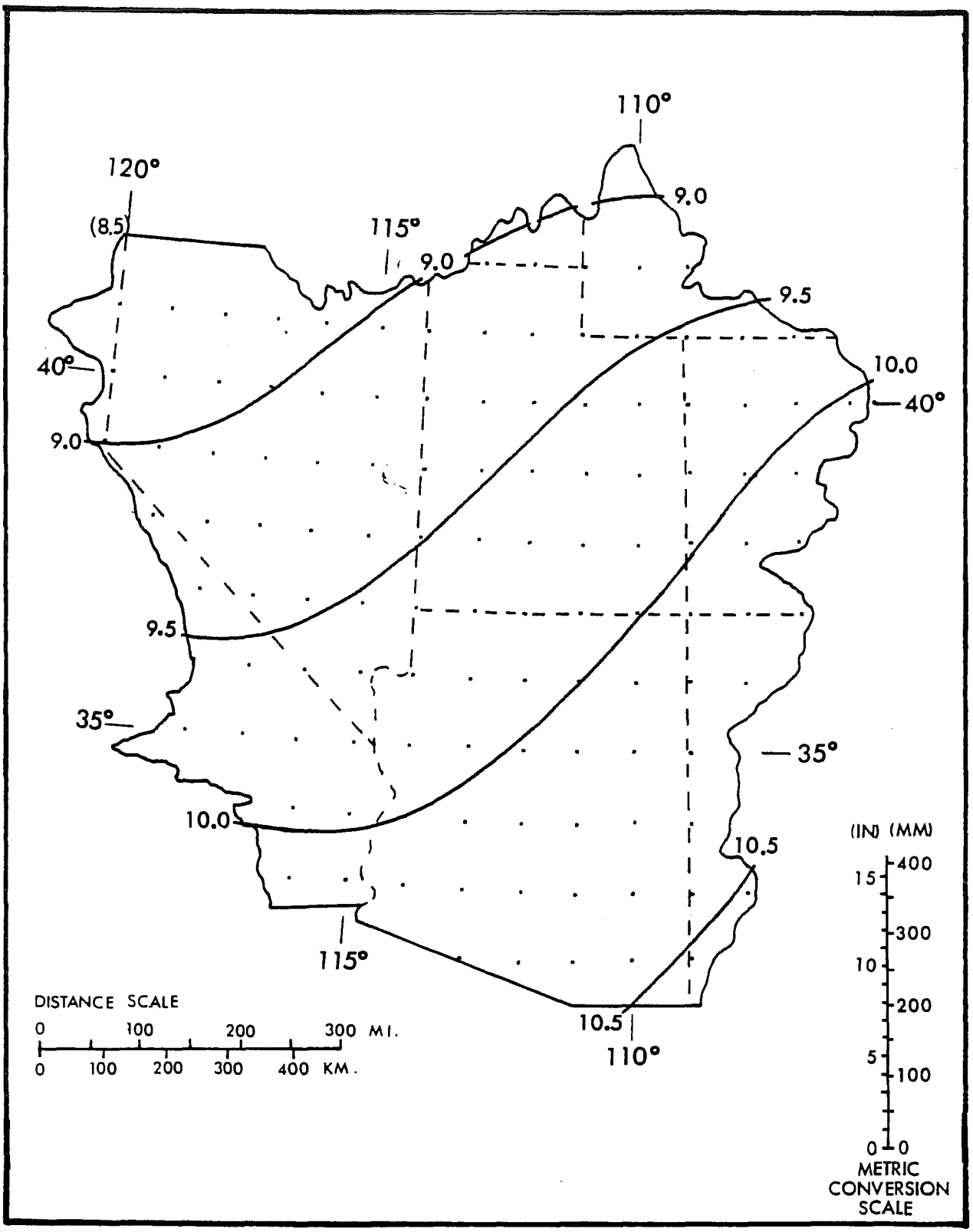

Figure 2.15.--1000-mb (100-kPa) 24-hr convergence PMP (inches) for 10 mi^2 (26 km^2) for November. Values in parentheses are limiting values and are to facilitate extrapolation beyond the indicated gradient.

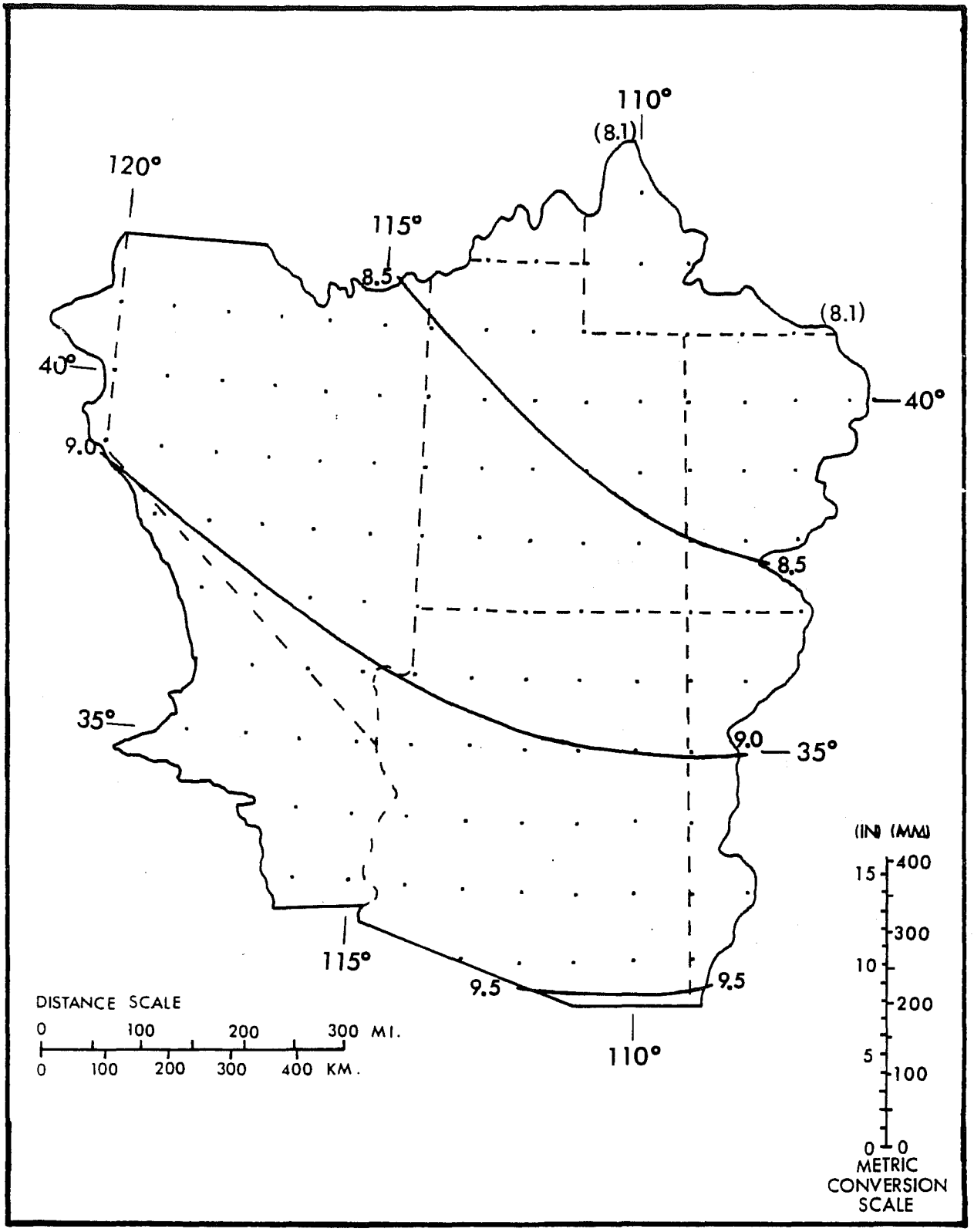

Figure 2.16.--1000-mb (100-kPa) 24-hr convergence PMP (inches) for 10 mi^2 (26 km^2) for December. Values in parentheses are limiting values and are to facilitate extrapolation beyond the indicated gradient.

2.3 Effect of Barrier and Elevation

The adopted convergence PMP is for 1000 mb (100 kPa) or sea level. For locations at higher elevations or to the lee of mountain barriers, the 1000-mb (100-kPa) convergence PMP must be decreased. This is accomplished by reductions for barrier and elevation.

2.3.1 Effective Barrier and Elevation Map

During strong inflow of saturated or near saturated air, moisture is depleted on windward slopes by the higher elevations. Moisture is depleted for areas to the lee of upwind barriers by the effect of the barrier.

Elevations used in this study were based on smoothed elevation contours of a 1:1,000,000 scale topographic map. The smoothing moved the actual terrain elevation slightly upwind. This "effective" elevation, as differentiated from the actual elevation, provided for greater moisture into a region because precipitation particles can be carried along by the wind to higher elevations.

The "effective" barrier for the lee areas was determined from the height of the upwind barrier. These effective barriers may differ from the maximum elevation of the barrier since allowance was made for moisture flow through substantial breaks in the ridgeline.

Inflows from southwest through south-southeast were of prime importance in deriving the effective barrier and effective elevation chart for a large portion of the Southwestern States. Winds from westerly to northwesterly directions were involved near the northwest corner of the region. A reasonable tie-in was maintained with the effective barrier and elevation charts of studies for adjoining areas. Also, inflow into southwestern Wyoming and northeastern Utah from the east to northeast resulted from the prototype storm for this portion of the study region. This is consistent with extreme rains to the east of the Continental Divide caused by easterly flow in late spring storms.

With some variability permitted in the direction of moist inflow, isolated mountains and ridges less than 10 miles (16 km) long (measured at the base relative to the wind direction) are not effective in reducing moisture. The effective barriers were in many instances phased out, downwind, at a distance about 1 to 1.5 times their length, implicitly allowing recharge of moisture behind such obstacles. The amount of recharge is similar to that of bordering generalized reports (HMR Nos. 36 and 43). Recharge toned down or eliminated effects of ridges somewhat longer than the initial 10-mi (16-km) criterion. Figure 2.17 shows the combined barrier/elevation map for the for the Southwest.

2.3.2 Reduction for Effective Barrier and Elevation

Variation of nonorographic PMP with barrier height and elevation has been made proportional to the variation with elevation of precipitable water in a saturated column. It is the same as that used for convergence PMP in HMR No. 36 for California and for some of the variation in HMR No. 43 for the

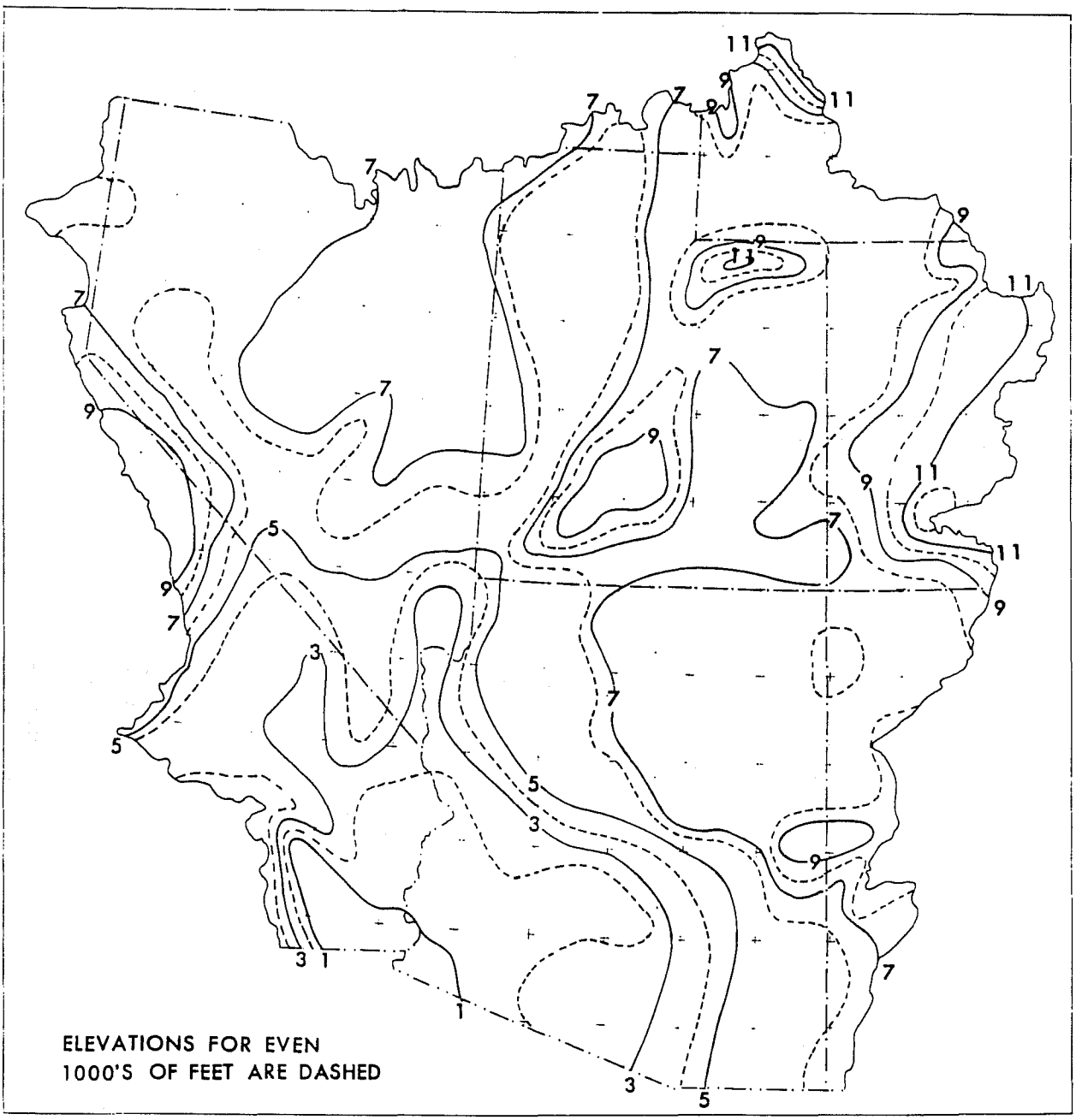

Figure 2.17.--Effective barrier and elevation heights (1000's of feet) for Southwestern States.

Columbia River drainage. The adopted variation with elevation, which is proportional to the variation in precipitable water, is consistent with the method used for moisture-maximizing the greatest observed least-orographic rains for guidance in setting the level of 1000-mb (100-kPa) convergence PMP.

The maximum 12-hr persisting 1000-mb (100-kPa) dew points for August general storms (Schwarz and Hansen 1978) of 73° (23°C) were used for determining the percent reduction due to effective barriers and elevations. The August dew points tend to give less reduction than winter dew points. High-elevation rainfall would be unreasonably reduced if winter dew points were used, particularly because the use of a single moisture chart does not allow for the high wind and therefore higher rainfall capability at the higher elevation in the cool season.

Figure 2.18 shows the reduction (in percent) of 1000-mb (100-kPa) convergence PMP for effective barrier and elevation over the Southwestern States. There is agreement between the patterns shown in figures 2.17 (barrier/elevation) and 2.18 (reduction of 1000-mb (100-kPa) convergence PMP) with one exception. Figure 2.18 contains a large area of 45% reduction in northeastern Arizona, to the lee (northeast) of the Mogollon Rim. A continuous approximate 8,000-ft (2,440-m) barrier does not exist to support the 45% feature directly. We believe this factor is justified, since the effect of downslope motion behind the major barrier is to produce additional drying of the air which is equivalent to a higher effective barrier. Further downwind, the 45% reduction line has been closed off to indicate the gradual influence of recharge of moisture below 8,000 ft (2,440 m).

When using figure 2.18 to determine a percent of convergence PMP for a specific basin, interpolate between the isopleths. However, for locations that lie within closed contours or at the end of gradients, (within the 95% contour in southern California, and within the 50% contour in north-central Nevada, for example), the correct value is that of the last identified contour, i.e., do not extrapolate.

2.4 Depth-Duration Variation

The 24-hr mid-month convergence PMP values can be extended to other durations through application of rainfall depth-duration relationships. Durations between 6 and 72 hours are required. Relationships were developed from 6/24-hr, 48/24-hr and 72/24-hr ratios of rainfall in selected severe storms and from maximum rainfalls of record at recorder stations. Seasonal and regional variations of depth-duration relations are given.

2.4.1 Data

Hourly precipitation data for up to 25 years (1948-72) were available on magnetic tapes for recorder stations listed in table 2.4. These stations are located in the least-orographic regions shown in figure 2.1. Stations A, B, C, D, and F in table 2.4 are geographically close to stations 3, 10, 11, 13, and 23, respectively, in table 2.2. An additional station at Baker, California (station E in table 2.4) was included in the southern Nevada subregion. Although some of these stations (A to F) had records exceeding 20 years, only

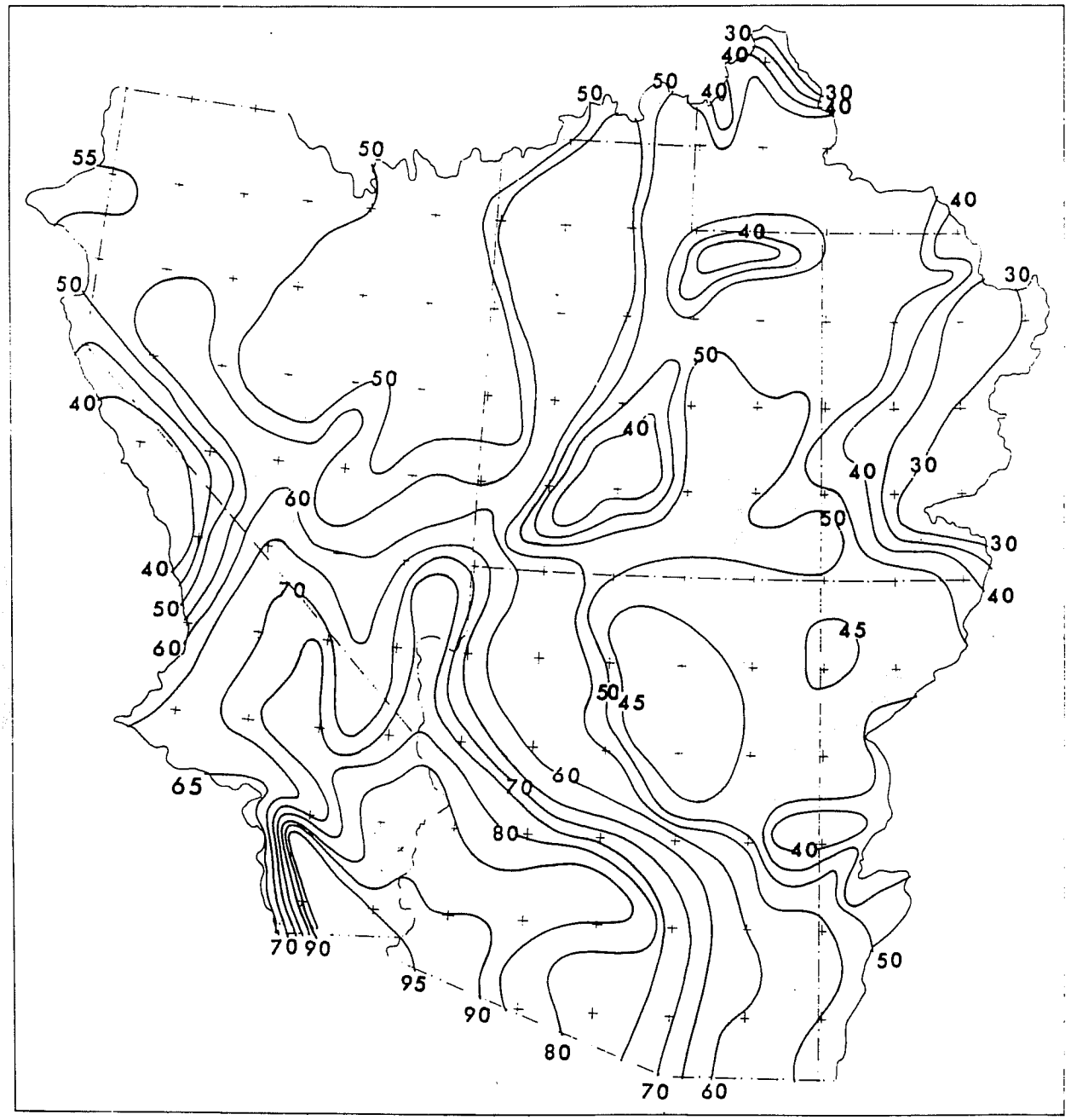

Figure 2.18.--Percent of 1000-mb (100-kPa) convergence PMP resulting from effective elevation and barrier considerations. Isolines drawn for every five percent.

Table 2.4.--Stations within least-orographic regions for which hourly precipitation data were available for the period 1948 through 1972.

	Station	Latitude	Longitude	Elevation ft	(m)
	Southwest Arizona				
	Ajo, Ariz.	33°22	112°52	1763	(537)
A*	Casa Grande Ruins, Ariz.	33°00	110°32	1419	(433)
	Phoenix, Ariz.	33°28	112°04	1083	(330)
	Yuma, Ariz.	32°44	114°36	138	(42)
	Blythe, Calif.	33°37	114°36	268	(82)
B	El Centro, Calif.	32°46	115°34	- 37	(- 11)
	Iron Mt., Calif.	34°08	115°08	922	(281)
C	Thermal, Calif.	33°38	116°10	- 112	(- 34)
	Northeast Arizona				
D	Keems Canyon, Ariz.	35°49	110°12	6205	(1893)
	Winslow, Ariz.	35°01	110°44	4880	(1487)
	Green River, Utah	39°00	110°09	4087	(1246)
	Hanksville, Utah	38°25	110°41	4456	(1358)
	Crownpoint, N. Mex.	35°40	108°13	6978	(2128)
	Farmington, N. Mex.	36°43	108°12	5300	(1615)
	Western Utah				
F	Delta, Utah	39°20	112°35	4626	(1410)
	Dugway, Utah	40°10	113°00	4359	(1329)
	Enterprise B. Jct., Utah	37°43	113°39	5220	(1598)
	Milford, Utah	38°25	113°01	5029	(1535)
	Wendover, Utah	40°44	114°02	4239	(1292)
	Malad, Idaho	42°11	112°16	4420	(1347)
	Southern Nevada				
	Beatty, Nev.	36°54	116°45	3314	(1010)
	Caliente, Nev.	37°37	114°31	4402	(1342)
	Las Vegas, Nev.	36°10	115°09	2006	(611)
	Searchlight, Nev.	35°28	114°55	3540	(1079)
E	Baker, Calif.	35°16	116°04	940	(287)
	Needles, Calif.	34°46	114°38	913	(278)
	Northwest Nevada				
	Elko, Nev.	40°50	115°47	5075	(1548)
	Lovelock, Nev.	40°12	118°28	3977	(1212)
	McDermitt, Nev.	42°00	117°43	4427	(1349)
	Winnemucca, Nev.	40°54	117°48	4314	(1315)

*Locators in figure 2.1.

the longer record station was used in the studies for determining the magnitude and regional and seasonal variation of convergence PMP.

Additional data were sought from major storms of record for which there were large rainfalls in least-orographic regions. Almost all major storms in the Southwest have their centers in orographic regions; thus, it is difficult to obtain large amounts (more than one inch in 24 hours) in least-orographic regions. Data from the August 1951 and the northern center of the September 1970 storms along with seven lesser nonsummer storms were considered for guidance in establishing the seasonal variation of durational relations. The latter storms are listed in table 2.5.

Table 2.5.--Nonsummer storms in the Southwest and the number of stations with relatively large rainfalls in least-orographic regions, used in duration analysis of convergence PMP.

Date	No. of stations	Location
Dec. 14-17, 1908	4	W. Cent. Arizona
Dec. 17-24, 1914	6	S. Arizona
Jan. 14-20, 1916	5	S. Arizona
Feb. 01-07, 1905	5	SE Calif., S. Ariz.
Feb. 10-22, 1927	3	S. Utah
Mar. 11-17, 1941	3	SE Calif., S. Ariz.
Apr. 05-10, 1926	2	S. Arizona

2.4.2 Depth-Duration Relation

A depth-duration relation of PMP for an area size indicates the relationship between PMP values for various durations. It can be specified by a smooth curve of duration vs. depth (either in inches or percent of the value for a selected duration) or mathematically by ratios of the depths for various durations to that say of 24 hours. A PMP depth-duration relation is based on the concept that the average intensity of rainfall decreases with increasing duration. This concept is analogous to that in depth-area relations of PMP in which precipitation decreases with increasing area size. It might be well to point out that a depth-duration relation of PMP does not specify the time sequence in which incremental rain will fall. A smooth depth-duration relation can be quite well defined by the 6/24- and 72/24-hr ratios of rainfall.

Some regional PMP studies have used one depth-duration relation for the entire region. From preliminary examination of 6/24-hr ratios of rainfall, it was apparent that seasonal and regional variations precluded use of a single relation for the Southwestern States.

As an alternative, a concept of a family of smooth depth-duration relations was envisioned that would cover the range of probable relations required. When expressed in percent of the 24-hr amount, the concept of a smooth family of curves that require a continually decreasing rate of rainfall intensity involves an inverse relationship: Where the short-duration value is high, the long-duration value with which it is associated is low, and vice versa. In effect, this implies that high 6/24-hr ratios relate to low 72/24-hr ratios, and that low 6/24-hr ratios relate to high 72/24-hr ratios.

A tendency to support the inverse relation can be seen in the data plotted in figure 2.19. These ratios are selected within-storm (paired 6/24- and 72/24-hr ratios from the same storm) values from the stations in table 2.4. All storms were used where the 24-hr amount equalled or exceeded 1.0 inch (25 mm). To aid in understanding seasonal variations the data were stratified according to winter (Jan. and Feb.) and summer (Jul. and Aug.) months. An attempt was made to reduce the influence of thunderstorms by purging the data to eliminate 6/24-hr ratios greater than or equal to 0.90 and 72/24-hr ratios less than or equal to 1.10. An envelopment of the data in figure 2.19 supports an inverse relation. Similarly, a rough average through all the points, aside from the wide scatter, supports an inverse relation.

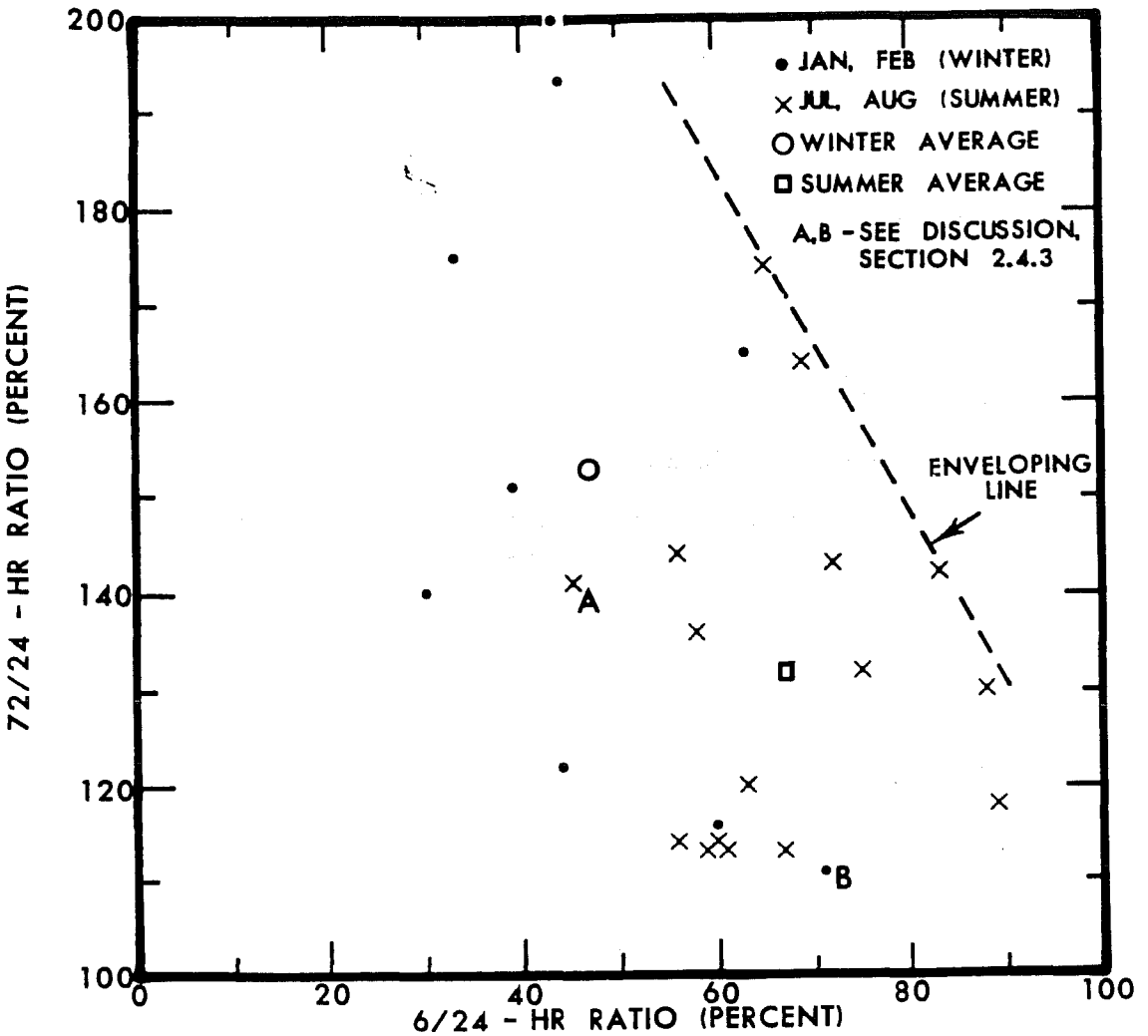

Figure 2.19.--Relation between 6/24-hr and 72/24-hr ratios for within-storm cases of 3 consecutive day rainfall for all stations listed in table 2.4 (see text for criteria for selection). Points identified as winter or summer.

A family of depth-duration curves that would cover the range required in the Southwest was then developed. First, a base depth-duration curve was established using all recorder data for least-orographic stations in the August 1951 and September 1970 storms. These storms are the closest to the prototype PMP storm for most of the Southwest. Averages of 6/24-, 12/24-, 18/24-, 48/24-, and 72/24-hr ratios are shown by the large dots in figure 2.20. The 72-hr dot is based solely on August 1951 data. A smooth line was drawn through these dots.

Next, we expanded this base depth-duration curve to a family of curves constrained by the limits:

a. Contant rainfall rate. A straight line from 0 to 100% at 24 hours to 300% at 72 hours.

b. All rain in the first instant, or 100% at all durations.

These two constraints are represented by the straight lines in figure 2.20. There is great flexibility in how to draw additional curves between these two lines. We selected 6/24-hr ratios at increments of 30, 40,..., 90% and drew smooth curves between 0 and 24 hours that were consistent with the curvature of the basic relation and somewhat symmetrical about a perpendicular bisector to the curves.

The 6 additional curves were then extended to 48 and 72 hours as smooth (not necessarily straight) lines. Further adjustments were made to the increments between curves beyond 24 hours in order to maintain a gradual increase (smooth gradient) in the increment between successive curves as the 72/24-hr ratios increased. The control for this gradient was the range in individual recorder durational curves for the stations used in the August 1951 and September 1970 storms. Although the family of curves in figure 2.20 suggests a broad range of 72/24-hr ratios, a much smaller range is applicable to the Southwest as discussed under seasonal and regional variations.

The PMP study for the Northwestern States, HMR No. 43, used a similar generalized set of depth-duration relations for convergence PMP. While not developed in the same manner as in the present study, the results are similar. Adopted smooth relations from the two studies are compared in figure 2.21.

2.4.3. Seasonal variation

It is to be expected that the 6/24-hr ratio should have a seasonal variation, i.e., because of greater convective activity ratios should be higher in summer than in winter.

In figure 2.19, a check was made of two points (labelled A and B) that appear to be extremes relative to the seasonal distribution of points indicated in this figure. Hourly precipitation records and synoptic weather analyses indicate that point A is the result of 3 days of isolated afternoon thundershowers. Thus, it is not representative of a general-storm summer rainfall. Point B results from one-day rainfall associated with a rapidly moving and dissipating low-latitude cold front with light post-frontal showers on the

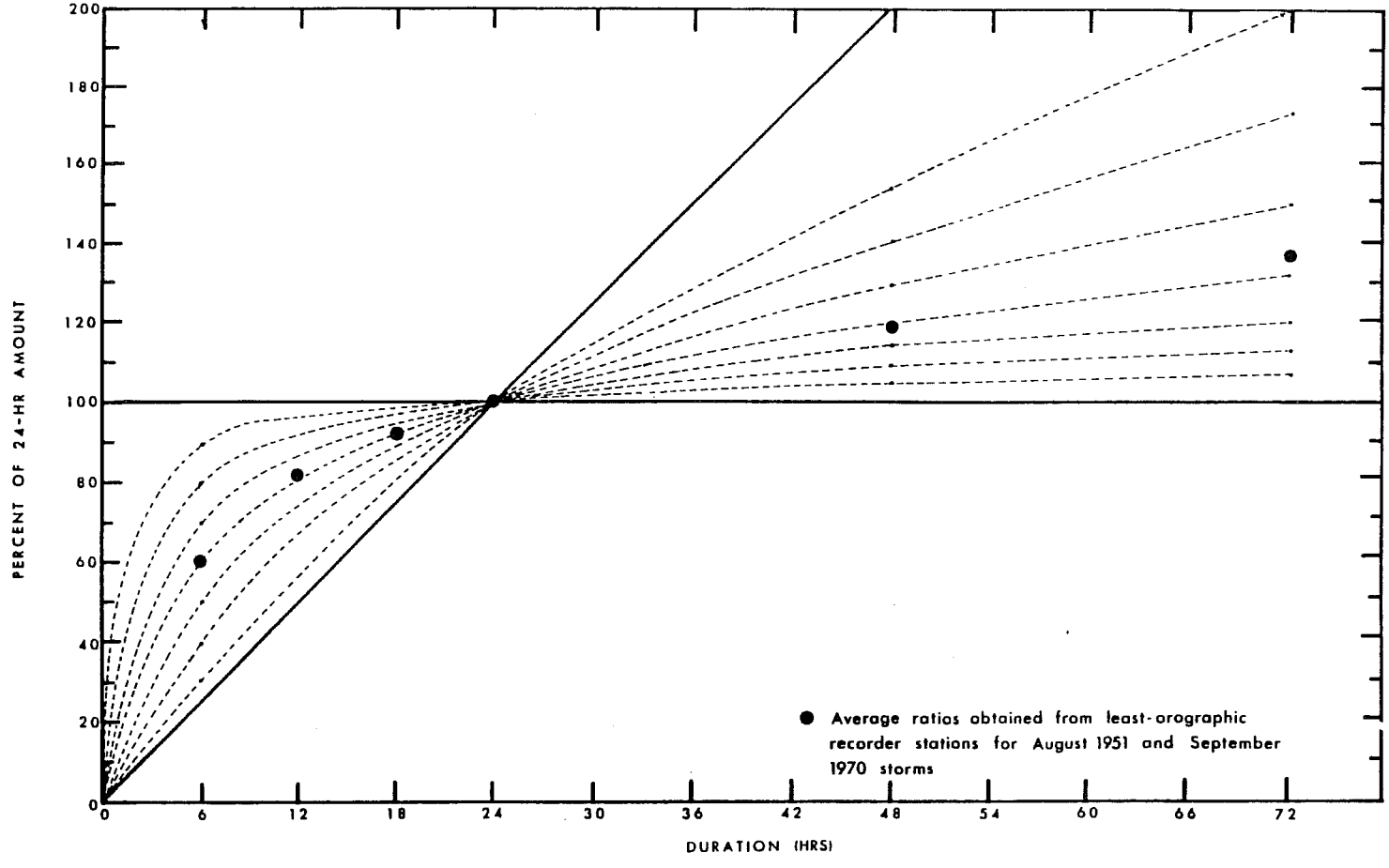

Figure 2.20.--Idealized depth-duration curves in percent of 24-hr amount. For development of this diagram see section 2.4.2. Selected durational values from this diagram are presented in table 2.9 for various 6/24-hr ratios used in figures 2.25 to 2.27.

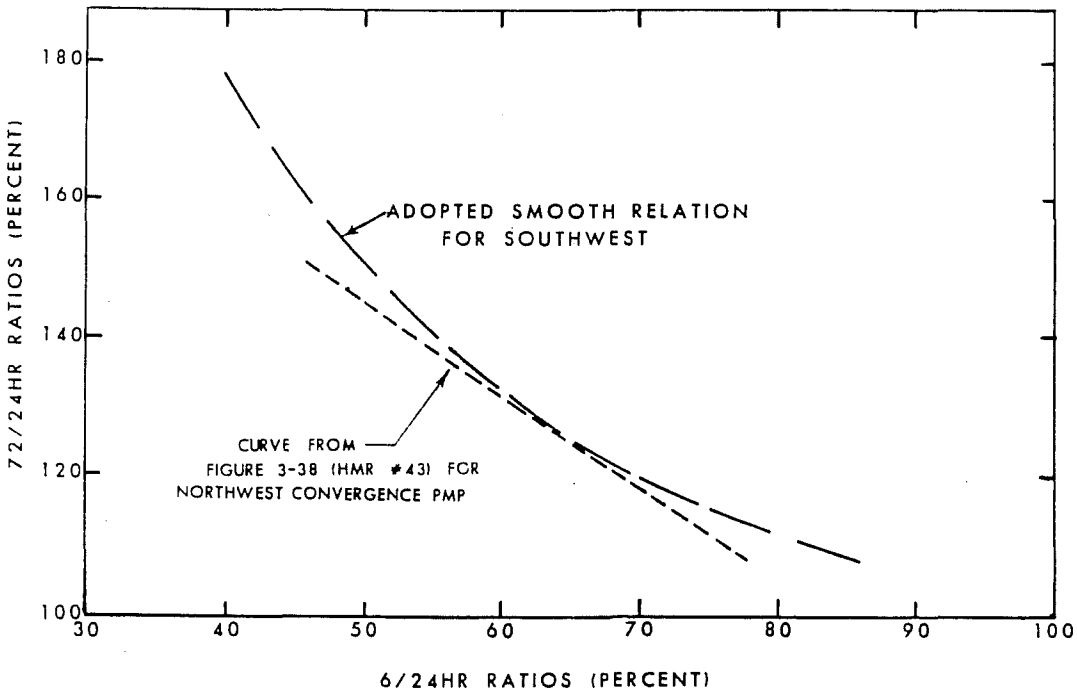

Figure 2.21.--Adopted 6/24-hr vs. 72/24-hr convergence PMP ratios.

next two days. Again, most of the rain during frontal passage was caused by thunderstorms and therefore make this case unrepresentative of a major winter storm. As to the meteorological cause for the other data in figure 2.19, no check was made, but it is believed they tend to support a seasonal distribution in the ratios shown.

The recorder rainfall data for stations in least-orographic areas, table 2.4, were processed to determine monthly average 6/24-hr within-storm ratios for maximum 24-hr rainfalls. This was done by selecting the 20 highest 24-hr rainfalls of record for each month and station and purging to reduce the influence of short term thunderstorm events. The purging was accomplished by eliminating 6/24-hr ratios greater than 0.90. In many instances, particularly during the summer months, fewer than 20 cases were available. From these cases that met the purging criterion, ratios from the five highest 24-hr rainfalls for each station were averaged to obtain mid-month subregional ratios. Some monthly averages had less than five cases. The subregional values are shown on a seasonal plot in figure 2.22. Although there is considerable scatter this may be due to the limited sample. There is a definite trend for higher 6/24-hr ratios in the warm season. These monthly averages are plotted on a seasonal plot, figure 2.23, as short dashes. Four other sets of data have been added to this figure to aid in determining the seasonal variation. Among-storm 6/24-hr ratios (highest monthly 6-hr rainfall divided by the highest monthly 24-hr rainfall) were averaged for 6 stations that were helpful in determining the initial seasonal variation of convergence PMP (fig. 2.4). These are shown by Xs in figure 2.23. A third set of 6/24-hr ratios were monthly averages of station data in the storms listed in table 2.5 along with the August 1951 and September 1970 storm (open circles in fig. 2.23).

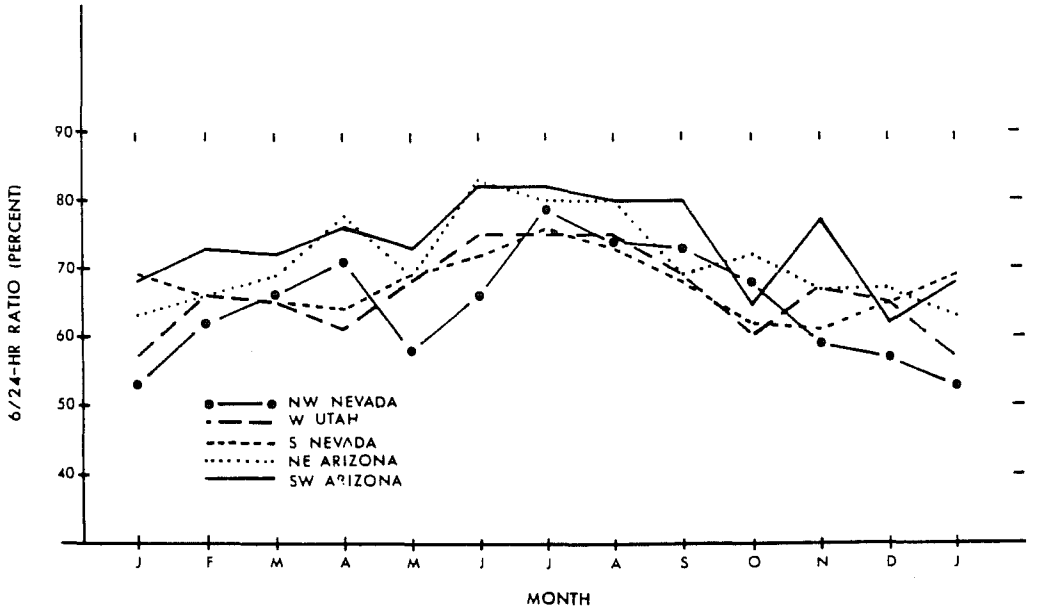

Figure 2.22.--Seasonal variation of 6/24-hr ratios at least-orographic subregion midpoints. Based on averages of station data (table 2.4) for maximum 24-hr rainfalls.

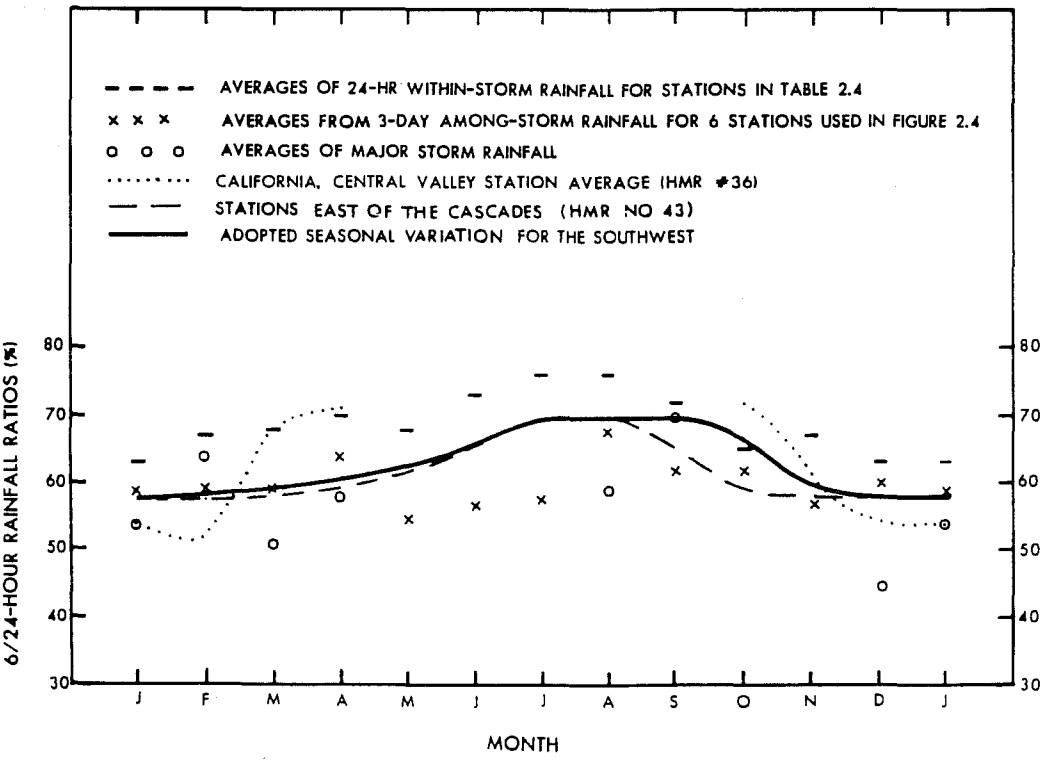

Figure 2.23.--Seasonal variation of 6/24-hr durational rainfall ratios for Southwest and adjacent regions.

No major storm data was available for the months of May, June, July, October, and November. Seasonal variation of 6/24-hr ratios used for convergence PMP in adjoining regions, are also shown in figure 2.23.

We have adopted the mean seasonal variation indicated by the solid curve in figure 2.23. This curve is quite similar to that used in the Northwest. The major difference is an extension of the summary maximum to include September and early October. The occurrence of general tropical storm rainfall, e.g., September 1970 into Utah and the October 1911 into Colorado, this late in the year is the basis for this extension. The smooth adopted curve with highest ratios in summer is generally supported by an average of the Southwest data (dashes, Xs, and open circles).

2.4.4 Regional Variation

The seasonal plots of 6/24-hr ratios for each least-orographic area (fig. 2.22, in addition to higher values in summer, also show some tendency for higher ratios throughout the year for the southern subregions than for the northern subregions. For example, the ratios for southwestern Arizona give the highest ratios for 7 of the months, and only slightly lower ratios than some other area for 3 other months. Ratios for northwestern Nevada are lowest for 6 months and near-lowest for 2 other months. This latitudinal trend in ratios was preserved by using the adopted seasonal variation for all locations from figure 2.23 as a guide in smoothing the curves. Shifting the adopted seasonal variation curve to fit the distribution of 6/24-hr ratios for each region shown in figure 2.22 resulted in a set of smooth curves similar to that shown in figure 2.24. Because the magnitude of the ratios shown in figure 2.22 is somewhat greater than the adopted curve in figure 2.24, the set of smooth regional curves was adjusted downward to center their range about the adopted curve as is shown in figure 2.24.

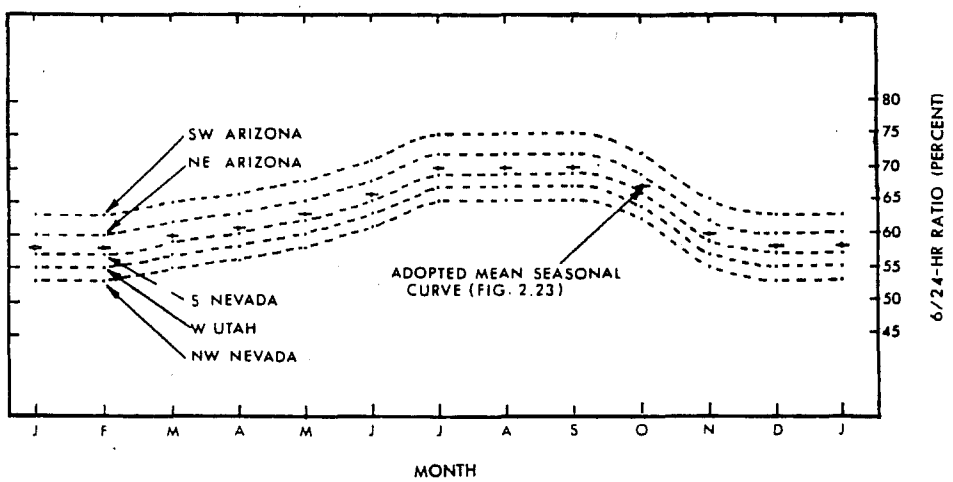

Figure 2.24.--Smoothed variation of 6/24-hr ratios at subregional midpoints.

Ratios from figure 2.24 were plotted at regional centers on a series of monthly maps. Analysis of these data resulted in the monthly maps of regional variation in 6/24-hr ratios shown in figures 2.25 to 2.27. With the exception of magnitude, the analyzed maps show similar patterns.

A comparison between ratios from figures 2.25 to 2.27 and data from HMR No. 43 for a coincident location (42°N, 113°W) is given in table 2.6. Except

Table 2.6.--Comparison of 6/24-hr ratios in the Northwest and Southwest studies at 42°N, 113°W.

	Month											
	O	N	D	J	F	M	A	M	J	J	A	S
Northwest	.62	.61	.59	.59	.59	.61	.62	.64	.69	-	-	-
Southwest	.62	.55	.54	.54	.54	.55	.57	.59	.62	.66	.66	.66

for October, the Southwest ratios are generally about 6% lower than those of the northwest at this location. The larger northwest data ratios are to be expected as they were not purged of bias toward rain showers. Another source of difference results from the difference in development of regional analyses in these two studies. The two studies agree in that the gradient of ratios presented is oriented from high ratios in the southeast to lower ratios in the northwest.

Meteorological support for the pattern of 6/24-hr ratios shown in figures 2.25 to 2.27 comes from the moisture potential in storms. The Sierra Nevada range represents a major barrier to deep moisture flows from the southwest through northwest. Storms that enter the Southwest around the north end of this range are characteristic of cool-season storms of higher latitudes. Major storms that pass south of the Sierra Nevada pick up unstable air from lower latitudes. As the storms continue eastward, additional moist unstable air from over the Pacific is supplied. In terms of 6/24-hr ratios the supply of moist unstable air is shown by higher values, and we believe the more rapid increase in gradient as one passes across the southern portion of the region is realistic.

In figures 2.25 to 2.27 the combined seasonal-regional variation in 6/24-hr ratios is evident. These ratios vary between 0.50 and 0.69 during the cool season (Nov. to Mar.) and between 0.59 and 0.79 during the warm season (June to Oct.). Thus, the spread of depth-duration relations applicable to the Southwest convergence PMP is considerably reduced from the possible relations initially developed in figure 2.20. Furthermore, the gradients shown in figures 2.25 to 2.27 imply a greater potential for sustained precipitation in the northern portion of the Southwest than in the southern portion during the summer season. This can be explained as possibly caused by extratropical influences that modify the prototype storm as it penetrates farther inland.

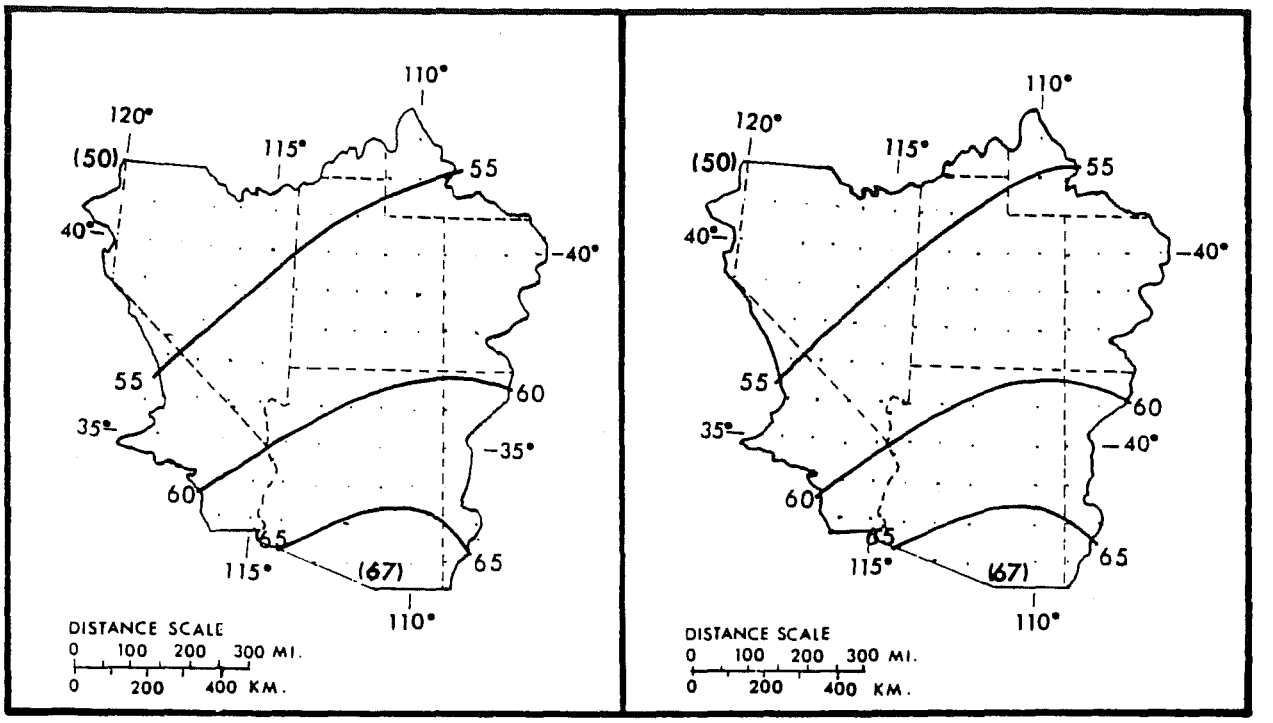

January *February*

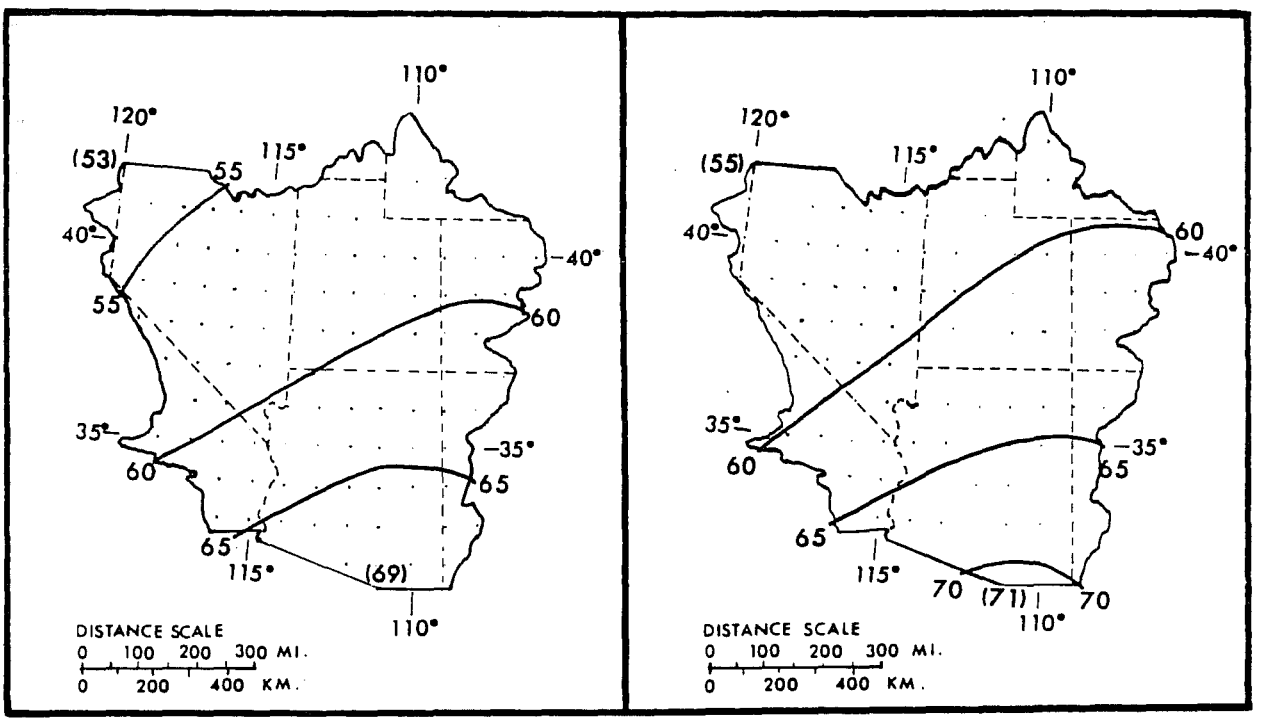

March *April*

Figure 2.25.--Regional variation of 6/24-hr ratios by month (percent). Values in parentheses are limiting values and are to facilitate extrapolation beyond the indicated gradient.

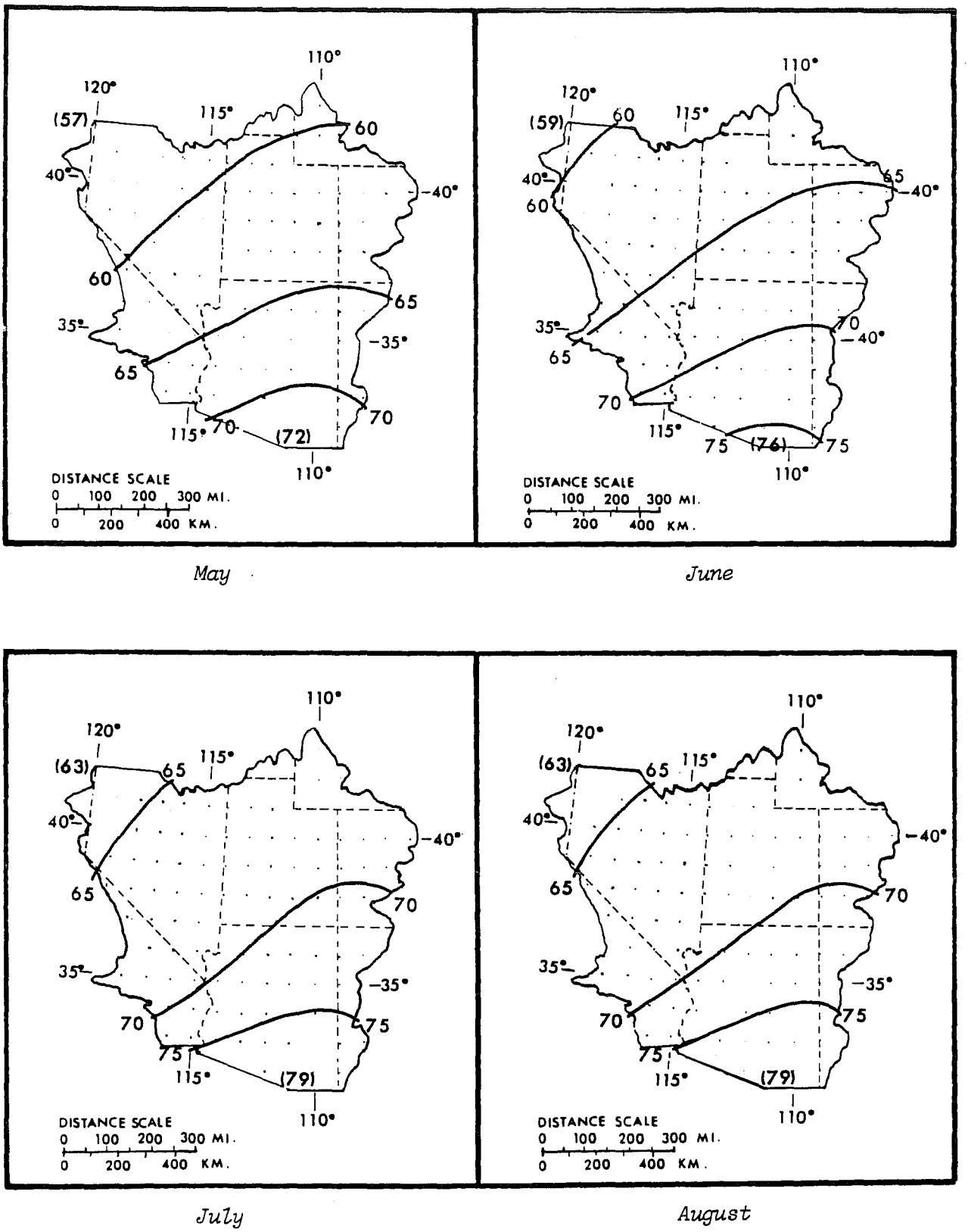

Figure 2.26.--Regional variation of 6/24-hr ratios by month (percent). Values in parentheses are limiting values and are to facilitate extrapolation beyond the indicated gradient.

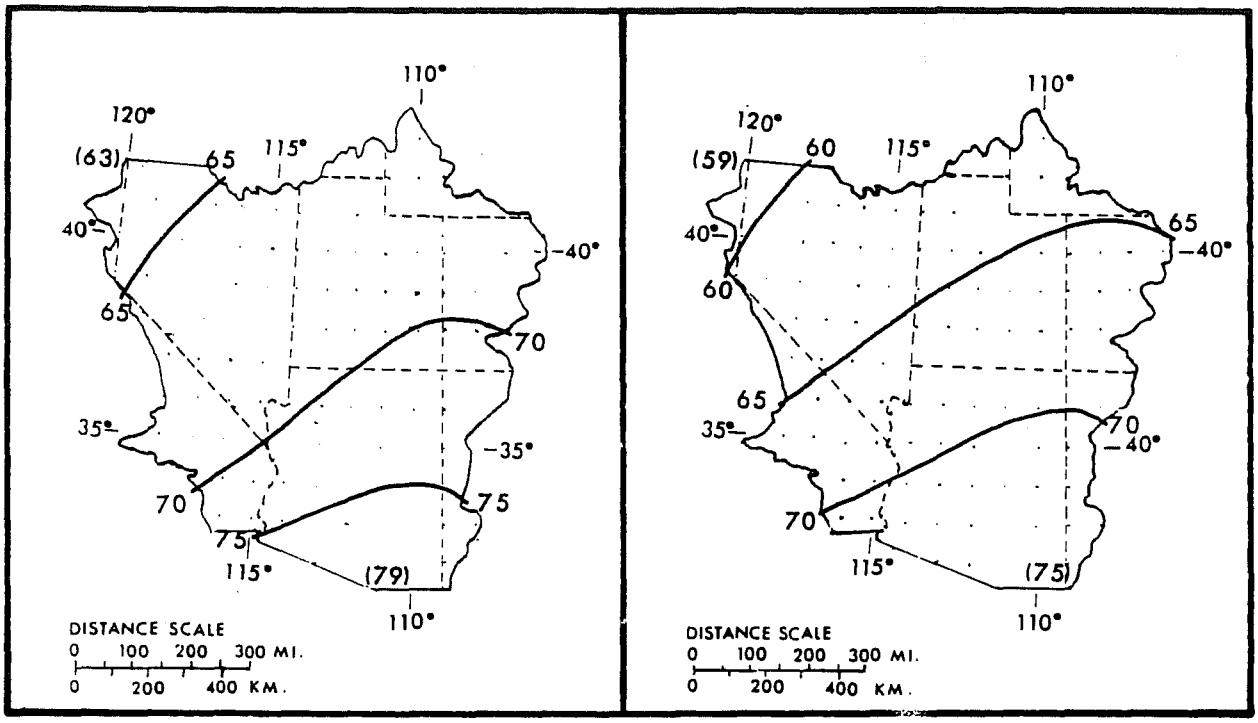

September *October*

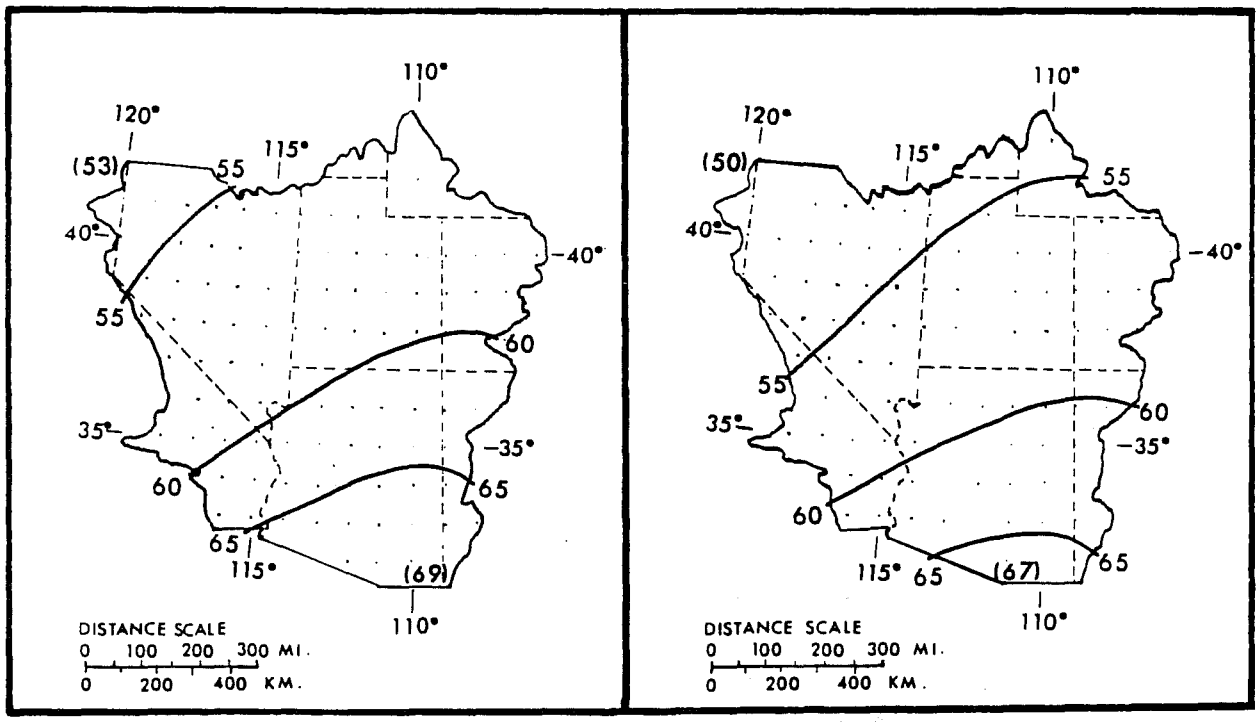

November *December*

Figure 2.27.--Regional variation of 6/24-hr ratios by month (percent). Values in parentheses are limiting values and are to facilitate extrapolation beyond the indicated gradient.

For the range of 6/24-hr ratios included in figures 2.25 to 2.27, depth-duration values in percent of 24-hr amounts are found in table 2.7. The regional ratio maps, and the depth-duration curves presented in figure 2.20 were used in adjusting the major storm data to 24-hr amounts listed in table 2.1.

Table 2.7.--Durational variation of convergence PMP (in percent of 24-hr amount).

Duration (Hrs)						Duration (Hrs)					
6	12	18	24	48	72	6	12	18	24	48	72
50	76	90	100	129	150	66	84	93	100	116	124
51	77	90	100	128	148	67	85	94	100	116	123
52	77	90	100	127	146	68	85	94	100	115	122
53	77	91	100	127	144	69	86	94	100	115	121
54	78	91	100	126	142						
55	78	91	100	125	140	70	87	94	100	114	120
56	79	91	100	124	138	71	87	95	100	114	119
57	79	92	100	123	137	72	88	95	100	113	118
58	80	92	100	122	135	73	88	95	100	113	118
59	80	92	100	121	134	74	89	95	100	112	117
						75	89	96	100	112	116
60	81	92	100	120	132	76	90	96	100	111	115
61	81	92	100	120	131	77	90	96	100	110	114
62	82	93	100	119	129	78	91	96	100	110	114
63	82	93	100	118	128	79	92	97	100	109	113
64	83	93	100	117	126						
65	84	93	100	117	125	80	92	97	100	109	113

Note: For use, enter first column (6 hr) with 6/24-hr ratio from figures 2.25 to 2.27.

2.5 Areal Reduction for Basin Size

For operational use, basin average values of convergence PMP are needed rather than 10-mi^2 (26-km^2) values. Preferably, the method for reducing 10-mi^2 (26-km^2) values to basin average rainfalls should be derived from depth-area relations of storms in the region. However, all general storms in the region include large proportions or orographic precipitation.

Our solution was to use generalized depth-area relations developed for PMP estimates within bordering zones in the Central and Eastern United States (Riedel et al. 1956). The smoothed areal variations adopted for the Southwestern States are shown in figures 2.28 and 2.29 for each month or a combination of months where differences are insignificant.

Figures 2.28 and 2.29 give depth-area relations that reduce 10-mi^2 (26-km^2) convergence PMP for basin sizes up to 5,000 mi^2 (12,950 km^2) for each month. Areal variations are given for the 4 greatest (1st to 4th) 6-hr PMP increments. After the 4th increment no reduction for basin size is required. Application of these figures will become clear through consideration of an example of PMP computation in chapter 6.

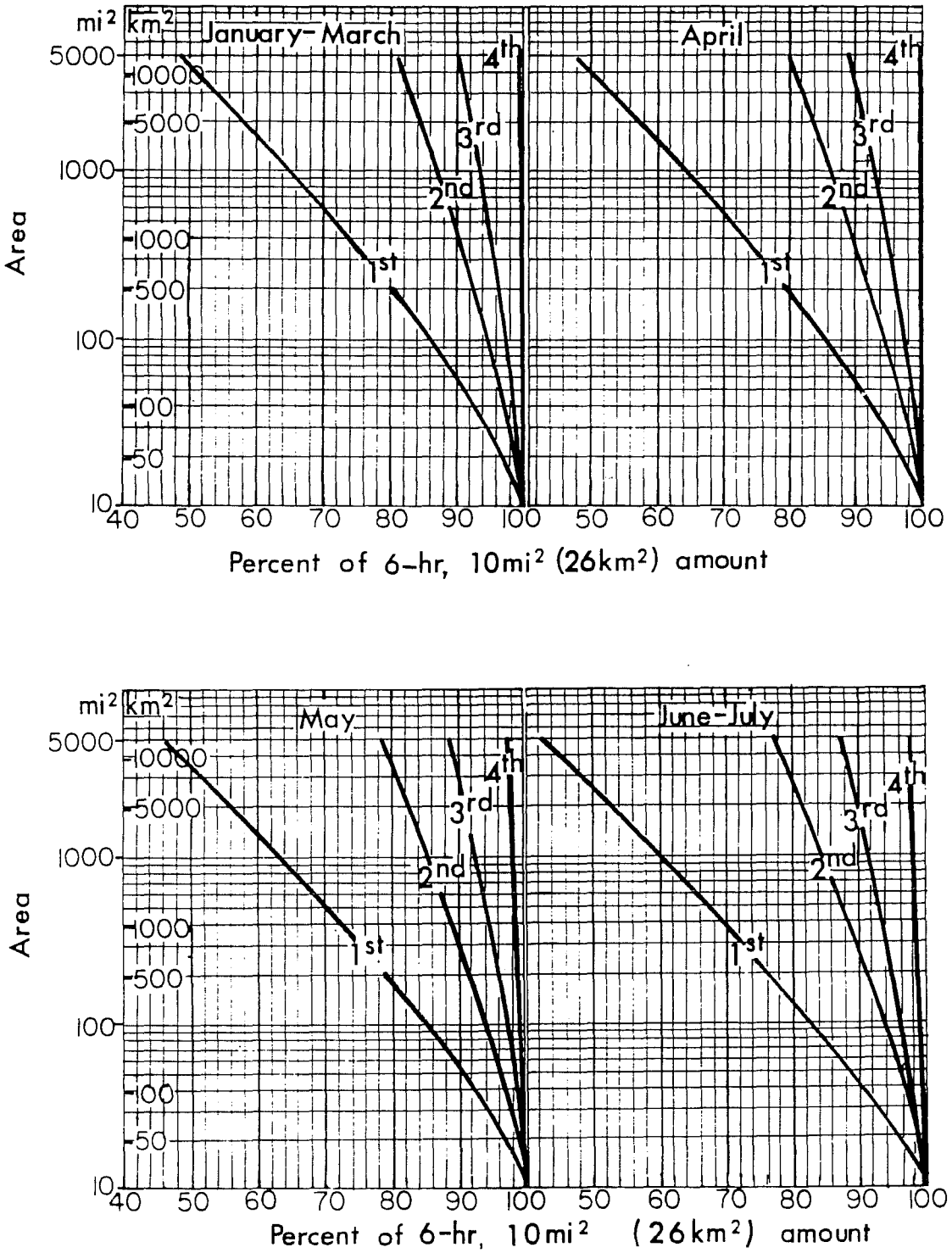

Figure 2.23.--Depth-area variation for convergence PMP for first to fourth 6-hr increments.

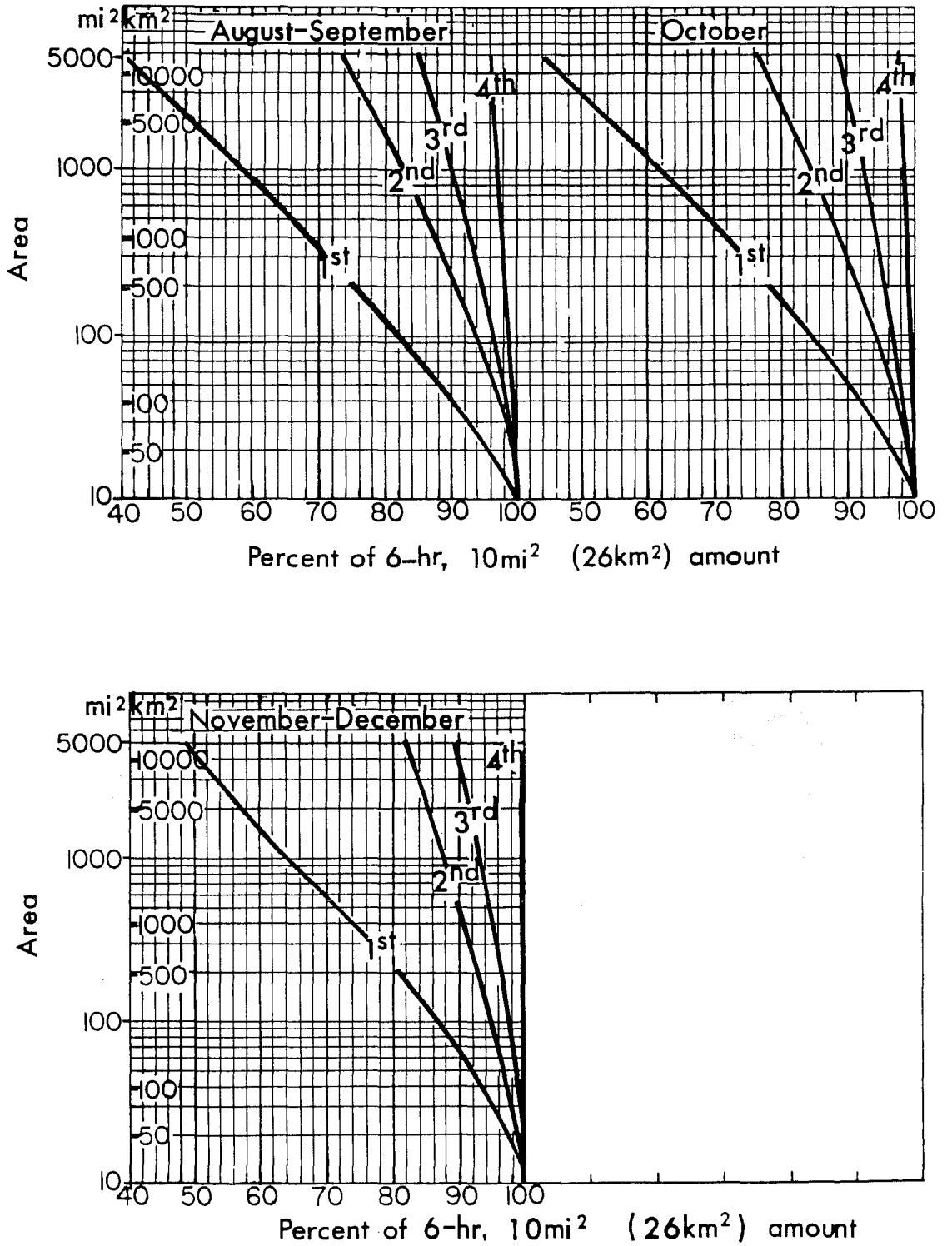

Figure 2.29.--Depth-area variation for convergence PMP for first to fourth 6-hr increments.

3. OROGRAPHIC COMPONENT OF PMP

3.1 Introduction

3.1.1 Methods for Determining Orographic Effects on Rainfall

Recent PMP studies in mountainous terrain have used one of two methods for determining the orographic effects on precipitation magnitude and distribution. One computes precipitation with a numerical orographic windflow model based on physical principles. Examples of the use of this method are HMR No. 36 and HMR No. 43. The other, used where the windflow model does not apply is a more empirical approach in which observed rains on slopes and in nearby least orographic areas (fig. 3.1, see discussion in 3.2.3.2) are compared and the differences are assumed to be orographic. This procedure was used in studies for the Hawaiian Islands (Schwarz 1963), the Yukon River in Alaska (U. S. Weather Bureau 1966b), and the Tennessee River drainage (Schwarz and Helfert 1969).

The western slopes of California mountains (HMR No. 36) are one of the better locations for use of the orographic windflow model for estimating PMP in winter. The Sierras form a barrier to stable moist air. A large number of representative rainfall measurements are available for checking the model. The west slopes of the Cascades (HMR No. 43), are almost as suitable for model calculations but have fewer rainfall measurements. Using the model in the interior of the Northwest, resulted in problems stemming mainly from short mountain ridges and complicated terrain.

In major storms, moisture transport into the Southwestern States involves less stable air than in the Northwestern States and the orographic model with its assumed laminar flow is less applicable. Much rainfall, as in the September 4-6, 1970 storm in Arizona and Colorado, results mainly from an effect called "stimulation" in earlier reports, that is, the initiation of non-laminar convection, including thunderstorms, by mountain slopes.

Because of these factors the orographic windflow model has limited use in estimating PMP for the Southwestern States, where it is more practical to base the estimation of orographic effects primarily on observed variations in precipitation and terrain.

3.1.2 Definition of Orographic Precipitation

In this report orographic precipitation for the general storm is defined as the excess over nonorographic precipitation, and includes stimulation. In this report orographic PMP also includes some local details that were omitted from the smooth convergence PMP index maps.

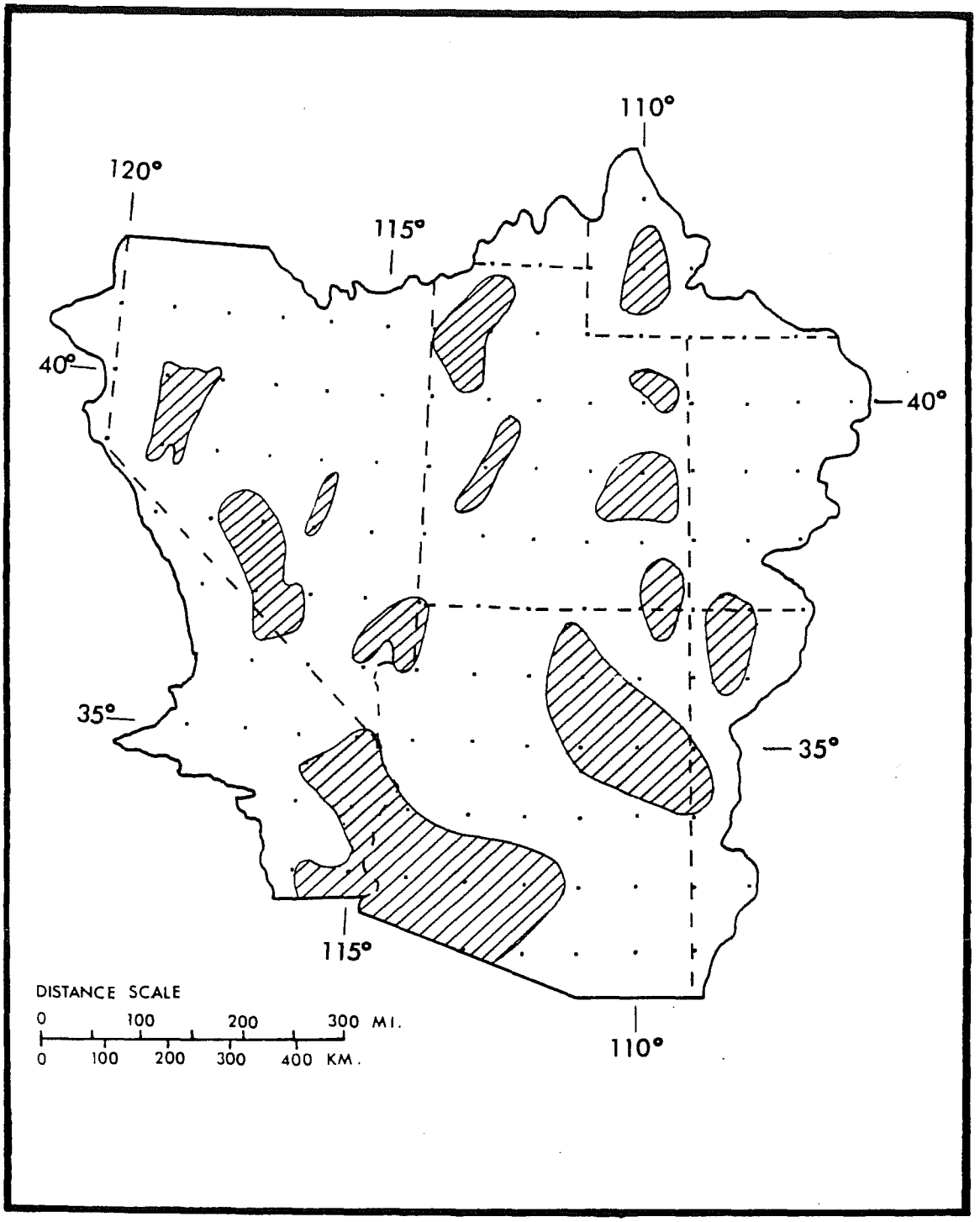

Figure 3.1.--Areas of minimum orographic effects in Southwest States.

3.1.3 Detail in Orographic PMP

Mean annual precipitation (MAP) charts[1] and rainfall frequency maps (Miller et al. 1973) show details quite closely related to terrain. This close a relation to terrain features may not be warranted for PMP. As the magnitude of a storm increases, the energy involved in the dynamic processes also increases and the effect of terrain features is less important.

Inadequate knowledge of the complex mechanisms involved in precipitation in mountainous regions also must be considered. Many of these problems were highlighted in papers presented at a symposium on precipitation in mountainous regions (World Meteorological Organization 1972).

In generalized PMP studies, effects of many wind directions, moisture sources, and storm types must be evaluated. This may be particularly important when small terrain features are considered. Factors pertinent to judging the proper amount of detail follow.

a. A single orographic index map was developed. This is a simplifying step that does not take completely into account differences in terrain effects due to month-to-month variation in moisture, wind, and height of freezing level. Use of a single index map using near highest moisture is a slight maximizing factor.

b. With a condensation level near the surface for the PMP storm, differences between lower and upper reaches of slopes become less than in ordinary storms. This reduces the detailed response to elevation.

c. From several empirical terrain-rainfall studies, discussed later, we concluded that in extrapolation to the general-storm PMP prototype, rainfall is intensified more on large, steep slopes than on smaller, gentler slopes. On the other hand, some regions (with minimum upwind barriers) where conditions are particularly favorable for orographic rainfall, the stimulation of rain at low levels (with a low condensation level in the PMP) may tend to decrease the gradient of rainfall on the slope.

Throughout development of orographic PMP several forms of topographic charts were used to identify primary terrain features. This information was transferred to, and final smoothing made on a 1:2,000,000 scale map. This scale was adopted for the final orographic index map.

---

[1]Charts considered were:

a. Normal Annual Precipitation (NAP) for New Mexico (State of New Mexico), Arizona (State of Arizona), Utah (State of Utah), and Colorado (State of Colorado) prepared by National Weather Service, NOAA for data period 1931-1960.

b. NAP for Upper Colorado River drainage (U. S. Geological Survey 1964) for data period 1921-1950.

c. MAP for southeastern Idaho prepared jointly by Soil Conservation Service and U. S. Weather Bureau (1965).

3.2 Orographic Index Map

Rainfall frequency analyses for the Western States have recently been developed by Miller et al. (1973). These analyses were based on multiple correlations relating precipitation to physiographic factors. The resulting charts thus qualitatively show variations that will also be present in the PMP. Following this reasoning, a first approximation of the 24-hr 10-mi^2 (26-km^2) orographic component to PMP was based on an estimate of the orographic component of the 100-yr 24-hr rainfall values.

The first approximation orographic index map was modified by considering a number of other precipitation/terrain effects to arrive at a finalized map. Figure 3.2 is a schematic of the procedure.

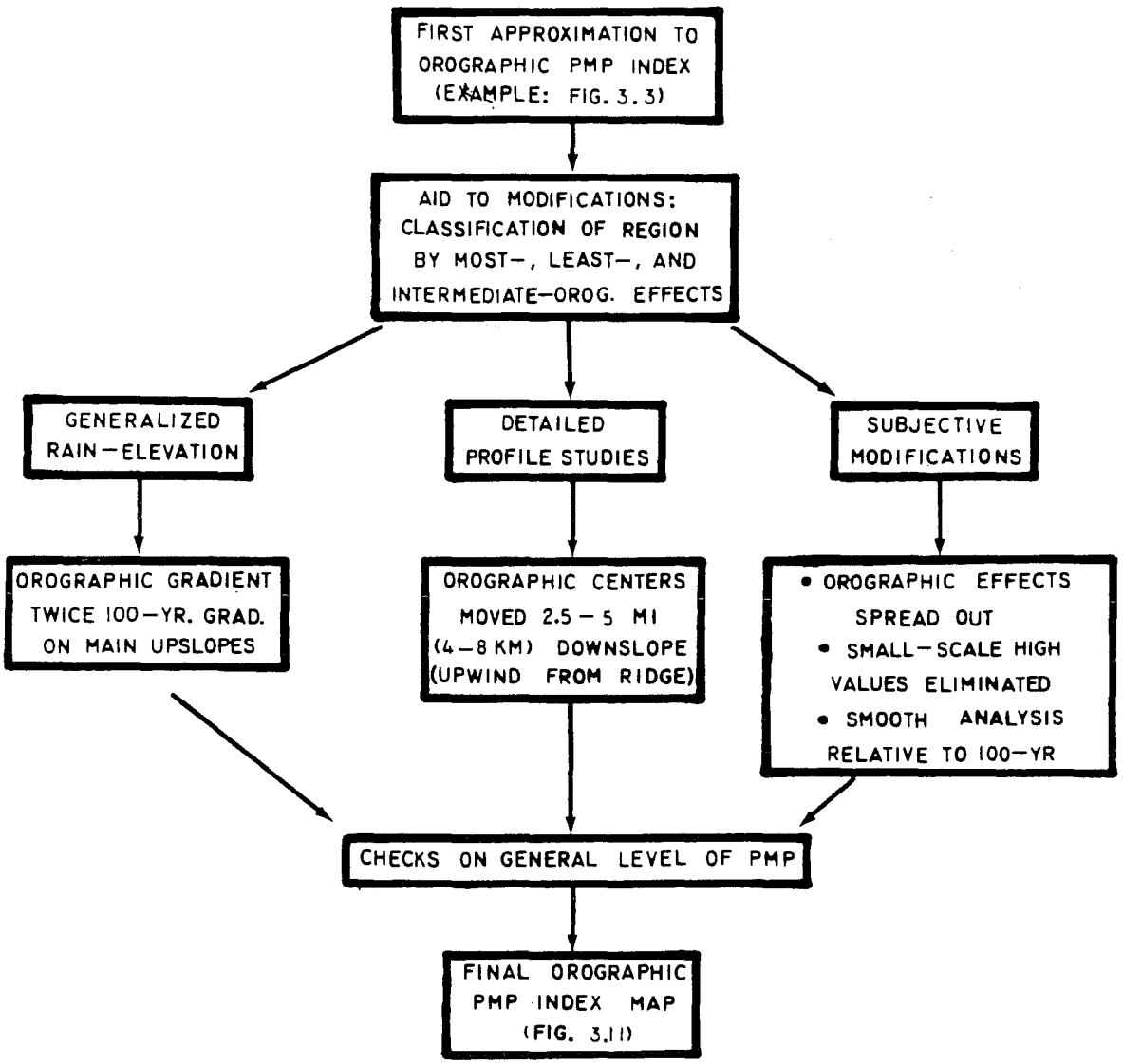

Figure 3.2.--Schematic of orographic PMP index map development.

3.2.1 Development of First Approximation

The 100-yr 24-hr rainfall of 4.0 inches (102 mm) over the nearly flat area of southwestern Arizona and southern California was assumed to be entirely convergence rainfall. Comparable convergence values over the entire Southwestern States were estimated by first applying reductions for effective barrier and elevation[1]. The total 100-yr 24-hr rainfall was then expressed as a percent of this convergence component. These percents (minus 100) are a preliminary approximation to orographic effects.

The convergence component of PMP has been shown to have a regional gradient (See section 2.2.6, and figures 2.5 to 2.16). An adjustment to the preliminary approximation to orographic effects incorporated a regional gradient. For the sake of simplicity, the August 1000-mb (100-kPa) convergence PMP was used as a single index map. This month was selected since a decadent tropical storm is the PMP prototype over much of the region. The preliminary approximation values were multiplied by the convergence PMP values adjusted for effective barrier and elevation. Figure 3.3 shows an example of the first approximation of the orographic PMP for central Arizona.

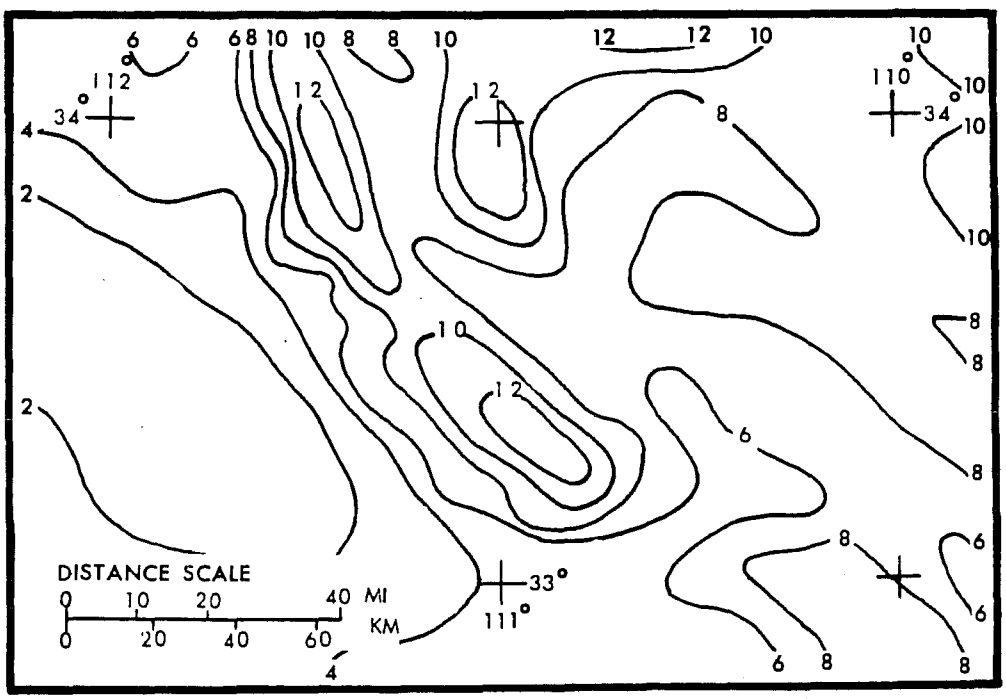

Figure 3.3.--A first approximation to the orographic PMP (inches) for 10 mi^2 (26 km^2) 24 hr in southeast Arizona.

[1]The effective barrier-elevation chart used was less smooth than the final version shown in figure 2.17.

Implicit in the procedure is the assumption that the orographic and convergence components of PMP have the same relation to each other as the relation between the orographic and convergence components of the 100-yr 24-hr rainfall each appropriately adjusted for elevation and barrier. We have thus estimated the orographic component of PMP utilizing the equation:

$$PMP_o = PMP_c \frac{100\text{-yr}_o}{100\text{-yr}_c}$$

where subscript "o" denotes the orographic component and "c" the convergence component of precipitation. Numerous departures from this assumption were made through modifications discussed in the following sections.

3.2.2 Guidance to Modification

The result of several studies using various data gave guidance to modifying the first approximation to the orographic PMP index.

3.2.2.1. Rain Ratios for Line Segments. We first cover the variations of rainfall along lines or segments across major ridges. Figure 3.4 shows the segments selected for the study region and figure 3.5 shows the segments for Arizona. This last figure also shows the 100-yr 24-hr rainfall. In addition to 100-yr and 2-yr 24-hr values, storm rainfall and normal annual precipitation were considered.

For each of the line segments, we determined the rain ratio or the change in rainfall per 1000 feet (305 m), divided by the low-elevation rainfall. For example, if along a line segment the 100-yr 24-hr rainfall is 2.0 inches (51 mm) at the base and 4.0 inches (102 mm) at the ridge with a 4,000-foot (1,219-m) difference in elevation, the rain ratio is 0.25, or $\frac{4.0-2.0}{4}/2.0$. This rain ratio is an index of the variation of rainfall with elevation, related to the low-elevation value.

Various rain ratios for this study region and the Northwest States (HMR No. 43) were determined. These ratios are summarized in table 3.1. Rain ratios for the Northwest States in table 3.1a were computed for the orographic PMP index values and 100-yr 24-hr rainfall for various regions with significant orographic effects.

The rain ratios for the segments in figure 3.4 are summarized in table 3.1b, for two rainfall categories; 100-yr 24-hr, and mean annual precipitation. The high 100-yr 24-hr average ratio for southeast California implies low values of rainfall at the beginning point of many of the segments. The large rain ratios from the mean annual precipitation, compared to those for the 100-yr rainfall, are due to the greater frequency of rains at higher elevations. Adjustment of the mean annual precipitation rain ratios for frequency would make them more nearly similar to those for the 100-yr 24-hr rainfall. The comparisons with HMR No. 43 indicate that PMP ratios ought to be larger than 100-yr rain ratios for areas of significant upslope.

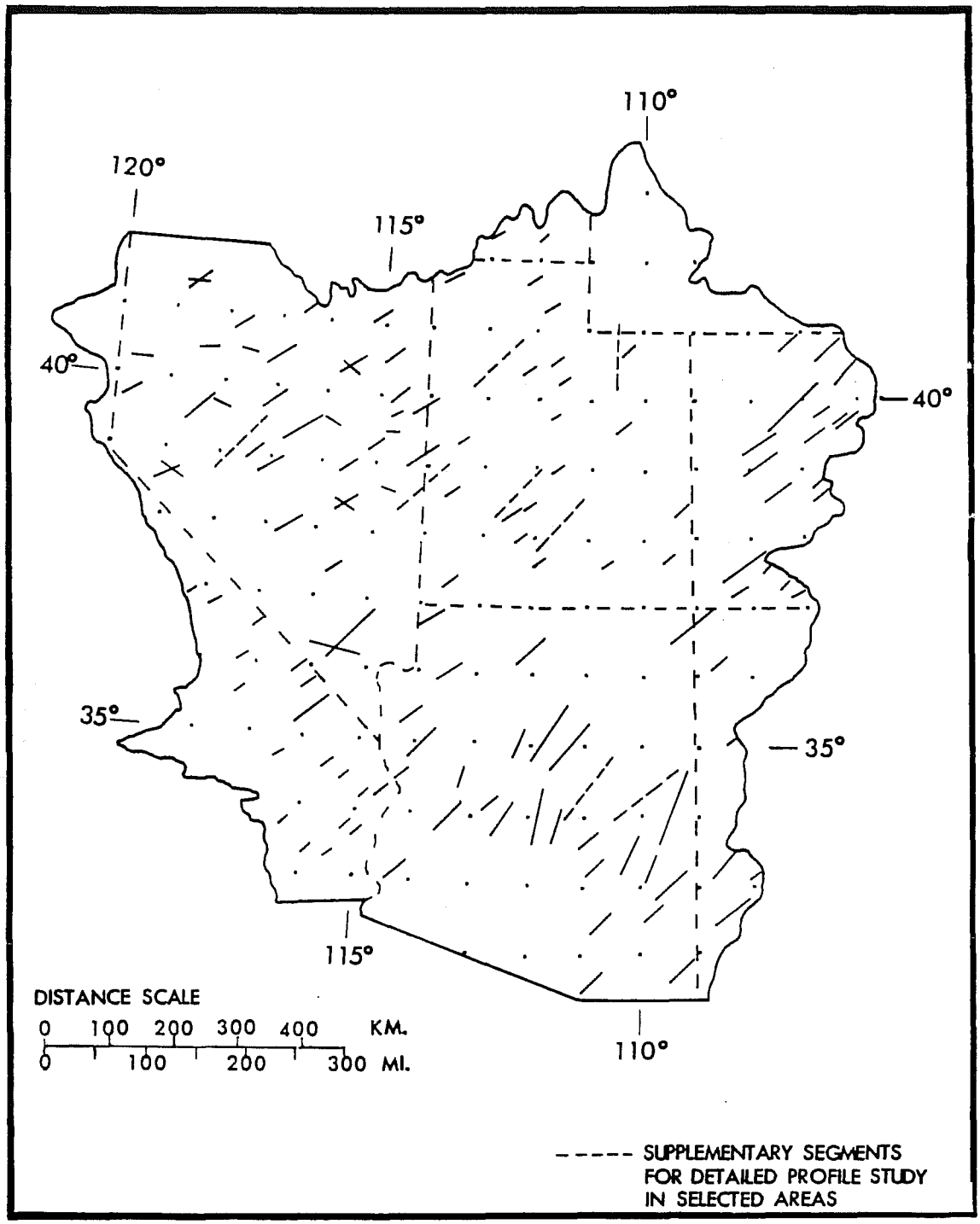

Figure 3.4.--Segments across major ridges in Southwest States used in rain ratio study.

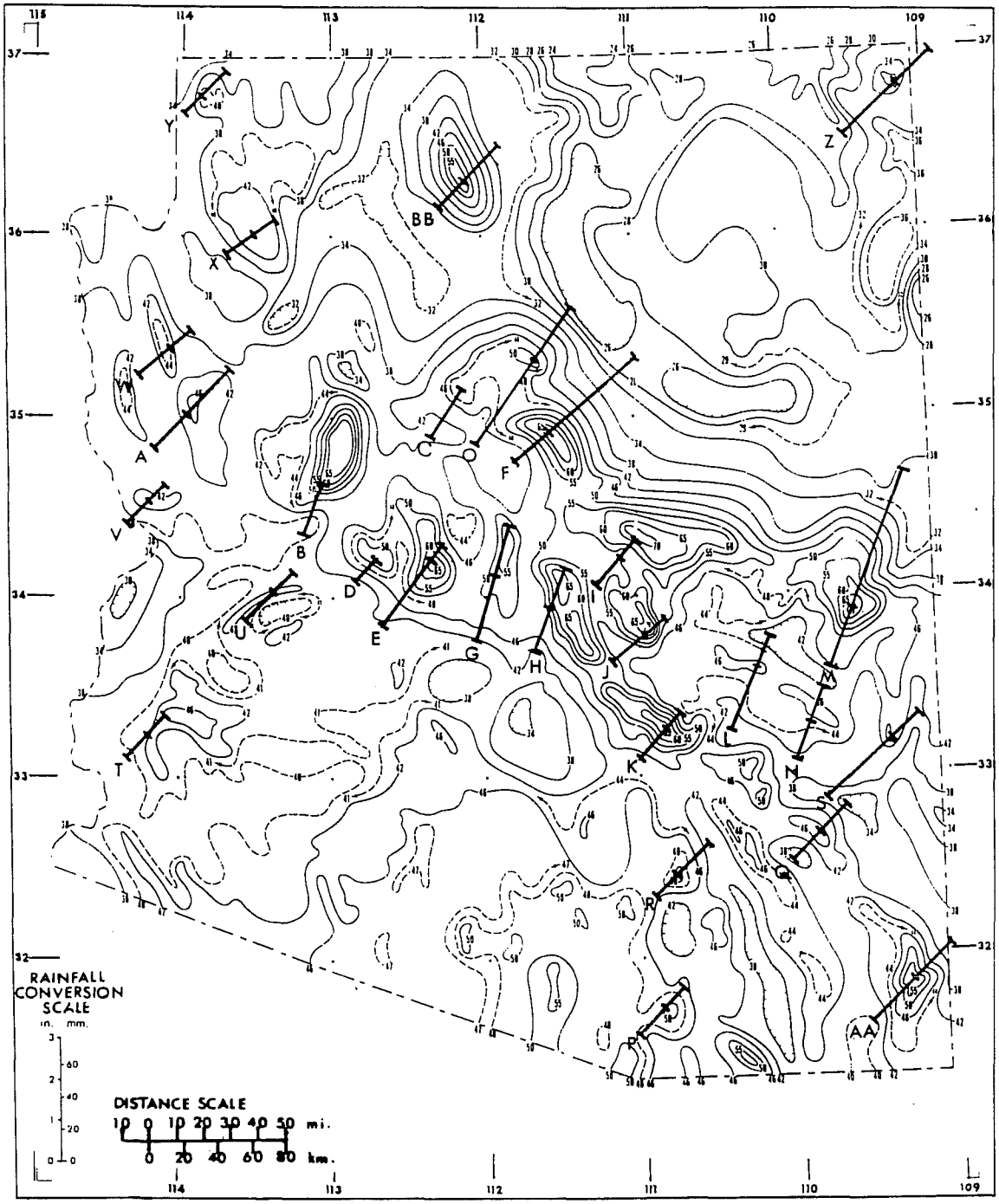

Figure 3.5.--Segments across major ridges in Arizona superimposed on analysis of 100-yr 24-hr precipitation (in tenths of an inch).

Table 3.1.--Summary of average rain ratios [change in rainfall per 1000-ft (305-m) elevation difference divided by low-elevation rainfall]

State or portion of State	Average ratio for segments in indicated region for:		
	Mean annual precipitation	100-yr 24-hr	Orog. PMP index (HMR No.43)
a. Northwest States			
Montana (W. of Continental Divide)		.13	.34
Western Washington		.15	.61
Eastern Washington		.21	.47
Southwest Idaho		.09	.82
Northern Idaho		.14	.98
b. Southwest States			
Arizona	.26	.07	
Utah	.46	.10	
Nevada*	--	.12	
Western New Mexico	.56	.10	
Southeast California*	--	.22	
Western Colorado	.39	.12	
Mean	.42	.12	

*The available MAP chart for Nevada did not provide an isohyetal analysis that could be used for computing rain ratios. The southeast California MAP was considered too uncertain in orographic areas for computing reliable ratios.

One other set of rain ratios is shown in table 3.2. This compares the average rain ratios (as previously defined) for 9 selected segments (B, D, E, F, G, H, I, J, K in fig. 3.5) which had considerable rain in the August 1951 and September 1970 storms, with the ratios for the 100-yr 24-hr rainfall. These data show that rainfall from the 2 storms was affected more by the slopes than the 100-yr 24-hr rainfall (rain ratios of 0.31, 0.21 and 0.11, respectively, for the September 4-6, 1970, August 25-30, 1951 and 100-yr 24-hr rainfalls).

Table 3.2.--Average rain ratios for 9 selected upslope segments in Arizona (B, D, E, F, G, H, I, J, K in fig. 3.5).

Source	Ratio
100-yr 24-hr rainfall	.11
August 25-30, 1951 rainfall	.21
September 4-6, 1970 rainfall	.31

3.2.2.2 Rain Ratios for Central Arizona. Other sets of data analyzed were for the prominent slopes north and east of Phoenix. Figure 3.6 is a map of the region with generalized contours and precipitation stations. Figure 3.7 shows the rainfall for these stations during the August 25-30, 1951 and September, 4-6 1970 storms, plotted vs. station elevation. An eye-fitted curve is shown for the August 1951 storm data. If one computes the rain ratio of the curve in figure 3.7, a value of 0.28 is obtained (1.05 in. per 1000 ft/ 3.7 in.)

Rains of one month or longer could be useful for guidance on rain-elevation relations for this same region (fig. 3.6.) We used mean July to September rainfall after adjusting it by a frequency-of-rain vs. elevation relation (not shown). The resulting rain ratio was 0.18, not greatly different from the approximate 0.28 of figure 3.7 for the August 1951 storm and the average rain ratio of 0.21 in table 3.2 for the same storm.

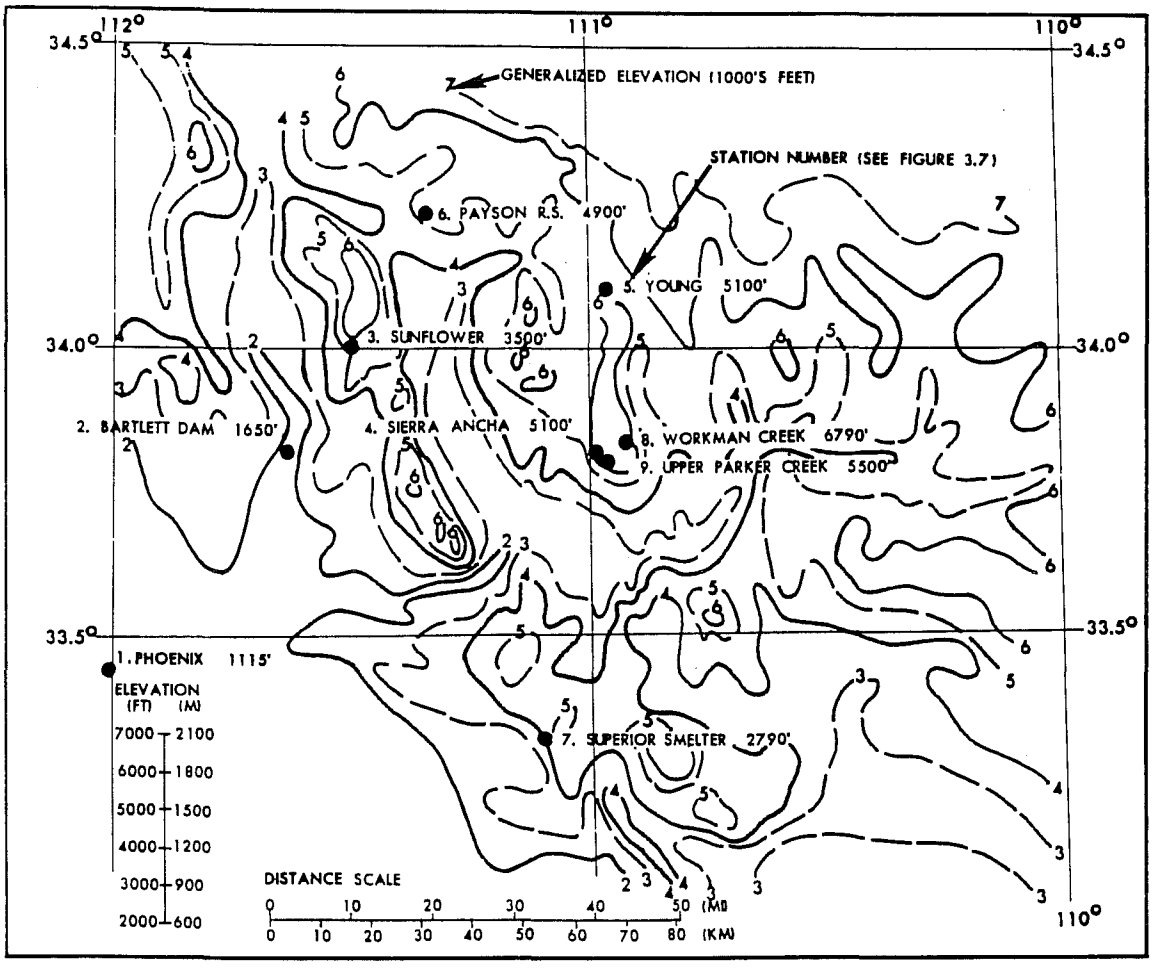

Figure 3.6.--Generalized topography and station locator map in vicinity of Workman Creek, Arizona.

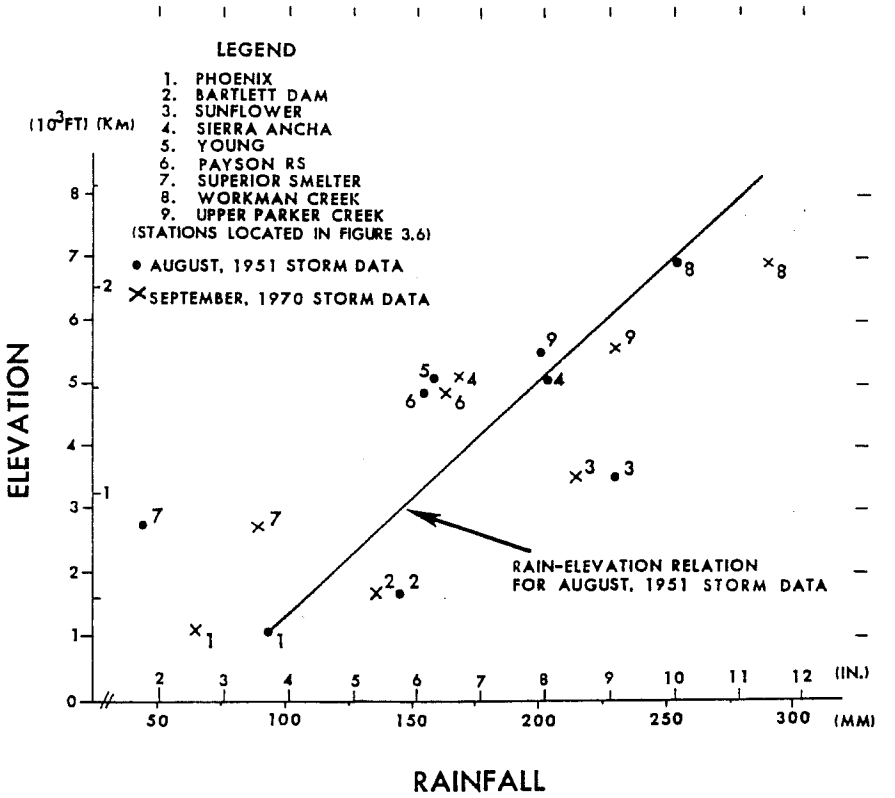

Figure 3.7.--Rainfall-elevation relation for August 1951 storm, and rainfall for September 1970 storm.

For maximum monthly rains in the same region, the variation with elevation is not as closely tied to the frequency of rains. The air in such months would tend to be more nearly saturated at low elevations, (as with the rains for the PMP-type storm), in comparison to mean monthly rainfall cases. With the above in mind, a relation between rain increases and elevation for warm-season maximum monthly rain was developed. These rains give a rain ratio of about 0.19. This appears to give reasonably good agreement with the rain ratio from major storms that are the prototype for the PMP in this portion of the study region.

3.2.2.3 Effects to Lee of Ridges. The decrease of rainfall to the lee of a major ridge in Arizona for each of the two important warm-season PMP-prototype storms of August 1951 and September 1970 was compared to the decrease in the 100-yr 24-hr rainfall. The rainfall along a line through the rainfall centers extending leeward normal to the ridge is the basis for the comparison. Figures 3.8a to 3.8c show the analyzed isohyets and figure 3.9 shows the comparisons.

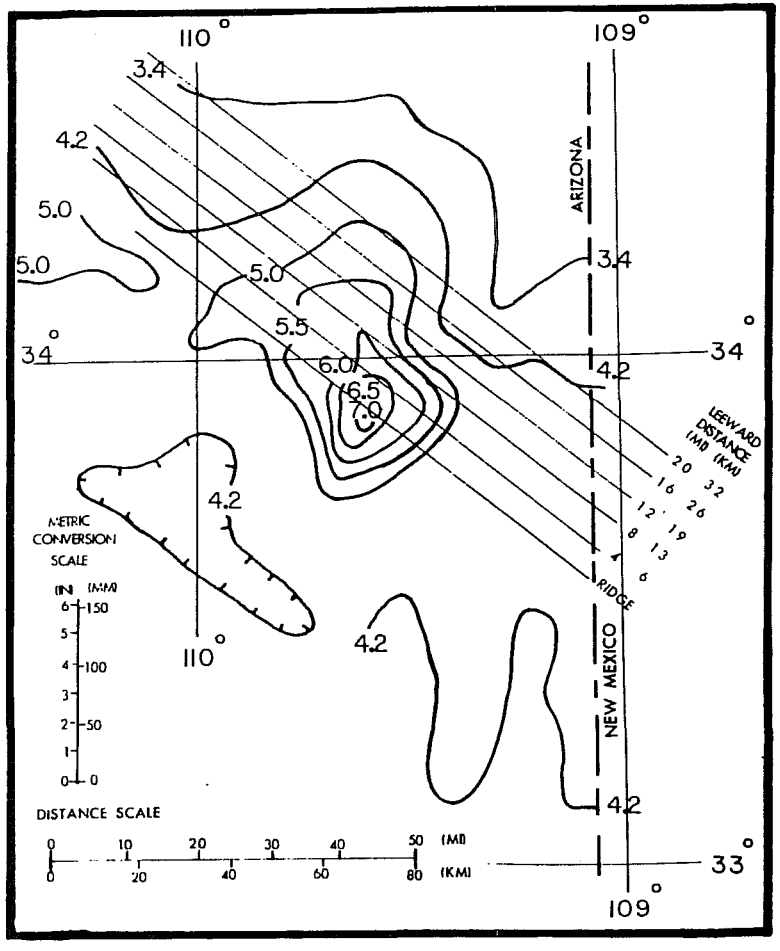

a. *100-yr 24-hr rainfall*

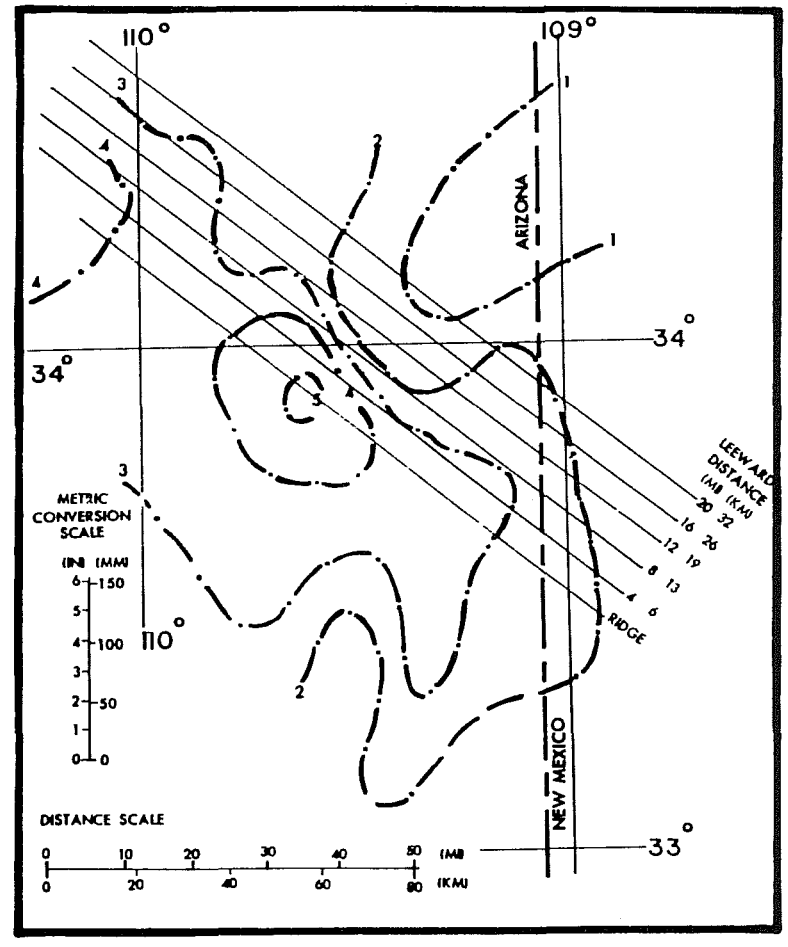

b. *August 1951 storm.*

Figure 3.8.--Leeward isohyetal patterns.

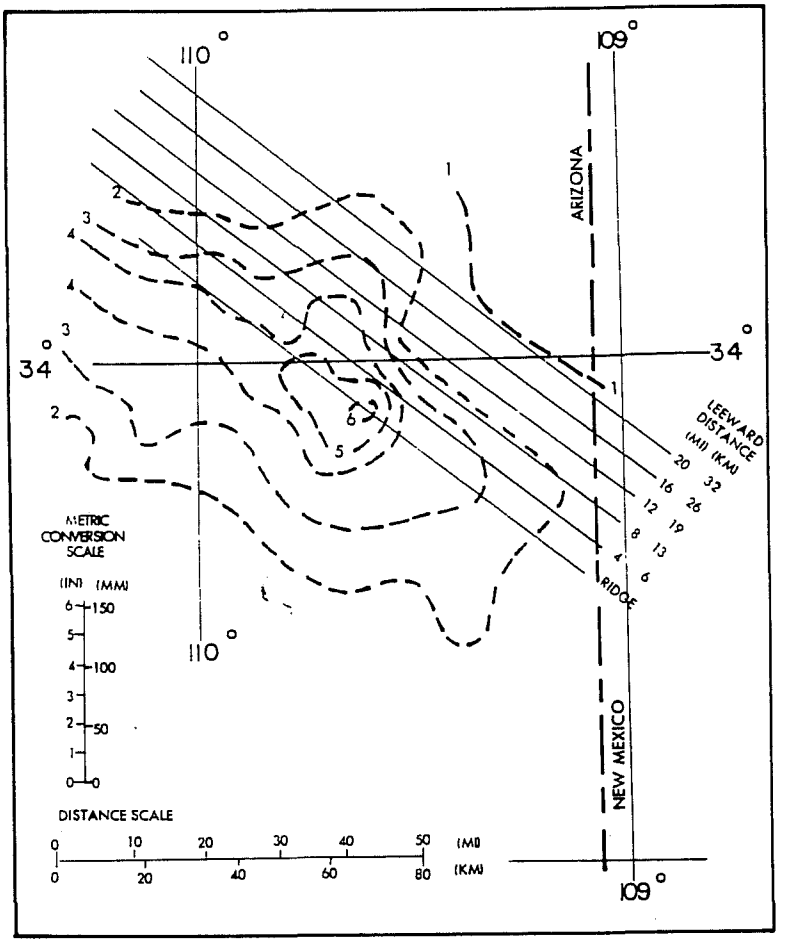

c. September 1970 storm.

Figure 3.8.--Leeward isohyetal patterns.

The storm rainfall (both August 1951 and September 1970) decreases more rapidly to the lee than the 100-yr 24-hr rainfall. This result should not be surprising. The 100-yr rainfall is probably made up of isolated storms to the lee of the major ridge. In contrast, the two major storms provided rain over a large region and were associated with inflow from a southerly direction, across the ridge which would decrease the rainfall to the lee.

3.2.2.4 Summary

a. For areas of pronounced orographic uplift, the gradients of PMP should be approximately double that shown by the 100-yr 24-hr precipitation. This is supported by the comparisons of rain ratios of the 100-yr 24-hr precipitation with those of large general storms (table 3.2).

b. To the lee of ridges, PMP should decrease faster with distance than the 100-yr 24-hr rainfall values.

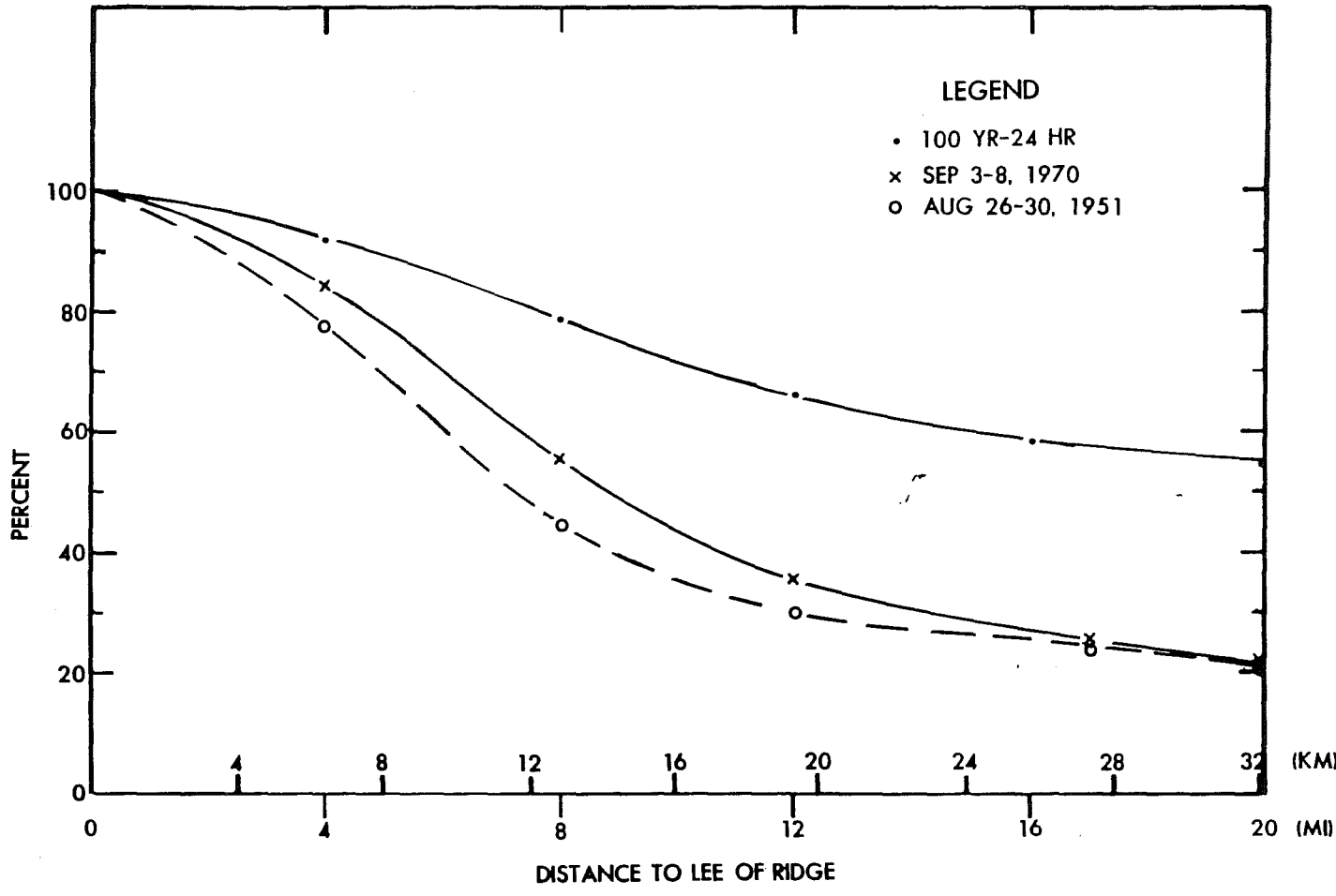

Figure 3.9.--Leeward rainfalls in percent of ridge value for major storms and 100-yr 24-hr rains. Based on fig. 3.8.

c. Mean monthly or mean annual precipitation maps exaggerate orographic effects because of a greater frequency of rains at higher elevations. Such maps should be used with caution as guidance to PMP distribution.

3.2.3 Modifications to Index Map

The guidelines summarized above and other aids, were used to modify the first approximation to the orographic PMP index. For such modifications it was expedient to first classify the region into three terrain categories: areas with (1) most- (2) least- and (3) intermediate-orographic effects.

3.2.3.1 In Areas of Most-Orographic Effects. The most important guideline for these areas was to try to make the gradient of total PMP about twice that of the 100-yr 24-hr rainfall. Additional detailed analyses in prominent upslope regions (see example in fig. 3.10) resulted in the rule of moving orographic rainfall centers from 2.5 miles (4.0 km) to 5.0 miles (8.0 km) downslope from the ridgelines. This helped meet the criterion for the gradient of PMP to be twice that of the 100-yr 24-hr rainfall. In some terrain, i.e., where the ridges are small or close together such rules do not apply.

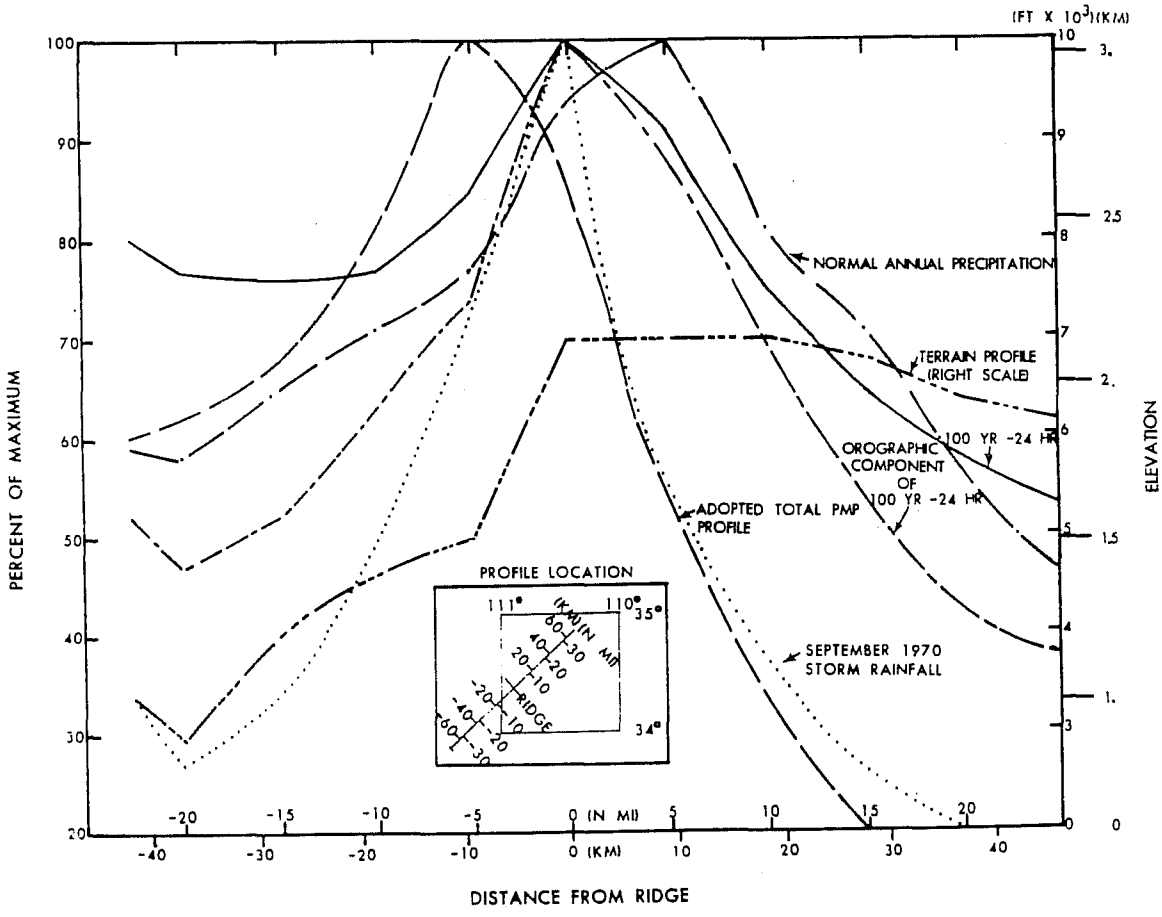

Figure 3.10.--Example of profiles of several rainfall indices (in percent of maximum values).

The objective procedure of moving the orographic center downslope was also, in some instances, largely negated by the subjective increases for nearby slopes facing differing directions. Maintaining an allowance for stimulation on the lower slopes also tended to negate the initial aim of doubling the upslope gradients of the 100-yr 24-hr precipitation.

3.2.3.2 In Areas of Least-Orographic Effects. A map of least-orographic areas was useful in establishing limits to orographic precipitation gradients, delineating sheltering effects, and providing guidance in modifying the first approximation orographic index map. Figure 3.1[1] integrates the independent interpretation of least-orographic areas by three meteorologists in accord with the following guidelines:

a. Areas where mean annual precipitation was less than 8 inches.

b. Areas where the first approximation to an orographic index map showed less than 10% increase over the convergence component developed for August in chapter 2.

c. Areas where the orographic component of total PMP from the method described in section 5.7 was less than 50% greater than the convergence component.

For the Southwest States a lower limit of 1.0 inch (25 mm) orographic PMP in 24 hours was set in least-orographic regions. Such rainfall in these regions is attributed to either spillover from upwind ridges or to a generalizing (spreading out of the influences of small ridges or hills that make up a part of most areas classified as least-orographic.

Within portions of the outlined least-orographic areas, the threshold of 1.0 inch (25 mm) in 24 hours was increased. For example, rainfall gradients to the lee of upwind ridges at times suggested higher values. In effect, the original areas of least-orographic rainfall, figure 3.1, were decreased in size and their bounds smoothed.

3.2.3.3 In Areas of Intermediate-Orographic Effects. Intermediate orographic areas were those remaining after areas of most- and least-orographic effects were considered. The intermediate areas are usually a mix of nearly flat areas with enough small orographic features to preclude classification as least orographic.

The following factors should be kept in mind in connection with the intermediate areas.

a. With light winds predominating in ordinary rain situations (producing values contributing significantly to MAP charts and lesser values in the series of precipitation amounts used in developing frequency maps), the effect of small orographic features are overly emphasized relative to what one can expect from strong winds in a PMP storm situation.

[1]Note that figure 3.1 differs somewhat from least-orographic regions of figure 2.1. The latter was influenced by availability of station rainfal data.

b. With the varying wind directions possible in PMP storms, orographic effects can be spread out in numerous directions from small areas that act as foci (or stimulation points) for rainfall.

To get away from the overemphasis of orographic effects (point a.), the overall orographic precipitation increase for a particular orographic feature was reduced by 50%. However, a compensating feature stemming from point b. was to spread influences from foci or orographic increases over a larger area. We increased by fourfold the area influenced by small orographic features.

3.2.3.4 Other Modifications

a. Isohyetal peak rainfall centers in the most-orographic regions, covering areas of up to about 100 mi^2 (260 km^2), were eliminated. Most indices of rainfall have a built-in increase with elevation derived from depending too closely on MAP. Where peak MAP values over small areas are supported by data, we feel they must be due to ordinary rains as compared with the strong diversion of air that must take place in major storms.

b. Additional smoothing was done in areas where 100-yr 24-hr rain values were low and had a small range (2.2 to 2.8 inches, 56 to 71 mm). We believe the small range in 100-yr values indicated such smoothing as realistic. This was done regardless of orographic classification.

3.2.4 Modified Orographic PMP Index MAP

Figures 3.11 a, b, c and d are the adopted orographic PMP index maps covering the Southwest States. Figure 3.11a covers the northernmost portion (down to latitude 40°N) while figure 3.11d covers the southernmost portion with figures 3.11b and 3.11c covering the intervening region. The maps overlap by one degree of latitude. This index is for 24 hr 10 mi^2 (26 km^2). Linear interpolation may be used between the isolines for obtaining an average index over a basin. However, within any closed high or low center, the value of the last enclosed isoline should be used.

The remainder of this chapter covers extension of orographic PMP to all 12 months, to durations from 6 to 72 hours and basin sizes from 10 to 5000 mi^2 (26 to 12,950 km^2).

3.3 Seasonal Variation

3.3.1 Introduction

Seasonal variation of PMP is always difficult to define because the rainfall sample is increasingly limited.

For the Western States the problem is especially difficult because of complicated terrain influences which do not permit direct transposition of storms. The approach adopted for the Southwest States was to tie into the seasonal variations of HMR No. 43 and 36 near the boundaries and utilize various rainfall indices within the region.

3.3.2 Boundary Regions

Seasonal variation for the Northwest States (HMR No. 43) is given for the months October through June. A separate variation was determined for each of four zones, three of which border our study region. Elevation plays a part in differentiating among the zones.

By analysis of station maximum observation-day precipitation of record, the seasonal variations for the three zones were smoothly extended through the remaining 3 months. Percent of the August values for each month are shown in table 3.3.

Table 3.3.--Seasonal variation east of Cascade Ridge in Northwest States as percent of August

Zone in HMR No. 43	Jan	Feb	Mar	Apr	May	Jun	Jul	Aug	Sep	Oct	Nov	Dec
B	91	91	95	87	74	67	84	100	107	108	107	104
C (5000 ft) (1524 m)	92	92	91	94	98	97	98	100	100	100	99	96
D	90	90	90	95	100	100	100	100	100	98	97	94

The seasonal variations of HMR No. 43 stress winter maximum values west of the Cascade Ridge and in a region to the east of the ridges (Zone B). May through October are the maximum months near the eastern borders of the Columbia River drainage (Zone D). Between these is a transition zone with a maximum from late summer to early winter; the importance of winter maximum increasing with elevation in zone C.

From HMR No. 36, the seasonal variation for the west slopes of the Sierras is adopted for use at the western border of the Southwest Region. Again it was necessary to extend the seasonal variation given there throughout the year or over the months of May through September. Maximum observation-day precipitation amounts for high elevation orographic stations were used for this extension. The results in percent of August are shown in table 3.4.

Table 3.4.--Seasonal variation in Pacific drainage of California as percent of August

Jan	Feb	Mar	Apr	May	Jun	Jul	Aug	Sep	Oct	Nov	Dec
106	106	102	97	91	91	96	100	103	104	104	105

FIGURE 3.11b (Revised) — 10-mi² (26-km²) 24-hr orographic PMP index map (inches), north-central section.

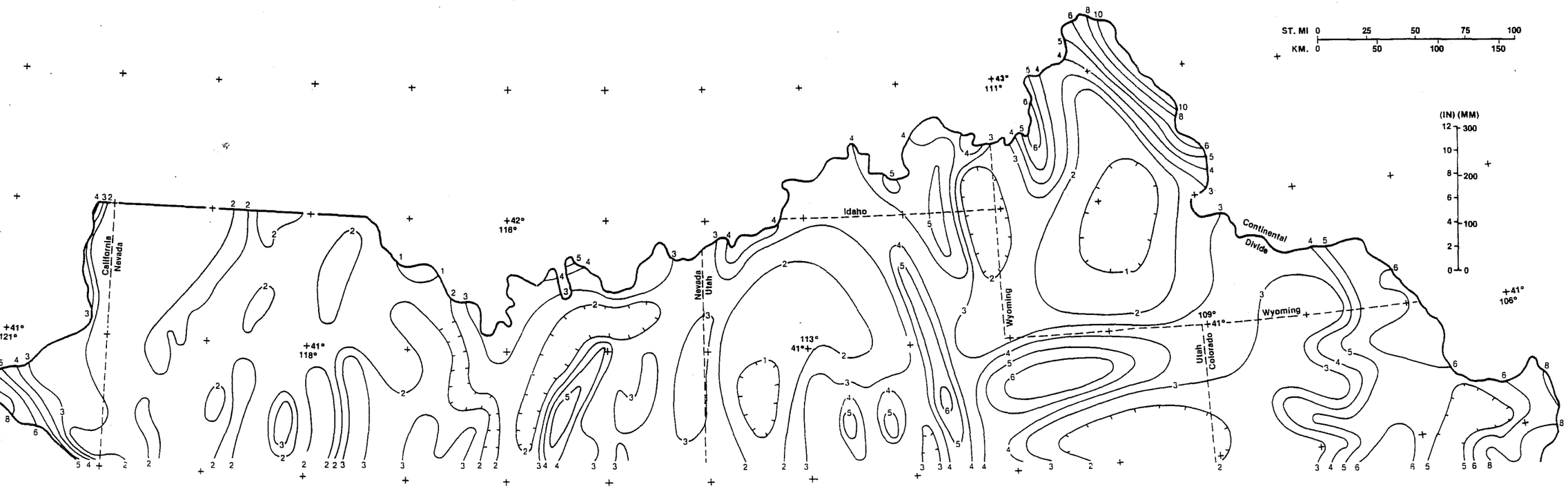

FIGURE 3.11a (Revised) — 10-mi² (26-km²) 24-hr orographic PMP index map (inches), northern section.

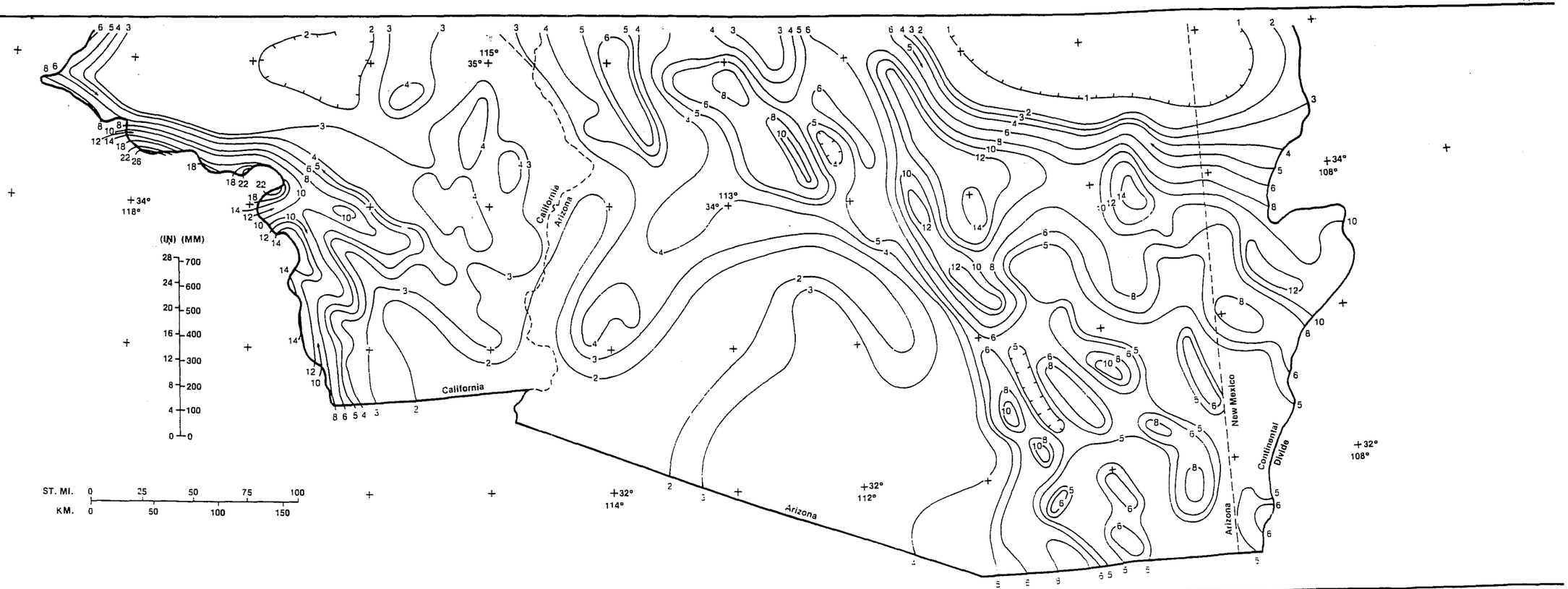

FIGURE 3.11d (Revised) — 10-mi² (26-km²) 24-hr orographic PMP index map (inches), southern section.

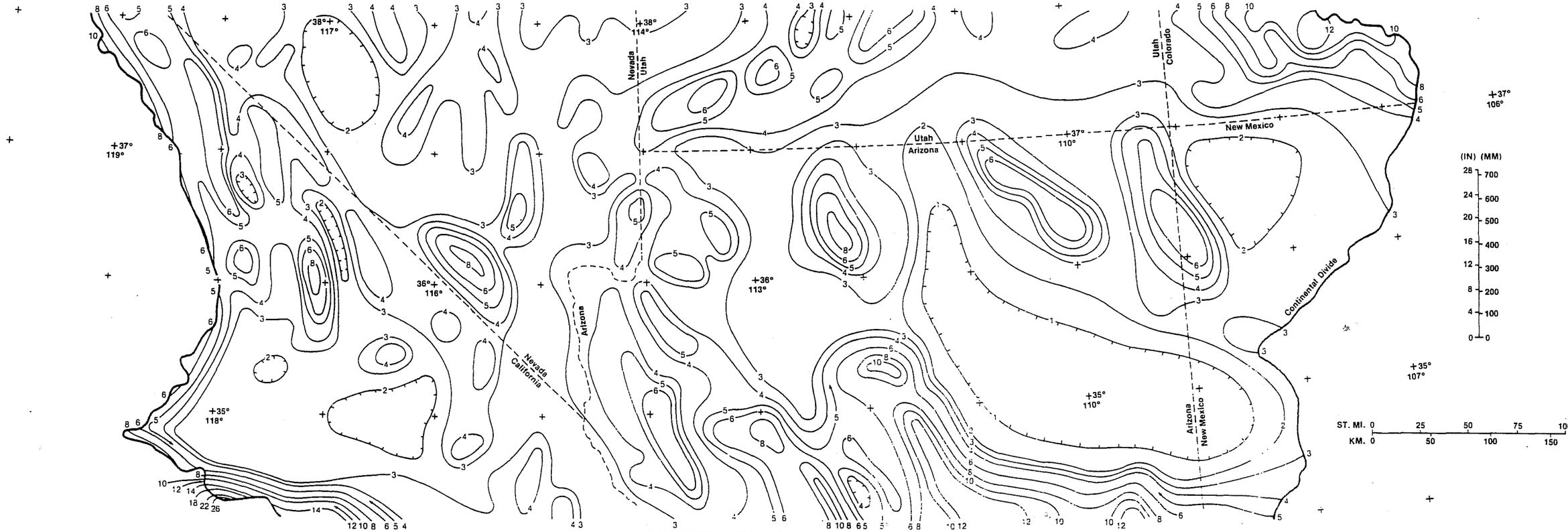

FIGURE 3.11c (Revised) — 10-mi² (26-km²) 24-hr orographic PMP index map (inches), south-central section

3.3.3 Indices Within the Region

3.3.3.1 Maximum Precipitation at High Elevations. On the mountain slopes north and east of Phoenix, Ariz. the maximum observation-day rainfalls of record for seven stations for each month of record were averaged. Highest average values were equal for August and September. Lowest values (61% of highest) were in May. Use of these data as an index to seasonal variation of orographic precipitation assumes either that the precipitation is entirely orographic or that the seasonal variation is the same as that for convergence precipitation. Probably these stations come closer to being an index to orographic variation than any other stations in the Southwestern States where the terrain is more broken and complex. It would also assume no regional variation in the pattern of seasonal variation.

The seasonal variation of maximum observation-day precipitation (by month) was further evaluated at high-elevation stations at various locations in the Southwest States. In northern Nevada, a seasonal plot of the data showed a fall maximum with relatively little variation through the winter. In southwestern Wyoming and extreme northeastern Utah, spring maximums predominate with a secondary maximum in early fall. Stations in Colorado north of about 39° N indicate a broad summertime maximum extending from June through September. These data, when averaged, gave an estimate of seasonal variation near the center of the region (the northern border of Arizona.) July, August, and September gave about equally high values. The lowest values, in May and June, averaged 80% of summer.

3.3.3.2 Maximum Winds and Moisture. A physical index of intensity of orographic precipitation at a given location is the product of the strength of the horizontal wind normal to the mountain and the moisture content of the air column. This index was evaluated seasonally from upper-air observations at Tucson, Ariz.

From the twice-a-day observations (1956-69) a series of maximum southerly wind components were determined for each month for the 900-, 700-, 500-, and 300-mb (90-, 70-, 50-, and 30-kPa) levels. The 0.01 probability southerly components were then computed using the log-normal distribution. These monthly wind components were then expressed in percent of the highest value of the 12 months for each level.

Precipitable water through the 300 mb level associated with the maximum 12-hr persisting 1000-mb (100-kPa) dew points assuming a saturated pseudo-adiabatic atmosphere for each month at Tucson were also expressed in percent of the highest value. Multiplication of the percentages of wind and moisture for each month gives an index to the magnitude of moisture transport. The highest value of this index was about the same for August through October. December through May averaged 78%.

3.3.3.3 Orographic Model Computations. The detailed orographic precipitation computation model described in HMR Nos. 43 and 36 was applied to 10

profiles in a steep upslope region. Five of these were north-south slopes north of Phoenix; the others were SW-NE slopes near the same location. Input to the model were maximum winds at Tucson described previously and moisture based on maximum 12-hr persisting 1000-mb (100-kPa) dew points. The computed precipitation for the 10 slopes was used as another seasonal index to orographic PMP. September gave the highest orographic precipitation of the 12 months followed by October (92% of September) and July (81%). December and January were the months of lowest values (68% of September).

3.3.4 Smoothed Maps

Recommended seasonal variation of orographic PMP is provided by mid-month maps, figures 3.12 to 3.17, showing isolines of percent of the orographic index. The several different indices discussed were used as guidance in these analyses. The maps have been adjusted to yield smooth seasonal curves at grid points covering the region.

3.3.5 Supporting Evidence

Division of total storm precipitation into two components (convergence and orographic) is uncertain; therefore, direct use of rainfall data to check the seasonal variation of orographic PMP was not attempted. We prefer to evaluate the seasonal variation of <u>total</u> PMP as determined from the criteria developed.

Twenty-four-hr 10-mi^2 (26-km^2) PMP for each month was computed for each point on a 1° grid covering the Southwestern States. The regional pattern of month of maximum is shown in figure 3.18. June gives maximum total PMP for a small portion of the northeast corner of the Southwest. Winter or fall months dominate the northwest portion. The tropical cyclone during August and September dominates three-fourths of the Southwestern States.

In recorded history only a small number of such storms have had important effects on the Southwestern States, mainly Arizona. The storms of September 1939, October 1911, August 1951, and September 1970 were most intense.

A map was plotted (not shown) that presented a composite of all pertinent tropical storm rainfalls greater than 2.0 inches (51 mm), regardless of duration. A large void in tropical cyclone rainfall existed across most of Nevada eastward to the Wasatch Mountains in Utah. Yet, composite weather maps for some of the tropical storm situations suggest that at some time in the future, only slight changes in synoptic features could bring tropical cyclone-related rainfall into nearly all of Utah and much of Nevada. The infrequency of this storm type means a very long record is needed to delineate the effects of such storms.

Checks were also made from more commonly observed precipitation. One analysis of the month of maximum 24-hr station precipitation in the Western States appears in a study by Pyke (1972). His analysis of these data revealed that much of the Southwest experienced a bimodal distribution of precipitation. Figure 3.19 shows Pyke's results, where the season and

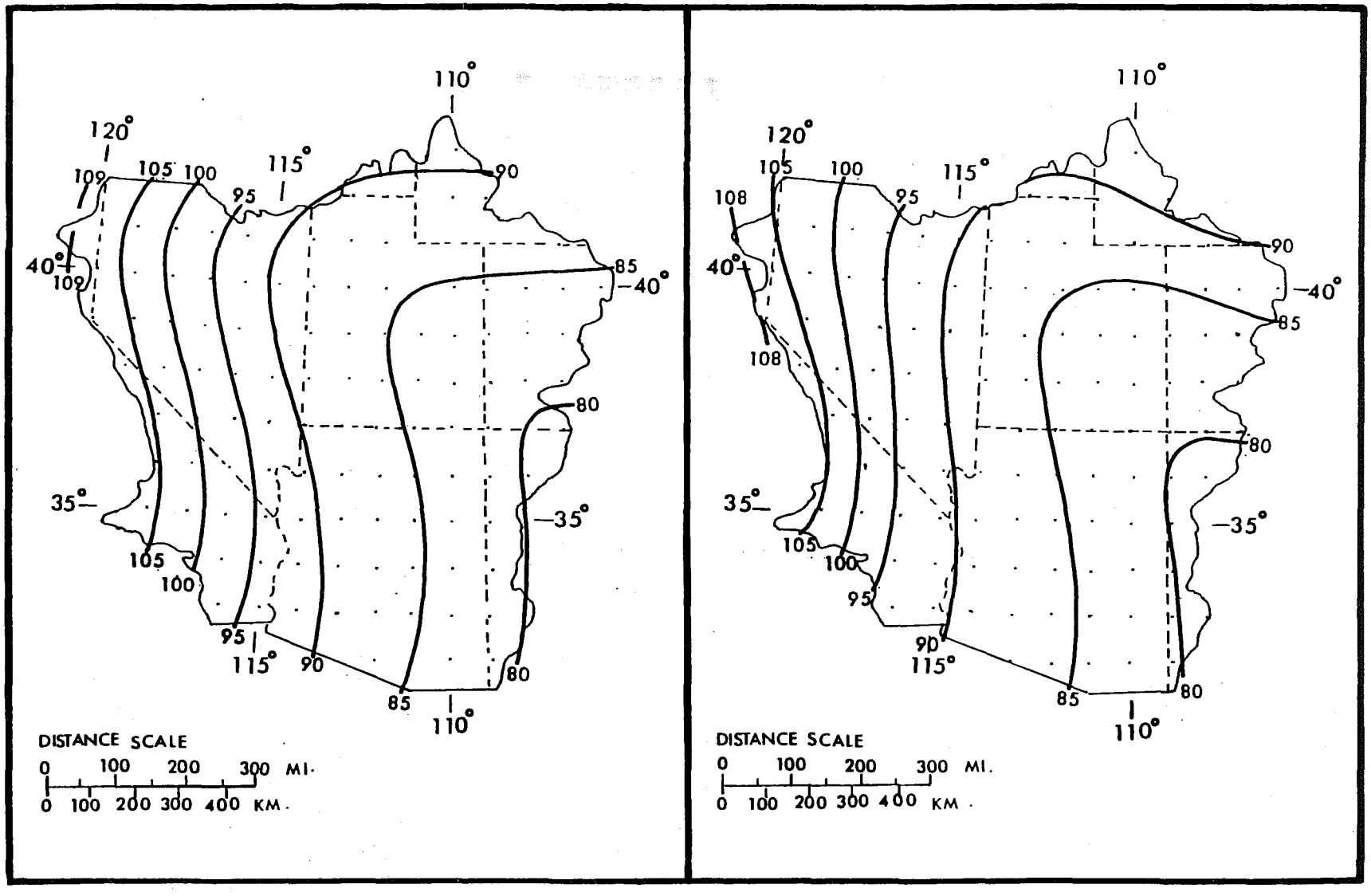

Figure 3.12.--Seasonal variation in 10-mi^2 (26-km^2) 24-hr orographic PMP for the study region (in percent of values in figure 3.11).

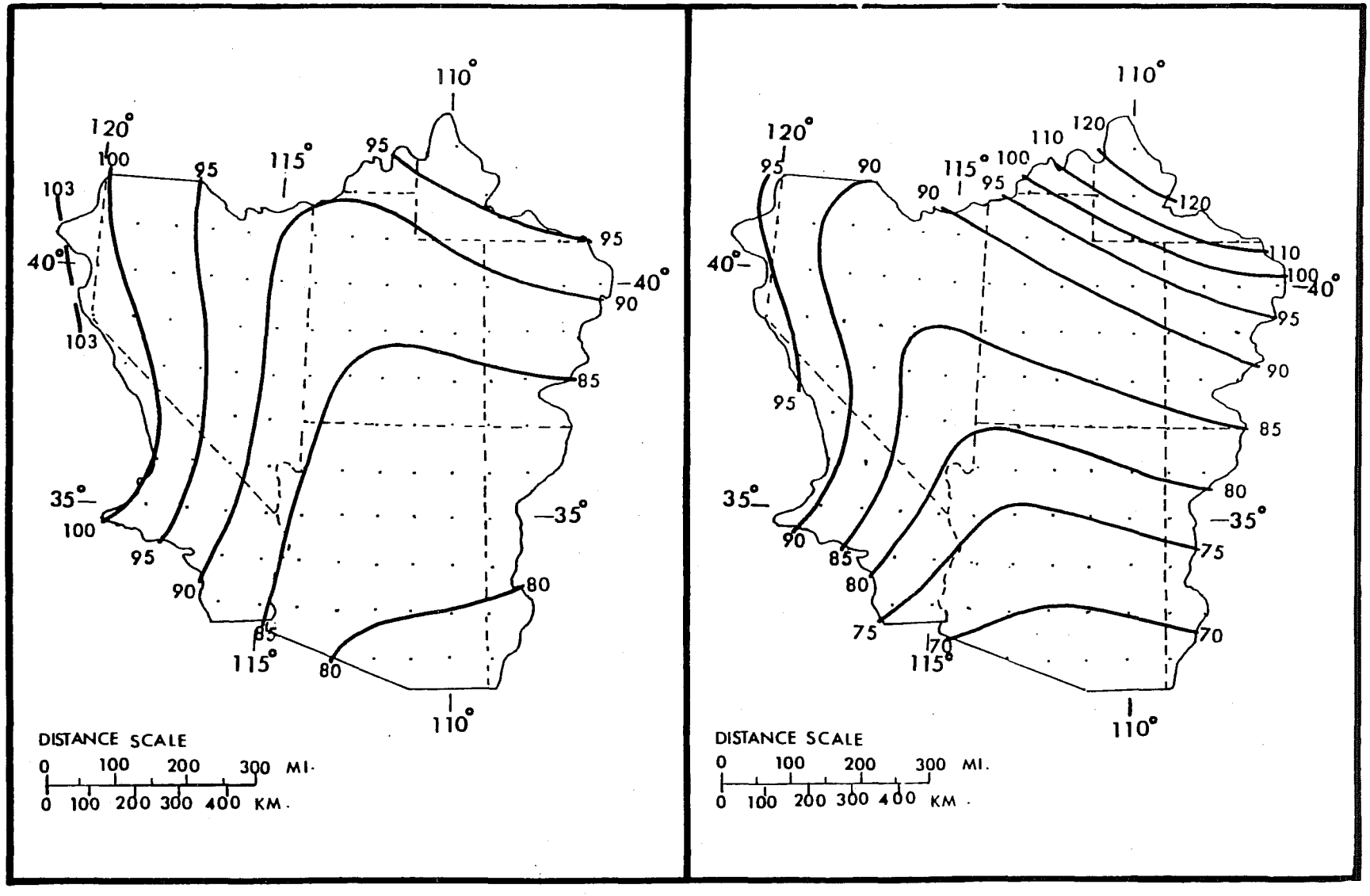

March *April*

Figure 3.13.--Seasonal variation in 10-mi^2 (26-km^2) 24-hr orographic PMP for the study region (in percent of values in figure 3.11).

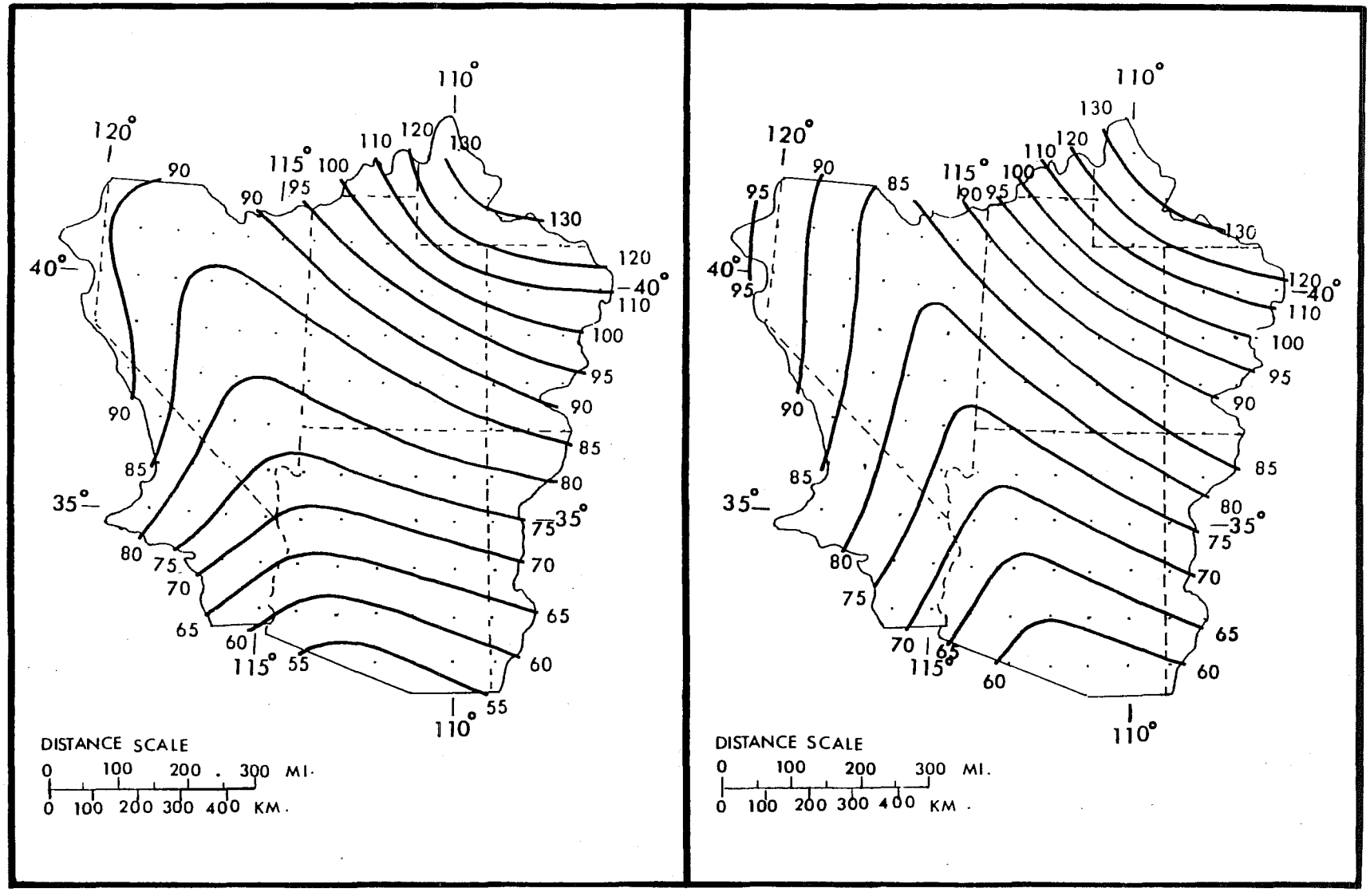

Figure 3.14.--Seasonal variation in 10-mi^2 (26-km^2) 24-hr orographic PMP for the study region (in percent of values in figure 3.11).

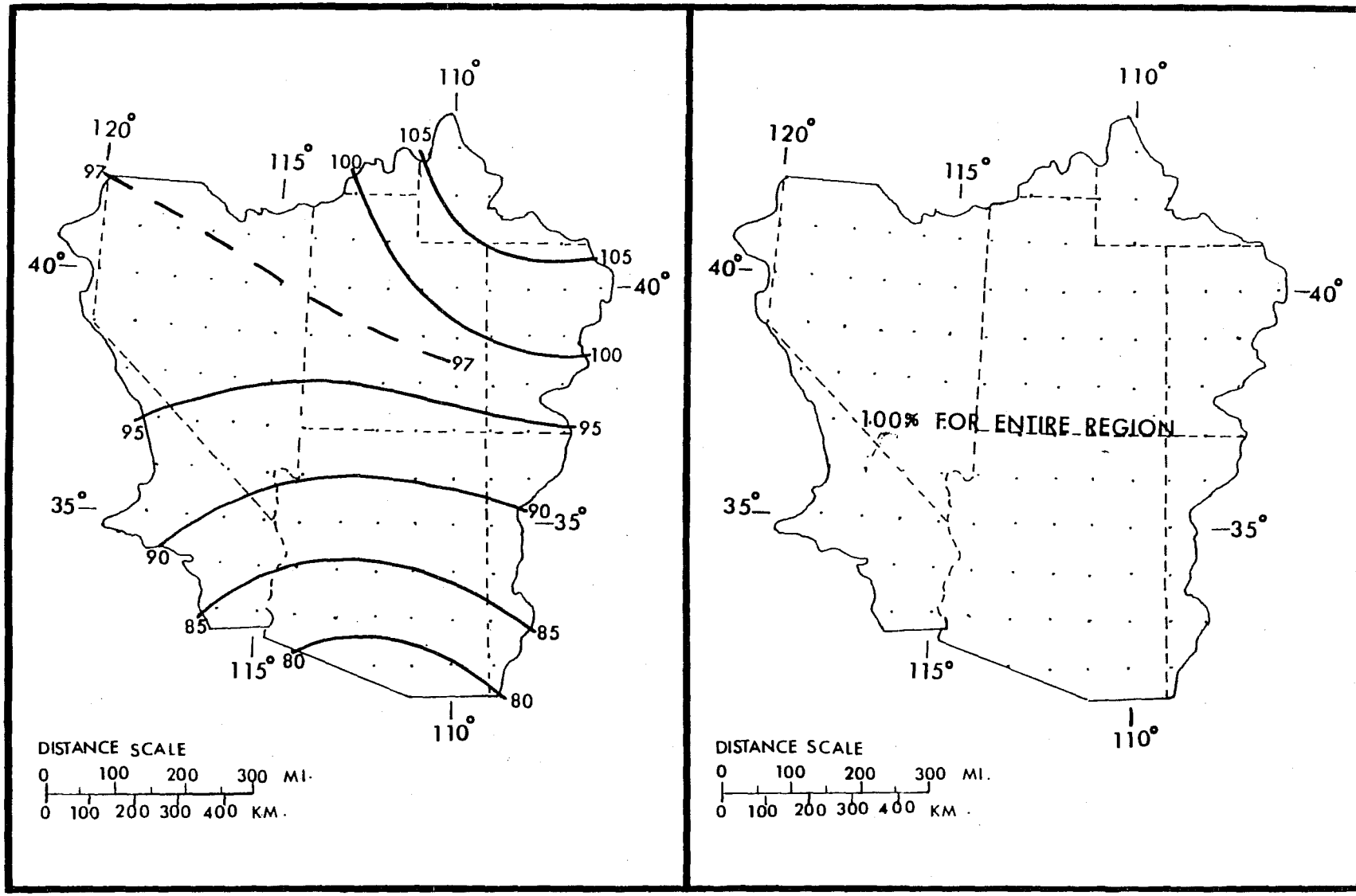

July *August*

Figure 3.15.--Seasonal variation in 10-mi^2 (26-km^2) 24-hr orographic PMP for the study region (in percent of values in figure 3.11).

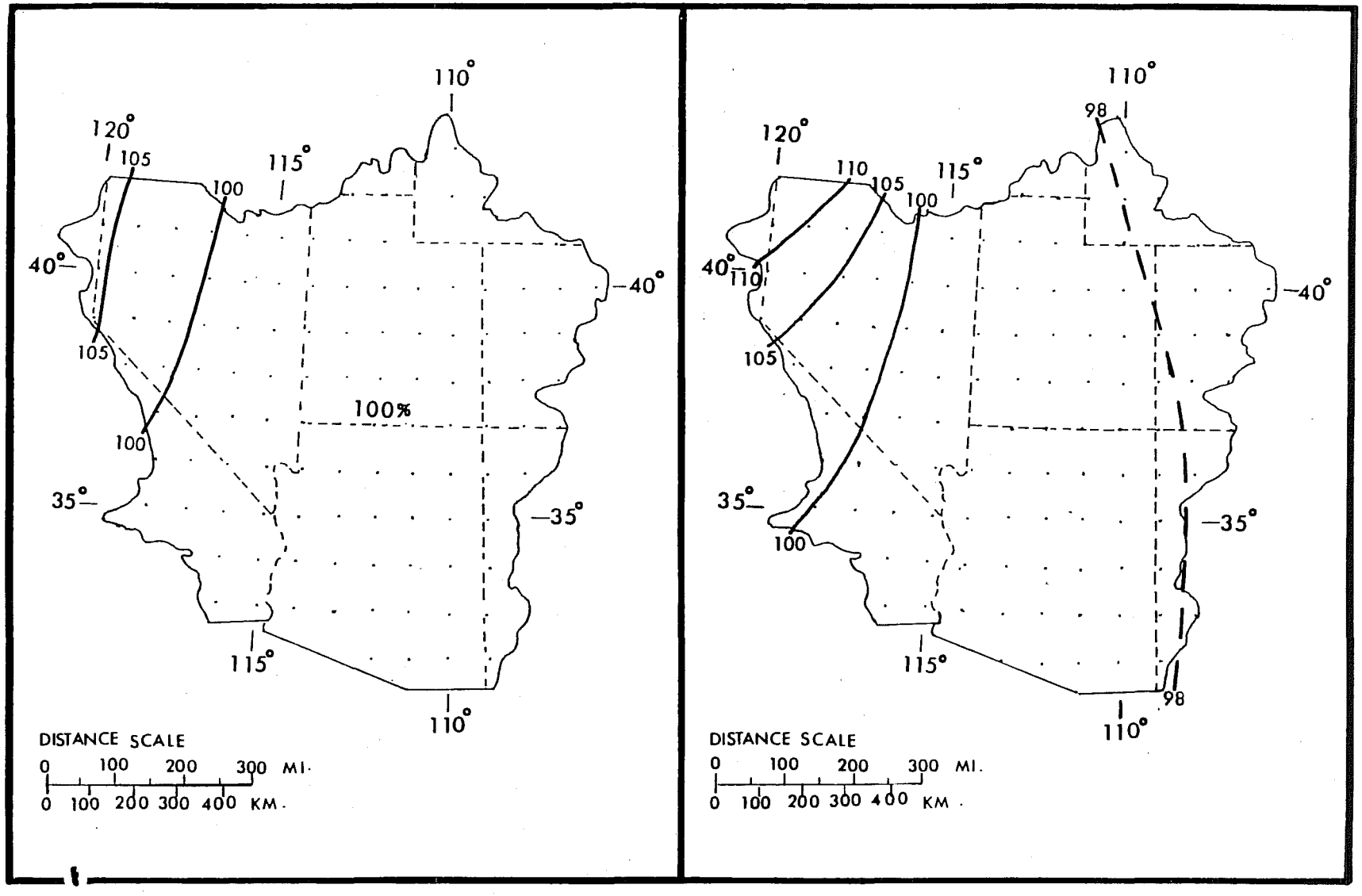

September *October*

Figure 3.16.--Seasonal variation in 10-mi^2 (26-km^2) 24-hr orographic PMP for the study region (in percent of values in figure 3.11).

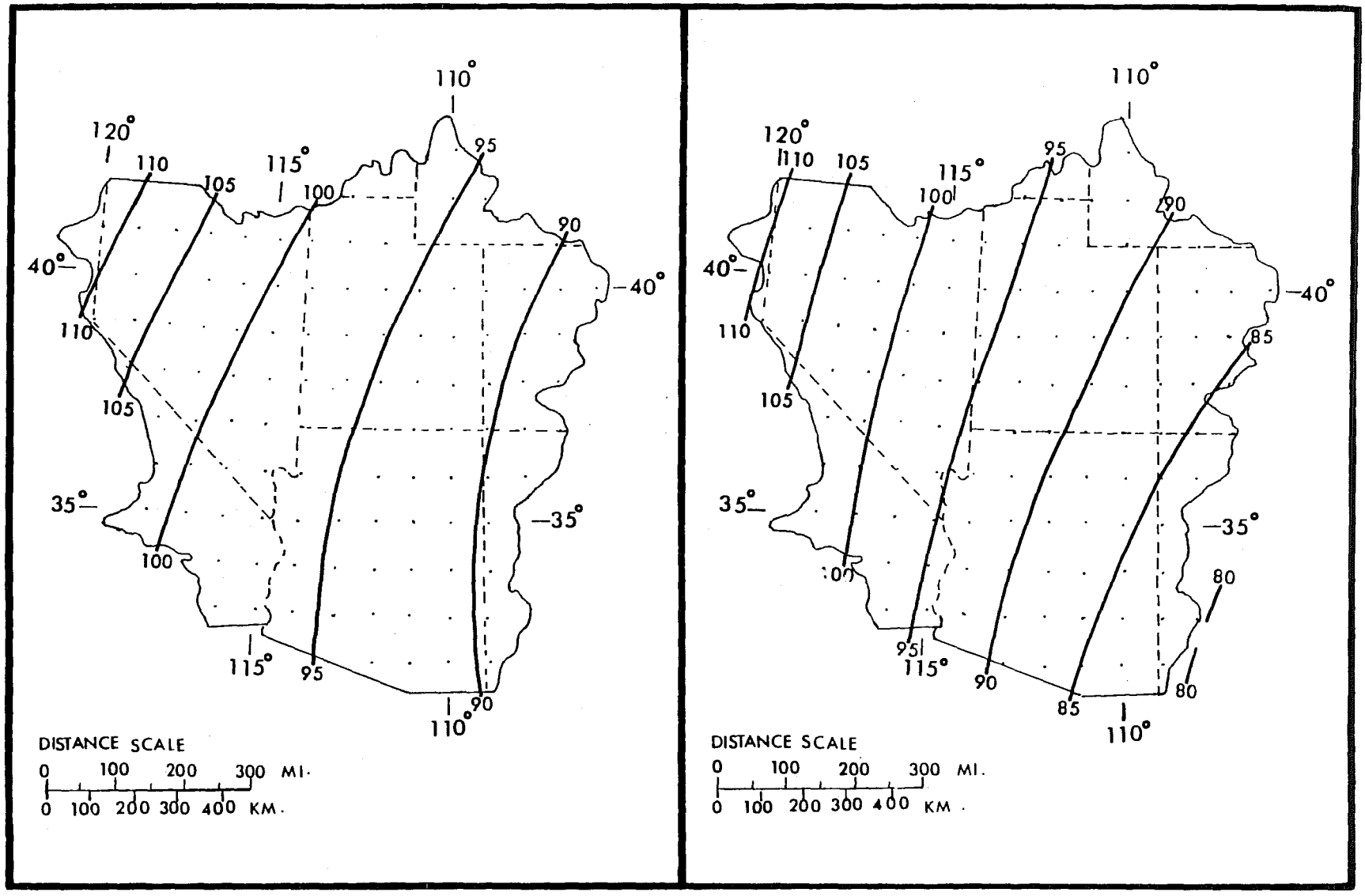

November *December*

Figure 3.17.--Seasonal variation in 10-mi^2 (26-km^2) 24-hr orographic PMP for the study region (in percent of values in figure 3.11).

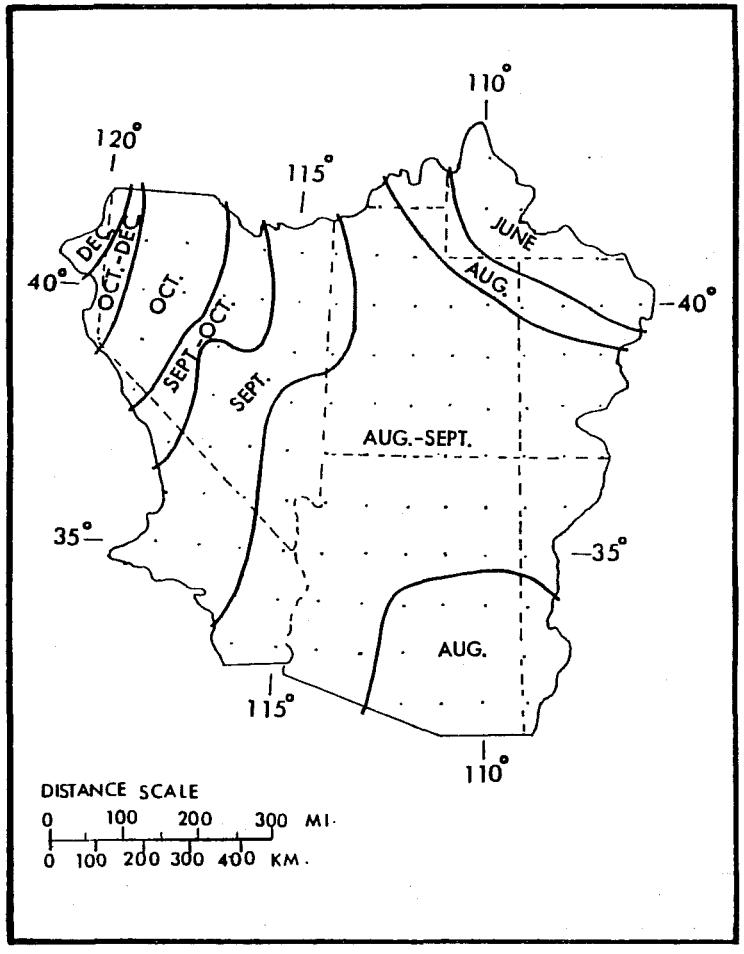

Figure 3.18.--Months of maximum total general-storm PMP for Southwest States, 10 mi^2 (26 km^2) 24 hr.

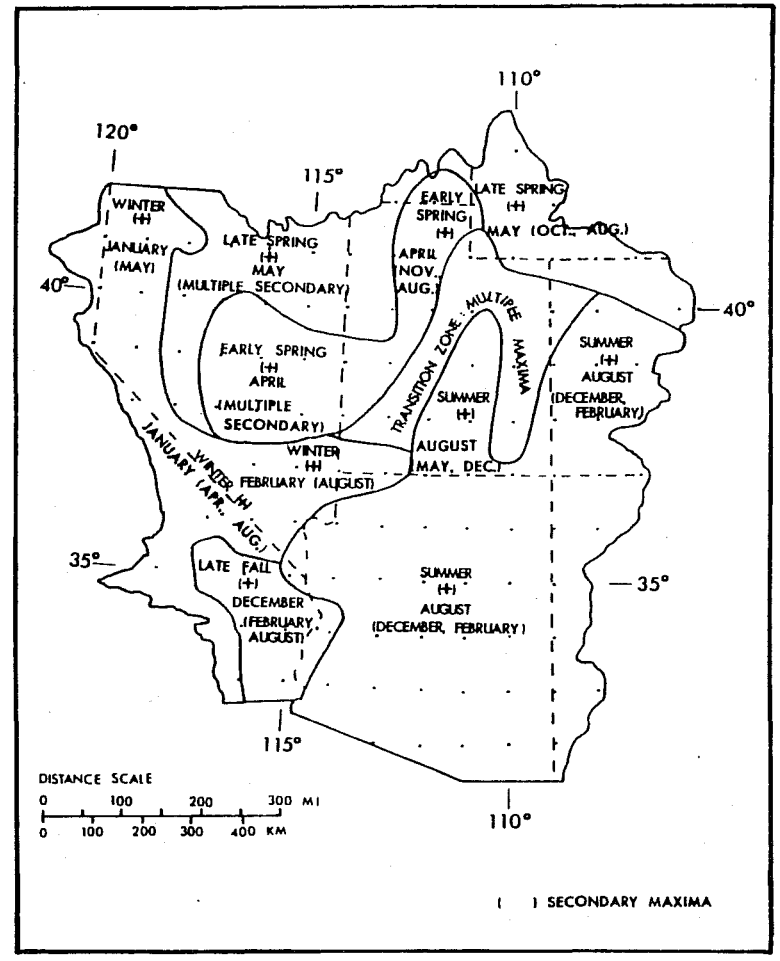

Figure 3.19.--Season and month of maximum and secondary maximum 24-hr station precipitation after Pyke (1972).

month of primary maximum is indicated, and the secondary maximum is given in parenthesis. There is general agreement between month of maximum shown in figure 3.19 and that of this PMP study shown in figure 3.18, particularly considering the need to extend beyond the raw data, which necessarily has in it much bias toward showers. August has a maximum on the southeastern third of the region in Pyke's study and is a secondary maximum through much of the remainder except the northwestern corner. The month of May dominates along the northeast to north-central border of the region, while April appears to dominate in central Nevada to northwestern Utah. The winter maxima of 24-hr precipitation in January and February along the western portion of the Southwest differ from the month of maximum PMP in a similar way. While both areal and point storm rainfall show a winter or spring maximum, the latent possibility of tropical storms, so infrequent in the storm data shifts the PMP to late summer.

An analysis of season of maximum monthly precipitation over the Great Basin was made by Houghton (1969). While monthly precipitation is not a good index to PMP for durations up to 3 days, the comparisons with PMP may be of interest. His conclusions apply to the Great Basin, roughly the northwestern half of the Southwestern States. There is general correspondence between Houghton's results and those of Pyke. The larger expanse of spring maximum in Houghton's work is the major disagreement with the PMP analysis. The seasonal analysis of PMP shown in figure 3.18 is considered justified on the basis of the PMP storm prototypes and the relative potential for precipitation in the various months.

3.4 Variation With Basin Size

3.4.1 Introduction

The orographic PMP index (figures 3.11 a to d) is for the 24-hr duration and a 10-mi^2 (26-km^2) area. For application to specific basins, it is necessary to define a depth-area relation.

Depth-area relations for the orographic PMP index maps are controlled by the steepness, height, length, orientation, and exposure of each slope relative to moisture bearing winds. There is a limit to the lateral extent over which moisture can be transported over mountain slopes without some decrease in intensity. This was assessed for the Sierra Mountains in HMR No. 36 by a study of the variation of pressure gradients with distance between stations that take pressure observations. Figure 3.20 shows this variation by the dashed curve.

An additional factor is required for the present orographic index. This is the way the index was developed. Inflow from several directions was considered in determining the magnitude and gradient of orographic PMP. However, for any particular 6-hr period of the PMP storm over a given drainage, the winds would generally be from one direction and thus have an orographic influence for slopes normal to that direction only.

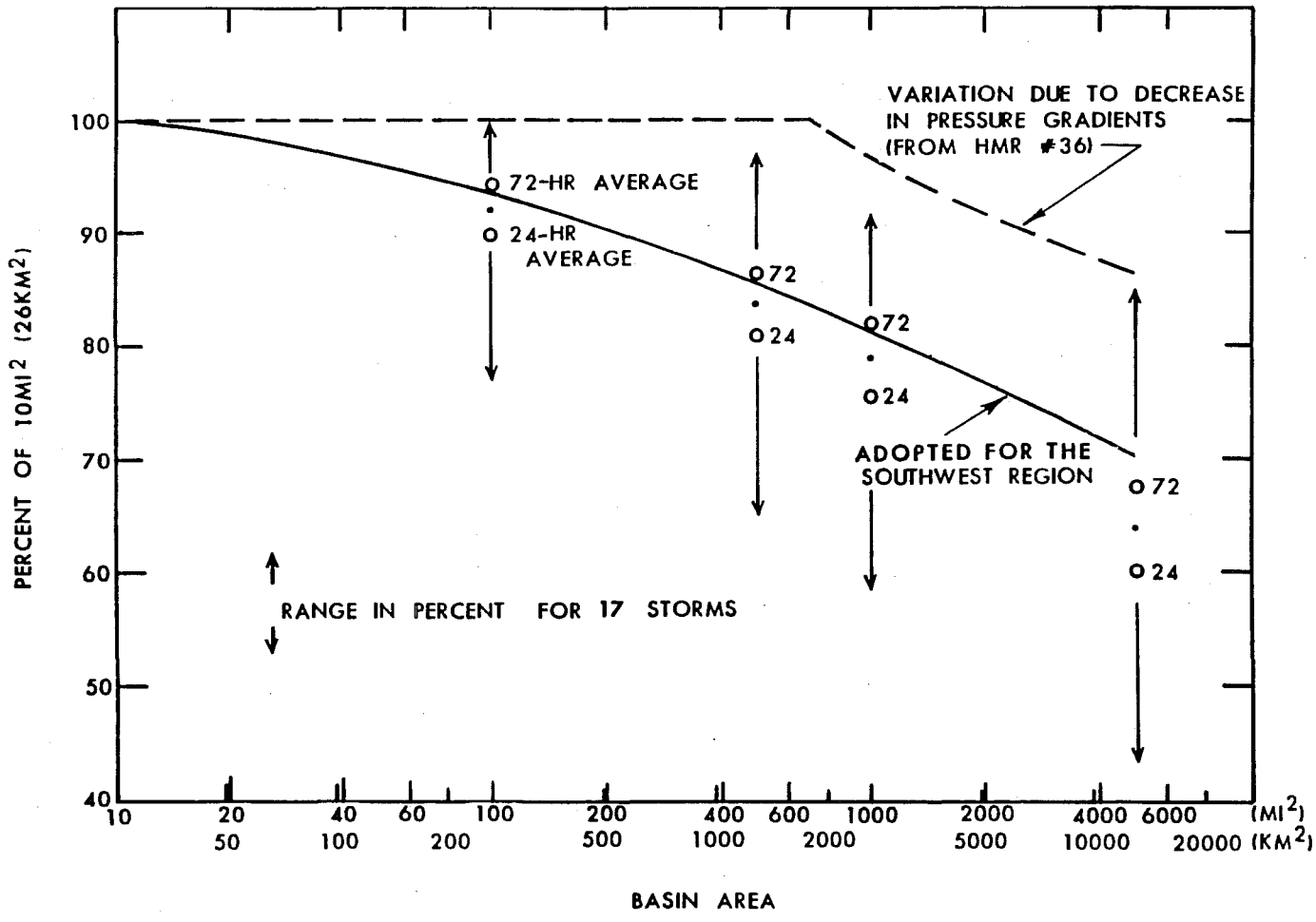

Figure 3.20.--Variation of orographic PMP with basin size.

An approximate method was used to take into account both the reduction due to lateral extent of a basin and the fact that at a given time slopes oriented in only one direction can be effective. This was to analyze the depth-area relations of most orographically-influenced rainfalls for major storms of record in the Southwestern States. The approximation is that we assume precipitation at high elevations is mostly orographic.

3.4.2 Storm Data.

The storms used in the analysis are listed in table 3.5 along with the 10-mi^2 (26-km^2) precipitation for 24 and 72 hours. The 1000-mi^2 (2590 km^2) values for 24 and 72 hours are given in percentages of the 10-mi^2 (26-km^2) values. Some storms with centers at lower elevations, such as the September 3-9, 1939 storm in California, were omitted from the storm sample. If the duration of the storm is less than 72 hours, the actual duration is asterisked in the right-hand column of table 3.5. All storms occurred within the southwest study region.

Figure 3.21 shows 1000-mi^2 (2590-km^2) 72-hr precipitation expressed in percent of the 10-mi^2 (26-km^2) value. The data do not suggest a simple relation between magnitude of rainfall at 10 mi^2 (26 km^2), and the percent at 1000 mi^2 (2590 km^2). A similar plot (not shown) for 24-hr durations

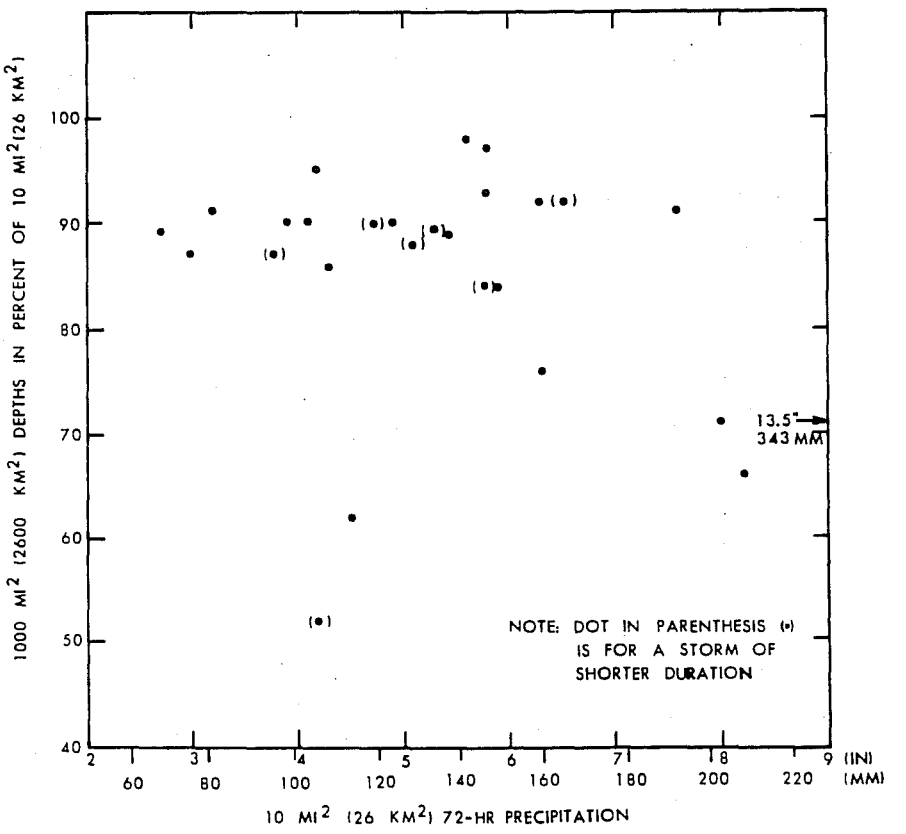

Figure 3.21.--1000-mi^2 (2590-km^2) storm depths relative to 10-mi^2 (26-km^2) depths for 72-hr rainfalls.

Table 3.5.--Data analyzed for determining depth-area variation of orographic PMP

Storm date	24-hr 10-mi^2 rainfall in.	(mm)	24-hr 1000-mi^2 rainfall in % of 10-mi^2 value	72-hr 10-mi^2 rainfall in.	(mm)	72-hr 1000-mi^2 rainfall in % of 10-mi^2 value	
Arizona							
Feb. 1-7, 1905	2.3	(58)	100	5.8	(147)	97	
Mar. 12-20, 1905	3.0	(76)	80	4.3	(109)	86	
Apr. 9-13, 1905	3.2	(81)	78	3.9	(99)	90	
Nov. 25-28, 1905	4.4	(112)	82	4.9	(124)	90	
Dec. 1-4, 1906	2.7	(69)	85	5.1	(130)	88	60*
Dec. 14-17, 1908	3.9	(99)	90	6.3	(160)	92	
Dec. 17-24, 1914	3.1	(79)	77	5.9	(150)	83	
Jan. 14-20, 1916	2.7	(69)	82	5.8	(147)	93	
Jan. 25-30, 1916	4.0	(102)	73	5.8	(147)	84	66*
Apr. 4-9, 1926	4.0	(102)	88	4.7	(119)	90	60*
Feb. 10-22, 1927	4.3	(109)	79	7.6	(193)	91	
Feb. 3-8, 1937	4.9	(124)	84	5.3	(185)	89	54*
Feb. 26-Mar. 4, 1938	5.8	(147)	90	6.5	(165)	92	66*
Mar. 11-17, 1941	3.3	(84)	67	6.3	(160)	76	
Aug. 26-31, 1951	6.9	(175)	71	13.5	(343)	71	
Sept. 3-7, 1970	4.7	(119)	64	8.0	(203)	71	
Colorado							
Dec. 14-17, 1908	3.7	(94)	89	5.6	(142)	98	
Sept. 3-7, 1909	2.9	(74)	93	4.1	(104)	90	
Oct. 4-6, 1911	8.1	(206)	59	8.2	(208)	66	
Mar. 19-21, 1912	2.6	(66)	92	3.8	(96)	87	54*
June 26-29, 1927	2.8	(71)	89	5.4	(137)	89	
Sept. 6-10, 1927	2.4	(61)	87	4.2	(107)	95	
July 27-Aug. 7, 1929	2.5	(64)	84	3.0	(76)	87	
Aug. 25-29, 1932	2.2	(56)	77	2.7	(69)	89	
Sept. 18-23, 1941	3.0	(76)	90	3.2	(81)	91	
June 1-3, 1943	2.2	(56)	91	4.2	(107)	52	42*
Utah							
May 31-June 5, 1943	3.1	(79)	65	4.5	(114)	62	

Note: 10 mi^2 = 26 km^2 and 1000 mi^2 = 2590 km^2.
*Storm duration when less than 72 hours.

indicates a slight trend of lower percents for the greater 10-mi^2 (26-km^2) values; however we do not believe this trend is significant. We chose to use a depth-area relation not related to magnitude of the 10-mi^2 (26-km^2) value.

Another aspect of depth-area variation is whether one relation can be used for all months of orographic PMP. The 1000-mi^2 (2590-km^2) rainfall for 24 hours, in percent of 10-mi^2 (26-km^2) values, column 2 of table 3.5, were averaged for each month. The results did not show a clear-cut seasonal trend. Similar analysis of 72-hr values was also inconclusive. The limited number of storms and their uneven seasonal distribution are handicaps in defining seasonal trends. Without data to indicate otherwise, and to avoid unduly complicating one aspect of the PMP criteria, we recommend use of one depth-area relation for all months.

3.4.3 Adopted Variation

An average depth-area relation was developed from the 17 storms in table 3.5 with 10-mi^2 (26-km^2) 24-hr amounts $\geq$ 3.0 inches (76 mm). These averages are shown in figure 3.20 separately for the 24- and 72-hr durations along with the range in ratios from the two durations indicated by arrow points. The averages are somewhat less than the adopted areal variation used in the adjoining Northwest Region (HMR No. 43). Considering the ranges in the data, and that nonorographic precipitation in the data would tend to lower the ratios, we recommend the same areal variation as in the Northwest Region. This is the solid curve shown in figure 3.20.

3.5 Durational Variation

3.5.1 Background

Variation of orographic precipitation with duration depends on the durational variation of winds and moisture. The measure of moisture used in this study is surface dew point. During major storms there are periods when depth of the moist layer is limited by drier air aloft. In a study for the Northwest (HMR No. 43) a variation in relative humidity with duration during the 3-day PMP storm was introduced, based upon some recent storms of record. For computations of PMP with the orographic model on the Sierra slopes of California (HMR No. 36) an equivalent procedure was used for taking into account the variation of relative humidity. This was to calibrate the computed orographic precipitation by comparison with observed values. The longer the duration, the lower the calibration factor. We postulated that the lowering in relative humidity was responsible for variation of the calibration factor with duration.

In this section durational variation of winds, moisture, and relative humidity for data in the Northwest and California study areas will be compared with similar data for the Southwest. Finally, an adopted variation will be described.

3.5.2 Variation of Maximum Winds

The variation with duration of maximum 6-hr incremental winds for 500- and 900-mb (50- and 90-kPa) pressure levels is shown for Tucson, Ariz. by the solid curves in figure 3.22. These variations are the average of 10 windy periods for each level that contained the highest instantaneous winds at

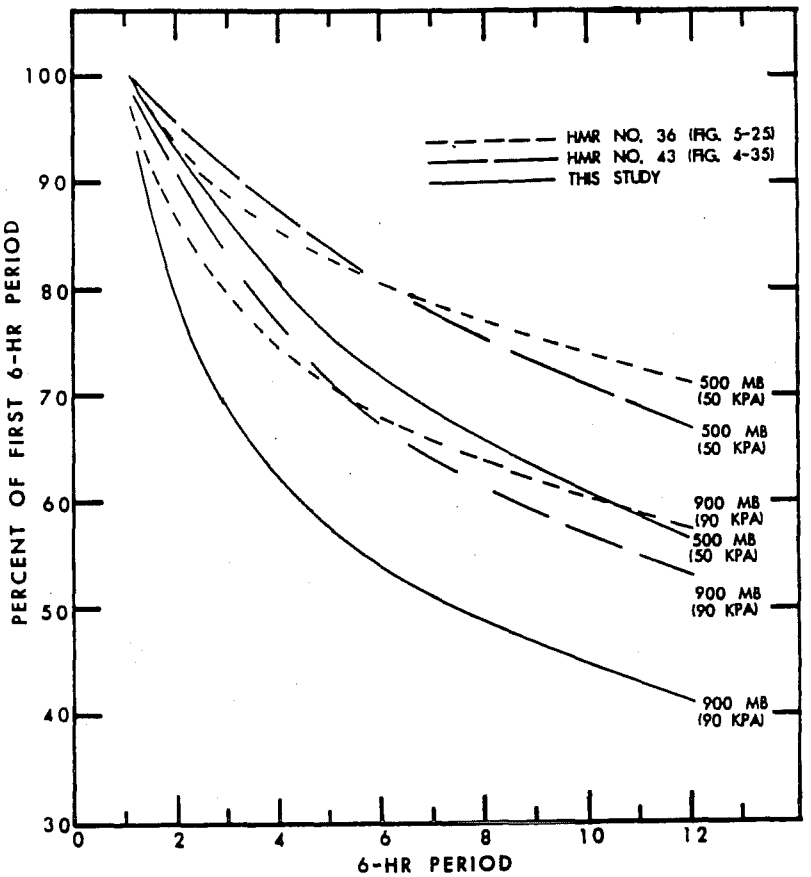

Figure 3.22.--Durational variation of maximum winds at Tucson, Arizona compared with variations for adjoining regions.

Tucson (1956-69). While the instantaneous winds were definitely greater during the winter months, the amount of variation with duration did not show a consistent correlation with time of year. For each of the windy periods, the highest average wind for consecutive observations was determined, and each durational average expressed in percent of its instantaneous highest value. From twice-a-day observations, 2 consecutive observations were considered for a 12-hr average, etc., to 7 consecutive observations for a 72-hr average. The durational decay of winds was then converted to give the durational variation of 6-hr incremental winds. The 10 cases were then averaged.

For comparison the durational variations for these same two levels for the Northwest (HMR No. 43, fig. 4-35) and California (HMR No. 36, fig. 5-25) are shown in figure 3.22 by long and short dashes, respectively. The variations for the two adjoining regions are quite similar because most of the basic data was the same. The Tucson winds have a decidedly greater decrease with duration. This is reasonable from the standpoint that the Tucson winds were restricted to the southerly component, the important direction to moisture inflow for most of the Southwest study region. Extreme westerly winds are stronger and longer lasting.

3.5.3 Variation of Maximum Moisture

Highest 12-hr persisting 1000-mb (100-kPa) dew points are used as the index to moisture assuming a pseudo-adiabatic lapse rate. For the Southwest States, 12-hr persisting 1000-mb (100-kPa) dew points for durations extending out to 3 days (U. S. Weather Bureau 1948) were considered at 7 stations well spaced over the region.

The maximum persisting dew points for 6, 12, 24, 36, 48, 60 and 72 hours for each of the 12 months at each station were expressed in inches of precipitable water assuming a saturated psuedo-adiabatic atmosphere and then in percent of the 12-hr values.

Smooth seasonal curves (not shown) of these percents for each duration were then constructed. These curves showed small random fluctuations in percents for each station not forming a discernible regional pattern. Table 3.6 lists the 7 stations and the 12-month average 3-day moisture in percent of the 12-hr moisture. One durational curve was adopted, as shown in figure 3.23. Similar curves for California and the Northwest are shown for comparison in the figure.

Table 3.6.—Durational variation of maximum moisture of the Southwest

Station	3-day moisture in percent of max. 12-hr moisture
Grand Junction, Colo.	84
Salt Lake City, Utah	82
Winnemucca, Nev.	80
Tonopah, Nev.	80
Yuma, Ariz.	84
Phoenix, Ariz.	82
Modena, Utah	79

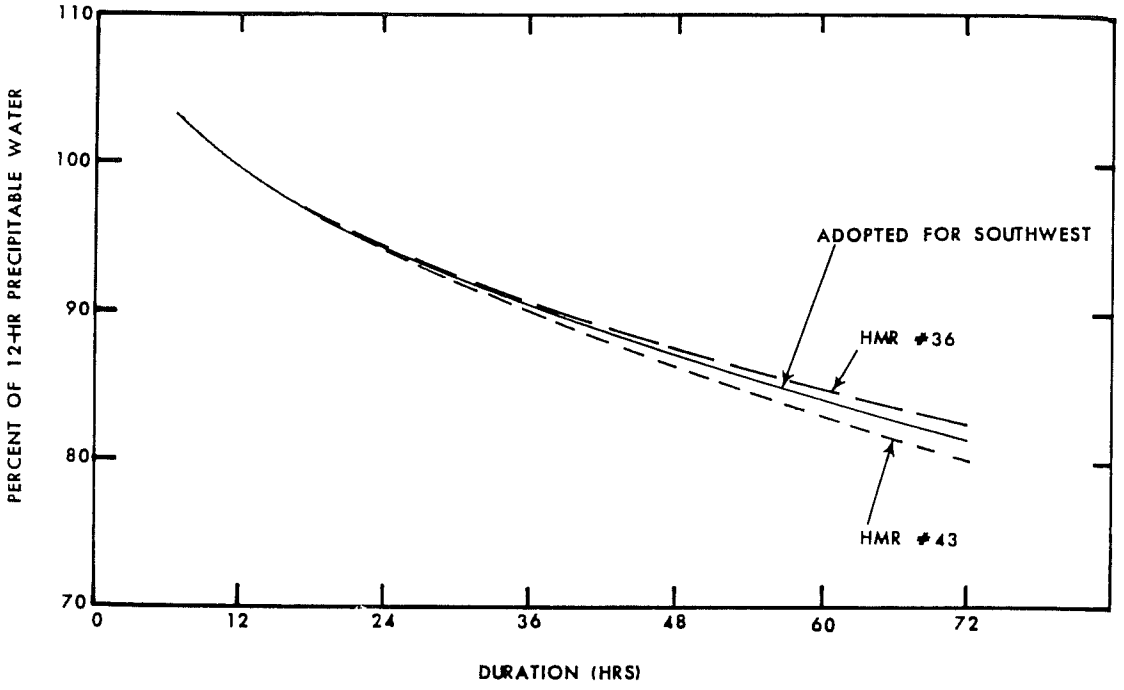

Figure 3.23.--Durational variation of precipitable water.

3.5.4 Variation of Relative Humidity

Four recent storms in Arizona (two in winter and two in summer) were selected for analysis of relative humidity (RH) from the surface to 500 mb (50 kPa). The average surface to 500-mb relative humidity for each of two soundings was plotted on a time graph for each storm. From a smooth curve joining these data, the maximum 6-, 12-, 18-, 24- ... hr relative humidity for the surface to 500 mb was determined and expressed in percent of the 6-hr value. The storms considered and the durations averaged are shown in figure 3.24. An envelopment of these percents is given by the upper solid curve in this figure. For comparison with the variation used in HMR No. 43, the durational curve was expressed in terms of 6-hr incremental RH values. This is shown by the lower solid curve. The comparable RH values from HMR No. 43 are given by the dashed curve. The variation based on four Arizona storms generally shows a greater decrease with succeeding 6-hr increments.

3.5.5 Orographic Model Computation

One method of evaluating the durational variation of precipitation is to make computations with the orographic computation model. Tests of the detailed model (which includes consideration of the slope of the inflow wind profile) show that resulting durational variations are strongly dependent on the height and length of the slope so that a different durational variation would result for each different ground profile.

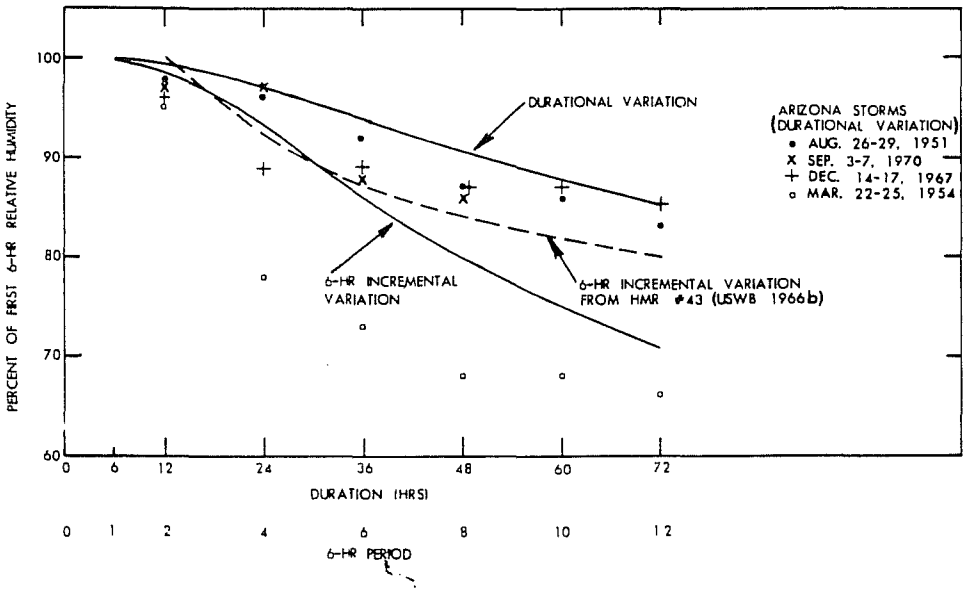

Figure 3.24.--Adopted durational variation in relative humidity and supporting data.

A simplified orographic model (World Meteorological Organization 1973) was used to evaluate differences in precipitation with duration. This is

$$R = \overline{V}_1 \left(\frac{W_1 - W_2 \frac{\Delta p_1}{\Delta p_2}}{Y} \right) \qquad (3.1)$$

where:

R = precipitation
$\overline{V}_1$ = mean inflow wind
W_1, W_2 = inflow and outflow precipitable water
Δp_1, Δp_2 = inflow and outflow pressure differences
Y = horizontal distance.

This model also yields somewhat different durational variations depending on the height of the terrain profile, but the differences are not as great with this simplified model since the inflow wind profile is given as one average value. We believe it is a satisfactory tool where only relative magnitudes are required.

For the computations, the winds, moisture, and relative humidity for the northern border of the region were obtained from HMR No. 43. Near the southern border we used the values of parameters in Arizona described in 3.5.2 to 3.5.4. A lift of 150 mb (15 kPa) was assumed at both locations. For the southern location the slope is from 1000 mb (100 kPa) to 850 mb (85 kPa). For the northern location it is from 850 mb (85 kPa) to 700 mb (70 kPa). The Y distance is held constant. A nodal surface of 300 mb (30 kPa) is assumed. The mean inflow wind for the southern location is an average of the 900-,

700-, and 500-mb (90-, 70- and 50-kPa) winds. For the northern location, it is an average of the 700- and 500-mb (70- and 50-kPa) winds. Table 3.7 shows details of the computations made for the 1st, 4th, 8th and 12th 6-hr periods. Rainfall computations were made for January and August in both locations. The 12th period averages 33% of the 1st for the southern border and 39% for the northern border (fig. 3.25). The southern location shows 6% more decrease in precipitation than the northern border region (relative to the first 6-hr value) for each of the 6-hr periods.

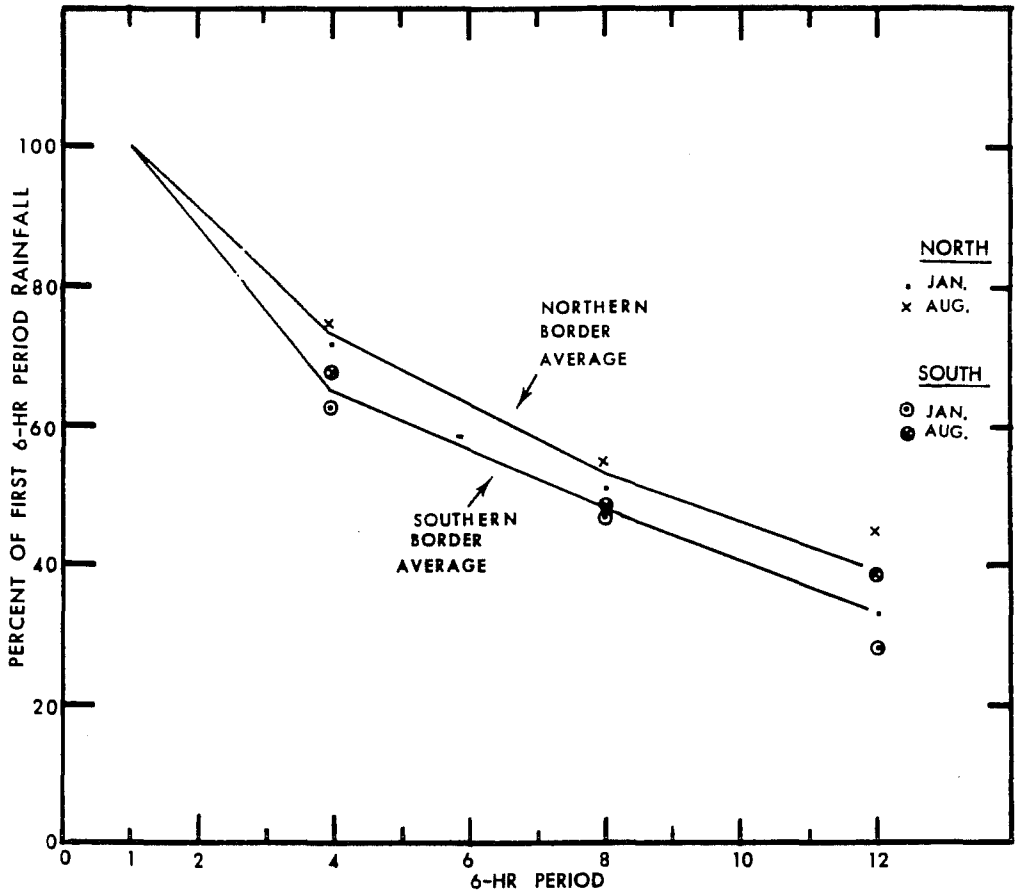

Figure 3.25.--Durational variation in orographic precipitation near northern and southern borders of Southwest region (from orographic model).

3.5.6 Guidance from Observed Precipitation

HMR No. 36 Rev. (U.S. Weather Bureau 1969) shows a tendency in more intense storms for less decrease in rain for longer durations in the north than in the south. This latitudinal variation in the durational variation of orographic PMP was based on observed precipitation along the Coastal and Sierra Mountains of California at high elevation stations during major storms.

Since orographic precipitation is dependent on the strength of moisture-bearing winds flowing against the mountains, one could expect a greater de-

Table 3.7. --Computation of durational variation of orographic precipitation for the Southwest States using a simplified orographic model (eq. 3.1)

	Near northern border	Near southern border
	ΔP_1 = 850-300 = 550 mb (85-30 = 55 kPa)	ΔP_1 = 1000-300 = 700 mb (100-30 = 70 kPa)
	ΔP_2 = 700-300 = 400 mb (70-30 = 40 kPa)	ΔP_2 = 850-300 = 550 mb (85-30 = 55 kPa)

Precipitable water, in. (mm), considering decrease in RH

6-hour period	January		August		January		August	
	W_1	W_2	W_1	W_2	W_1	W_2	W_1	W_2
	in. (mm)	in. (mm)	in. (mm)	in. (mm)	in. (mm)	in. (mm)	in. (mm)	in. (mm)
1	0.60 (15)	0.27 (7)	1.68 (43)	0.93 (24)	1.45 (37)	0.85 (22)	3.85 (85)	2.21 (56)
4	.47 (12)	.20 (5)	1.34 (34)	.71 (18)	1.19 (30)	.67 (17)	2.76 (70)	1.76 (45)
8	.39 (10)	.16 (4)	1.13 (29)	.58 (15)	.97 (25)	.53 (14)	2.27 (58)	1.42 (36)
12	.32 (8)	.16 (4)	.95 (24)	.47 (12)	.80 (20)	.42 (11)	1.87 (48)	1.13 (29)

Average wind (percent of first 6-hour period) for the pressure levels to 500 mb (50 kPa)

	Near northern border	Near southern border
1	100	100
4	84	72
8	68	58
12	60	50

R (from substitution in equation 3.1) in percent of 1st 6-hr period value

	January	August	January	August
1	100	100	100	100
4	72	75	63	68
8	51	55	47	50
12	33	45	28	39

crease with duration in Arizona than in California because maximum winds for California (HMR No. 36) decay less with duration than those in Arizona. A study was made of the durational variation of precipitation for high elevation stations in Arizona during major storms. The storms and stations used are shown in table 3.8, along with 48/24- and 72/24-hr durational ratios. The table also gives similar ratios for high elevation stations during major storms in southern California. All the ratios are based on scaling the largest 24-, 48-, and 72-hr consecutive rains from mass rainfall curves. For the earlier winter Arizona storms, only one station's rainfall was considered, that with the greatest rainfall.

The 72/24-hr ratios for the data of table 3.8 are compared on figure 3.26. The points labeled "A" are from southern California; those labeled "B" are from Arizona. Averages of the 72/24-hr rain ratios are 1.78 for southern California and 1.45 for Arizona. The southern California data are part of the information used to revise HMR No. 36 (U. S. Weather Bureau 1969).

A question may be raised about seasonal variation in the depth-duration relation. The Arizona storms show both high and low 72/24-hr rain ratios for the same months; in February the ratios for four storms range from 2.13 to 1.08. The August 1951 storm 72/24-hr ratios averaged 1.66, the September 1970 storm, 1.38. There are not enough storms to establish a seasonal trend.

3.5.7 Adopted Variation

We have discussed several aspects of the durational variation of orographic precipitation. Some conclusions for variations in the Southwest are:

a. Comparisons of durational variations of high wind cases indicate more decrease with increasing duration than in the Northwest.

b. The variation of moisture with duration is about the same as in California and the Northwest.

c. Relative humidity in upper air soundings during four major Arizona storms shows more decrease with duration than in the Northwest.

d. No definitive seasonal variation in the durational variations of wind, moisture or relative humidity could be found.

e. Computations with the simplified orographic model using the adopted durational variations of wind and moisture show more decrease with duration for southern Arizona compared to northern Nevada.

f. Observed major rains decidedly show more decrease with duration than rains on western slopes in southern California.

Based on this guidance, recommended durational variation near the southern boundary of the Southwest (latitude 31°) is shown in figure 3.27 with other comparisons. We recommend phasing into the relation adopted for the Northwest (HMR No. 43) at the northern boundary to the study region. Table 3.9 shows the durational variations expressed in percent of the 24-hr values.

Table 3.8.--Durational variation in major storms in orographic locations; southern California and Arizona

Storm date Arizona	Elevation ft	Elevation m	Station	Rain ratios $\frac{48}{24}$ hr	Rain ratios $\frac{72}{24}$ hr	Average ratio $\frac{48}{24}$ hr	Average ratio $\frac{72}{24}$ hr
Sept. 3-6, 1970	6900	2103	Flagstaff	1.28	1.28		
	7405	2257	Beaver Creek	1.15	1.15		
	6000	1829	Crown King	1.15	1.15		
	6300	1920	Gordon Cnyn.	1.43	1.43		
	7650	2332	Woods Cnyn.	1.10	1.10		
	6970	2124	Workman Creek	1.09	1.09		
	6700	2042	Cagle Cabin	1.07	1.07		
	8180	2493	Hawley L.	1.51	1.51		
	6875	2096	Kitt Peak	1.27	2.18		
	7945	2422	Palisade R.S.	1.48	1.87		
						1.25	1.38
Aug. 26-31, 1951	5708	1740	Camp Wood	1.59	1.32		
	5500	1676	Upper Prkr.Cr.	1.35	1.67		
	6970	2124	Workman Creek	1.34	1.65		
	8400	2560	Bright Angel R.S.	1.28	1.28		
	6000	1829	Crown King	1.93	2.11		
	6000	1829	Tonto Creek	1.31	1.58		
	5100	1554	Sierra Ancha	1.16	1.31		
	4500	1372	Pinal Ranch	1.25	1.35		
	5000	1524	Payson	1.69	2.03		
	4607	1404	Natural Bridge	1.47	1.86		
						1.44	1.66
Dec. 14-17, 1908	4607	1404	Natural Bridge	1.36	1.62		
Nov. 25-28, 1905	4500	1372	Pinal Ranch	1.11	1.11		
Feb. 11-17, 1927	4607	1404	Natural Bridge	1.51	1.77		
Dec. 17-24, 1914	4800	1463	Rosemont	1.21	1.33		
Feb. 1-7, 1905	4700	1433	Yarnell	1.61	2.13		
Mar. 12-20, 1905	5345	1629	Prescott	1.43	1.43		
April 3-11, 1926	6000	1829	Crown King	1.03	1.25		
Feb. 5-8, 1937	5345	1629	Prescott	1.08	1.08		
Feb. 27-Mar.4, 1938	6903	2104	Flagstaff	1.03	1.17		
Arizona storm averages						1.28	1.45

Table 3.8.--Durational variation in major storms in orographic locations; southern California and Arizona - Continued

Storm date Southern California	Elevation ft	Elevation m	Station	Rain ratios $\frac{48}{24}$ hr	Rain ratios $\frac{72}{24}$ hr	Average ratio $\frac{48}{24}$ hr	Average ratio $\frac{72}{24}$ hr
Jan. 20-23, 1943	4254	1297	Opids Camp	1.42	1.48		
	5709	1740	Mt. Wilson	1.41	1.42		
	2290	698	Big Tujunga Dam	1.33	1.35		
	2650	808	Hoegee's Camp	1.41	1.44		
	5239	1594	Squirrel Inn	1.27	1.36		
	4320	1317	Camp Baldy	1.38	1.43		
	5740	1750	Crystal Lake	1.41	1.46		
	6800	2073	Big Bear Dam	1.50	1.58		
						1.39	1.44
Feb. 27-Mar 3, 1938	4254	1297	Opids Camp	1.18	1.49		
	5850	1783	Mt. Wilson	1.22	1.71		
	2050	625	Big Tujunga Dam	1.25	1.59		
	2650	808	Hoegee's Camp	1.21	1.76		
	5239	1594	Squirrel Inn	1.12	1.47		
	4320	1317	Camp Baldy	1.26	1.55		
	5740	1750	Crystal Lake	1.17	1.59		
	6800	2073	Big Bear Dam	1.18	1.34		
						1.20	1.56
Feb. 10-22, 1927	4254	1297	Opids Camp	1.41	2.00		
	5850	1783	Mt. Wilson	1.34	2.11		
	2650	808	Hoegee's Camp	1.39	1.91		
	5239	1594	Squirrel Inn	1.43	2.09		
	4300	1310	Camp Baldy	1.43	1.97		
	6800	2073	Big Bear Dam	1.46	1.96		
						1.41	2.01
April 3-11, 1926	4254	1297	Opids Camp	1.24	1.63		
	5850	1783	Mt. Wilson	1.28	1.55		
	2650	808	Hoegee's Camp	1.28	1.81		
	5239	1594	Squirrel Inn	1.50	1.87		
	4300	1310	Camp Baldy	1.38	1.62		
	6800	2073	Big Bear Dam	1.42	1.54		
						1.35	1.66
Dec. 18-28, 1921	5850	1783	Mt. Wilson	1.40	1.66		
	5239	1594	Squirrel Inn	1.79	2.27		
	4300	1310	Camp Baldy	1.56	1.90		
						1.58	1.94
Jan. 13-16, 1916	5850	1783	Mt. Wilson	1.43	1.55		
	5239	1594	Squirrel Inn	1.29	1.46		
	4300	1310	Camp Baldy	1.44	1.48		
						1.39	1.50
Feb. 17-22, 1914	5850	1783	Mt. Wilson	1.89	2.47		
	5239	1594	Squirrel Inn	1.63	2.39		
	6800	2073	Big Bear Dam	1.41	2.29		
						1.64	2.38
California Storm Averages						1.38	1.78

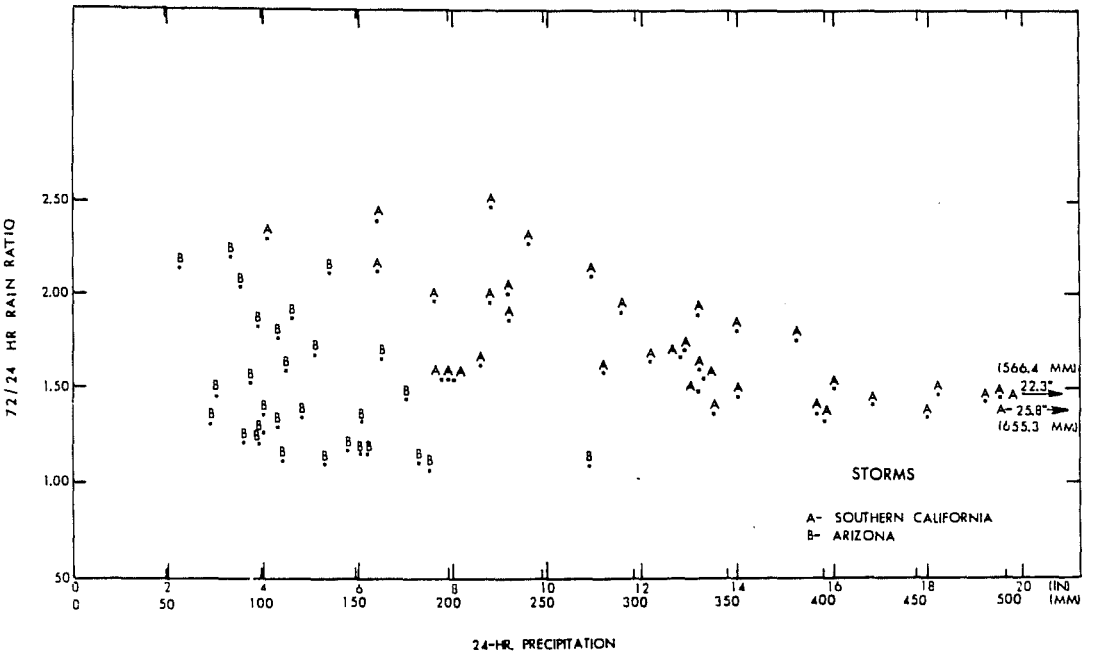

Figure 3.26.--Ratios of 72/24-hr rains at high elevations from major storms in southern California and Arizona.

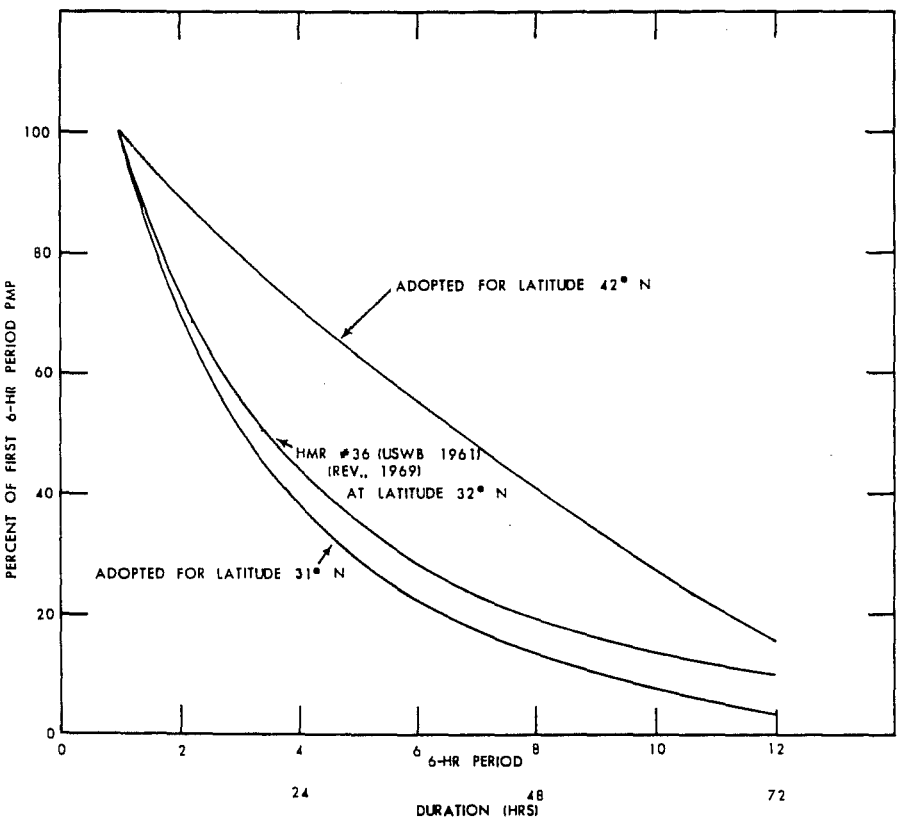

Figure 3.27.--Adopted durational variation in orographic PMP. (Percent of first 6-hr period value at latitudes near the northern and southern borders of the Southwest States.

Table 3.9.--Durational variation of orographic PMP

Latitude °N	Percent of 24-hr value					
	6 hr	12	18	24	48	72
42	28	55	79	100	161	190
41	29	56	79	100	160	189
40	30	57	80	100	159	187
39	30	57	80	100	157	185
38	31	58	81	100	155	182
37	32	59	81	100	152	177
36	33	60	82	100	149	172
35	34	61	82	100	146	167
34	35	62	83	100	143	162
33	36	63	84	100	139	157
32	37	64	84	100	135	152
31	39	66	85	100	132	146

4. LOCAL-STORM PMP FOR THE SOUTHWESTERN REGION AND CALIFORNIA

4.1 Introduction

This chapter provides generalized estimates of local or thunderstorm probable maximum precipitation. By "generalized" is meant that mapped values are given from which estimates of PMP may be determined for any selected drainage.

4.1.1 Region of Interest

Local-storm PMP was not included in the "Interim Report, Probable Maximum Precipitation in California" (HMR No. 36). During the formulation of the present study, we decided that the local-storm part of the study should include California west of the Sierra Nevada. It was also noted that PMP for summer thunderstorms was not considered west of the Cascade Divide in the Northwestern Region (HMR No. 43). As stated in the latter report, "No summer thunderstorms have been reported there (west of the Divide) of an intensity of those to the east, for which the moisture source is often the Gulf of Mexico or Gulf of California. The Cascade Divide offers an additional barrier to such moisture inflows to coastal areas where, in addition, the Pacific Ocean to the west has a stabilizing influence on the air to hinder the occurrence of intense summer local storms." Therefore, it was necessary to establish some continuation of the Cascade Divide into California so that the local-storm PMP definition would have continuity between the two regions.

The stabilizing influence of the Pacific air is at times interrupted by the warm moist tropical air from the south pushing into California, although it is difficult to determine where the limit of southerly flow occurs. General storms having the tropical characteristic of excessive thunderstorm rains are observed as far north as the northern end of the Sacramento Valley. Thus, a northern boundary has been selected for this study, excluding that portion of

California north and west of a line extending from the Cascade Divide at the California-Oregon border, southwestward along the coastal mountain ridge-line to a point near 41°N, 123°W, and then directly to Cape Mendocino on the California coast, (see fig. 4.1).

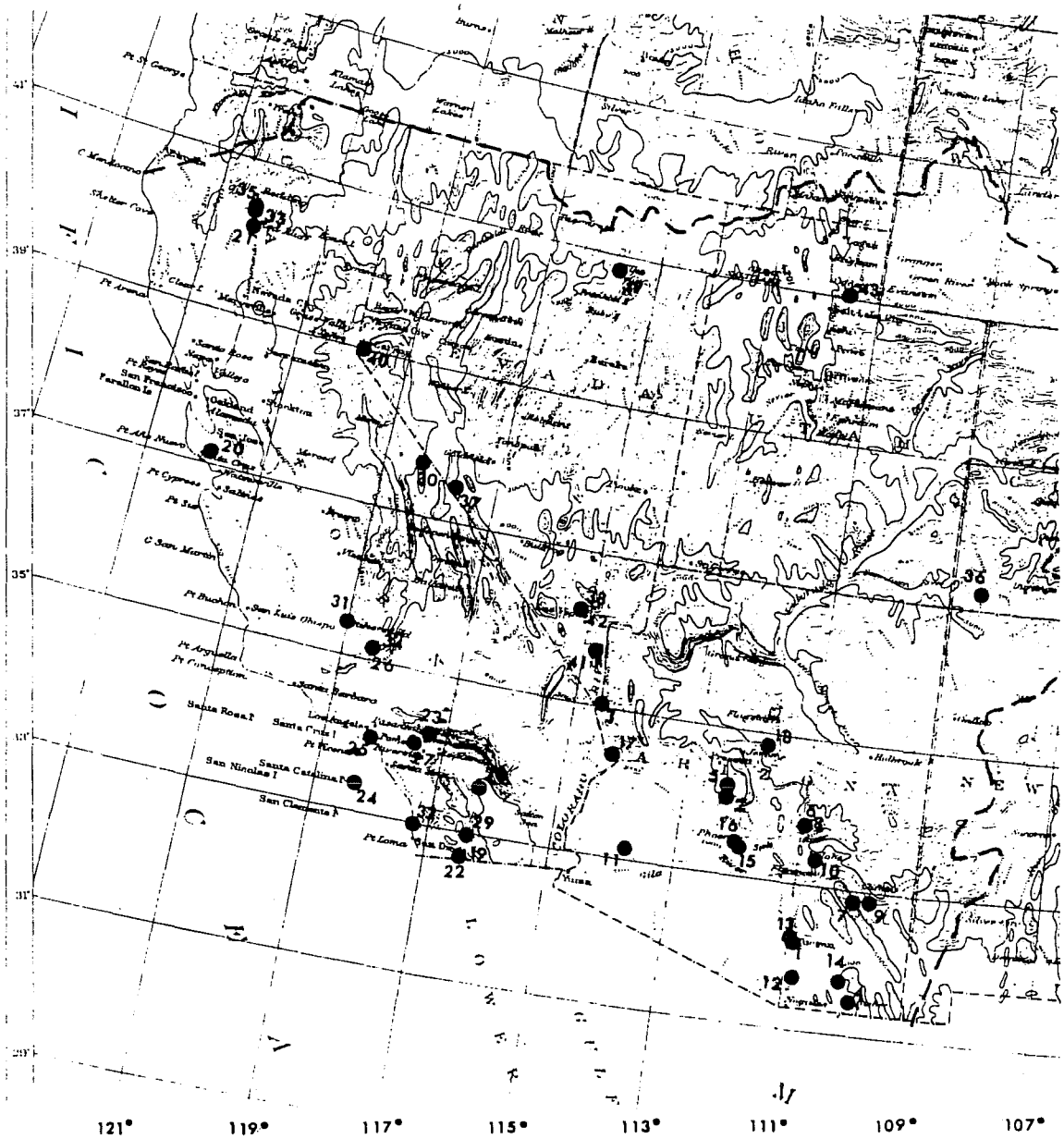

Figure 4.1.--Location of short-duration extreme rainfalls. (See table 4.1 for storm identification).

4.1.2 Definition of Local Storm

One of the most important processes in extreme local storms is the strong convective lifting of moist air. Most storms are thunderstorms, but because thunder is not necessarily heard during extreme rainfall, the term local storm is used.

Record storms used as the basis for local-storm PMP are defined as unusually heavy rains exceeding 3.0 inches (75 mm) in 3 hours or less that are reasonably isolated from surrounding rains. This definition was chosen to provide a basis for selection of candidate storms (generally point rainfall amounts), and because many of the most extreme storms are independent of widespread rain patterns. Thunderstorms with point rainfalls less than the most intense of record have of course been observed in general-storm situations.

The records for California west of the Sierra Nevada contained only a few storms meeeting the criteria set for local storms. Thunderstorm frequency within the Central Valley is one of the lowest in the region studied. Because of the absence of prototype local storms as defined above a decision was made, for California west of the Sierra Nevada, to include extreme point rainfalls that were imbedded in general-type precipitation patterns and that occurred during the warm season.

Our sample of extreme local storms (thunderstorms) in the Southwestern Region have short lifetimes as compared to the supercells observed over the Great Plains. Their lifetime is usually 1 to 2 hours, occasionally as long as 3 hours. Some isohyetal patterns are the combined result of rains within a 6-hr period from two or more storms. Thus 6 hours has been used as the duration limit for local PMP estimates.

PMP values derived in this chapter are estimates of the upper limit of rainfall resulting from summer or early fall local storms. Such storms, while producing the most intense point rainfalls of record, characteristically show a rapid decrease in rainfall with increasing area. We have extended the criteria out to 500 mi^2 (1,295 km^2).

4.2 Storm Record

Determination of PMP for a region is based in part on the most extreme precipitation of record. A survey was made of extreme rains within the study region meeting the definition of local storms in section 4.1.2. The most intense short-period rains found are listed chronologically by State in table 4.1, except for the four long-duration storms in California.

Records, although not complete, permit us to examine a period of about 90 years. Within this span, the number of observers has increased and the manner and detail in recording unusual events has improved, so the storm record is strongly biased toward more recent events. Furthermore, the storms listed in table 4.1 represent only those known to the NWS Hydrometeorological

Table 4.1.--Major short-period rains of record in the Southwestern States and all of California

	Location		Lat., N ° '	Long., W ° '	Elevation ft	Elevation m	Date	Duration min	Amount in.	Amount mm	Reference †	Remarks
Arizona												
1.	Tucson	(n.d.)	32 13	110 58	2360	720	7/11/78*	105	5.10	130	MWR, 7/1878	
2.	Farley's Camp	(n.d.)	34 02	112 18	2700	825	8/28/91*	90	3.10	79	MWR, 8/1891	
3.	Ft. Mohave		35 03	114 36	540	165	8/28/98*	45	~8	203	CCSB, 8/1898	Amount questionable.
4.	Bisbee	(n.d.)	31 27	109 55	5440	1650	7/22/10	70	4.25	108	Green and Sellers,1964	
5.	Crown King	(n.d.)	34 12	112 20	6000	1830	8/11/27	170	4.90	124	Leopold, 1943	
6.	Sierra Ancha	(n.d.)	33 48	110 58	5100	1550	9/10/33	105	4.28	109	1	At experimental forest site.
7.	Pima	(n.d.)	32 51	110 02	4000	1220	8/02/39	60	3.10	79	Langbein, 1941	
8.	Sierra Ancha	(n.d.)	33 48	110 58	5100	1550	8/05/39	140	5.02	128	USCE, 1961	
9.	Thatcher	(n.d.)	32 51	109 46	2800	855	9/16/39	90	4.1	104	USCE, 1961	
10.	Globe		33 20	110 43	3540	1080	7/29/54	40	3.5	89	2	
11.	Welton (25NE)	(n.d.)	33 10	113 45	2800	855	8/23/55	180	~6	~150	3	
12.	Santa Rita		31 45	110 51	4400	1340	6/29/59	60	4.5	114	4	
13.	N. Tucson	(n.d.)	32 18	111 00	2450	750	9/06/64	~120	~5	~125	5	
14.	Walnut Gulch		31 42	110 05	4600	1400	9/10/67	45	3.35	85	Osborn and Renard,1969	
15.	Tempe	(n.d.)	33 23	111 58	1180	360	9/14 69	60	3.52	89	6	
16.	Phoenix		33 27	112 04	1100	355	6/22/72	120	5.25	133	USCE, 1972	
17.	Lk. Havasu City	(n.d.)	34 26	114 20	~500	~150	7/19/74	~60	~4.5	~115	7	
18.	Sedona	(n.d.)	34 53	111 46	~4800	~1460	7/14/75	~60	3.5	89	Selvidge, 1975	
California												
19.	Campo		32 36	116 28	2590	760	8/12/91*	80	11.5	292	USWB, 1960	Amount is a minimum.
20.	Wrights		37 08	121 55	1600	490	9/12/18	~60	~3.5	~90	Weaver, 1962	Tropical cyclone influence.
21.	Red Bluff		40 09	122 15	340	104	9/14/18	180	4.70	119	Weaver, 1962	Tropical cyclone influence.
22.	Campo		32 36	116 28	2590	760	7/18/22	120	7.1	180	CD, 7/1922	
23.	Squirrel Inn		34 14	117 15	5280	1610	7/18/22	90	5.01	127	CD, 7/1922	
24.	Avalon		33 21	118 19	10	3	10/21/41	210	5.53	140	Weaver, 1962	Imbedded in general storm.
25.	Los Angeles		34 00	118 10	500	152	3/03/43	180	3.32	84	Weaver, 1962	Imbedded in general storm.
26.	Tehachapi		35 08	118 27	3975	1210	10/06/45	~120	3.17	81	8	
27.	Cucamonga	(n.d.)	34 05	117 25	1650	500	9/29/46	80	3.2	81	9	
28.	La Quinta	(n.d.)	33 40	116 19	50	15	7/22/48	~210	~3	~75	USCE, 1957	
29.	Vallecito		32 58	116 21	1450	440	7/18/55	70	7.1	180	10	
30.	Chiatovich Flat		37 44	118 15	10320	3140	7/19/55	150	8.25	210	Kesseli and Beaty, 1959	Location uncertain.
31.	Bakersfield		35 25	119 03	475	145	6/07/72	75	3.5	89	Bryant, 1972	Tropical cyclone influence.
32.	Encinitas	(n.d.)	32 59	117 15	100	30	10/12/89*	8 hr	7.58	192	MWR, 10/1889	Possible tropical cyclone.
33.	Kennett		40 23	122 12	730	222	5/09/15	8 hr	8.25	210	Weaver, 1962	Imbedded in general storm.
34.	Tehachapi		35 08	118 27	3975	1210	9/30/32	5 hr	~6.2	~155	CD, 10/1932	Tropical cyclone influence.
35.	Newton		40 22	122 12	700	212	9/18/59	5 hr	~10.6	~270	Weaver, 1962	Imbedded in general storm.
Colorado (west of Continental Divide)												
36.	Mesa Verde N.P.	(n.d.)	37 12	108 29	7070	2160	8/03/24	45	3.50	89	CD, 8/1924	Duration from Bureau of Reclamation, Denver.

† See footnotes at end of table, p. 107

Table 4.1.--Major short-period rains of record in the Southwestern States and all of California--Continued

	Location		Lat., N ° '	Long., W ° '	Elevation ft	Elevation m	Date	Duration min	Amount in.	Amount mm	Reference †	Remarks
Nevada												
37.	Palmetto		37 27	117 42	6700	2040	8/11/90*	60	8.8	224	USWB, 1960	Amount questionable.
38.	Las Vegas		36 11	115 11	2175	660	6/13/55	~120	3.4	86	11	
39.	Elko		40 50	115 40	5075	1660	8/27/70	60	3.64	92	CD, 8/1970	
40.	Genoa	(n.d.)	38 59	119 50	4700	1450	8/07/71	58	3.50	89	12	Most of rain fell in 15 min.
41.	Nelson	(n.d.)	35 43	114 49	3500	1050	9/14/74	45	3.25	83	Glancy and Harmsen, 1975	
42.	Las Vegas		36 11	115 11	2175	660	7/03/75	~210	~3	~75	Randerson, 1975	
New Mexico (west of Continental Divide)												
No reports of amounts exceeding 3 in. (75 mm) in 3 hr or less.												
Utah												
43.	Morgan		41 03	111 38	5150	1570	8/16/58	60	~6.75#	~170	Peck, 1958	

† Reference identification:

MWR: Monthly Weather Review, U.S. Weather Bureau, Washington, D.C.
CCSB: Climate and Crop Service Bulletin, Dept. of Agriculture (early series published monthly for each state).
CD: Climatological Data, U.S. Weather Bureau, Washington, D.C. (published monthly for each state).
USCE: U.S. Army, Corps of Engineers, Washington, D.C.
USWB: U.S. Weather Bureau, Washington, D.C.
USGS: U.S. Geological Survey, Washington, D.C.

Unpublished material; copies available from Hydrometeorological Branch, National Weather Service.

1. Letter from USCE, Los Angeles District (LAD), April 27, 1964.
2. Report from USCE, LAD, August 24, 1954.
3. Report from USCE, LAD, September 15, 1955.
4. Letter from U.S. Dept. of Agriculture, Exp. Rg. Sta., August 21, 1959.
5. Communication from USGS, Tucson, Arizona (undated).
6. Letter from Flood Control District of Maricopa Co., Arizona, October 8, 1969.
7. Communication from USCE, LAD (undated).
8. Joint Review of Flood Damage, Exerpts Kern and Inyo Counties, California, January 17, 1946.
9. Report from San Bernardino Co. Flood Control District, California, October 4, 1946.
10. Report from USCE, LAD, August 5, 1955.
11. Report from USCE, LAD, July 6, 1955.
12. Communication from USGS, Carson City, Nevada (undated).

(n.d.)- no detailed storm study made.
* - storm date prior to 1900.
\# - reported 7 in. questionable.

Branch. Information may exist about other local-storm rains that meet our criteria but are unknown to us. It is doubtful, however, that there are any observed storms that exceed the most extreme of those listed in table 4.1. The file of record storm rainfall is only as complete as is possible from the observational network, through which many extreme local storms can pass unrecorded.

Table 4.1 lists the location, date, duration, amount, and source[1] of each major local storm. Figure 4.1 shows the storm locations. The distribution of storms by State shows greatest frequency closest to warm moisture sources. Storms at Avalon and La Quinta, California and Las Vegas, Nevada exceed the 3-hr duration limit by about one-half hour, but were included because they appeared to be exceptional cases at their respective locations. The 1941 Avalon storm, and the Los Angeles storm of 1943 appear to be general-storms, but their maximum point amounts were the result of imbedded thunderstorms and were notably larger than the surrounding general-storm rains. In addition, four extreme storm values that came from durations much longer than 3 hours are listed in table 4.1 for California (Encinitas, Kennett, Tehachapi, and Newton). The meteorological description of these four storms has been presented elsewhere (Weaver 1962). They all were from either early or late cool-season general storms, or from rains produced by tropical storm moisture, but whose maximum value was very localized. Tropical storms usually affect only the southern half of California while the general frontal-type events occur mostly in the northern half of the State. On a few occasions tropical moisture penetrates northward nearly to the Oregon border. Since few cases of large rainfall from isolated storms were found in coastal California, it was believed important to this study to consider these few exceptions.

Meteorological analyses of the synoptic weather surrounding most of the other significant events listed in table 4.1 are included in a companion report to this study (Schwarz and Hansen 1978). Characteristics of moisture, instability, and inflow believed pertinent to the development of the local storm and the effects of movement and terrain on maximizing rainfall are also discussed in that volume.

4.3 Development of 1-Hr PMP

4.3.1 Introduction

The development of local-storm PMP has several steps: First, 1-hr PMP is estimated over the region for 1 mi^2 (2.6 km^2). Then, durational and areal variations are determined. The method for developing the 1-hr PMP is comparable in many respects to basic PMP approaches used in studies for other parts of the country.

Some studies, particularly those in the region east of the 105th meridian, make widespread use of the transposition of extremes within meteorologically homogeneous regions to supplement sparse data. In the Southwest, however,

[1]Published references are listed at the end of this report, unpublished material is numerically referenced at the end of table 4.1.

terrain limits explicit transposition of observed local-storm maxima. The final 1-hr PMP map however is drawn in part by smoothing between data points thus implicitly introducing transposition.

4.3.2 Data adjustments

In studies of PMP it is assumed that observed data come from storms in which the contributing factors were not all at their maximum. Where there is sufficient storm data, a procedure for adjustment to maximum moisture, storm transposition, and smooth envelopment durationally, areally, and over a region is considered adequate for an estimate of PMP. This is the method of this study.

The following adjustments were made on the data:

a. Adjustment for maximum moisture. As in the case of convergence PMP for general storms discussed in chapter 2, moisture maximization was used to adjust short-term storms to potential moisture considered possible for the location and date. The procedure for maximization is similar to that stated in section 2.2.1; however, maximum 12-hr persisting 1000-mb (100-kPa) dew points for local storms were used (Schwarz and Hansen 1978).

b. Adjustment for elevation. The elevations of observed maximum local-storm rains in table 4.1 vary from sea level to over 10,000 feet (3,048 m). No discernable relation appears between rainfall amount and elevation for these data.

Guidance on adjustment for elevation was sought from maximum 6-consecutive clock-hour rainfall for the months of May through September at recorder stations. Plots of these data vs. station elevation for three states are presented in figure 4.2. The dashed lines envelop the body of data, and show a tendency for rainfall to decrease for stations above 4,000 to 5,000 feet (1,219 - 1,524 m).

In chapter 2, the elevation adjustment allowed for reduced moisture with increased elevation above sea level. For general-type storms, the need for sustained inflows and the effects of barriers warrented such an adjustment. In our study of local storms, however, conditions of local moisture and the evidence in figure 4.2 suggest that maximum precipitation could occur through some range of elevations. Theoretically, such a condition could result from a combination of factors, such as vertical mixing, vertical velocities, convergence effects, etc. Above some level, there must be a reduction in precipitation potential with height. At what height this reduction begins is not evident from meteorological knowledge.

We have chosen 5,000 feet (1,524 m) as the elevation of the limit to maximum effective precipitation in this study. A limit of 5,000 feet is somewhat in agreement with the results shown in figure 4.2, and is compatible with the limit established in HMR No. 43. No adjustment in precipitation is made for elevations up to 5,000 feet (1,524 m). Above this level, a decrease of 5

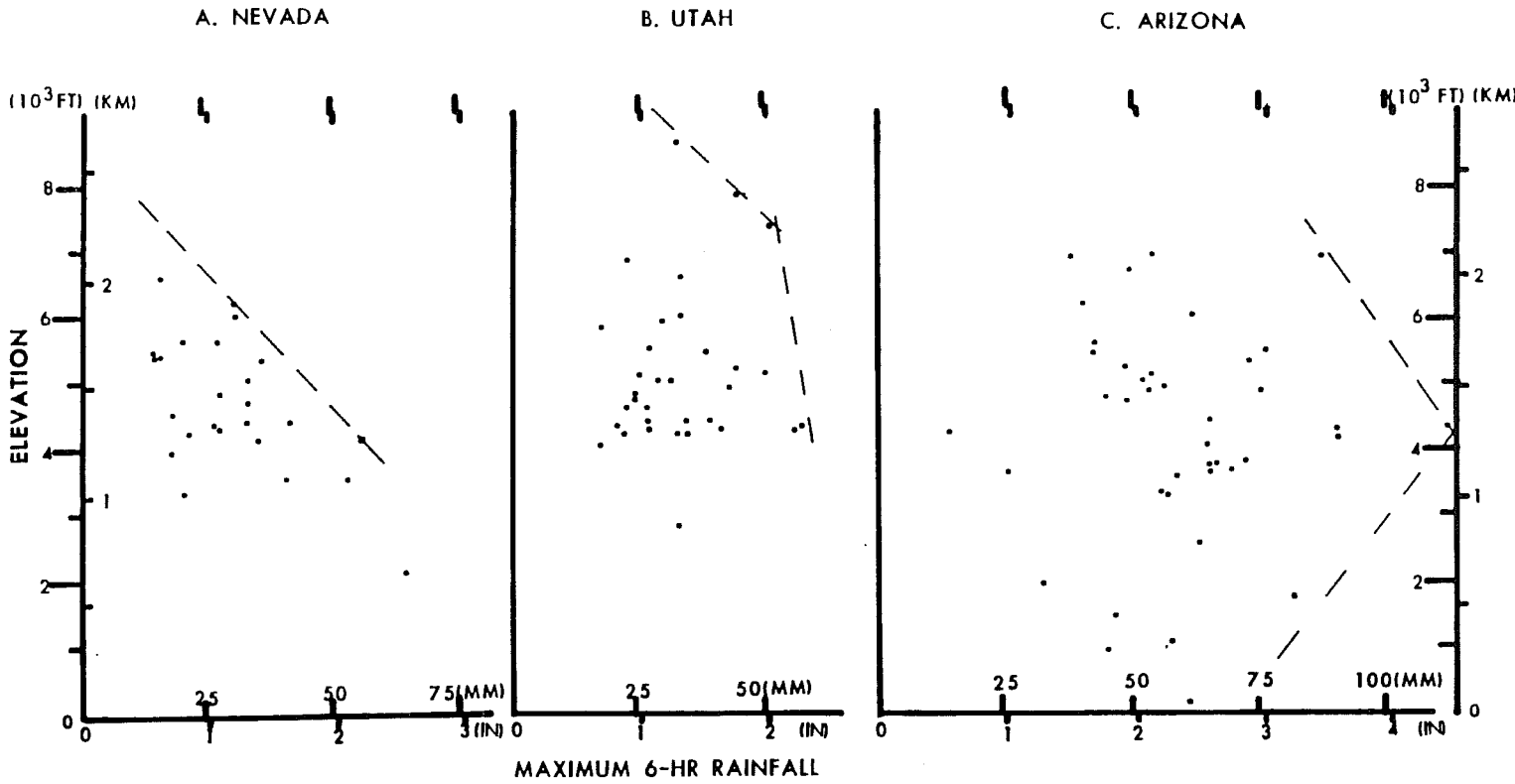

Figure 4.2.--Variation of maximum 6-hr summer recorder rainfall with elevation (period of record is 1940-1972).

percent per 1,000 feet (305 m) of additional elevation is applied. This adjustment was used to normalize all observations in table 4.1 for elevation. Similarly, this adjustment must be applied to PMP for elevations above 5,000 feet (see chapter 6).

c. Adjustment for duration. The storms in table 4.1 had durations ranging between 15 and 210 minutes (except for the four relatively longer duration storms in California). All the durations in this table were adjusted to a common duration of 1 hour. Normalization for duration has been accomplished through use of the depth-duration relations shown in figure 4.3. These relations were developed from local-storm rainfalls for May through September in the study region (see discussion, section 4.4).

4.3.2.1 Application of Adjustments to Data. Of the 43 storms listed in table 4.1, the 16 most intense and widely distributed over the region were selected. Table 4.2 shows the results of moisture maximizing and normalizing (for elevation and duration) the 16 storm amounts. Note in column 3 of table 4.2 that the effect of the elevation adjustment for those observations above 5,000 feet (1,524 m) is to increase the rain amount by 5% per 1,000 feet (305 m) above that elevation.

The maximized, normalized values given in column 7 of table 4.2 were plotted on a map at their respective locations as the lower bounds to PMP for those locations. Data were insufficient to define a regional pattern.

4.3.3 Analysis

Maximum 1-hr amounts from recorder stations (1940-72) were examined for guidance to a regional pattern of 1-hr PMP. Not all stations had complete 33-yr records. The largest 1-hr amounts at each station for the months May to September were plotted and an analysis made at 1-in. (25 mm) isohyetal interval (fig. 4.4).

All amounts exceeding 1.5 inches (38 mm) have been underlined as an aid to locating zones of maxima. Noticeable are the number of underlined amounts extending SE-NW across Arizona. These observations reflect the interaction between the terrain and moist southerly flows from the Gulf of California. A much smaller zone of maxima occurs in southern California. Large zones of minimum amounts occur over portions of the Great Basin, the Central Valley of California, and along the Pacific coast.

Further guidance was obtained from the shape of the maximum moisture pattern for August (see fig. 2.3). Lowest moisture occurs along the Pacific coast with a push of maximum values northward through east central Arizona. There is a tendency for lower values in northern New Mexico and western Colorado.

The analysis in figure 4.4 has been influenced by knowledge of the terrain. This includes allowing for stimulation of convective activity which leads to triggering of rainfall in upslope areas.

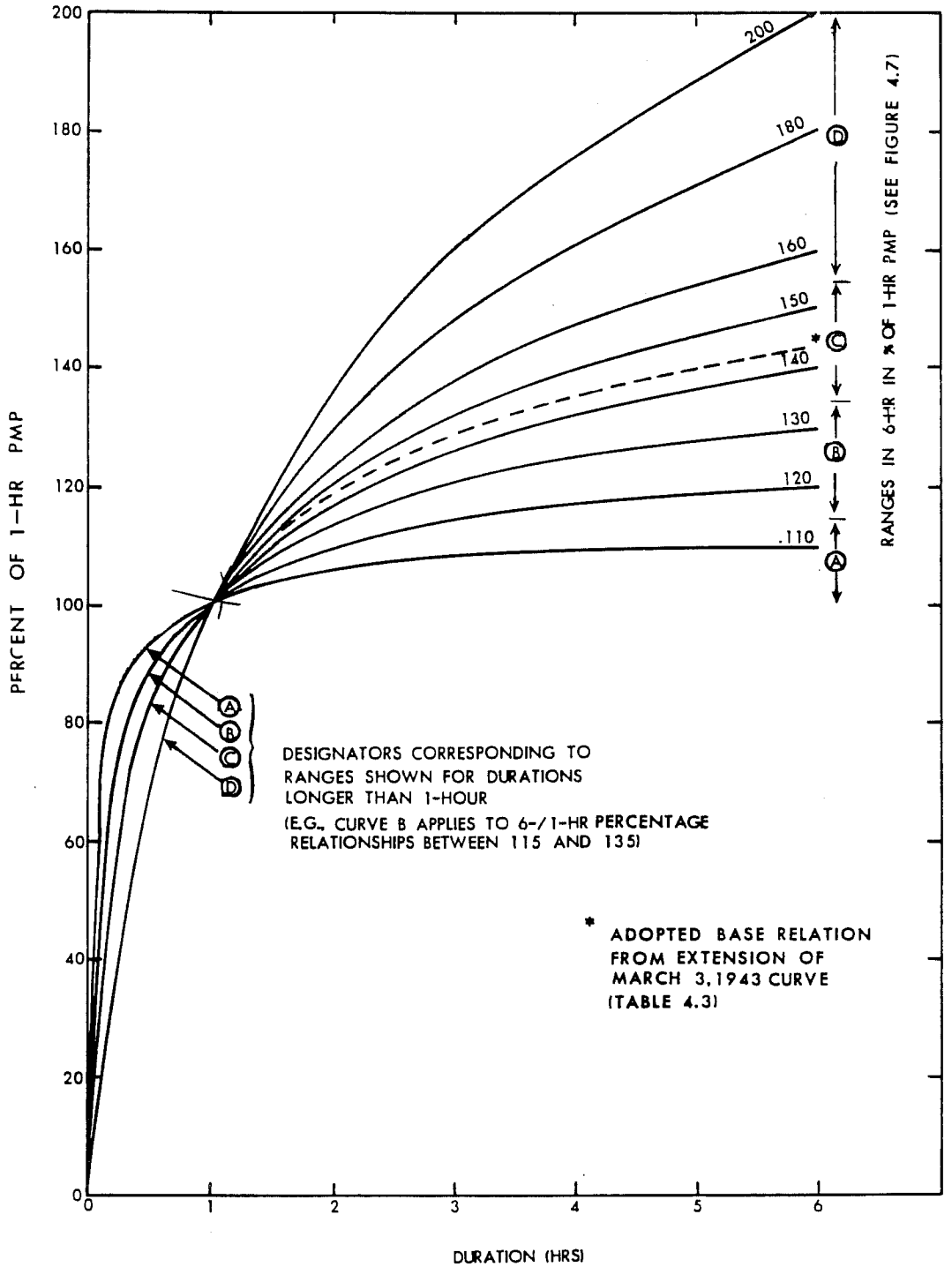

Figure 4.3.--Variable depth-duration curves for 6-hr PMP in the Southwest States and all of California.

Table 4.2.--Adjustment to most critical local-storm rainfalls

Column:	1		2		3		4		5		6	7	
Storm location	Date	Observed amount in.	(mm)	Col. 1 normalized to 1-hr amount in.	(mm)	Col. 2 adjusted to 5000 ft (1524 m)# in.	(mm)	Storm dewpoint °F	(°C)	Maximum dewpoint °F	(°C)	Moisture adjustment factor	Col. 3 multiplied by Col. 6 in.	(mm)
Palmetto, Nev.	8/11/90*	8.8**	(224)	8.8	(224)	9.5	(241)	70	(21)	74	(23)	1.22	11.6	(294)
Campo, Calif.	8/12/91*	11.5	(292)	10.4	(264)	10.4	(264)	72	(22)	75	(24)	1.16	12.1	(307)
Ft. Mohave, Ariz.	8/28/98*	8	(203)	8.4	(213)	8.4	(213)	72	(22)	77	(25)	1.28	11.8	(274)
Mesa Verde N.P., Colo.	8/03/24	3.50	(89)	3.71	(94)	4.08	(103)	65	(18)+	77	(25)	1.80	7.4	(188)
Globe, Ariz.	7/29/54	3.5	(89)	3.7	(94)	3.7	(94)	70	(21)	78	(26)	1.48	5.5	(140)
Vallecito, Calif.	7/18/55	7.1	(180)	6.8	(173)	6.8	(173)	68	(20)	75	(24)	1.41	9.6	(244)
Chiatovich Flat, Calif.	7/19/55	8.25	(219)	6.90	(175)	8.60	(218)	70	(21)	73	(23)	1.16	10.0	(254)
Morgan, Utah	8/16/58	6.75	(171)	6.75	(171)	6.75	(171)	67	(19)	75	(24)	1.48	10.0	(254)
Santa Rita, Ariz.	6/29/59	4.5	(114)	4.5	(114)	4.5	(114)	70	(21)	77	(25)	1.41	6.3	(160)
Elko, Nev.	8/27/70	3.64	(92)	3.64	(92)	3.64	(92)	68	(20)	74	(23)	1.34	4.9	(125)
Bakersfield, Calif.	6/07/72	3.5	(89)	3.1	(79)	3.1	(79)	64	(18)	68	(20)	1.16	3.6	(91)
Phoenix, Ariz.	6/22/72	5.25	(133)	4.57	(116)	4.57	(116)	70	(21)	75	(24)	1.28	5.8	(147)
Encinitas, Calif.	10/12/89*	7.58	(192)	4.00	(101)	4.00	(101)	65	(18)	72	(22)	1.41	5.6	(142)
Wrights, Calif.	9/12/18	3.5++	(89)	3.5	(89)	3.5	(89)	62	(17)	69	(21)	1.41	4.9	(125)
Avalon, Calif.	10/21/41	5.53	(141)	3.50	(89)	3.50	(89)	54	(12)	66	(19)	1.82	6.4	(163)
Newton, Calif.	9/18/59	10.6	(270)	6.5	(165)	6.5	(165)	59	(15)	68	(20)	1.56	10.1	(256)

*Storm date prior to 1900.
**Amount is questionable.
+Based on Phoenix and Grand Junction dewpoints and on estimatdd dewpoint at Durango determined from minimum temperatures.
++24-hr amount of 8.75 in. (222 mm) reduced to 1-hr approximation by subtracting 24-hr amount at a nearby station.
#Adjustment for elevation made for stations above 5000 ft (1524 m), no adjustment for those below 5000 ft.

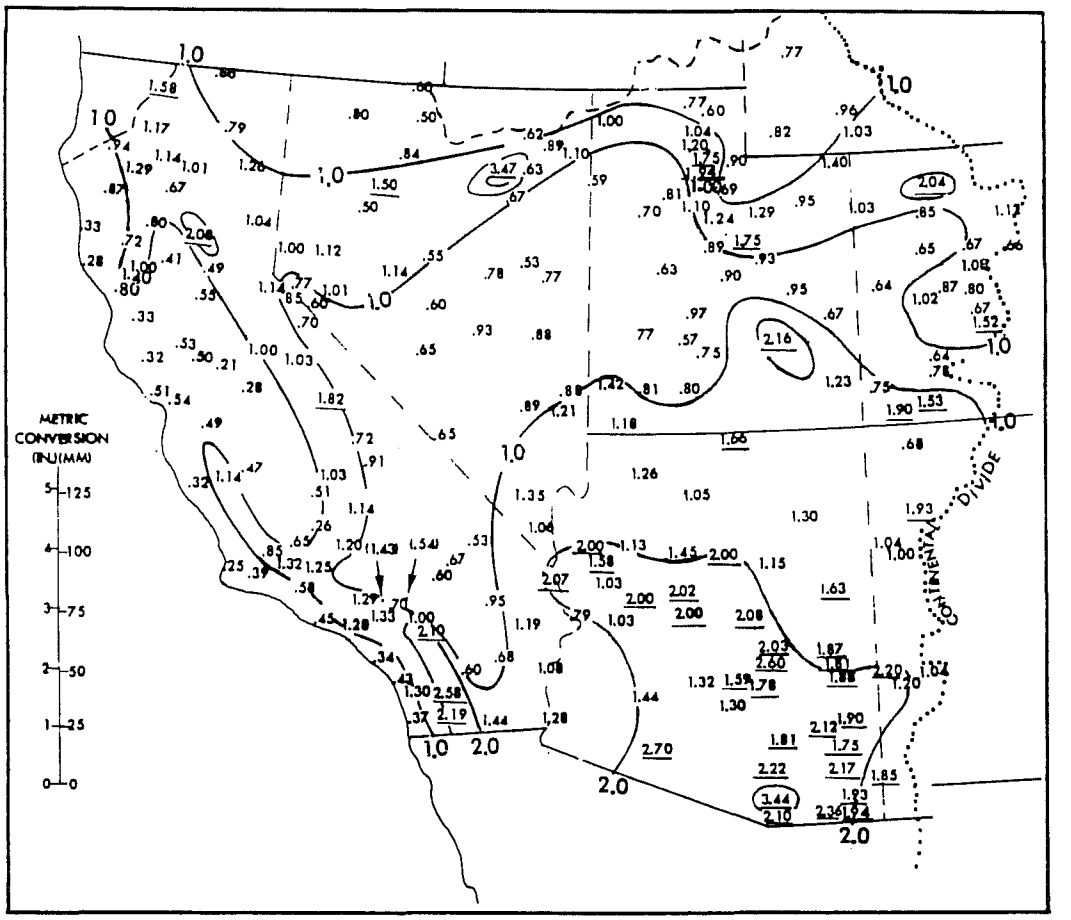

Figure 4.4.--Maximum clock-hour rainfalls at stations with records for period 1940-1972. Underlined values exceed 1.5 inches (38 mm).

The analysis of maximum 1-hr rains in figure 4.4 is a step toward the analysis of the 1-hr PMP in figure 4.5. The primary basis for the 1-hr PMP analysis was the maximized rains in table 4.2, with guidance from the analysis in figure 4.4. Controlling maxima are those at Newton, Chiatovich Flat, Morgan, Ft. Mohave, Avalon, and Campo (underlined on the figure). In addition, maximum moisture and the effects of terrain on the inflow of moisture from source region to storm center was taken into account. The assumption is made that near-maximum moisture necessary to produce a PMP-type event must enter the Southwest from the warm waters of the Gulf of California and the subtropical southeastern Pacific. This assumption is supported by studies of many of the major rainfalls listed in table 4.1. Major terrain barriers obstruct or channelize the inflow of moisture. Figure 4.5 shows a tongue of maximum PMP exceeding 12.0 inches (305 mm) extending northward along the Imperial Valley of southern California. This is part of a broader tongue that penetrates into much of the lower Colorado River drainage and into the Great Basin. It envelops both the Chiatovich Flat, Calif. and Morgan, Utah

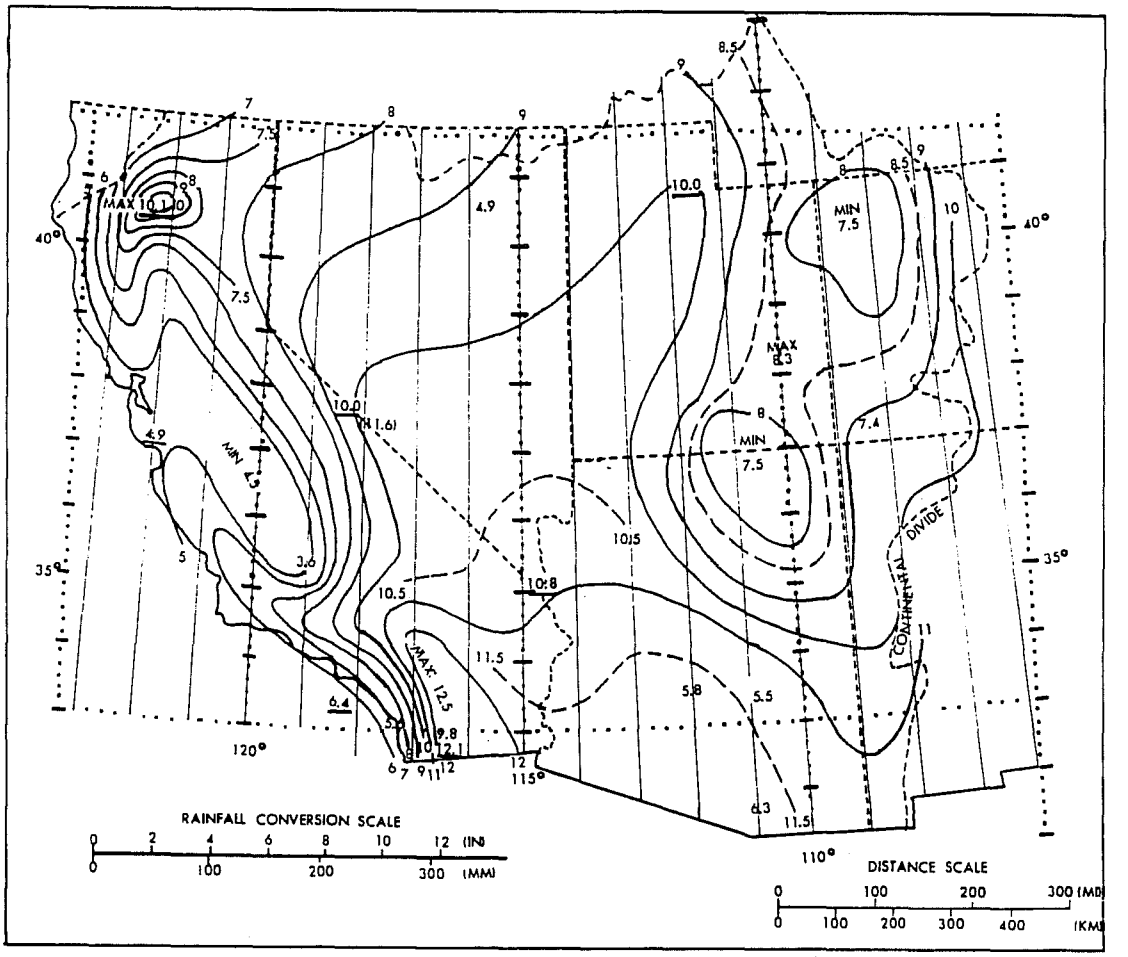

Figure 4.5--Local-storm PMP for 1 mi^2 (2.6 km^2) 1 hr. Directly applicable for locations between sea level and 5000 ft (1524 m). Elevation adjustment must be applied for locations above 5000 ft.

events. In contrast to figure 4.4, figure 4.5 maintains a maximum between these two locations. There is no known meteorological basis for a different solution. The analysis suggests that in the northern portion of the region maximum PMP occurs between the Sierra Nevada on the west and the Wasatch range on the east.

A discrete maximum (> 10 inches, 254 mm) occurs at the north end of the Sacramento Valley in northern California because the northward-flowing moist air is increasingly channeled and forced upslope. Support for this PMP center comes from the Newton, Kennett, and Red Bluff storms (fig. 4.1). Although the analysis in this region appears to be an extension of the broad maximum through the center of the Southwestern Region, it does not indicate the direction of moist inflow. The pattern has evolved primarily as a result of attempts to tie plotted maxima into a reasonable picture while considering inflow directions, terrain effects, and moisture potential.

The last mentioned considerations were important in establishing the gradients through north-central Arizona and the northeastern quadrant of the region of interest. The Mogollon Rim, a range 5,000 to 7,000 feet (1,524 to 2,134 m) in elevation appears to be a prominent obstacle to the low-level moist flows coming northward from the Gulf of California. We believe this barrier is the principle reason why no large local-storm rainfall has been observed to the northeast, and that a sheltering effect is reasonable for the PMP analysis. To the south and southwest of the Mogollon Rim, the PMP increases to a maximum, to reflect the available moisture.

4.4 Durational Variation

4.4.1 Duration of Local-Storm PMP

We postulated that the most extreme or PMP-type local storm could last for 6 hours. A large portion of the total storm should occur in the first hour and almost all within 3 hours. An exception lies in the coastal drainage areas of California where a more continuous inflow of moisture is possible, particularly when synoptic scale systems are involved. Thus, PMP of up to 6 hours probably comes from a moisture resupply that is more typical of the general-storm situation.

4.4.2 Data and Analysis for Durations from 1 to 6 Hours

To obtain local-storm PMP for durations from 1 to 6 hours a number of types of rainfall data were studied. One source of data was recorder station maxima (1940-72). Amounts for 1, 6 and 24 consecutive clock-hour amounts were chosen that met the following conditions.

a. A criterion of minimum clock-hour amounts was established on a regional basis as shown in figure 4.6. The criterion recognizes differences in the magnitude of extremes over the region.

b. The 1-, 6-, and 24-hr consecutive clock-hour amounts at a station must occur on the same date.

c. The 24-hr amount could not exceed the 6-hr amount by more than 0.1 inch (2.5 mm). This helped avoid general type storms.

From data meeting the above criteria, 6/1-hr ratios of rainfall were determined. Averages of ratios for stations within 2° latitude-longitude grid units were used to smooth the data. An analysis of the grid averaged data is shown in figure 4.7.

This analysis needed only slight adjustment to reflect anticipated sheltering influences of major terrain barriers. Especially noteworthy is the strong gradient along the eastern slopes of the Sierra Nevada. East of this gradient the ratios range between 1.10 and 1.40. A zone of minimum ratios (1.10 to 1.20) is centered in the plateau region of southeastern Utah and northeastern Arizona. This minimum can be ascribed to the sheltering effects of the Wasatch range on the west, the Mogollon Rim on the south,

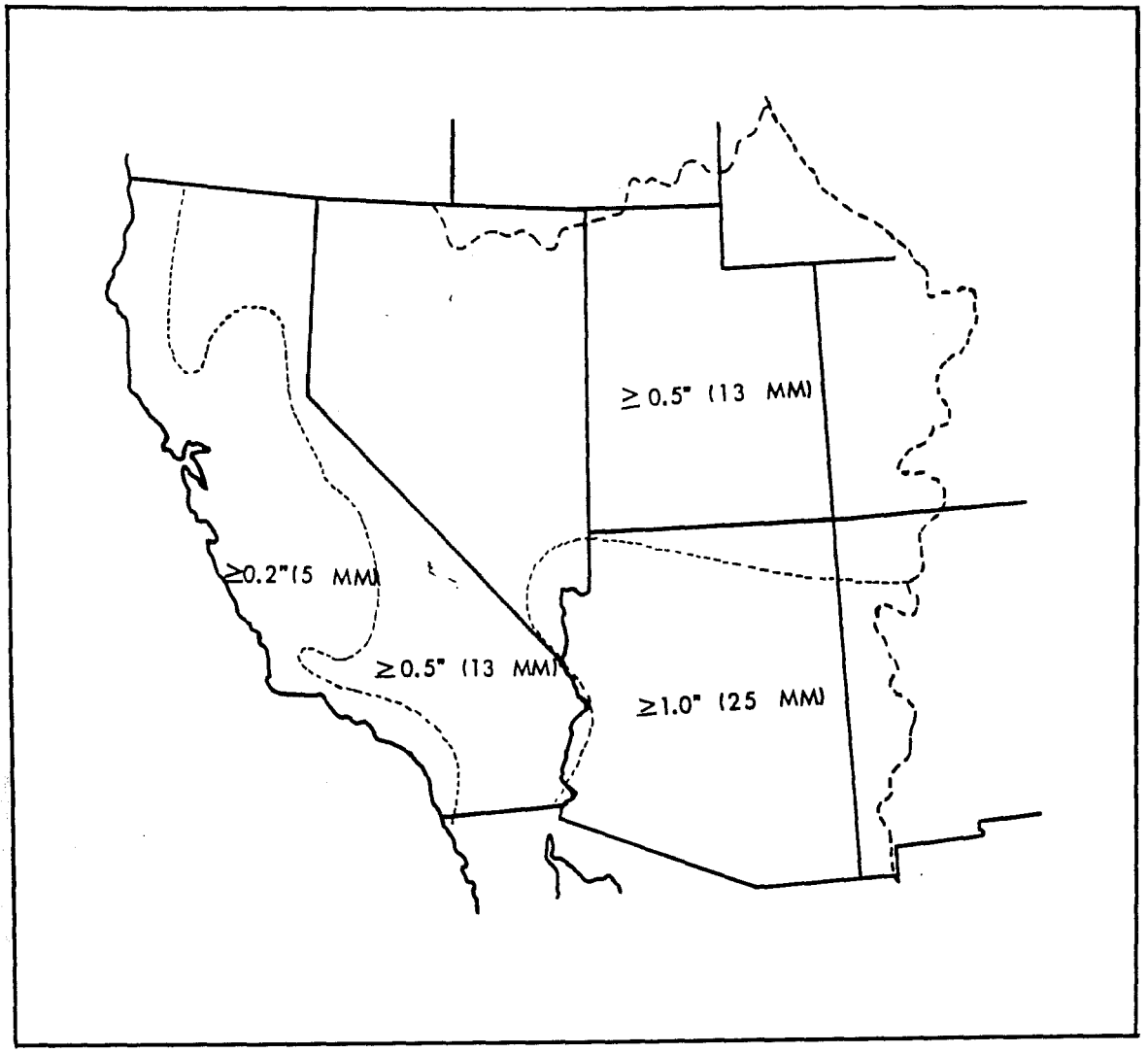

Figure 4.6.--Criteria of clock-hour rainfall amounts used for selection of storms at recorder stations for depth-duration analysis.

and the Rockies on the east. The apparent minimum in Nevada shown by the data is questionable since there are no broadscale topographic features blocking moisture flow. The result may be due to a deficiency of data.

With the exception of the Mojave Desert, the analysis in California shows considerably higher ratios. The maximum along the coast and into the upper Central and Sacramento Valleys exceeds 1.80. Farther inland, terrain barrier effects reduce the ratios.

The wide range of 6/1-hr ratios shown in figure 4.7 suggests that the entire region cannot be represented by a single depth-duration relation. The problem is similar to the depth-duration problem of general-storm PMP (see section 2.4) and we used a similar solution: Find a suitable relation to

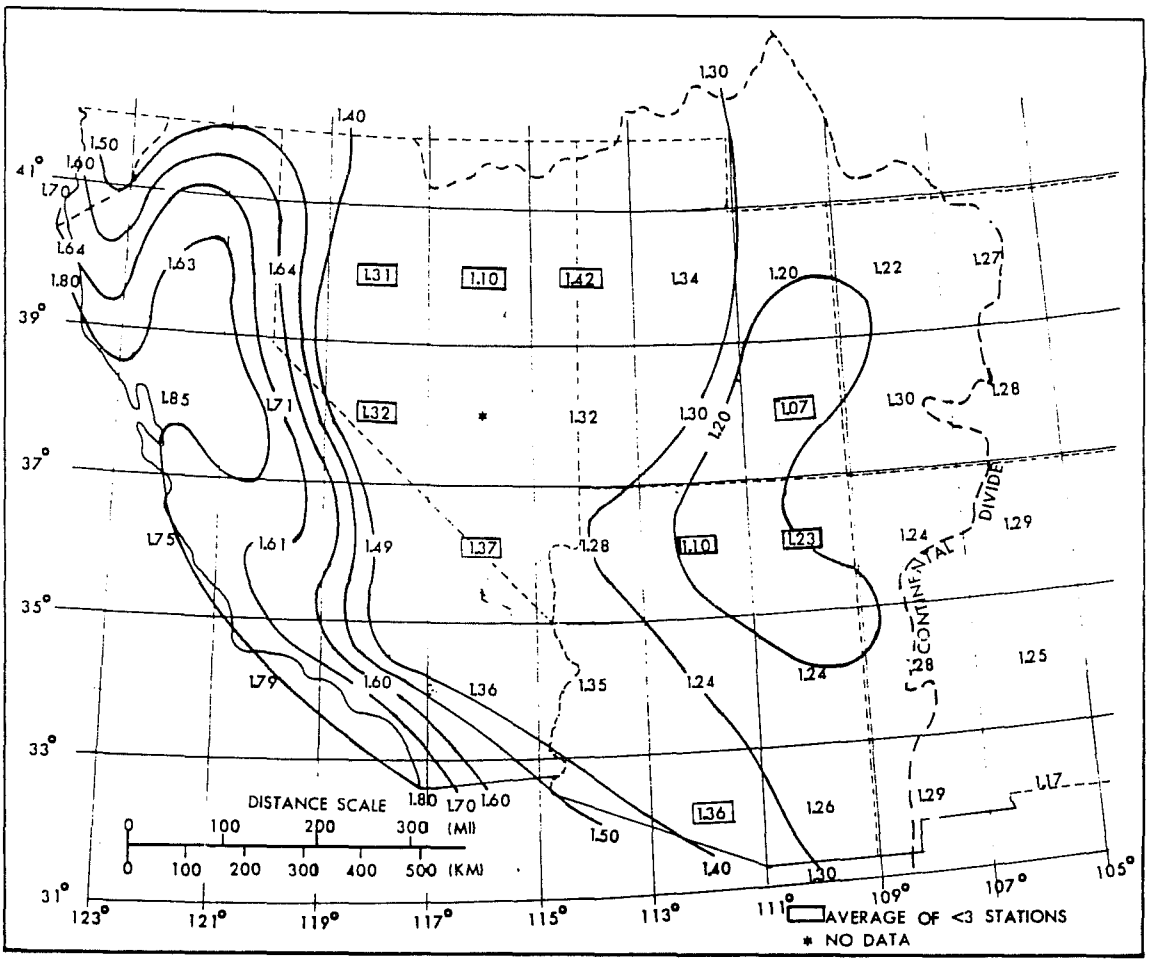

Figure 4.7.--Analysis of 6/1-hr ratios of averaged maximum station data (plotted at midpoints of a 2° latitude-longitude grid).

establish the basic depth-duration curve, then structure a variable set of depth-duration curves to cover the range of 6/1-hr ratios that are needed.

Three sets of data were considered for obtaining a base relation (see table 4.3 for depth-duration data).

a. An average of depth-duration relations from each of 17 greatest 3-hr rains from summer storms (1940-49) in Utah (U. S. Weather Bureau 1951b) and in unpublished tabulations for Nevada and Arizona (1940-63). The 3-hr amounts ranged from 1 to 3 inches (25 to 76 mm) in these events.

b. An average depth-duration relation from 14 of the most extreme short-duration storms listed in Storm Rainfall (U. S. Army, Corps of Engineers 1945-). These storms come from Eastern and Central States and have 3-hr amounts of 5 to 22 inches (127 to 559 mm).

Table 4.3.--Depth-duration relations of severe local storms

	Duration (hr)			
	1	2	3	6
	Percent of 1-hr value			
1. Average of 17 storms Utah, Nevada, and Arizona (recorder data)	100	125	133	152
2. Average of 14 most extreme short-duration storms in Storm Rainfall (U. S. Corps of Engineers 1945-)	100	125	135	166
3. March 3, 1945, Los Angeles storm (U. S. Corps of Engineers 1958)	100	118	128	(144)

c. The depth-duration variation from one of the best documented thunderstorm rainfalls of record in the Southwest. This is the 3-hr, 3.3-in. (84-mm) fall in Los Angeles County, Calif. on March 3, 1943 (U. S. Army, Corps of Engineers 1958). Even though this rainfall was imbedded in more general storm rains, March 3-6, 1943, covering parts of several states, the large amount of reliable data for the event make it useful.

Most of the extreme local storms in the study region (table 4.1) lasted less than 3 hours and little depth-duration data are available for them. We would expect that a representative PMP depth-duration curve would have a lower 6/1-hr ratio than either of the first relations listed. We chose to adopt the relation for the March 3, 1943 storm as guidance for the basic depth-duration curve for the local-storm PMP. A smooth extension of this relation to 6 hours gave a 6-hr value that is 144% of the 1-hr amount. This relation is quite similar to the local storm depth-duration curve of HMR No. 43 in which major Southwest storms were considered. For a variable relation, a family of curves (fig. 4.3) was established where the 6-hr values were incrementally 10% greater than the 1-hr amount. A smooth curve was drawn between the 1-hr (100%) point and the 6-hr (110%) point. The remaining curves were determined by the ratio of the 6-hr value to the difference between 110% and the basic depth-duration (dashed line fig. 4.3) curve.

4.4.3 Data and Analysis for Less Than 1-Hr Duration

Durational relationships for durations less than 1 hour were obtained from data at first-order stations in Utah, Arizona, Nevada and southern California for a period of record between 1954 and 1970. Tables of excessive precipitation at these stations are summarized in the Annual Summary of Climatological Data (U. S. Weather Bureau 1954-) for durations of 5 to 180 minutes. These data showed that storms with low 3/1-hr rain ratios had higher 15-min to 1-hr

ratios than storms with high 3/1-hr ratios. The geographical distribution of 15-min to 1-hr ratios also were inversely correlated with magnitudes of the 6/1-hr ratios of figure 4.7. For example, Los Angeles and San Diego (high 6/1-hr ratios) have low 15-min to 1-hr ratios (approximately 0.60) whereas the 15-min to 1-hr ratios in Arizona and Utah (low 6/1-hr ratios) were generally higher (approximately 0.75).

Depth-duration relations for durations less than 1 hour were then smoothed to provide a family of curves consistent with the relations determined for 1 to 6 hours, as shown in figure 4.3. Adjustment was necessary to some of the curves to provide smoother relations through the common point at 1 hour.

We believe we were justified in reducing the number of the curves shown in figure 4.3 for durations less than 1 hour, letting one curve apply to a range of 6/1-hr ratios. The corresponding curves have been indicated by letter designators, A-D, on figure 4.3. As an example, for any 6-hr amount between 115% and 135% of 1-hr, 1-mi^2 (2.6-km^2) PMP, the associated values for durations less than 1 hour are obtained from the curve designated as "B".

Table 4.4 lists durational variations in percent of 1-hr PMP for selected 6/1-hr rain ratios. These values were interpolated from figure 4.3.

To determine 6-hr PMP for a basin, use figure 4.3 (or table 4.4) and the geographical distribution of 6/1-hr ratios given in figure 4.7.

Table 4.4.--Durational variation of 1-mi^2 (2.6-km^2) local-storm PMP in percent of 1-hr PMP (see figure 4.3)

6/1-hr ratio	Duration (hr)								
	1/4	1/2	3/4	1	2	3	4	5	6
1.1	86	93	97	100	107	109	110	110	110
1.2	74	89	95	100	110	115	118	119	120
1.3	74	89	95	100	114	121	125	128	130
1.4	63	83	93	100	118	126	132	137	140
1.5	63	83	93	100	121	132	140	145	150
1.6	43	70	87	100	124	138	147	154	160
1.8	43	70	87	100	130	149	161	171	180
2.0	43	70	87	100	137	161	175	188	200

4.5 Depth-Area Relation

We have thus far developed local-storm PMP for an area of 1 mi^2 (2.6 km^2). To apply PMP to a basin, we need to determine how 1-mi^2 (2.6-km^2) PMP should decrease with increasing area. We have adopted depth-area relations based on rainfalls in the Southwest and from consideration of a model thunderstorm.

Figure 4.8 is a plot of available depth-area data for major local storms listed in table 4.1. The durations given with the 7 storms are longer than for the point value because of the areal pattern. Most of the data from which areal patterns were drawn came from bucket surveys and other unofficial observations.

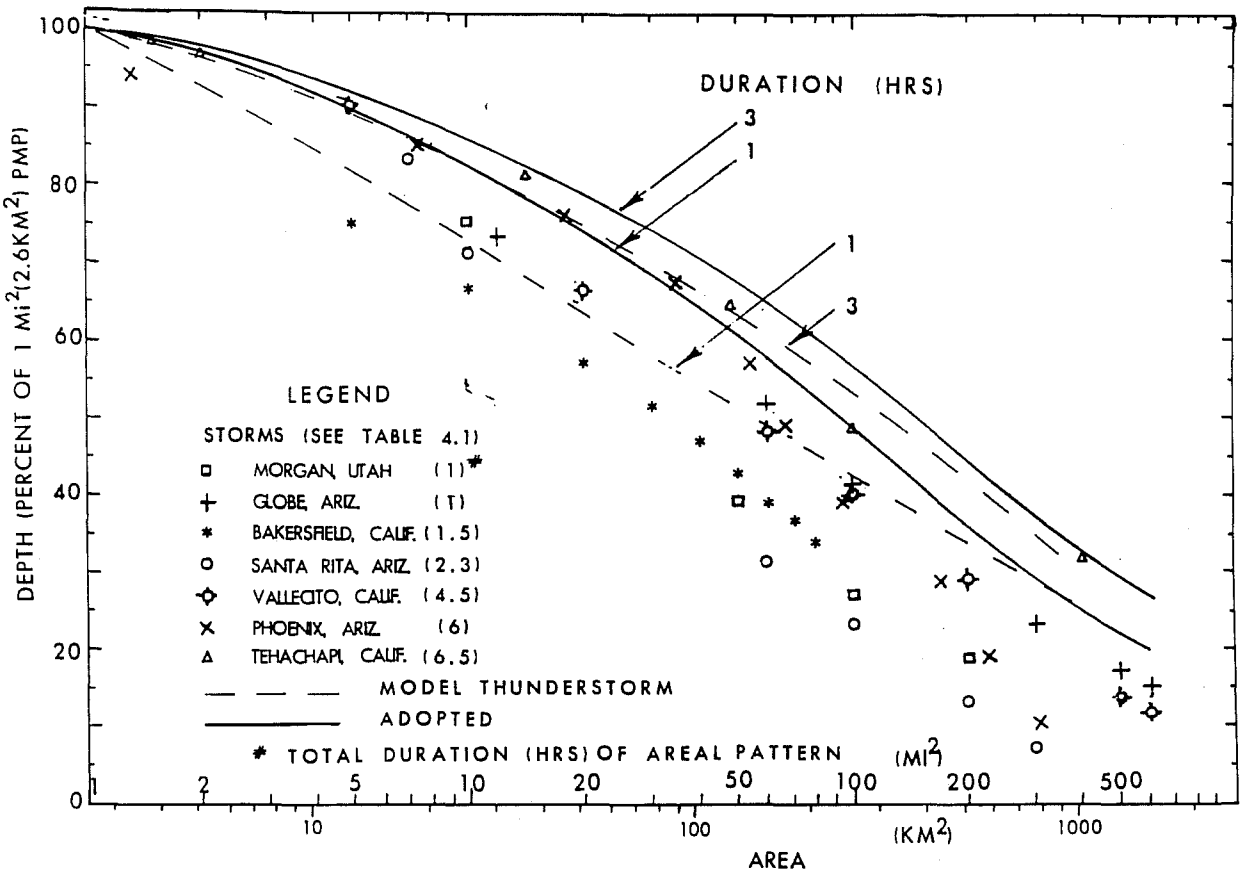

Figure 4.8.--Depth-area relations adopted for local-storm PMP in the Southwest and other data.

Also shown on figure 4.8 are 1- and 3-hr curves from a model thunderstorm. The following conditions comprised the model:

a. A depth-duration relation for 1 mi^2 (2.6 km^2) based on a 6-hr percent of 1 hr of 144% (fig. 4.3).

b. Circular isohyets.

c. A storm rate of travel of 4 mph (1.8 m/sec).

d. A rate of change in storm intensity due to storm motion the same throughout the areal pattern as at a point.

Both the data and the model thunderstorm results were used in determining the adopted depth-area relations for 1 and 3 hours shown on figure 4.8. A first consideration is that the relation must envelop the data. The adopted 1-hr curve shown in figure 4.8 envelops the 1-hr rains (Globe, Morgan and Bakersfield) by roughly 10%. Only data for the two 6-hr rains (Phoenix and Tehachapi) exceed the 1-hr curve. The adopted 3-hr curve envelops all the storm data. The model thunderstorm curves are also enveloped. In the model thunderstorm we assume that if the rate of travel were reduced, the model curves would approach the adopted curves.

A depth-area curve for the Southwest for 6 hours was estimated from relations given in HMR No. 43 based on selected storms for the Eastern United States. Using the curves for 1-, 3-, and 6-hr durations, relations were interpolated for intermediate durations. Depth-duration curves based on these relations and for a number of area sizes were used to obtain values to approximate curves for durations less than 1 hour. The adopted depth-area relations are shown in figure 4.9.

4.6 Distribution of PMP Within a Basin

Idealized elliptically shaped isohyets patterned after the few available storms have been developed for distribution of PMP. The extreme storms at Globe and Vallecito were examples from which an isohyetal pattern having a 2:1 axial ratio was adopted for application throughout the Southwest. The pattern, shown in figure 4.10, is drawn to a 1:500,000 scale. Isohyets are shown on this idealized pattern labeled A (1 mi^2, 2.6 km^2) to J (500 mi^2, 1,295 km^2).

Table 4.5 gives isohyets labeled in percent of 1-hr 1-mi^2 (2.6-km^2) PMP for the 4 highest 15-min incremental PMP values. Incremental labels are given for each of the four indexed 6/1-hr ratio categories (see fig. 4.3). These labels when multiplied by the 1-hr 1-mi^2 (2.6-km^2) PMP for a specific drainage give drainage PMP isohyetal labels for the 4 highest 15-min increments. Table 4.5 also gives isohyetal labels for 1-hr PMP. The resulting isohyetal values take into account the depth-duration relations of figure 4.9.

For obtaining PMP out to 6 hours duration (remaining five lesser 1-hr increments of PMP), use the isohyetal values given in table 4.6. The 1-hr increments of PMP are listed in successively decreasing order of magnitude. The percents by which the 1-hr 1-mi^2 (2.6-km^2) PMP are to be multiplied to obtain isohyetal values are categorized by the 6/1-hr ratios. Steps outlining the application of these percents are presented along with an example in chapter 6.

4.7 Time Distribution of Incremental PMP

We have little information about the time sequence of incremental 1-hr rainfalls for intense local storms. A study of sequences of increments in each of 38 six-hr storms (U. S. Weather Bureau 1947) resulted in an average mass curve in which the maximum intensities occurred in the middle of the

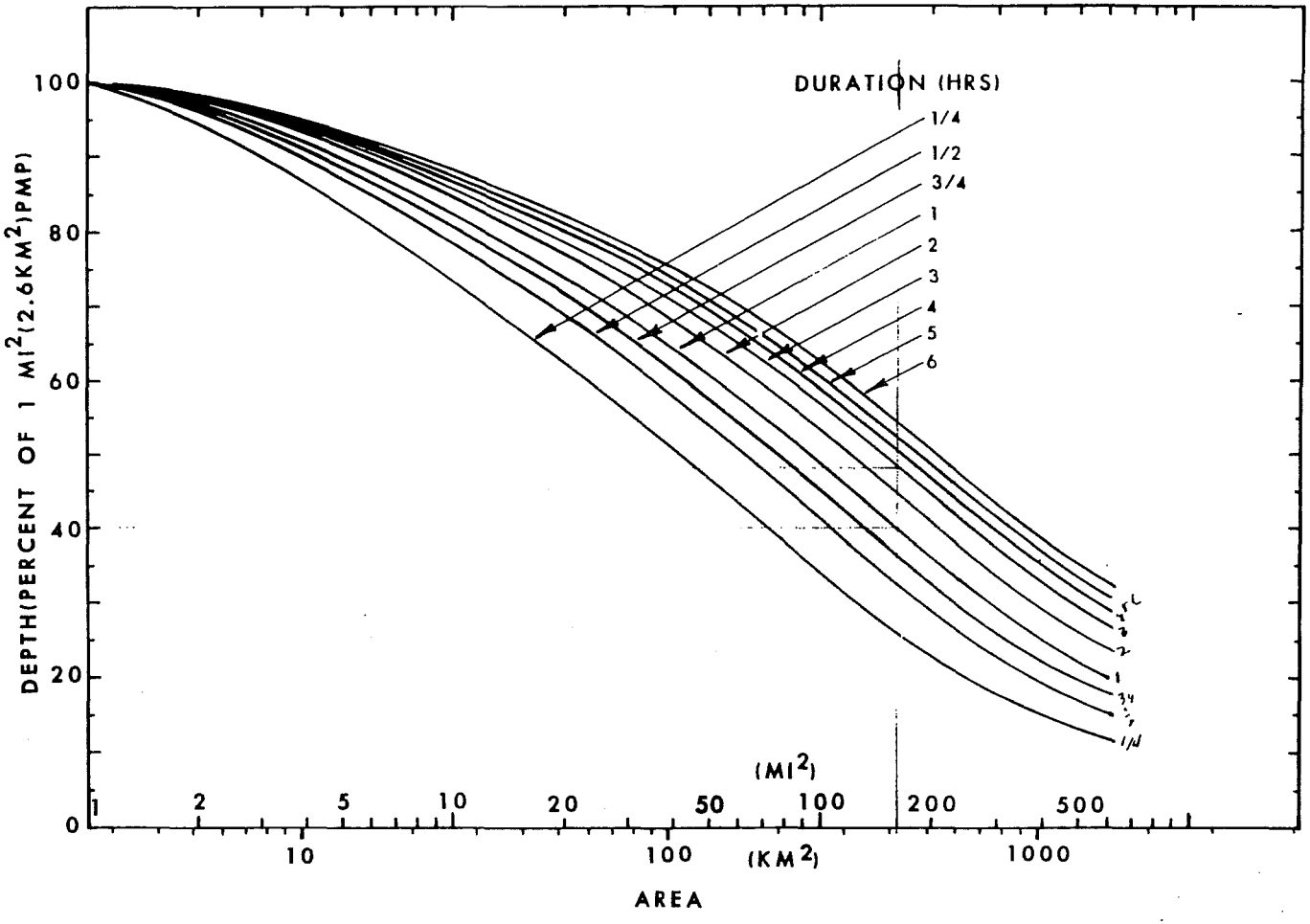

Figure 4.9.--Adopted depth-area relations for local-storm PMP.

Table 4.5.--Isohyetal labels for the 4 highest 15-min PMP increments and for 1-hr PMP

6/hr ratio (%)	PMP Increment	Isohyet A	B	C	D	E	F	G	H	I	J
		Enclosed area mi^2 (km^2)									
		1 (2.6)	5 (13)	25 (65)	55 (142)	95 (246)	150 (388)	220 (570)	300 (777)	385 (997)	500 (1,295)
		Percent of 1-hr, 1-mi^2 (2.6-km^2) PMP									
<115 (A)	Highest 15-min.	86	68	44	30	18	10	7	6	5	4
	2nd. 15-min.	7	7	7	7	7	6	4	3	3	3
	3rd. 15-min.	4	4	4	4	4	4	3	2	2	2
	4th. 15-min.	3	3	3	3	3	3	2	2	2	2
116-135 (B)	Highest 15-min.	74	56	32	21	14	8	7	6	5	4
	2nd. 15-min.	15	15	15	12	9	6	4	3	3	3
	3rd. 15-min.	6	6	6	6	5	5	3	2	2	2
	4th. 15-min.	5	5	5	5	4	4	2	2	2	2
136-155 (C)	Highest 15-min.	63	45	27	18	11	7	6	5	4	4
	2nd. 15-min.	20	20	15	12	9	6	4	3	3	3
	3rd. 15-min.	10	10	9	8	7	5	3	3	3	3
	4th. 15-min.	7	7	7	6	5	5	3	2	2	2
>156 (D)	Highest 15-min.	43	31	19	14	9	7	5	4	4	4
	2nd. 15-min.	27	23	16	12	8	6	4	3	3	3
	3rd. 15-min.	17	16	13	10	8	5	4	3	3	2
	4th. 15-min.	13	12	10	8	7	5	3	3	2	2
	1-hr.PMP	100	82	58	44	32	23	16	13	12	11

Table 4.6.--Isohyetal labels for second to sixth hourly incremental PMP in perceont of 1-hr 1-mi^2 (2.6-km^2) PMP

6/1-hr ratio	Isohyet A	B	C	D	E	F	G	H	I	J
					Second highest 1-hr PMP increment					
1.1	7	7	7	7	7	7	6	4	4	4
1.2	11	11	11	11	10	8	7	5	5	5
1.3	14	14	14	12	11	9	7	5	5	5
1.4	17	17	16	14	12	10	8	6	6	6
1.5	21	20	18	16	13	11	8	6	6	6
1.6	24	23	20	18	15	12	9	7	7	6
1.7	27	26	23	20	16	13	10	7	7	7
1.8	30	29	25	21	17	14	10	8	8	7
1.9	34	32	27	23	18	14	11	8	8	8
					Third highest 1-hr PMP increment					
1.1	2	2	2	2	2	2	2	2	2	2
1.2	4	4	4	4	4	4	4	4	4	4
1.3	6	6	6	6	6	6	5	5	5	5
1.4	9	9	9	9	8	7	6	5	5	5
1.5	11	11	11	11	10	8	7	5	5	5
1.6	14	14	14	13	11	10	8	6	6	6
1.7	17	17	17	14	13	11	8	7	6	6
1.8	19	19	18	16	14	12	9	7	6	6
1.9	21	21	20	18	15	13	10	8	7	7
					Fourth highest 1-hr PMP increment					
1.1	1	1	1	1	1	1	1	1	1	1
1.2	3	3	3	3	3	3	3	3	3	3
1.3	5	5	5	5	5	5	5	4	4	4
1.4	6	6	6	6	6	5	5	4	4	4
1.5	7	7	7	7	7	6	5	4	4	4
1.6	8	8	8	8	7	6	5	5	5	5
1.7	10	10	10	9	8	7	6	5	5	5
1.8	12	11	11	10	9	8	7	6	5	5
1.9	14	13	12	11	10	9	7	6	6	6
					Fifth highest 1-hr PMP increment					
1.1	1	1	1	1	1	1	1	1	1	1
1.2	2	2	2	2	2	2	2	2	2	2
1.3	3	3	3	3	3	3	3	3	3	3
1.4	5	5	5	5	5	5	4	4	4	4
1.5	6	6	6	6	6	5	5	4	4	4
1.6	7	7	7	7	7	6	5	5	5	5
1.7	9	9	9	9	8	7	5	5	5	5
1.8	10	10	10	10	9	7	6	6	5	5
1.9	12	12	12	11	9	8	6	6	6	6
					Sixth highest 1-hr PMP increment					
1.1	1	1	1	1	1	1	1	1	1	1
1.2	1	1	1	1	1	1	1	1	1	1
1.3	2	2	2	2	2	2	2	2	2	2
1.4	4	4	4	4	4	4	4	4	4	3
1.5	5	5	5	5	5	5	4	4	4	4
1.6	6	6	6	6	6	5	5	5	5	5
1.7	7	7	7	7	7	6	5	5	5	5
1.8	8	8	8	8	8	6	5	5	5	5
1.9	9	9	9	9	9	8	6	6	5	5

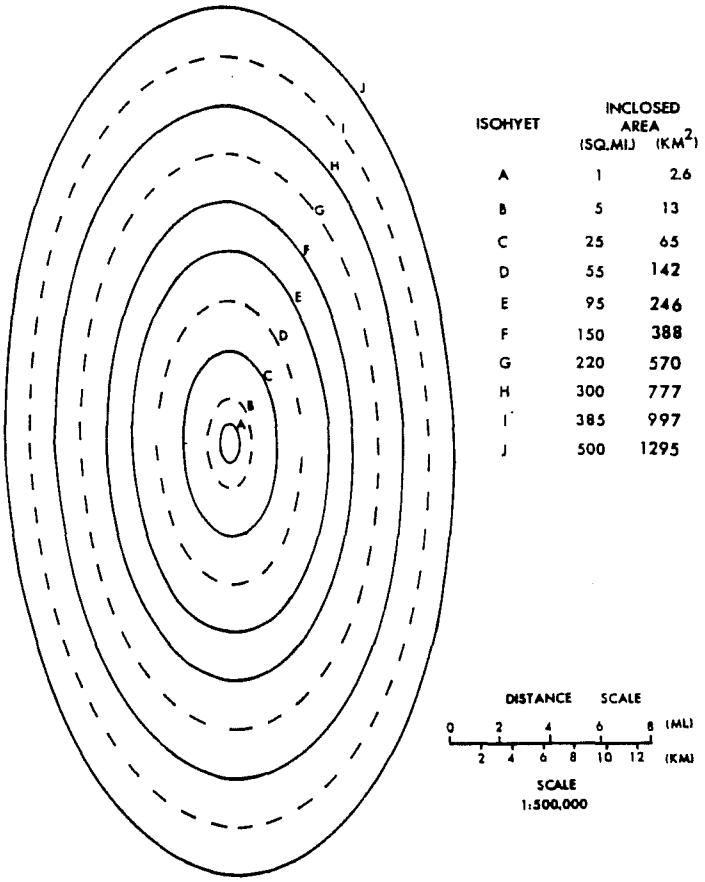

Figure 4.10.--Idealized local-storm isohyetal pattern.

storm period. The sequence of hourly incremental PMP for the Southwest 6-hr thunderstorm in accord with this study is presented in column 2 of table 4.7. A small variation from this sequence is given in Engineering Manual 1110-2-1411 (U. S. Army, Corps of Engineers 1965). The latter, listed in column 3 of table 4.7, places greater incremental amounts somewhat more toward the end of the 6-hr storm period. In application, the choice of either of these distributions is left to the user since one may prove to be more critical in a specific case than the other.

Table 4.7.--Time sequence for hourly incremental PMP in 6-hr storm

	HMR No. 5[1]	EM1110-2-1411[2]
Increment	Sequence Position	
Largest hourly amount	Third	Fourth
2nd largest	Fourth	Third
3rd largest	Second	Fifth
4th largest	Fifth	Second
5th largest	First	Last
least	Last	First

[1]U. S. Weather Bureau 1947.
[2]U. S. Corps of Engineers 1952.

Also of importance is the sequence of the four 15-min incremental PMP values. We recommend a time distribution, table 4.8, giving the greatest intensity in the first 15-min interval (U.S. Weather Bureau 1947). This is based on data from a broad geographical region. Additional support for this time distribution is found in the reports of specific storms by Keppell (1963) and Osborn and Renard (1969).

Table 4.8.--Time sequence for 15-min incremental PMP within 1 hr.

Increment	Sequence Position
Largest 15-min amount	First
2nd largest	Second
3rd largest	Third
least	Last

4.8 Seasonal Distribution

The time of the year when local-storm PMP is most likely is of interest. Guidance was obtained from analysis of the distribution of maximum 1-hr thunderstorm events through the warm season at the recording stations in Utah, Arizona, and in southern California (south of 37°N and east of the Sierra Nevada ridgeline). The period of record used was for 1940-72 with an average record length for the stations considered of 27 years. The month with the one greatest thunderstorm rainfall for the period of record at each station was noted. The totals of these events for each month, by States, are shown in table 4.9.

Table 4.9.--Seasonal distribution of thunderstorm rainfalls.

(The maximum event at each of 108 stations, period of record 1940-72.)

	Month						
	M	J	J	A	S	O	No. of Cases
Utah	1	5	9	14	5		34
Arizona		4	16	19	4		43
S. Calif.*		14	10	7			31
No. of cases/mo.	1	23	35	40	9	0	

*South of 37°N and east of Sierra Nevada ridgeline.

This distribution, by months, agrees well with the month of occurrence of the extreme thunderstorm rainfalls for the Southwest listed in table 4.1. July and August have the greatest frequency of extreme rains in both sets of data.

For the coastal drainages of California, most thunderstorms are associated with general-storm rainfalls (see discussion in the companion volume, Schwarz and Hansen 1978). The occurrence of these cool-season mid-latitude and tropical storm systems is apparently limited to the spring and fall months. Figure 4.11 presents the regional variation of the months of greatest potential for a 1-hr thunderstorm event approaching the magnitude of PMP.

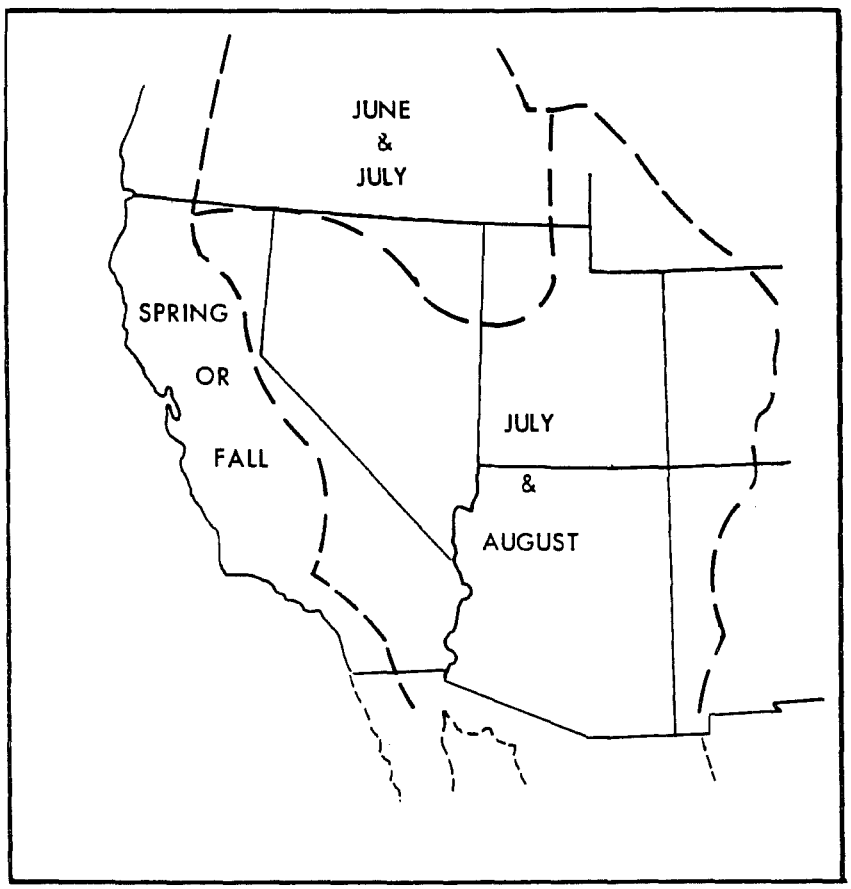

Figure 4.11.--Regional variation of month of maximum local-storm rainfall. (boundaries are not precise)

5. CHECKS ON THE GENERAL LEVEL OF PMP

5.1 Introduction

All probable maximum precipitation estimates involve some degree of uncertainty. Decisions leading to a level that provides safety, while not introducing unrealistically large estimates of precipitation amounts, requires experience and meteorological judgment. Guidance for such decisions includes evaluating maximum observed precipitation depths, and meteorological studies of storm characteristics such as moisture sources and storm mechanism. PMP must exceed the envelop of maximum observed values. For most regions, nature has not yet given us the biggest storm; rainfalls occasionally exceed the previous maximum from over 50 years of record by factors of 2 or 3.

In this chapter PMP estimates are compared with known maximum precipitation amounts in the Southwest States. We also show comparisons of the general level of PMP in this study with values in an earlier study and with PMP estimates in adjoining regions. In chapters 2 and 3 we pointed out how convergence and orographic PMP index maps compare with similar maps in HMR Nos. 43 and 36 for adjoining regions to the north and west, respectively. These discussions will not be repeated here. Rather, the general level of total PMP will be compared. Comparisons are also made with 100-yr rainfall and with some statistically estimated PMP values. Finally, we evaluate the rain potential from a hypothetical tropical cyclone, one that has the most extreme characteristics for producing rainfall for the Southwest States that such a storm might have.

5.2 Comparisons with Greatest Known General-Storm Areal Rainfalls

From a catalog of greatest known areal rainfall depths (Shipe and Riedel 1976) the greatest depths for various portions of the study region were extracted for the winter, spring, summer and fall seasons. Four standard areas: 100, 500, 1,000 and 5,000 mi^2 (259, 1,295, 2,590 and 12,950 km^2) for 6, 12, 18, 24, 48, and 72 hours were considered.

Table 5.1 lists the storm date, latitude and longitude of rainfall center, general location by section of the State, and the ratio of observed to general-storm PMP for the month of the storm for the selected area sizes. Of these comparisons, the September 1970 rainfall center in southwestern Colorado and southeastern Utah stands out with a high ratio of observed to PMP of 0.88 for 6 hours over 100 mi^2 (259 km^2). [The local-storm PMP (chapter 4) at this location exceeds the general-storm values, for this size area and duration, giving a ratio of observed to PMP of 0.69.] The more intense rainfall center of the September 1970 storm in central Arizona (where the ratios of observed to PMP are smaller than at the northern center) is not as rare an event. Comparisons with mean annual precipitation and other rainfall indices also lead to this conclusion.

Examination of the variation of the ratios of observed to PMP with duration shows the ratios decrease with increasing duration. This trend is considered reasonable in that nature has given us a larger number of extreme short-duration storms than longer ones over any given basin. There are rare

Table 5.1.--Comparison of storm areal rainfall depths with general-storm PMP for the month of the storm

Date	Latitude-longitude (of center)		General location	Area mi^2	Area (km^2)	Duration (hrs) 6	12	18	24	48	72
						obs/PMP					
11/25-28/05	34°13'	112°45'	Central Ariz.	100	(259)	.54	.38	.35	.33	.27	
				500	(1295)	.60	.40	.38	.36	.31	
				1000	(2590)	.60	.40	.38	.37	.34	
2/1-5/07	41°45'	115°25'	NE Nev.	100	(259)	.60	.68	.52	.59	.50	.51
				500	(1295)	.62	.67	.50	.56	.48	.49
				1000	(2590)	.61	.68	.64	.63	.54	.55
12/14-17/08	37°30'	108°30'	SW Colo.	100	(259)	.48	.53	.50	.53	.50	.52
				500	(1295)	.50	.52	.53	.53	.51	.53
				1000	(2590)	.50	.51	.50	.50	.47	.50
				5000	(12950)	.60	.58	.60	.55	.53	.55
12/14-17/08	34°22'	111°25'	Central Ariz.	5000	(12950)	.35	.44	.35	.35	.38	.36
8/28-9/2/09	40°00'	111°00'	N Utah	100	(259)	.34	.42	.34	.47	.39	.37
				500	(1295)	.32	.39	.31	.42	.34	.32
				1000	(2590)	.33	.39	.31	.40	.32	.31
				5000	(12950)	.31	.34	.26	.34	.27	.26
10/4-6/11	37°49'	107°40'	SW Colo.	100	(259)	.53	.64	.65	.60	.46	
				500	(1295)	.36	.45	.47	.43	.33	
				1000	(2590)	.39	.47	.52	.49	.38	
				5000	(12950)	.40	.41	.48	.47	.37	
4/5-10/26	34°51'	112°00'	Central Ariz.	100	(259)	.52	.41	.41	.37	.30	
				500	(1295)	.51	.43	.44	.41	.32	
				1000	(2590)	.51	.45	.47	.42	.33	
				5000	(12950)	.39	.36	.37	.35	.27	
2/11-17/27	34°19'	111°27'	Central Ariz.	100	(259)	.40	.39	.36	.38	.45	.48
				500	(1295)	.43	.39	.38	.39	.47	.52
				1000	(2590)	.40	.34	.35	.36	.44	.42
				5000	(12950)	.34	.28	.28	.29	.37	.43

Table 5.1.--Comparison of storm areal rainfall depths with general-storm PMP for the month of the storm--Continued

Date	Latitude-longitude (of center)		General location	Area mi^2	Area (km^2)	Duration (hrs) 6	12	18	24	48	72
						obs/PMP					
10/11-14/28	40°36'	110°24'	N Utah	100	(259)	.43	.50	.57	.48	.34	.36
				500	(1295)	.37	.44	.49	.42	.30	.33
11/12-17/30	41°45'	115°25'	NE Nev.	100	(259)	.55	.63	.49	.60	.55	.52
				500	(1295)	.50	.58	.45	.55	.51	.48
				1000	(2590)	.48	.51	.40	.51	.47	.44
2/1-3/36	40°36'	111°42'	N Utah	100	(259)	.37	.22	.17	.28		
				500	(1295)	.35	.20	.16	.26		
2/27-3/4/38	34°57'	111°44'	Central Ariz.	100	(259)	.49	.57	.50	.43	.31	.32
				500	(1295)	.58	.66	.60	.52	.38	.38
				1000	(2590)	.63	.70	.64	.55	.39	.41
				5000	(12950)	.56	.60	.46	.40	.28	.35
2/27-3/4/38	37°30'	112°30'	S Utah	100	(259)	.55	.38	.40	.50	.37	.38
				500	(1295)	.62	.41	.42	.46	.34	.37
				1000	(2590)	.77	.43	.43	.47	.35	.36
5/4-9/43	40°21'	106°55'	N Colo.	100	(259)	.20	.17	.15	.17	.12	.14
				500	(1295)	.22	.18	.15	.16	.13	.15
				1000	(2590)	.25	.18	.15	.16	.13	.16
				5000	(12950)	.23	.17	.15	.15	.13	.16
5/31-6/6/43	40°36'	111°36'	N Utah	100	(259)	.27	.25	.30	.27	.24	.23
				500	(1295)	.28	.27	.30	.27	.25	.23
				1000	(2590)	.27	.28	.32	.28	.26	.24
				5000	(12950)	.28	.30	.34	.32	.28	.25
10/27-29/46	37°30'	114°00'	SW Utah	100	(259)	.63	.44	.37	.80	.61	.55
				500	(1295)	.52	.35	.29	.66	.49	.44
				1000	(2590)	.43	.28	.23	.51	.38	.33
				5000	(12950)	.35	21	.17	.42	.30	.26

Table 5.1.—Comparison of storm areal rainfall depths with general-storm PMP for the month of the storm—Continued

Date	Latitude-Longitude (of center)		General location	Area mi^2	Area (km^2)	Duration (hrs) 6	12	18	24	48	72
						obs/PMP					
8/25-30/51	34°07'	112°21'	Central Ariz.	100	(259)	.35	.41	.41	.41	.55	.56
				500	(1295)	.40	.47	.43	.46	.58	.59
				1000	(2590)	.45	.48	.46	.48	.58	.59
				5000	(12950)	.30	.34	.38	.40	.44	.47
9/3-5/70	37°38'	109°04'	SW Colo. SE Utah	100	(259)	.88	.81	.71	.63	.53	
				500	(1295)	.80	.73	.64	.58	.49	
				1000	(2590)	.81	.74	.64	.59	.52	
				5000	(12950)	.49	.46	.47	.46	.39	
9/3-5/70	33°49'	110°56'	Central Ariz.	100	(259)	.63	.58	.56	.54	.43	
				500	(1295)	.54	.47	.45	.45	.36	
				1000	(2590)	.50	.48	.48	.47	.38	
				5000	(12950)	.52	.50	.51	.47	.37	

occasions when rains repeat or are continuous over a basin for a 3-day period. Continuation of an extreme inflow of moisture for longer durations is less likely, but yet a possibility. The August 1951 storm is an example of an event where a high level of moisture inflow and a continuation of the mechanism for causing rain produced an extreme rainfall event of 3-day duration.

Figures 5.1 and 5.2 show scatter diagrams for two sets of data taken from table 5.1. The comparison between maximum observed 100-mi^2 (259-km^2) 24-hr storm amounts and corresponding PMP estimates is shown in figure 5.1. Storms whose observed amounts come within 50% of PMP are identified. Note that for 24 hours duration, a southwest Utah storm in October 1946 more closely approaches PMP than any other storm. Figure 5.2 shows the comparison of known greatest rainfall amounts to PMP for 5,000 mi^2 (12,950 km^2). Only one storm comes within 50% of PMP. The validity of the trend toward lower ratios with larger areas is supported by the fact that fewer large-area storm depths have been recorded than small-area storm depths.

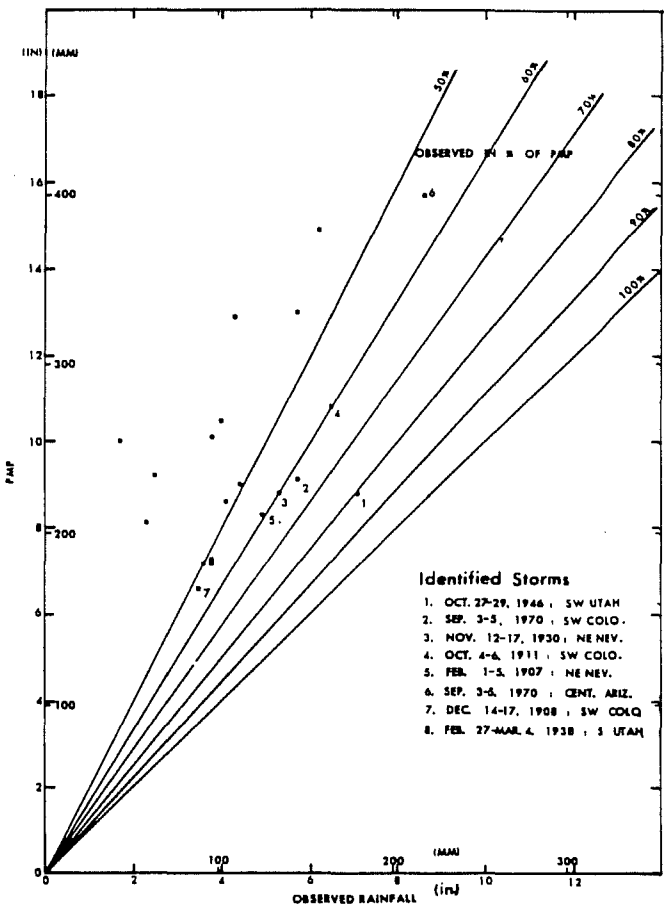

Figure 5.1.--Comparison between observed rainfall depths and general-storm PMP for 100 mi^2 (259 km^2) 24 hr.

5.3 Comparisons with Greatest Known Local-Storm Rainfalls

Local-storm PMP estimates were determined for the location of the 39 major local storms given in table 4.1. This does not include the four long-duration California storms. A scatter diagram of maximum observed total-storm amount vs. the PMP estimate for that duration is shown in figure 5.3.

Envelopment of local-storm data by PMP is less than that for general-storm data. The Campo and Chiatovich Flat, California rains come within 15% of the local-storm PMP estimates. Because of the doubt that has been given to the Palmetto, Nev. observation (U.S. Weather Bureau 1960), a question mark has been placed at this point in figure 5.3.

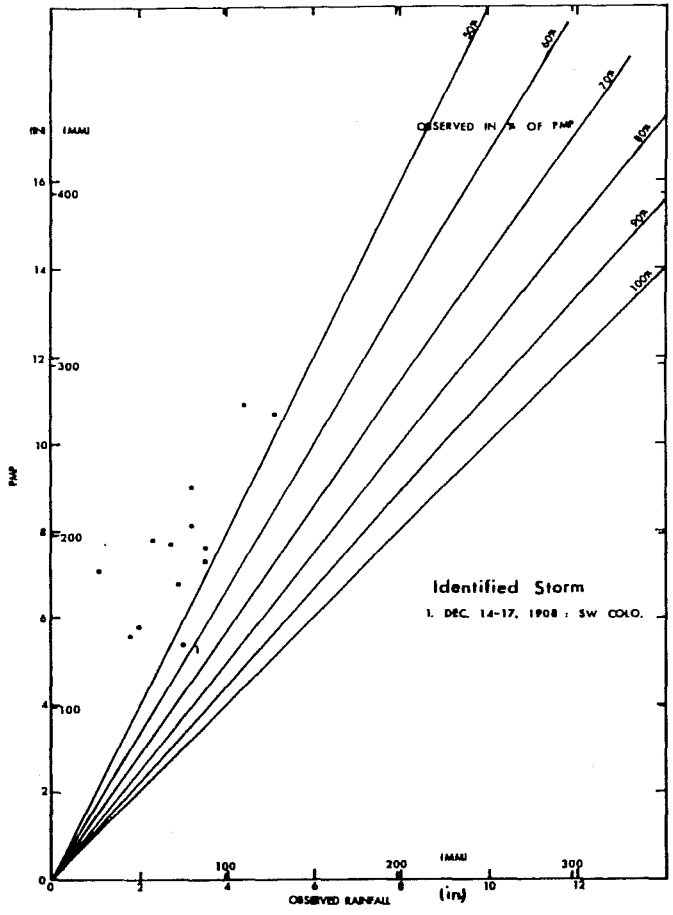

Figure 5.2.--Comparison between observed rainfall depths and general-storm PMP for 5000 mi^2 (12,950 km^2) 24 hr.

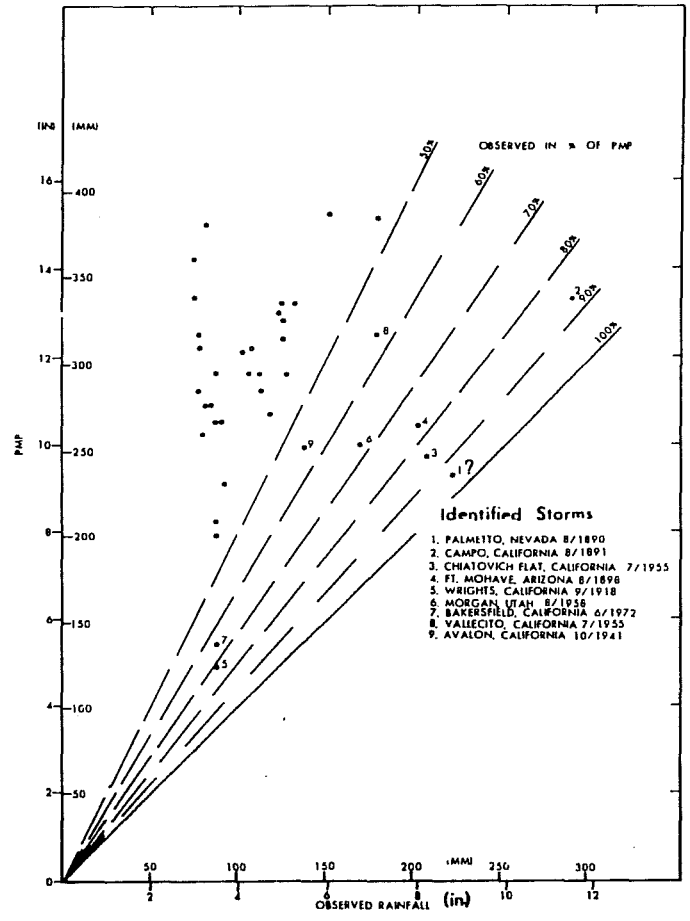

5.3.--Comparison between observed rainfall depths from local storms and local-storm PMP for the duration of the storm.

5.4 Comparisons with Estimates from a Previous Study

Technical Paper No. 38 (U.S. Weather Bureau 1960) gives all-season PMP estimates for the Western States for durations to 24 hours and areas up to 400 mi^2 (1,035 km^2). For the Southwest the 24-hr PMP of Technical Paper No. 38 is largely controlled by extreme summer thunderstorms. PMP from the present study for both the local storm and the general storm were computed for 10 mi^2 (26 km^2) on a 1° latitude-longitude grid (fig. 5.4). The upper value at each point is the general-storm 24-hr PMP. The 6-hr local-storm PMP exceeds the 24-hr general-storm value at many points. No attempt was made to draw an analysis of the data because of important topographic effects between the grid points.

Figure 5.5 compares the grid point amounts from Technical Paper No. 38 with the larger of the amounts shown for each point in figure 5.4. Although figure 5.5 shows considerable scatter there is general agreement that high estimates in the earlier study are also high in the present study. The cluster of points having PMP less than 16 inches (406 mm) in the 1960 study are in general from the less-orographic locations, whereas the more widely scattered values greater than this amount come from mountainous locations.

For 10 mi^2 (26 km^2) 24 hours, it is apparent from figure 5.5 that PMP from this study generally is less than the PMP estimated in 1960, and that there is a greater reduction for high PMP values (mountainous points) than for low values (less-orographic points). The level of PMP is partially a function of the amount of detail and data included in each study. The 1960 study covered a large region, while the present study considered more detail over an area about one-third as large. More conservative (higher) PMP estimates tend to result from broadscale analyses. Interpretation of figure 5.5 should not be applied to other durations, area sizes, or regions covered by Technical Paper No. 38.

5.5 Comparisons with 100-yr Return Period Rainfalls

Comparison was also made between PMP estimates and published 100-yr 24-hr rainfall values in the Western United States (Miller et al. 1973). In the frequency studies an effort was made to utilize all available data, but many gaps remained. Multiple regression screening techniques were used to interpolate between data points. These techniques placed greater emphasis on meteorological factors and topography than previous frequency studies for this region.

The frequency data are heavily weighted by thunderstorm rains; therefore, the greater of the local 6-hr PMP and general-storm PMP for 24 hours over 10-mi^2 (26 km^2) was compared to 100-yr 24-hr rainfall. Figure 5.6 shows a plot of 100-yr values vs. PMP for points on a 1° latitude-longitude grid covering the Southwest States. Most of the 100-yr amounts appear to be about 20 to 35% of the PMP. The results shown in figure 5.6 are not necessarily the same as would be found with other area sizes, durations or regions.

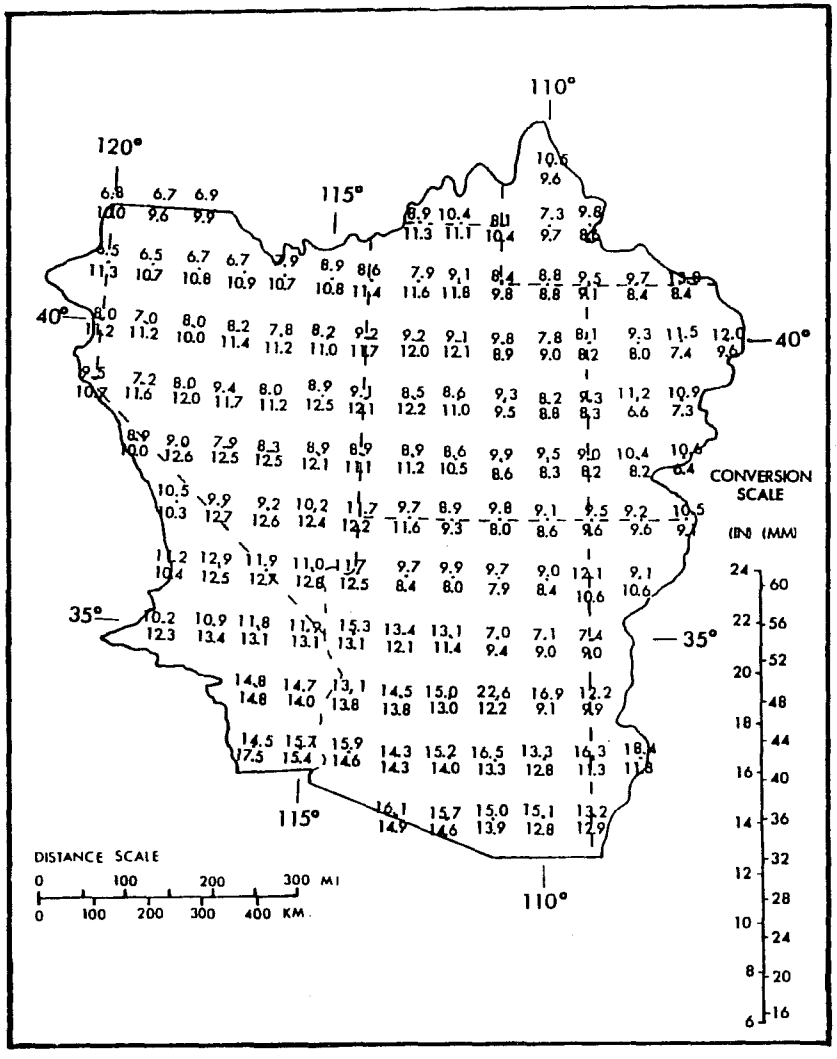

Figure 5.4.--General-storm PMP for 10 mi^2 (26 km^2) 24 hr in inches (upper number) and local-storm PMP for 10 mi^2 (26 km^2) 6 hr in inches (lower number) at 1° grid points.

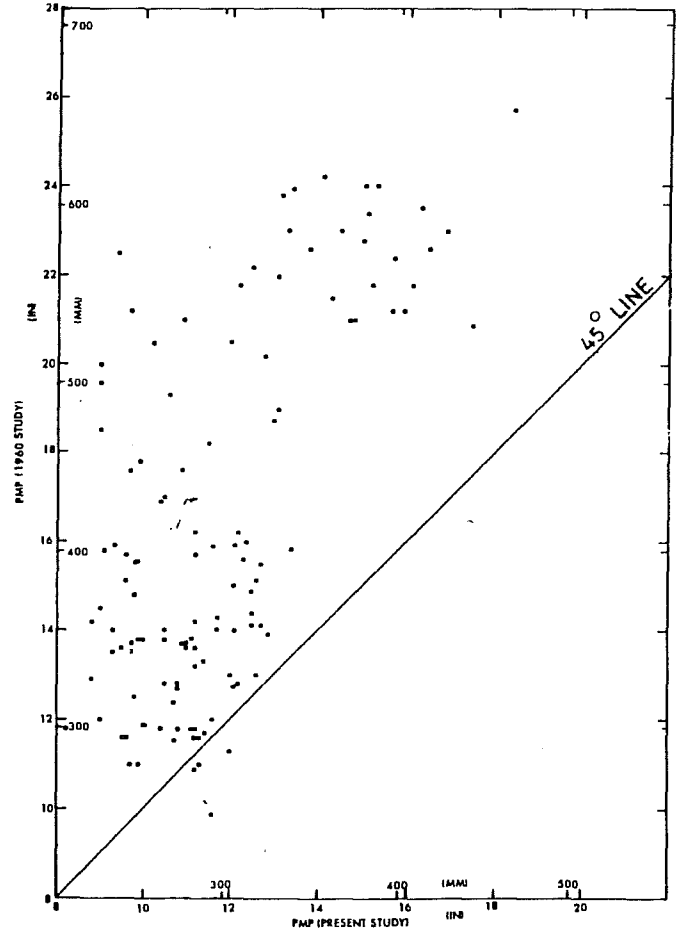

Figure 5.5.--Comparison between PMP from Technical Paper No. 38 (U. S. Weather Bureau 1960) and from this study. PMP values (present study) are the larger of the general- or local-storm amounts for 10 mi^2 (26 km^2) at 1° grid points.

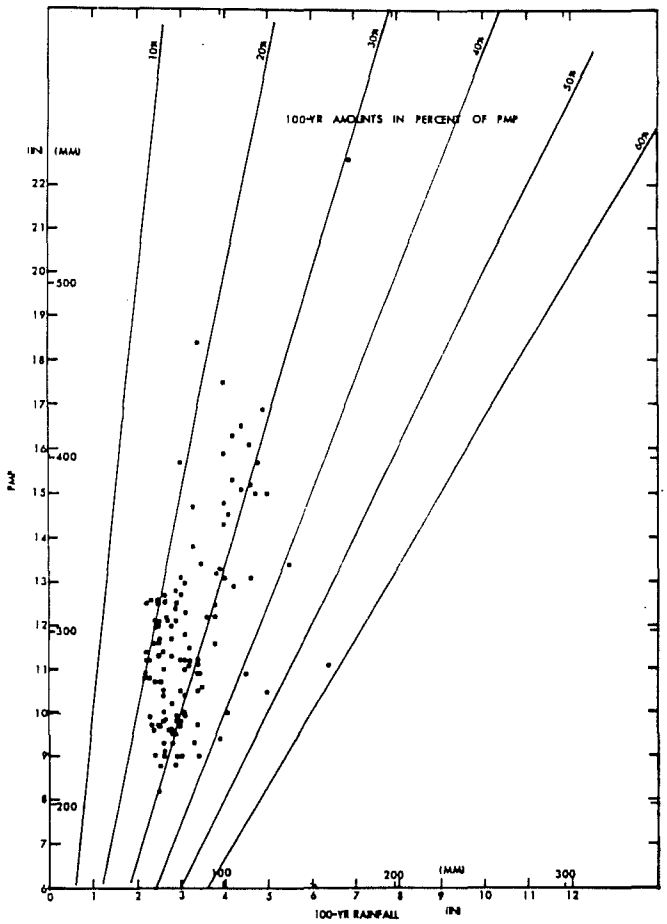

Figure 5.6.--Comparison between 100-yr rainfall (Miller et al. 1973) and PMP. PMP values are the larger of general- or local-storm amounts for 10 mi^2 (26 km^2) 24 hr at 1° grid points.

5.6 Mapped Ratios of 100-yr to PMP Values Over the Western States

Mapped ratios of 100-yr 24-hr rainfall to 24-hr PMP over a 1° latitude-longitude grid for most of the Western States and a portion of the Central States are shown in figure 5.7. For the Western States, PMP values came from this study, HMR Nos. 36 and 43. The Central States values are from HMR No. 51 (Schreiner and Riedel 1978). In figure 5.7, the larger of the local-storm and general-storm PMP estimates was used in the Western States.

Frequency data came from NOAA Atlas 2 (Miller et al. 1973). Although the volumes of this Atlas cover each of the Western States, they also include the eastern portions of those states along the Continental Divide. The eastern portions of Wyoming, Colorado and New Mexico enabled us to make a comparison of 100-yr 24-hr rainfall to PMP at a few points east of the Divide as shown in figure 5.7. Therefore, the comparisons for the Central States shown in figure 5.7 have been limited to these state boundaries.

Points where the 6-hr local-storm-PMP controls for 24 hours have been underlined in figure 5.7. Dominance of the local-storm PMP, through much of the Southwest extending into eastern Oregon and Washington and southern Idaho, is apparent. Essentially, the local-storm PMP controls in the less-orographic portions of the Western United States while the general storm prevails over the more mountainous regions for this area size.

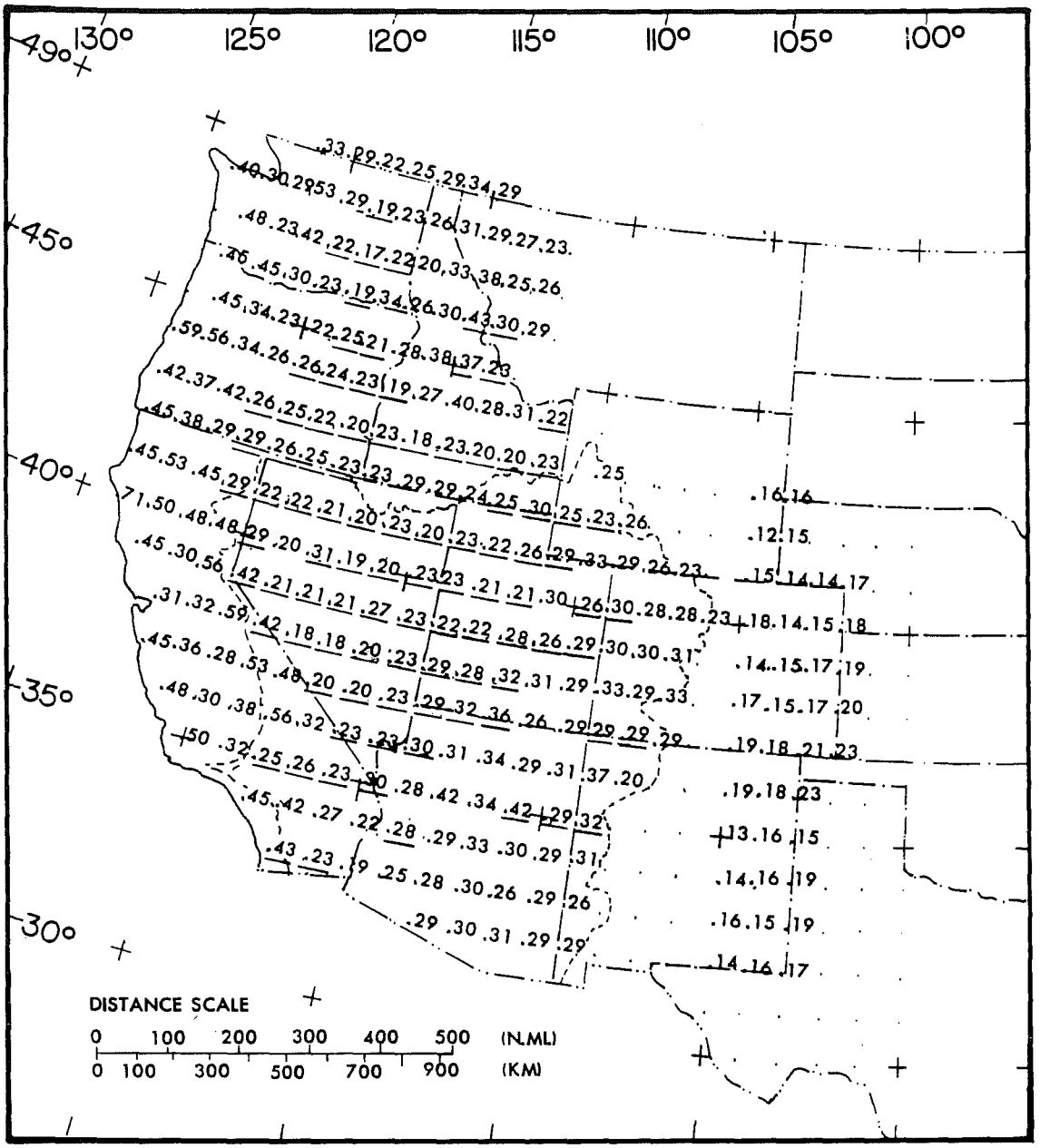

Figure 5.7.--Ratios of 100-yr point rainfall (Miller et al. 1973) to highest PMP for 10 mi^2 (26 km^2) 24 hr. Underlined ratios are points where 6-hr local-storm PMP controls. East of 105th meridian PMP taken from eastern states study (Schreiner and Riedel 1978).

The range of ratios shown in figure 5.7, 0.28 to 0.71 in the Pacific drainage of California, 0.17 to 0.59 in the Northwest, 0.18 to 0.56 in the Southwest, shows apparent consistency between the Northwestern and Southwestern Regions. East of the 105th meridian, the ratios range between 0.12 and 0.23. The trend in ratios that appears in going from the west coast to east of 105°W is what one might expect. There is a tendency for the ratios to decrease eastward from the Pacific coast and then increase again on windward slopes. This tendency is consistent with the results for similar ratios in HMR Nos. 36 and 43.

The ratios shown on figure 5.7 should not be used for basin PMP estimates. Variation in terrain features between 1° grid points could give a considerably different basin average PMP; i.e., because of topographic variations, the ratios are not necessarily representative of the area surrounding the grid point.

5.7 An Alternate Approach to PMP

An additional study was made of the variation in ratios of 100-yr rainfall to PMP estimates for the region most similar to the Southwest States that also had detailed estimates of both the precipitation criteria. This region is the Columbia River drainage east of the Cascade Divide. A conclusion of the study was that the 100-yr to PMP ratio should vary with the raininess of the location, and that a 90% envelope of a grid of ratios for the Northwest varies from 0.25 for a location with a MAP of 10 inches (254 mm) (dry region) to a ratio of 0.50 for a location with a MAP of 70 inches (1,780 mm) (wet region).

The curvilinear relation between 100-yr/PMP ratios and MAP (not shown) from the Columbia River drainage east of the Cascade Divide was used to estimate PMP for the Southwestern States over a 1° latitude-longitude grid[1]. Figure 5.8 gives the ratios of PMP by this alternate approach (100-yr/PMP vs. MAP) to the general-storm PMP of this study. It is important to point out that PMP estimates obtained by the ratio of 100-yr to PMP is not a recommended method for determining PMP. In any case, such a method includes transposition of an index relation without modification. Considerations such as the strength of the inflow wind and moisture potential would have an effect on the ratio of PMP to a lesser storm, such as the 100-yr precipitation, and the relation of the ratio to MAP.

The ratios can, however, be used as a check on the general level of the PMP estimates assuming we know the general level of PMP to the north, we have confidence in the 100-yr precipitation estimates, and accept the transposition of the index relation. Figure 5.8 indicates that the PMP estimates based on the transposed 100-yr/PMP relation vary from a low of 67% of the estimates in this study to a high of 223%. However, more than 60% of the values are within 25% of this report's PMP values. We believe this variation is acceptable, taking into account use of a transposed relation and unknowns in the generalized charts of mean annual precipitation and frequency values as well as in PMP.

---

[1]Charts used were for MAP and NAP referenced in section 3.1.3, and those for Nevada (Hardman 1965) and southern California (Rantz 1969).

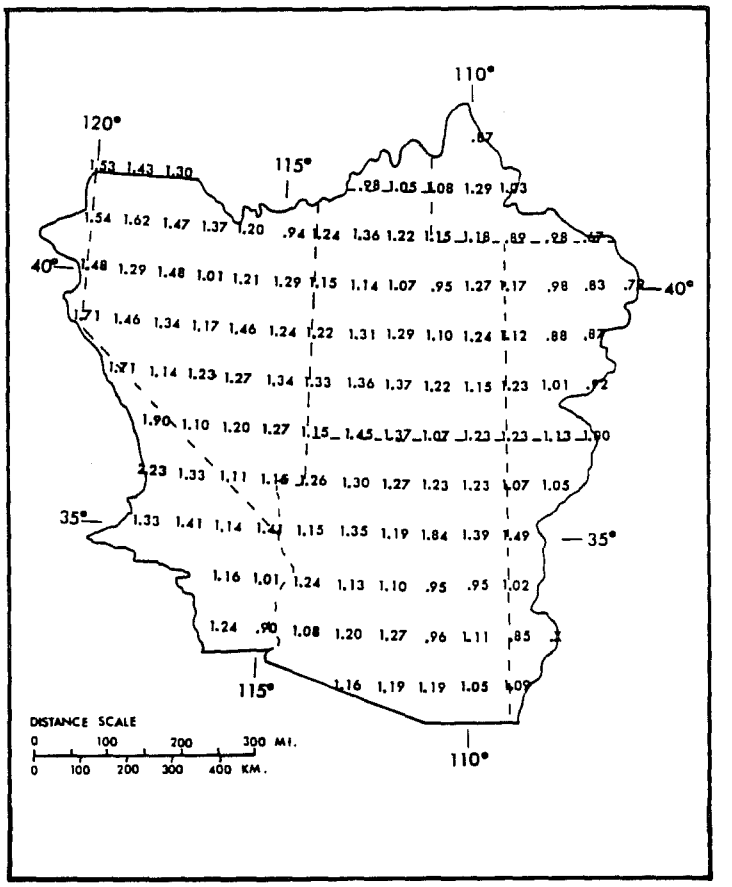

Figure 5.8.--Ratios of PMP determined from an alternate approach (see section 5.7) to that of this study for 10 mi² (26 km²) 24 hr.

5.8 Statistical Estimates of PMP

5.8.1 Background

A general formula for hydrologic frequency analysis (Chow 1951) demonstrated that the difference between various theoretical distributions is the value of K in the following formula:

$$x_T = \bar{x} + KS_n \qquad (5.1)$$

where x_T is the rainfall for return-period T, $\bar{x}$ is the mean of a series of annual maximum station precipitation, n is the sample size, and S_n is the standard deviation. Hershfield (1961) substituted the maximum observed rainfall (x_{max}) for x_T. K is then the number of standard deviations to add to $\bar{x}$ to obtain x_{max}. Using selected "world-wide" data, Hershfield originally adopted 15 as maximum K value for a statistical estimate of PMP.

Hershfield (1965) introduced a variable K-factor (K_m) related not only to the mean of the annual maximum rainfall but also to the duration. This modified relation in which K varies with rainfall magnitude was used in a statistical approach to PMP for the Southwestern States. The modified formula is:

$$X_m = \bar{x} + K_m S_n \qquad (5.2)$$

5.8.2 Computations

Computations of statistical PMP were made from data used in the rainfall-frequency analyses for the Western States (Miller et al. 1973). These data consisted of station values of mean and standard deviation of the annual maximum 24-hr rains. The variation of K as a function of the mean of the annual maximum 24-hr rains was taken from Hershfield's study (1965). The values of K necessary to cover the Southwestern States were mostly between 14 and 19. Arid regions have higher values of K than the worldwide average of 15. Given the K factors, one need only use the mean ($\overline{x}$) and standard deviation (S_n) from the series of annual maxima to solve equation 5.2.

5.8.3 Discussion

The highest PMP from the larger of general- and local-storm estimates for 24 hr and 10 mi^2 (26 km^2) were compared to statistical PMP computed from equation 5.2 at 98 stations in the Southwestern Region with rainfall records for 50 years or longer. Comparison of the two sets of values is shown in figure 5.9. Considerable scatter is apparent with the statistical PMP being less than the PMP from this report for all but two stations. The same results have been found for comparisons in other regions (World Meteorological Organization 1973).

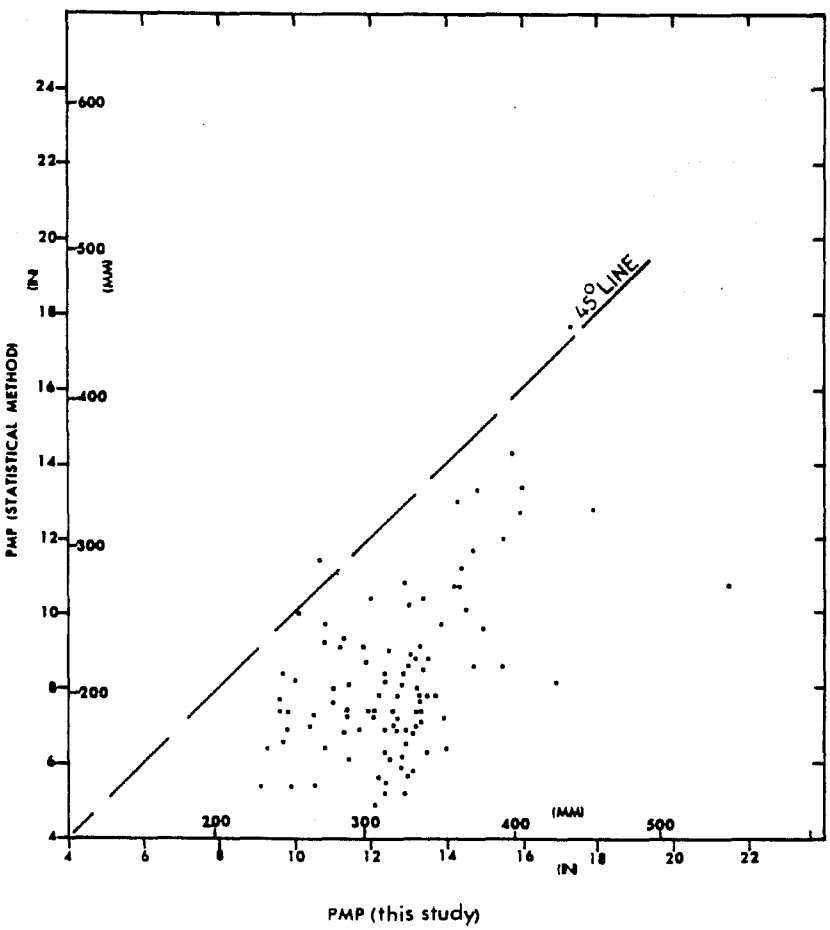

5.9.--Comparison between statistical PMP (Hershfield 1965) and the highest PMP for 10 mi^2 (26 km^2) 24 hr at stations with records exceeding 50 years.

Hershfield (1961, 1965) recommended some adjustments to the data. The first was an adjustment of $\bar{x}$ and S_n for a rare event, called an outlier. The ratio of the mean of the series excluding the outlier to that with the outlier could result in a downward adjustment to the mean by as much as 20%. Similarly, the ratio of S_n excluding the outlier to that with the outlier could bring about an adjustment to S_n of more than 50% depending on the record length.

A second adjustment normalizes daily data to 24-hr data. This factor can vary between 1.00 and 1.13 depending on the number of fixed time intervals considered in obtaining the maxima. Neither of these two adjustments was applied to the data in figure 5.9.

Another adjustment makes allowances for lengths of record less than 50 years. Adjustments up to 5% for the mean and up to 30% for S_n occur for records of only 10 years. In the present study only stations having records for 50 years or more were considered, so this adjustment was unnecessary.

Inclusion of the adjustments mentioned by Hershfield probably would have changed some of the points plotted in figure 5.9, but it is doubtful that they would have had much effect on the broad-scale scatter.

It is possible that the scatter would be reduced somewhat if the K factors had been averaged regionally prior to use in equation 5.2. Hershfield suggested regional averaging to eliminate some of the variability caused by local topographic features. However, the stations with records for 50 years or more were so widely separated that regional averaging would have been difficult and probably meaningless.

Direct application of equation 5.2 to obtain point PMP estimates, (considered equivalent to 10-mi^2 (26-km^2) values), is not recommended. There is no completely objective method for determining K. Different investigators have suggested different values for the same or similar regions. Some statistical PMP estimates have been exceeded by record storm amounts from supplementary rainfall surveys. Our use of equation 5.2 in this study, as in others, is solely to provide another comparison of the overall level of PMP. Other attempts to apply the statistical approach, and the problems encountered, are given by Lockwood (1967) for studies in Malaya and Dhar et al.(1975) in India.

5.9 Hypothesized Severe Tropical Cyclone

Some of the most intense general rainfalls for the Southwest States have resulted from tropical cyclones. The September 1970 event is the outstanding example. Pyke (1975) has speculated on the possibility of much more intense rains from such a storm assuming several optimum conditions. It would be a good check on our PMP to consider rains from such a storm. Evaluation of a storm of this intensity however, would require considerable speculation; e.g., on the extent that a hurricane circulation could be maintained into the study region and on the upwind terrain effects depleting the moisture (fueling) for the storm.

We have taken a somewhat different approach. This was to start with PMP based on the greatest known rainfall from a tropical cyclone in the United States and make adjustments in transposing it to our study region. We then compare results with our PMP. Considerable meteorological discussion is given in the companion volume (Schwarz and Hansen 1978) concerning the hypothetical storm. This is not repeated here.

5.9.1 Transposition and Adjustment of PMP Based on the Yankeetown, Fla. Storm of September 5-6, 1950

The most intense rainfall of record for the United States from a tropical cyclone is the Yankeetown, Fla., event of September 5-6 1950 (Gentry 1951). This storm gave 38.7 inches (983 mm) of rain in 24 hours. The 10-mi^2 (26-km^2) estimate for the Gulf of Mexico coast, based on this storm, is 47.1 inches (1196 mm) (Schreiner and Riedel 1978). We adjusted this PMP value for occurrence in our study region. As a starting place, we chose a point off the Baja California coast (28°N, 115°W) as a location for optimum rain. This location would not include depletion (or intensification) for terrain and would allow a large sea surface for fueling the storm.

Sea surface temperature represents a measure of moisture potential for fueling tropical cyclones. Sea surface temperatures that are exceeded 5% of the time in the warmest month (National Oceanic Atmosphereic Administration 1973), were considered a fairly stable index. A value of 87°F (31°C) is obtained for the moisture source of the Yankeetown storm, compared to 74°F (23°C) near 28°N off Baja California. The ratio of precipitable water for a saturated atmosphere associated with a 1000-mb (100-kPa) temperature of 74°F (23°C) to one of 87°F (31°C) is 0.45. Adjusting the sea surface temperatures downward by 5°F (3°C) at both locations, thereby giving realistic 12-hr persisting 1000-mb (100-kPa) dew points, results in approximately the same reduction for differences in moisture potential.

This gives us an adjusted 24-hr value of 25.9 inches (658 mm) at 28°N, 115°W. We then applied a distance-from-coast adjustment (Schwarz 1965, 1973, and Schreiner and Riedel 1978) in order to obtain values within the study region. This adjustment is based on the decrease inland in nonorographic tropical storm rainfalls of record along the gulf and east coasts of the United States. Table 5.2 shows the percentage reduction with distance inland and the reduced values. These reduced values are also shown on the left side of the hypothesized track in figure 5.10. For comparison, this report's 1000-mb (100-kPa) convergence PMP values are shown plotted to the right of the track in the figure. The distance-from-coast reduced values are higher than the convergence PMP estimates from chapter 2 at every point along the track. The greatest differences are near the southern border of Arizona close to the Gulf of California. At 700 n.mi. (1296 km), there is almost no difference.

There are at least three factors <u>not</u> accounted for that would tend to reduce these hypothesized tropical-storm rain values. These are:

a. Depletion of rainfall upwind of any location, including the starting point by mountain barriers in the Baja California peninsula.

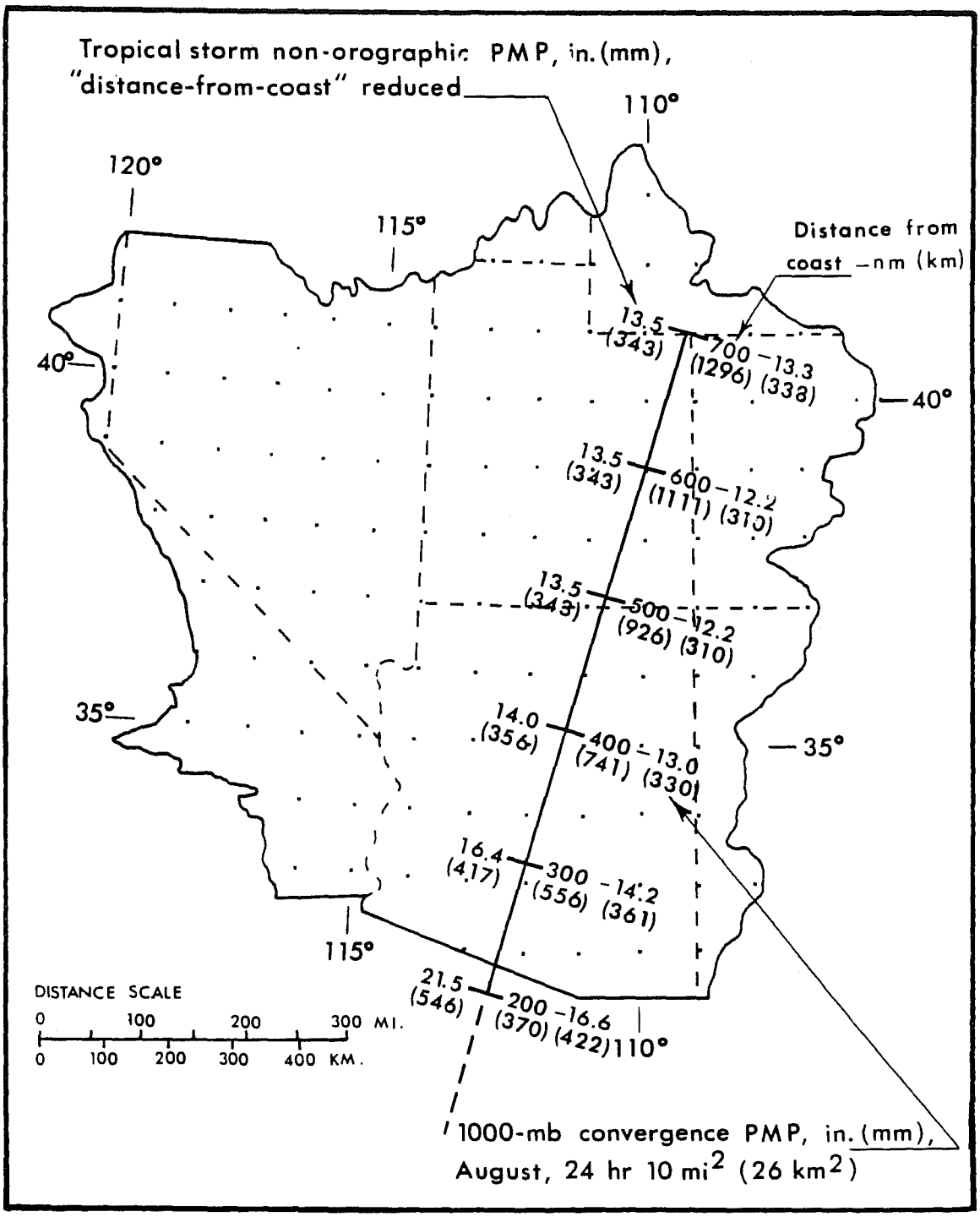

Figure 5.10--Distance-from-coast reduced tropical storm nonorographic PMP compared with 1000-mb (100-kPa) convergence PMP for August, 10 mi² (26 km²) 24 hr.

Table 5-2.--Adjustment of tropical storm PMP for distance-from-coast

Distance from coast n. mi.	(km)	Percent of Coastal Value	Adjusted rain in.	(mm)
0	0	100	25.9	(658)
100	185	96	24.6	(625)
200	370	83	21.5	(546)
300	556	63	16.4	(417)
400	741	54	14.0	(356)
500	926	52	13.5	(343)
600	1111	52	13.5	(343)
700	1296	52	13.5	(343)

b. Dampening effects of mountains on tropical cyclone circulation, assuming that maximum rainfall is produced by organized storms.

c. Effects of changing the speed of forward motion of the hypothetical tropical cyclone. (The Yankeetown storm was a slow-moving and looping storm that concentrated the rainfall. Such storm movement has not been duplicated off the Baja California coast.)

However, there is at least one factor that might contribute to even higher results than computed here. This is higher sea-surface temperatures than the 5% level postulated.

The authors believe that the combined effects of the three reducing factors outweigh the effect of higher sea surface temperatures. A hypothetical intense tropical cyclone moving northward over the Gulf of California, though taking advantage of the higher sea surface temperatures, would suffer considerably from the effects of the terrain and mountains on the circulation.

The authors further believe that the rainfall extremes determined from the generalized PMP study adequately allow for rain from a hypothesized severe tropical cyclone event in the Southwestern States.

5.10 Conclusion on PMP Checks

A variety of checks have been presented in this chapter on the general level of PMP. We conclude that the results show that the PMP and its seasonal, geographical, areal, and durational variations are appropriate and consistent.

6. PROCEDURES FOR COMPUTING PMP

6.1 Introduction

For estimating general-storm PMP for a specific drainage the maps, charts, and tables required are in chapters 2 and 3. A stepwise procedure for using these materials is given here with a computation form, table 6.1. This is followed by an example of the computations for a selected drainage (table 6.2).

The stepwise procedure and computation form are set up to give general-storm PMP for a given month. If the highest value over all months (called the "all-season" PMP) is needed, it may be necessary to compute PMP for several months and to then select the highest value.

The local-storm PMP for small drainages described in chapter 4 should be compared with general-storm PMP for any drainage and the most critical values selected. Depending on hydrologic characteristics of a particular drainage, its location, size, and the problem at hand, a 500-mi^2 (1,295-km^2) local storm, well placed on a drainage larger than 500 mi^2, may be the more critical of the two storm types. A step-wise procedure is given (sec. 6.3) for computing local-storm PMP. Part A gives the drainage average PMP while part B gives the areal distribution of PMP over the drainage. A computation form is provided in table 6.3, for computing these estimates. Table 6.4 is an example of these computations.

Local-storm PMP also covers the Pacific drainage of California. General-storm PMP for this region is given in HMR No. 36, with revisions (U.S. Weather Bureau 1969).

The procedures have been developed to give PMP in tenths of inches. Although in some instances it may be possible to discriminate values from figures and tables to hundredths of an inch or fractions of a percent, PMP estimates should be rounded to the nearest tenth of an inch.

6.2 Steps for Computing General-Storm PMP for a Drainage

A. Convergence PMP. The steps correspond to those in table 6.1.

1. Obtain drainage average 1000-mb (100-kPa) 24-hr 10-mi^2 (26-km^2) convergence PMP for month of interest from one of figures 2.5 to 2.16.

2. Obtain the 1000-mb (100-kPa) 24-hr 10-mi^2 (26-km^2) convergence PMP reduction factor for effective barrier and elevation in percent from figure 2.18.

3. Step 1 value times step 2 value gives barrier-elevation reduced 24-hr 10-mi^2 (26-km^2) convergence PMP average for the drainage.

4. Determine drainage 6/24-hr ratio for month of interest from figures 2.25 and 2.27. Enter table 2.7 with this ratio to obtain 6-, 12-, 18-, 24-, 48-, and 72-hr values in % of the 24-hr value.

5. Step 3 value times percents from step 4 provides convergence PMP for durations of step 4 for 10 mi^2 (26 km^2).

6. Incremental 10-mi^2 (26-km^2) convergence PMP is obtained by successive subtraction of values in step 5.

7. Areal reduction in percent for drainage area is obtained from figure 2.28 or 2.29 for the month of interest.

8. Values from step 6 times corresponding percents from step 7 are the areally reduced incremental convergence PMP in inches (mm).

9. Accumulation of incremental values from step 8 gives drainage average convergence component PMP for 6, 12, 18, 24, 48 and 72 hours.

B. Orographic PMP

1. Drainage average orographic PMP index for 24 hours 10 mi^2 (26 km^2) is read from one of figures 3.11a to d (foldout pages).

2. Areal reduction factor in percent for drainage size is read from figure 3.20.

3. To get seasonal adjustment, locate drainage on map for month of interest, figures 3.12 to 3.17, and read average percent for the drainage.

4. Areally and seasonally adjusted 24-hr orographic PMP in inches (mm) is obtained by multiplying values from step 1 by percents from steps 2 and 3.

5. Durational variation of orographic PMP in percent of the 24-hr value for 6, 12, 18, 24, 48, and 72 hours is read from table 3.9, which is entered with the latitude of the drainage (to the nearest 1°).

6. Orographic PMP in inches (mm) for listed durations results from multiplication of values in step 4 by corresponding values in step 5.

C. Total PMP

1. Add corresponding convergence and orographic PMP values in steps A9 and B6.

2. If PMP values are required for intermediate durations, plot a smooth curve and interpolate.

3. Compare with the local-storm PMP.

Table 6.2 shows an example of the computation of general-storm PMP for the month of October for the Humboldt River drainage above Devil's Gate damsite in Nevada. The table is self-explanatory.

6.3 Steps for Computing Local-Storm PMP

A. Drainage Average Depth Local-Storm PMP. Steps correspond to those in table 6.3A.

Use steps of section 6.3B if areal distribution within drainage is required.

Step

1. Locate drainage on figure 4.5 and read interpolated average PMP value for 1 hour 1 mi^2 (2.6 km^2) in inches (mm).

2. If the lowest elevation within the drainage is above 5,000 feet (1,524 m), decrease the PMP value from step 1 by 5% for each 1,000 feet (305 m) or proportionate fraction thereof above 5,000 feet (1,524 m). This gives elevation adjusted drainage average 1-hr 1-mi^2 (2.6-km^2) PMP.

3. Use figure 4.7 to find the 6/1-hr ratio for the drainage location.

4. Enter table 4.4 with the ratio from step 3 to obtain percentage durational variation.

5. Multiply each of the percentages of step 4 by the 1-hr PMP from step 2 to obtain PMP for 1/4 hr to 6 hours.

6. Enter the abscissa of figure 4.9 with the size of the drainage to obtain the areal reduction for each duration in terms of percent of 1-mi^2 (2.6-km^2) PMP.

7. Multiply the areal reduction percentages from step 6 by the PMP values from step 5 to obtain areally reduced PMP.

8. Determine the incremental PMP values by successive subtraction of values in step 7.

9. Arrange the hourly incremental values from step 8 in one of the time sequences shown in table 4.7. Use table 4.8 for sequence of 4 highest 15-minute increments.

Table 6.4A is an example of local-storm PMP computation for Sycamore Creek, Arizona.

B. Areal Distribution of Local-Storm PMP Within Drainage. The following steps are recommended for computing local-storm PMP and its areal distribution.

Step

1. Overlay a tracing of the drainage outline (adjusted to 1:500,000 scale) on figure 4.10. Rotate the outline to obtain the maximum rain volume in the drainage. (For particular problems, other placements may be hydrologically more critical.)

2. Note the isohyets that lie within the drainage.

3. Locate drainage on figure 4.5 and read interpolated PMP value for 1 mi^2 (2.6 km^2) in inches (mm).

4. If the lowest elevation within the drainage is above 5,000 feet (1,524 m) decrease the PMP value from step 3 by 5% for each 1,000 feet (305 m) or proportionate fraction thereof above 5,000 feet (1,524 m).

5. Use figure 4.7 to find the 6/1-hr ratio for the drainage.

6. Enter table 4.5 with 6/1-hr ratio of step 5 to obtain isohyetal labels for the 4 highest 15-min PMP increments in percent of 1-hr, 1-mi^2 (2.6-km^2) PMP.

7. Enter table 4.6 with 6/1-hr ratio of step 5 to obtain isohyetal labels for the 2nd highest to 6th highest (the lowest) 1-hr incremental PMP values in percent of 1-hr, 1-mi^2 (2.6-km^2) PMP.

8. Multiply the isohyetal percentages for each PMP increment from step 6 (for highest 1-hr PMP and 15-min incremental PMP) and step 7 (2nd to 6th highest 1-hr PMP) by the 1-hr, 1-mi^2 (2.6-km^2) PMP value from step 4. The results are incremental PMP isohyetal labels in inches (mm).

9. Arrange the hourly incremental values in one of the time sequences of table 4.7. Use table 4.8 for the sequence of 4 highest 15-min increments.

Note: An average depth equal to the value of the last isohyet (J) may be used for any portion of the drainage not covered by the isohyetal pattern.

Table 6.4B is an example of computation of local-storm PMP and its areal distribution for Sycamore Creek, Arizona.

Table 6.1.--General-storm PMP computations for the Colorado River and Great basin

Drainage _____ Area_____ mi^2 (km^2)

Latitude _____, Longitude ___ of basin center

Month _____

Step	Duration (hrs) 6	12	18	24	48	72
A. Convergence PMP						
1. Drainage average value from one of figures 2.5 to 2.16 ___in. (mm)						
2. Reduction for barrier-elevation [fig. 2.18] ___%						
3. Barrier-elevation reduced PMP [step 1 X step 2] ___in. (mm)						
4. Durational variation [figs. 2.25 to 2.27 and table 2.7].	___	___	___	___	___	___ %
5. Convergence PMP for indicated durations [steps 3 X 4]	___	___	___	___	___	___ in. (mm)
6. Incremental 10 mi^2 (26 km^2) PMP [successive subtraction in step 5]	___	___	___	___	___	___ in. (mm)
7. Areal reduction [select from figs. 2.28 and 2.29]	___	___	___	___	___	___ %
8. Areally reduced PMP [step 6 X step 7]	___	___	___	___	___	___ in. (mm)
9. Drainage average PMP [accumulated values of step 8]	___	___	___	___	___	___ in. (mm)
B. Orographic PMP						
1. Drainage average orographic index from figure 3.11a to d. ___ in. (mm)						
2. Areal reduction [figure 3.20] ___%						
3. Adjustment for month [one of figs. 3.12 to 3.17] ___%						
4. Areally and seasonally adjusted PMP [steps 1 X 2 X 3] ___in. (mm)						
5. Durational variation [table 3.6]	___	___	___	___	___	___ %
6. Orographic PMP for given durations [steps 4 X 5]	___	___	___	___	___	___ in. (mm)
C. Total PMP						
1. Add steps A9 and B6	___	___	___	___	___	___ in. (mm)
2. PMP for other durations from smooth curve fitted to plot of computed data.						
3. Comparison with local-storm PMP (see sec. 6.3).						

Table 6.2.--Example computation of general-storm PMP.

Drainage Humboldt R.(above Devils Gate), Nevada Area _____ mi^2 (km^2)
Latitude 41° 20', Longitude 115°48 of basin center
Month Oct.

Step		Duration (hrs) 6	12	18	24	48	72
A.	Convergence PMP						
1.	Drainage average value form one of figures 2.5 to 2.16	9.2 in. (mm)					
2.	Reduction for barrier-elevation [fig. 2.18]	50%					
3.	Barrier-elevation reduced PMP [step 1 X step 2]	4.6 in. (mm)					
4.	Durational variation [figs. 2.25 to 2.27 and table 2.7].	62	82	93	100	119	129 %
5.	Convergence PMP for indicated durations [steps 3 X 4]	2.8	3.8	4.3	4.6	5.5	5.9 in. (mm)
6.	Incremental 10 mi^2 (26 km^2) PMP [successive subtraction in step 5]	2.8	1.0	0.5	0.3	0.9	0.4 in. (mm)
7.	Areal reduction [select from figs. 2.28 and 2.29]	63	85	93	98	100	100 %
8.	Areally reduced PMP [step 6 X step 7]	1.8	0.8	0.5	0.3	0.9	0.4 in. (mm)
9.	Drainage average PMP [accumulated values of step 8]	1.8	2.6	3.1	3.4	4.3	4.7 in. (mm)
B.	Orographic PMP						
1.	Drainage average orographic index from figure 3.11a to d.	3.3 in. (mm)					
2.	Areal reduction [figure 3.20]	82%					
3.	Adjustment for month [one of figs. 3.12 to 3.17]	100%					
4.	Areally and seasonally adjusted PMP [steps 1 X 2 X 3]	2.7 in. (mm)					
5.	Durational variation [table 3.6]	29	56	79	100	160	189 %
6.	Orographic PMP for given durations [steps 4 X 5]	0.8	1.5	2.1	2.7	4.3	5.1 in. (mm)
C.	Total PMP						
1.	Add steps A9 and B6	2.6	4.1	5.2	6.1	8.6	9.8 in. (mm)
2.	PMP for other durations from smooth curve fitted to plot of computed data.						
3.	Comparison with local-storm PMP (see sec. 6.3).						

Table 6.3A.--Local-storm PMP computation, Colorado River, Great Basin and California drainages. For drainage average depth PMP. Go to table 6.3B if areal variation is required.

Drainage _____ Area _____ mi^2 (km^2)
Latitude _____ Longitude _____ Minimum Elevation _____ ft (m)

Steps correspond to those in sec. 6.3A.

1. Average 1-hr 1-mi^2 (2.6-km^2) PMP for drainage [fig. 4.5]. _____ in. (mm)

2. a. Reduction for elevation. [No adjustment for elevations up to 5,000 feet (1,524 m): 5% decrease per 1,000 feet (305 m) above 5,000 feet (1,524 m)]. _____ %

   b. Multiply step 1 by step 2a. _____ in. (mm)

3. Average 6/1-hr ratio for drainage [fig. 4.7]. _____

	Duration (hr)									
	1/4	1/2	3/4	1	2	3	4	5	6	
4. Durational variation for 6/1-hr ratio of step 3 [table 4.4].	___	___	___	___	___	___	___	___	___	%
5. 1-mi^2 (2.6-km^2) PMP for indicated durations [step 2b X step 4].	___	___	___	___	___	___	___	___	___	in. (mm)
6. Areal reduction [fig. 4.9].	___	___	___	___	___	___	___	___	___	%
7. Areal reduced PMP [steps 5 X 6].	___	___	___	___	___	___	___	___	___	in. (mm)
8. Incremental PMP [successive subtraction in step 7].				___	___	___	___	___	___	in. (mm)
				___	___	___	___			} 15-min. increments

9. Time sequence of incremental PMP according to:

   Hourly increments [table 4.7]. ___ ___ ___ ___ ___ ___ in. (mm)

   Four largest 15-min. increments [table 4.8]. ___ ___ ___ ___ in. (mm)

Table 6.3B.--Local-storm PMP computation, Colorado River and Great Basin, and California drainages. (Giving areal distribution of PMP).

Steps correspond to those in sec. 6.3B.

1. Place idealized isohyetal pattern [fig. 4.10] over drainage adjusted to 1:500,000 scale to obtain most critical placement.

2. Note the isohyets within drainage.

3. Average 1-hr 1-mi^2 (2.6-km^2) PMP for drainage [fig. 4.5]. _____ in. (mm)

4. a. Reduction for elevation. [No adjustment for elevations up to 5,000 feet (1,524 m), 5% decrease per 1,000 feet (305 m) above 5,000 feet (1,524 m)]. _____ %

   b. Multiply step 3 by step 4a. _____ in. (mm)

5. Average 6/1-hr ratio for drainage [fig. 4.7]. _____

6. Obtain isohetal labels for 15-min incremental and the highest PMP from table 4.5 corresponding 6/1-hr ratio of step 5.

PMP Increment	Isohyet A	B	C	D	E	F	G	H	I	J	
Highest 1-hr											
Highest 15-min.											
2nd "											
3rd "											in %
4th "											

7. Obtain isohyetal labels in % of 1-hr PMP for 2nd to 6th highest hourly incremental PMP values from table 4.6 using 6/1-hr ratio of step 5.

2nd Highest 1-hr PMP											
3rd "											
4th "											in %
5th "											
6th "											

8. Multiply steps 6 and 7 by step 4b to get incremental isohyetal labels of PMP.

Highest 15-min.											
2nd "											
3rd "											
4th "											
Highest 1-hr											in in. (mm)
2nd "											
3rd "											
4th "											
5th "											
6th "											

9. Arrange values of step 8 in time sequence [tables 4.7 and 4.8].

Table 6.4A.--Example of computation of local-storm PMP. Average values for the drainage.

Drainage Sycamore Ck. (above Verde River), Arizona Area 360 mi^2 (km^2)
Latitude 34°53' Longitude 112°08' Minimum Elevation 3850 ft (m)

Steps correspond to those in sec. 6.3A.

1. Average 1-hr 1-mi^2 (2.6-km^2) PMP for drainage [fig. 4.5]. 10.1 in. (mm)

2. a. Reduction for elevation. [No adjustment for elevations up to 5,000 feet (1,524 m): 5% decrease per 1,000 feet (305 m) above 5,000 feet (1,524 m)]. 100 %

   b. Multiply step 1 by step 2a. 10.1 in. (mm)

3. Average 6/1-hr ratio for drainage [fig. 4.7]. 1.2

	Duration (hr)								
	1/4	1/2	3/4	1	2	3	4	5	6
4. Durational variation for 6/1-hr ratio of step 3 [table 4.4].	74	89	95	100	110	115	118	119	120 %
5. 1-mi^2 (2.6-km^2) PMP for indicated durations [step 2b X step 4].	7.5	9.0	9.6	10.1	11.1	11.6	11.9	12.0	12.1 in. (mm)
6. Areal reduction [fig. 4.9].	16	20	23	26	30	34	37	38.5	40 %
7. Areal reduced PMP [steps 5 X 6].	1.2	1.8	2.2	2.6	3.3	3.9	4.4	4.6	4.8 in. (mm)
8. Incremental PMP [successive subtraction in step 7].				2.6	0.7	0.6	0.5	0.2	0.2 in. (mm)
	1.2	0.6	0.4	0.4	} 15-min. increments				

9. Time sequence of incremental PMP according to:

   Hourly increments [table 4.7]. 0.2 0.6 2.6 0.7 0.5 0.2 in. (mm)

   Four largest 15-min. increments [table 4.8]. 1.2 0.6 0.4 0.4 in. (mm)

Table 6.4B.--Example computation of local-storm PMP. Areal distribution over the drainage.

Steps correspond to those in sec. 6.3B.

1. Place idealized isohyetal pattern [fig. 4.10] over drainage adjusted to 1:500,000 scale to obtain most critical placement.
2. Note the isohyets within drainage.
3. Average 1-hr 1-mi^2 (2.6-km^2) PMP for drainage [fig. 4.5]. 10.1 in. (~~mm~~)
4. a. Reduction for elevation. [No adjustment for elevations up to 5,000 feet (1,524 m), 5% decrease per 1,000 feet (305 m) above 5,000 feet (1,524 m)]. 100 %
   b. Multiply step 3 by step 4a. 10.1 in. (~~mm~~)
5. Average 6/1-hr ratio for drainage [fig. 4.7]. 1.2
6. Obtain isohyetal labels for 15-min PMP from table 4.5 corresponding 6/1-hr ratio of step 5 and labels for highest 1 hr.

PMP Increment	Isohyet A	B	C	D	E	F	G	H	I	J
Highest 1-hr	100	82	58	44	32	23	16	13	12	11
Highest 15-min.	74	56	32	21	14	8	7	6	5	4
2nd "	15	15	15	12	9	6	4	3	3	3
3rd "	6	6	6	6	5	5	3	2	2	2
4th "	5	5	5	5	4	4	2	2	2	2

in %

7. Obtain isohyetal labels in % of 1-hr PMP for 2nd to 6th highest hourly incremental PMP values from table 4.6 using 6/1-hr ratio of step 5.

2nd Highest 1-hr	11	11	11	11	10	8	7	5	5	5
3rd "	4	4	4	4	4	4	4	4	4	4
4th "	3	3	3	3	3	3	3	3	3	3
5th "	2	2	2	2	2	2	2	2	2	2
6th "	1	1	1	1	1	1	1	1	1	1

in %

8. Multiply steps 6 and 7 by step 4b to get incremental isohyetal labels of PMP.

Highest 15-min.	7.5	5.7	3.2	2.1	1.4	0.8	0.7	0.6	0.5	0.4
2nd "	1.5	1.5	1.5	1.2	0.9	0.6	0.4	0.3	0.3	0.3
3rd "	0.6	0.6	0.6	0.6	0.5	0.5	0.3	0.2	0.2	0.2
4th "	0.5	0.5	0.5	0.5	0.4	0.4	0.2	0.2	0.2	0.2
Highest 1-hr	10.1	8.3	5.9	4.4	3.2	2.3	1.6	1.3	1.2	1.1
2nd "	1.1	1.1	1.1	1.1	1.0	0.8	0.7	0.5	0.5	0.5
3rd "	0.4	0.4	0.4	0.4	0.4	0.4	0.4	0.4	0.4	0.4
4th "	0.3	0.3	0.3	0.3	0.3	0.3	0.3	0.3	0.3	0.3
5th "	0.2	0.2	0.2	0.2	0.2	0.2	0.2	0.2	0.2	0.2
6th "	0.1	0.1	0.1	0.1	0.1	0.1	0.1	0.1	0.1	0.1

in in. (~~mm~~)

9. Arrange values of step 8 in time sequence [tables 4.7 and 4.8].

ACKNOWLEDGEMENTS

From the time this study was first begun, many members of the Hydrometeorological Branch have been involved. Some have since left the Branch, but should be remembered here. Robert Weaver did much of the groundwork and outlined the direction the study should take, and Albert Shipe aided computations with his programming ability. Many days of painstaking tasks were undertaken by former technicians Miriam McCarty, Ray Evans and Wallace Brewer. Currently, Roxanne Johnson, and particularly Marion Choate, our lead technician have carried out these tasks.

Appreciation is also given to John F. Miller, Chief of the Water Management Information Division (WMID) and to Dr. Vance A. Myers, Chief of the Special Studies Branch, WMID, for their helpful guidance and critical reviews of our efforts.

Thanks are also due Clara Brown for her typing of most of the final manuscript, and to Virginia Hostler and Cora Ludwig for their help.

REFERENCES

American Meteorological Society, 1959: *Glossary of Meteorology*, Boston, Mass., 638 pp.

Baum, R. A., 1974: Eastern North Pacific hurricanes of 1973. *Monthly Weather Review*, 102, 4, 296-305.

Bryant, W. C., 1972: Report on Bakersfield Storm, June 7, 1972. Kern County Water Agency, Bakersfield, Calif., 8 pp.

Chow, V. T., 1951: A general forumula for hydrologic frequency analysis. *Transactions of the American Geophysical Union*, 32, 231-237.

Dhar, O. N., Kulkarni, A. K., and Sangam, R. B., 1975: A study of extreme point rainfall over flash flood prone regions of the Himalayan foothills of North India. *Hydrological Sciences Bulletin*, International Assoc. of Hydrol. Sciences, United Kingdom, 20, 1, 61-67.

Environmental Science Services Administration, 1968: Climatic atlas of the United States. Environmental Data Service, U. S. Department of Commerce, Washington, D. C., 80 pp.

Gentry, R. C., 1951: Forecasting the formation and movement of the Cedar Keys hurricane September 1-7, 1950. *Monthly Weather Review*, 79, 6, 107-115.

Glancy, P. A., and Harmsen, L. 1975: A hydrologic assessment of the September 14, 1974 flood in El Dorado Canyon, Nevada. *Geological Survey Professional Paper* 930, U. S. Department of Interior, Washington, D. C., 28 pp.

Green, C. R., and Sellers, W. D., 1964: *Arizona Climate*. The University of Arizona Press, Tucson, Ariz., 503 pp.

Hansen, E. M., 1975a: Moisture source for three extreme local rainfalls in the southern intermountain region. *NOAA Technical Memorandum* NWS HYDRO 26, U. S. Department of Commerce, Washington, D. C., 57 pp.

Hansen, E. M. 1975b: Moisture analysis for specific cases of southwest summer rainfall. *Proceedings of National Symposium on Precipitation Analysis for Hydrologic Modeling, June 26-28, 1975, Davis, Calif.*, American Geophysical Union, Washington, D. C. 123-132.

Hardman, A., 1965: Nevada precipitation map. (Adapted from map printed in Experimental Station Bulletin No. 183, August 1949.)

Hershfield, D. M., 1961: Estimating the probable maximum precipitation. *Proceedings, ASCE Journal of Hydraulics Division*, 87, 99-106.

Hershfield, D. M., 1965: Methods for estimating probable maximum precipitation. *Journal of American Waterworks Association*, 57, 965-972.

Houghton, J. C., 1969: Characteristics of rainfall in the Great Basin. Desert Research Institute, University of Nevada, Reno, Nev., 205 pp.

Jennings A. H., 1952: Maximum 24-hour precipitation in the United States. *Technical Paper* No. 16, Weather Bureau, U. S. Department of Commerce, Washington, D. C., 284 pp.

Keppell, R. V., 1963: A record storm event on the Alamogordo Creek watershed in eastern New Mexico. *Journal of Geophysical Research,* 16, 4877-4880.

Kesseli, J. E., and Beaty, C. B., 1959: Desert flood conditions in the White Mountains of California and Nevada. *Technical Report* EP-108, Headquarters Quartermaster R & E Command, U. S. Army, Natick, Mass., 120 pp.

Langbein, W. B., (Geological Survey, U. S. Department of the Interior) 1941: Torrential rainstorms in Arizona and Utah, 22 pp. (unpublished manuscript).

Leopold, L. B., 1943: Characteristics of heavy rainfall in New Mexico and Arizona. *Proceedings of ASCE Papers* 69, 205-234.

Lockwood, J. G., 1967: Probable maximum 24-hr precipitation over Malaya by statistical methods. *Meteorological Magazine,* 96, 1134, 11-19.

Miller, J. F., Frederick, R. H., and Tracey, R. J., 1973: Precipitation frequency atlas of the Western United States. *NOAA Atlas* 2, National Weather Service, NOAA, U. S. Department of Commerce, Washington, D. C., 11 Vols.

National Oceanic Atmospheric Administration, 1973: Environmental conditions within specific geographic regions, (Offshore East and West coasts of the United States and in the Gulf of Mexico). *Final Report,* prepared for National Data Buoy Center, National Ocean Survey, by Interagency Ad Hoc Task Force.

Osborn, H. B., and Renard, K. G., 1969: Analysis of two major runoff producing southwest thunderstorms. *Journal of Hydrology,* 8, 3, 282-302.

Peck, E. L., 1958: Monthly flood report, September. U. S. Weather Bureau, Salt Lake City District Office, Salt Lake City, Utah, 2 pp.

Pyke, C. B., 1972: Some meteorological aspects of the seasonal distribution of precipitation in the Western United States and Baja California. *Water Resources Center Contribution* No. 139, University of California, Berkeley, Calif., 205 pp.

Pyke, C. B. (Los Angeles District Meteorologist, U. S. Army Corps of Engineers, Los Angeles, Calif.), 1975 (personal communication).

Randerson, D., 1975: Meteorological analysis for the Las Vegas, Nevada flood of 3 July, 1975. *Monthly Weather Review,* 104, 6, 719-727.

Rantz, S. E., 1969: Mean annual precipitation in the California region. U. S. Geological Survey, U. S. Department of Interior, Water Resources Division, Menlo Park, Calif., 5 pp.

Riedel, J. T., Appleby, J. F., and Schloemer, R. W., 1956: Seasonal variation of probable maximum precipitation east of the 105th meridian for areas from 10 to 1,000 square miles and durations of 6, 12, 24 and 48 hours. *Hydrometeorolgoical Report* No. 33, Weather Bureau, U. S. Department of Commerce, Washington, D. C., 55 pp.

Rosendal, H. E., 1962: Eastern North Pacific tropical cyclones, 1947-1961. *Mariners Weather Log*, 6, 6, 195-201.

Schreiner, L. G., and Riedel, J. T., 1978: All season probable maximum precipitation, United States east of the 105th meridian for areas from 10 to 20,000 square miles and durations 6 to 72 hours. *Hydrometeorological Report* No. 51, National Weather Service, NOAA, U. S. Department of Commerce, Washington, D. C., (in preparation).

Schwarz, F. K., 1963: Probable maximum precipitation in the Hawaiian Islands. *Hydrometeorological Report* No. 39, Weather Bureau, U. S. Department of Commerce, Washington, D. C., 98 pp.

Schwarz, F. K., 1965: Probable maximum and TVA precipitation over the Tennessee River basin above Chattanooga. *Hydrometeorological Report* No. 41, Weather Bureau, U. S. Department of Commerce, Washington, D. C., 148 pp.

Schwarz, F. K., and Helfert, N. F., 1969: Probable maximum and TVA precipitation for Tennessee River basins up to 3000 square miles in area and durations to 72 hours. *Hydrometeorolgical Report* No. 45, Weather Bureau, Environmental Science Services Administration, U. S. Department of Commerce, Silver Spring, Md., 166 pp.

Schwarz, F. K., 1973: A proposal for estimating tropical storms probable maximum precipitation (PMP) for sparse-data regions. *Proceedings of the Second International Symposium in Hydrology; Floods and Droughts*, September 11-13, 1972, Fort Collins, Colorado.

Schwarz, F. K., and Hansen, E. M., 1978: Meteorology of important rainstorms in the Colorado River and Great Basin drainages, *Hydrometeorological Report* No. 50, National Weather Service, NOAA, U. S. Department of Commerce, Washington, D. C. (in preparation).

Secretaria de Recursos Hidraulicos, 1970: Region No. 8, Northern Sonora. *Hydrologic Bulletin* No. 39, Mexico D. F., Mexico 1-03.8.

Selvidge, H., 1975: More about the Sedona Deluge. Paper published by the Laboratory of Climatology, Arizona State University, Tempe, Ariz., 3 pp.

Serra, S. C., 1971: Hurricanes and tropical storms of the west coast of Mexico. *Monthly Weather Review*, 99, 6, 302-308.

Shipe, A. P., and Riedel, J. T., 1976: Greatest known areal storm rainfall for the contiguous United States. *NOAA Technical Memorandum* NWS HYDRO-33, National Weather Service, NOAA, U. S. Department of Commerce, Washington, D. C., 174 pp.

Soil Conservation Service and U. S. Weather Bureau, 1965: Mean annual precipitation, State of Idaho (1930-1957).

State of Arizona: Normal October-April precipitation, normal annual precipitation and normal May-September precipitation. Prepared by National Weather Service, NOAA. Published by University of Arizona, Tucson, Arizona.

State of Colorado: Normal October-April precipitation, normal annual precipitation and normal May-September precipitation. Prepared by National Weather Service, NOAA. Published by Colorado Water Conservation Board, Denver, Colorado.

State of New Mexico: Normal October-April precipitation, normal annual precipitation and normal May-September precipitation. Prepared by National Weather Service, NOAA. Published by State Engineer Office, Santa Fe, New Mexico.

State of Utah: Normal October-April precipitation, normal annual precipitation and normal May-September precipitation. Prepared by National Weather Service, NOAA. Published by Utah State Engineer, Salt Lake City, Utah.

U. S. Army, Corps of Engineers, 1945-: Storm rainfall in the United States. Washington, D. C., (ongoing publication).

U. S. Army, Corps of Engineers, 1957: Hydrology, Tachevah Creek, Whitewater River Basin, California. Los Angeles District, Los Angeles, Calif. 11 pp.

U. S. Army, Corps of Engineers, 1958: Standard project rain-flood criteria, Sacramento-San Joaquin Valley, California, Sacramento, Calif., 16 pp.

U. S. Army, Corps of Engineers, 1961: Review report of the district engineer on survey for flood control, Winslow, Arizona and vicinity, Little Colorado River, Arizona and New Mexico. Los Angeles Distict, Los Angeles, Calif., 43 pp.

U. S. Army, Corps of Engineers, 1965: Standard project flood determinations. *Civil Engineer Bulletin* No. 52-8, Office of the Chief of Engineers, Washington, D. C., 33 pp.

U. S. Army, Corps of Engineers, 1972: Report on flood of 22 June 1972 in Phoenix metropolitan area, Arizona. Los Angeles District, Los Angeles, Calif., 57 pp.

U. S. Geological Survey, 1964: Normal annual precipitation for the Upper Colorado River above Lees Ferry, Arizona. *Professional Paper* No. 442. Department of Interior, Washington, D. C.

U. S. Weather Bureau, 1947: Thunderstorm rainfall. *Hydrometeorological Report* No. 5, Department of Commerce, Washington, D. C., 330 pp.

U. S. Weather Bureau, 1948: Highest persisting dew points in Western United States. *Technical Paper* No. 5, Department of Commerce, Washington, D. C., 27 pp.

U. S. Weather Bureau, 1951a: Tables of precipitable water. *Technical Paper* No. 14, Department of Commerce, Washington, D. C., 27 pp.

U. S. Weather Bureau, 1951b: Maximum station precipitation for 1, 2, 3, 6, 12, and 24 hours. Part 1, Utah, *Technical Paper* No. 15, Department of Commerce, Washington, D. C., 44 pp.

U. S. Weather Bureau 1954 -: Climatological data, annual summary. Department of Commerce, Washington, D. C., 27 pp. (ongoing publication).

U. S. Weather Bureau, 1960: Generalized estimates of probable maximum precipitation for the United States west of the 105th meridian. *Technical paper* No. 38, Department of Commerce, Washington, D. C., 66 pp.

U. S. Weather Bureau, 1961: Probable maximum precipitation in California. *Interim Report, Hydrometeorological Report* No. 36, Department of Commerce, Washington, D. C., 202 pp.

U. S. Weather Bureau, 1966a: Probable maximum precipitation, Northwest States. *Hydrometeorological Report* No. 43, ESSA, Department of Commerce, Washington, D. C.

U. S. Weather Bureau, 1966b: Meteorological conditions for the probable maximum flood on the Yukon River above Rampart, Alaska. *Hydrometeorological Report* No. 42, Environmental Science Services Administration, Department of Commerce, Washington, D. C., 97 pp.

U. S. Weather Bureau, 1969: Revisions to Hydrometeorological Report No. 36. Interim Report, probable maximum precipitation in California. Department of Commerce, Washington, D. C., 5 pp.

Weaver, R. L., 1962: Meteorology of hydrologically critical storms in California. *Hydrometeorological Report* No. 37, Weather Bureau, U. S. Department of Commerce, Washington, D. C., 205 pp.

World Meteorological Organization, 1972: *Proceedings of the International Symposium of Precipitation in Mountainous Areas, July 31-August 5, 1972, Geilo, Norway.* WMO/OMM No. 326, Geneva, Switzerland, Vol. 1, 228 pp; Vol. II, 587 pp.

World Meteorological Organization, 1973: Manual for estimation of probable maximum precipitation. *Operational Hydrology Report* No. 1, Geneva, Switzerland, 190 pp.

FIGURE 3.11b (Revised) — 10-mi² (26-km²) 24-hr orographic PMP index map (inches), north-central section

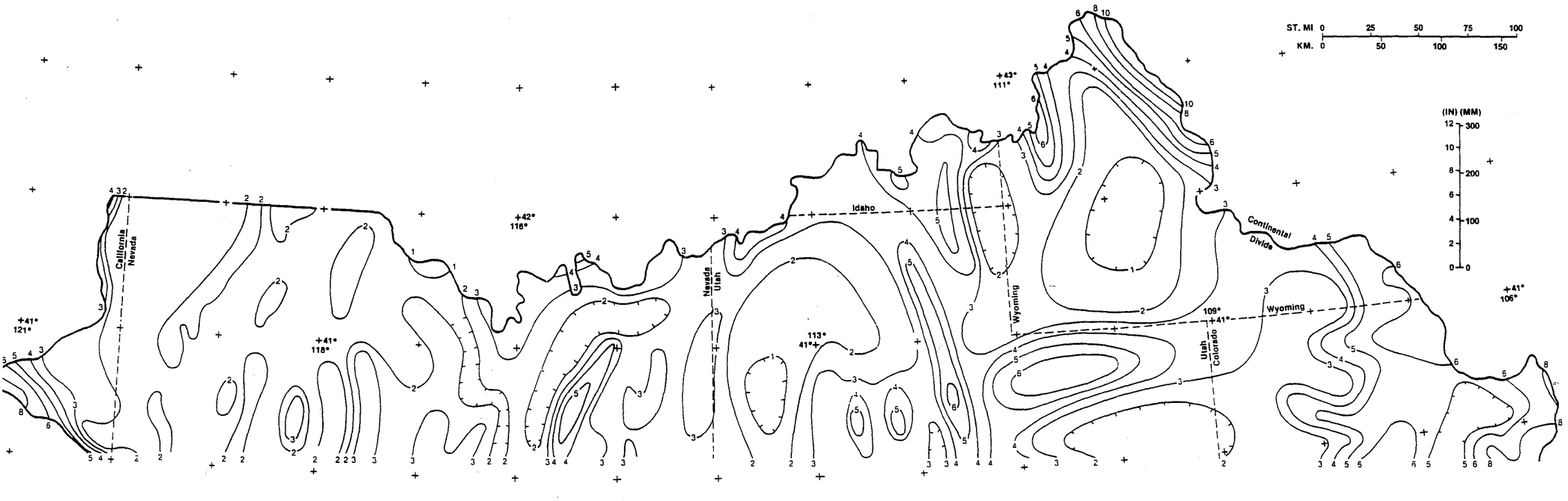

FIGURE 3.11a (Revised) — 10-mi² (26-km²) 24-hr orographic PMP index map (inches), northern section.

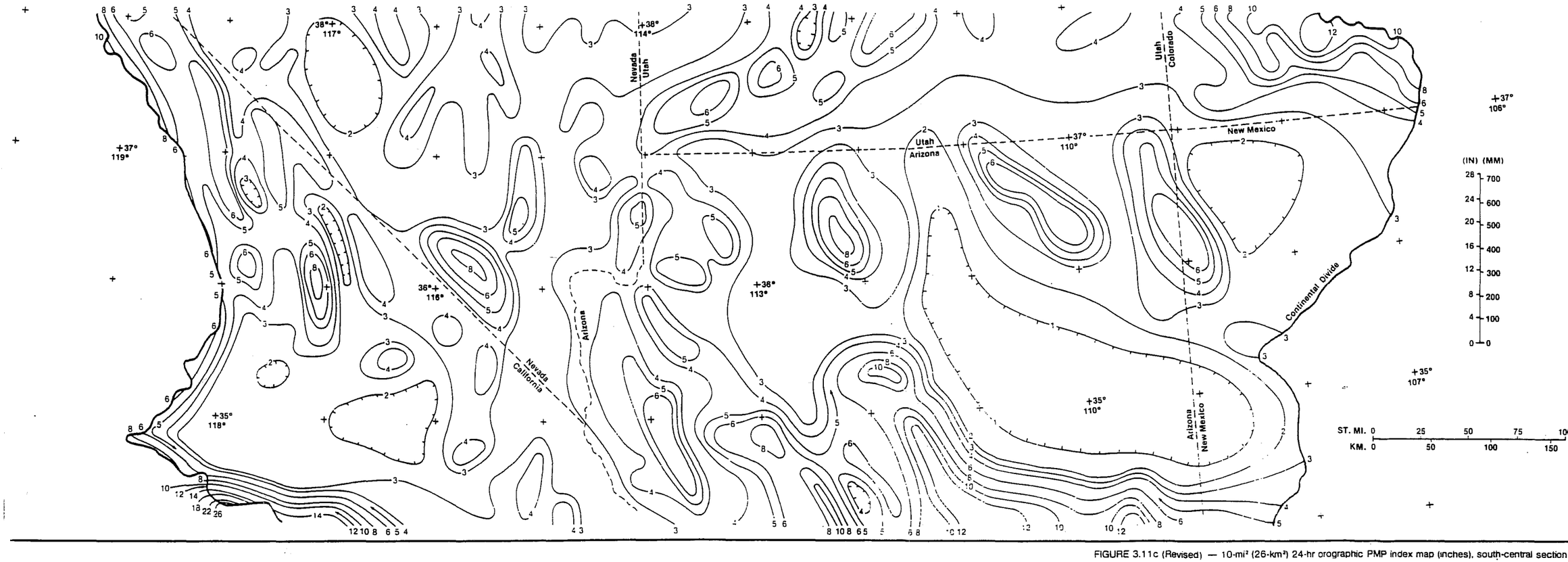

FIGURE 3.11c (Revised) — 10-mi² (26-km²) 24-hr orographic PMP index map (inches), south-central section

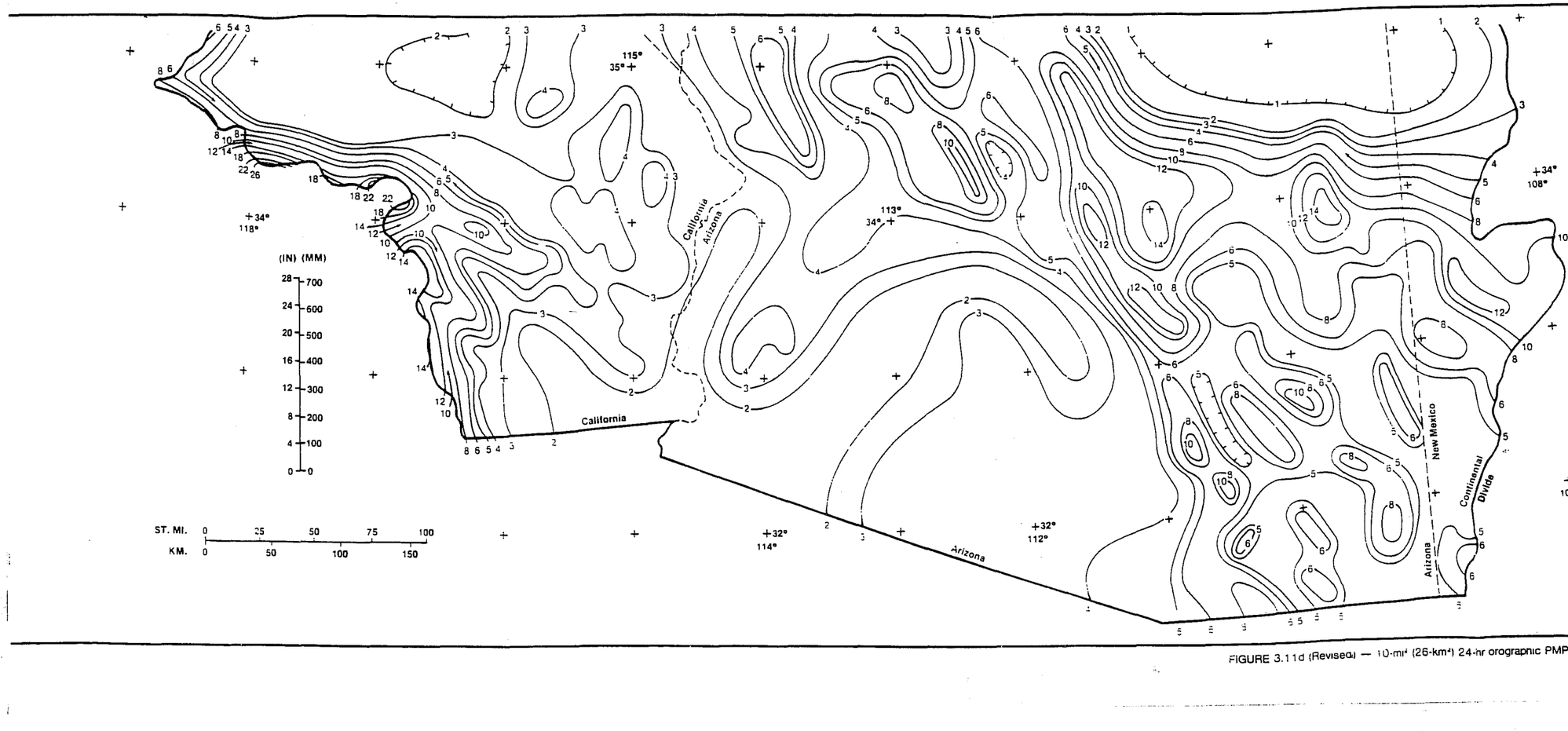

FIGURE 3.11d (Revised) — 10-mi² (26-km²) 24-hr orographic PMP index map (inches), southern section.

FIGURE 3.11b (Revised) — 10-mi² (26-km²) 24-hr orographic PMP index map (inches), north-central section